**The Dissertation Committee for Virginia Burton Smith Certifies that this is the approved version of the following dissertation:**

# Geomorphology of a coastal sand-bed river: lower Trinity River, Texas

**Committee:**

David Morhig, Supervisor

Charles Groat

Joel Johnson

Daene McKinney

Gary Parker

# Geomorphology of a coastal sand-bed river: Lower Trinity River, Texas

**by**

**Virginia Burton Smith, B.S.; M.S.E**

**Dissertation**

Presented to the Faculty of the Graduate School of

The University of Texas at Austin

in Partial Fulfillment

of the Requirements

for the Degree of

**Doctor of Philosophy**

**The University of Texas at Austin**

**December 2012**

# Acknowledgements

I would like to thank my advisor, David Mohrig, for his support, knowledge and guidance throughout my doctoral work. I would like to express my gratitude to my committee members Chip Groat, Joel Johnson, Daene McKinney and Gary Parker for sharing their insight, experience and expertise.

This project was accomplished through the assistance of many colleagues and fellow graduate students who have helped to make this project a success. I greatly appreciate their assisting with field work, discussing ideas, proofing reading and generally helping me along the way. In particular, I would like to thank Davaid Maidment, Bayani Cardenas, Gary Koucerek, Wonsuck Kim, Peter Wilcock, John Shaw, AymericPeyret, Jeff Nittrouer, Anjali Fernandes, Yao You, Travis Swason, Katie Delbecq, Lindsay Olinde, Peter Polito, Elizabeth Rinehart and all the members of Friends of Things that Meander. I would like to express my gratitude to the faculty for countless interesting, educational and inspirational lectures. I would also like to thank the staff of the Jackson School of Geosciences, who made my four years here very smooth and enjoyable.

I would like to thank the National Center for Earth-surface Dynamics (NCED) for financial support, as well as creating a wonderful intellectual experience. I would also like to thank the Deford Scholarship, the Walter L and Reta Mae Moore Graduate Fellowship for their financial support.

Finally, I would like to thank all of my family and close friends for their support of my pursuit of graduate studies. I would especially like to thank Bryan, my parents and my brother for their encouraging words, good humor, and willingness to proof read.

# Geomorphology of a coastal sand-bed river: Lower Trinity River, Texas

Virginia Burton Smith, PhD.

The University of Texas at Austin, 2012

Supervisor: David Mohrig

The lower Trinity River in Texas flows 180 river kilometers from Livingston Dam to Trinity Bay. Like many sandy coastal rivers the lower Trinity is geomorphically active. Within this 180-km reach, the river exhibits three styles of channel geometry and kinematic behavior that have been characterized using aerial photographs spanning the past 60 years, as well as bathymetric surveys and field work completed over the past 5 years. The three channel zones are connected to spatial change in properties of the sediment transport field. The upstream zone is defined by channel-bed incision, relatively small and coarse-grained bars, and relatively low rates of lateral channel migration. These properties of the upstream zone are connected to the discharge of water with effectively no bed-material load from Livingston Dam. Eventually the channel flow scours enough sediment from the channel bed and sidewalls to reestablish the predicted transport capacity for sand in the river, marking the transition to the central zone. This zone is defined by the largest bars and channel bends with the highest rates of lateral migration that persist downstream until the transport of sand and gravel is influenced by

the backwater hydraulics connected with the shoreline at Trinity Bay. This downstream river zone is characterized by very small point bars, the deepest flows at most discharges, and lower rates of channel migration. Studying the connections and transitions between these three river zones leads to a more complete understanding of the coevolution of river geometry and profile, channel kinematics, and downstream change in sediment transport in the coastal zone.

# Table of Contents

# List of Tables

# List of Figures

# Chapter 1: Introduction –
# Morphodyamics of the lower Trinity River, Texas

## INTRODUCTION

The science describing the dynamic morphology of rivers is important to understanding landscape development, fluvial deposits, and resource management. Coastal rivers frequently serve as water sources for population hubs, industry and support delicate coastal habitats, such as estuaries. Coastal rivers in particular play a critical role in producing sediment deposits that can counteract wetland loss and mitigate coastline loss due to storm surges. Sand-bed coastal rivers experience a high sediment transport rate, making the rivers physically dynamic (*Lagasse*, 2004). Texas, like areas around the world, has sand-bed coastal rivers. The lower Trinity River, from downstream of Livingston Dam to Galveston Bay, is an excellent system for studying the dynamics of sand-bed rivers.

This dissertation investigates the transport of sediment in a section of river, the lower Trinity River in Texas. The lower Trinity River, spanning from Livingston Dam to the coast, is composed of three distinct zones distinguished by channel dynamics and morphology: (1) a dam-influenced zone, (2) a zone with an actively migrating channel, and (3) backwater effected zone (Fig. 1.1). While all three channel segments appear to

share a relatively similar environment and geology *(Phillips et al*., 2004), the physical transport of sediment varies substantially between each zone. The homogeneity in environmental conditions (geology and land cover) coupled with the diversity in sediment transport characteristics provide an ideal opportunity to increase our understanding of how sediment transport affects the channel form and kinematics of alluvial rivers.

This research focuses on the measurement and modeling of river incision downstream of a dam, lateral channel migration, and modifications to sediment transport in the backwater zones. Incorporating observational data with analytical models allows for deeper comprehension of alluvial geomorphology. This dissertation provides insight towards answering several important questions in alluvial geomorphology, such as: how bed scour downstream of dams propagate further downstream overtime; which geometric variables describe the mechanics driving lateral migration; how sediment transport in the backwater zone alters bed conditions and channel and bar geometry; and, how the style of migration relates to point bar construction. This investigation was accomplished through surveys of the river-bed, banks and bars to identify the grain-size transition between zone transitions to identify features indicative of the sediment transport mechanics and bar construction. Additionally, this study used bridge and channel cross sections from the Texas Department of Transportation (TXDOT), historical aerial imagery of the river from the Texas Natural Resource Information System (TNRIS), bathymetry data from the Texas Parks and Wildlife Department (TPWD), Texas Water Development Board (TWDB), historical data from the Trinity River Authority (TRA), historical surveys from the U.S. Army Corps of Engineers (ASCE), and historical databases of flow and sediment transport from the US Geological Survey (USGS).

The upstream zone of the study area begins immediately downstream of Livingston Dam (Fig. 1.1). Lake Livingston retains sediment moving through the Trinity River (*Phillips et al*, 2005). While there have been thorough investigations into how the disruption of bed-load transport by dams impact the downstream sections of alluvial streams, the mechanics of the downstream geomorphic impacts are still being discovered (*Graf*, 2005). In the lower Trinity River, the Dam impedes the transport of bed-material, resulting in scouring of the river-bed downstream (*Phillips et al*., 2004). The Trinity appears to scour its bed and sidewalls until the eroded materials re-establish sediment transport equilibrium. Defining how and where the sediment transport equilibrium state is reached has not been fully explained.

The approximate re-establishment of an equilibrium sediment flux from mining the sediment from the channel bottom marks a change in channel kinematics, and the beginning of the second zone of the river. This zone is characterized by a substantially increased rate of lateral migration for the river channel (Fig 1.1c). In this portion of the river, net bed scour is replaced by roughly balanced sediment erosion from the outer banks of bends and deposition of sediment on the inner banks of bends (*Phillips et al*., 2004). This portion of the Trinity River experienced an average migration rate of 4.2 meters per year between 1952 and 2009, based on data from aerial photography and calculations by the Planform Statics GIS tool. Previous work on river meandering has primarily focused on how channel planform, particularly radius of curvature, governs rates of lateral migration (*Ikeda et al*., 1981, *Parker et al*., 1982, and *Parker and Andrews*, 1986, *Lagasse et al.*, 2004).

The most downstream Zone is influenced by the backwater of effect of Trinity Bay. In this stretch of river, coastal processes influence the flow. In comparing aerial photography from the past 60 years, it is evident that lateral migration of the river drastically decreases in the backwater zone. Previous studies have shown a correlation between migration rate and a spatial change in the sediment-transport field associated with backwater impacts of the Gulf of Mexico on the Mississippi River (*Hudson and Kesel*, 2000, *Jerolmack*, 2009 and *Nittrouer*, 2010). This study uses bathymetric and bank to examine the relationships between backwater influence on sediment transport and river-bed geometry.

The Trinity River is similar to many coastal rivers around the world. Like many coastal alluvial rivers, the lower Trinity is cut into alluvial deposits (*Phillips et al*., 2004), is dammed and supports local ecology, societies and economies (*Trinity River Authority*, 2010). The morphologic nature of coastal, alluvial rivers is typically highly active due to relatively high discharge and relatively fine grain size (*Lagasse et al.*, 2004). These rivers often support delicate eco-systems, provide critical water resources to population hubs and offer access to substantial economic resources (*Syvitski et al*., 2005). While these rivers play a vital role on several levels of our society, our physical models of sediment transport kinematics controlling their morphology are incomplete. This investigation seeks to better understand these rivers through their governing physical relationships between sediment transport, flow, dam impoundment, and coastal water.

## STUDY AREA

The Trinity River plays an important role as a water resource. Its basin is the largest fully contained within Texas. It serves as a water source for Dallas, Fort Worth and northern Houston, in addition to many industries, mines and farming located near the river. The lower Trinity River basin supports delicate coastal wetlands and serves as a habitat for several protected species of water fowl and alligator gar (*Trinity River Audubon Center,* 2009*).* The river terminates in Galveston Bay, and is part of the seventh largest estuary in the US; characterizing the river's flow as vital both economically and environmentally (*Trinity River Authority,* 2010).

Like many coastal rivers around the world, the relatively fine grain size and high discharge allows for sediment transport that in turn allows for rapid channel migration (*Lagasse et al.*, 2004). This can have implications effecting the floodplain and local infrastructure. For example, in this study area, as the river incised vertically downstream of the dam the bed exposes bridge pylons, resulting in bridge failure (Fig. 1.2). Lateral migration of rivers also threatens to undercut roads and to waste land along the banks. Also, like many coastal rivers, the Trinity is located near a major population hub, Houston. The Trinity River is subject to increasing stress to maintain a sound environmental flow due to a growing demand for water in the region (*Trinity River Authority*, 2010).

The lower Trinity River is an ideal location for this proposed research because it clearly exhibits distinct geomorphic regimes that span a range of qualities unique to coastal rivers. The study area begins downstream of Livingston Dam (the most

downstream dam of the river) and extends roughly 180 kilometers downstream to the Trinity River delta. In this study area the mean annual discharge is approximately 226 cubic meters per second (at USGS gage 8066350 at Goodrich, 11 river kilometers downstream of Livingston Dam). The geology surrounding the river is comprised of predominately of alluvial deposits. The exception to this occurs in the upstream stretch of the study area, where Miocene rocks can be found in the channel walls (Fig. 1.3). The river-bed and point bars are composed of medium to fine sand grains (*Phillips et al.*, 2004).

## DATA

Due to its strategic location and vital nature to the region, the river has been subject to substantial data collection. Records of the flow and suspended-sediment transport, beginning in the early 20$^{th}$ century, have been maintained by the USGS and the TWDB. Many surveys have also been done on the channel. The first official US survey was completed by the USACE in 1852 (*The Handbook of Texas*, 2010). Other surveys have been carried out by the Trinity River Authority, and the USGS. Aerial photographs and satellite imagery for the past 60 years have been assembled by the TNRIS. A TPWD completed a bathymetric survey of the lower Trinity River in 2007. Additionally, the USACE has recently provided river surveys dating back to 1909, including detailed cross sections from a 1939 survey, which will also be utilized in this investigation. However, many of the existing datasets are incomplete and, there is a lack of observational data describing the bathymetry and banks of the river.

Multiple field expeditions were taken on the Trinity to collect various types of data. The first few expeditions were to explore the river and make a photo survey of the diversity in the river zones. A bathymetric, land, and ditch transect surveys were completed in order to form a holistic picture of two bars in Zone Two of th lower Trinity River. Finally, a survey of the transition between zones was performed using a motorized canoe. This trip involved taking grain samples from the bars across the zone transitions to characterize the grain transition.

## RESEARCH TOPICS

This dissertation seeks to contribute to the science of geomorphology through furthering the understanding of alluvial coastal rivers mechanics. The lower Trinity River presents an excellent study area due to three distinct geomorphic zones previously discussed. This study investigates the geomorphic zones and coastal geomorphodynamics through the following chapters:

**Chapter Two: Dam Influenced Channel Incision:** Reservoirs behind dams act as sedimentation sites for the coarsest sediment being transported by rivers. As a result, the water exiting dams is relatively free of sediment and the river flow is well below the transport capacity for bed-material. The water flowing downstream from a dam tends to erode into beds of loose granular material. This occurrence is well documented in gravel-bed rivers, but has not been as completely studied in sand-bed channels such as the lower Trinity River, Texas. The mining of sediment from the bed of a gravel river acts to

coarsen the surface layer until the armoring shuts off any further erosion of the bed. This armoring control on the sediment discharge is not effective in a sand bed river. The relatively endless supply of sediment in sand bed alluvial rivers results in a unique response: the river bed is scoured of sediment until the river's sediment transport capacity is reached. This process is slope limiting, forcing the length of the sediment transport readjustment to expand downstream with time. Evidence of this is seen in the river profile, grain size, and cross-sectional relief of the channel.

**Chapter Three: Meander Mechanics:** Like many sandy coastal rivers, the lower Trinity is geomorphically active. From Livingston Dam to Trinity Bay the river meanders 180 kilometers, through 177 bends. The river exhibits three styles of channel geometry and kinematic behavior that have been characterized using aerial photographs spanning the past 60 years, as well as bathymetric and field surveys of the entire channel. The three channel zones correspond to spatial change in sediment transport properties. The upstream zone exhibits straightening and is defined by channel-bed incision, small bars, and relatively slow rates of lateral channel migration linked to sand retention behind Livingston Dam. Eventually the channel flow scours enough sediment from the channel bed to reestablish a transport capacity for sand in the river, marking the transition to the central zone. This second section is defined by fully developed point bars and a high rate of lateral channel migration. The second zone continues until the sediment transport is influenced by the backwater effect of Trinity Bay, defining a third segment. This backwater zone is characterized by very small point bars, steep channel walls, and lower channel migration rates. Migration in the channel segment is primarily translation with very little lengthening or shortening of bends, with no cutoffs or rapid straightening. For

this study a database with a myriad of physical variables describing the river was created to categorize the rivers shape as a function of downstream distance, by individual channel bend, and by bar. Studying connections between channel geometry, migration dynamics, sediment transport and fluid mechanics in each zone provides us with a more complete understanding of the relationships between channel shape and the mechanics at play.

**Chapter Four: Point Bar Construction:** Rivers exhibits two general styles of migration: persistent outward and downstream motion of bends and relatively abrupt adjustments in channel length due to bend cutoffs. Persistent lateral migration is primarily driven by the flow mechanics in bends that drive outer bank erosion and sedimentation along the inner bank of a bend. Cutoffs, on the other hand, quickly alter the course of a river, forcing a sequence of more rapid bed and bank adjustments to a set of neighboring channel bends. This chapter investigates the relationship between the two styles of channel motion and the growth of associated point bars. This is accomplished by examining two meander bends in the lower Trinity River of Texas. The lower Trinity River is a sandy coastal river of banks that are primarily composed of sandy Quaternary fluvial deposits. One of the studied bars is in a bend that has experienced rapid adjustment in response to an upstream cutoff. This bar is characterized by a steep adverse and lateral surface slopes at its upstream and an associated tear-drop shape in planview. The second bar is situated in a bend undergoing persistent lateral migration over the past 60 years. The bar has smaller adverse and lateral slopes at its upstream end and is crescent-like in plan form. I synthesized time-lapse planimetric maps, high-resolution topographic and bathymetric surveys, and trenching of the two point bars deposits to: 1) evaluate the cause-and-effect relationship between cutoffs and meander

adjustments, and 2) understand the relationship between channel plan form, bar morphology and bar sedimentation.

This dissertation demonstrates the relationship between morphodynamics, the sediment transport, and the physical geometry of the river channel. By describing the physical traits of the channel in quantitative detail over a large scale and over several decades the sediment transport and fluid mechanical kinematics and dynamics of the three channel environments can be identified. This studylinks three sandy coastal river environments: dam influenced flow, relative sediment transport equilibrium, and backwater, to their physical and mechanical traits. The following chapters will explore these ideas in greater detail.

**FIGURES**

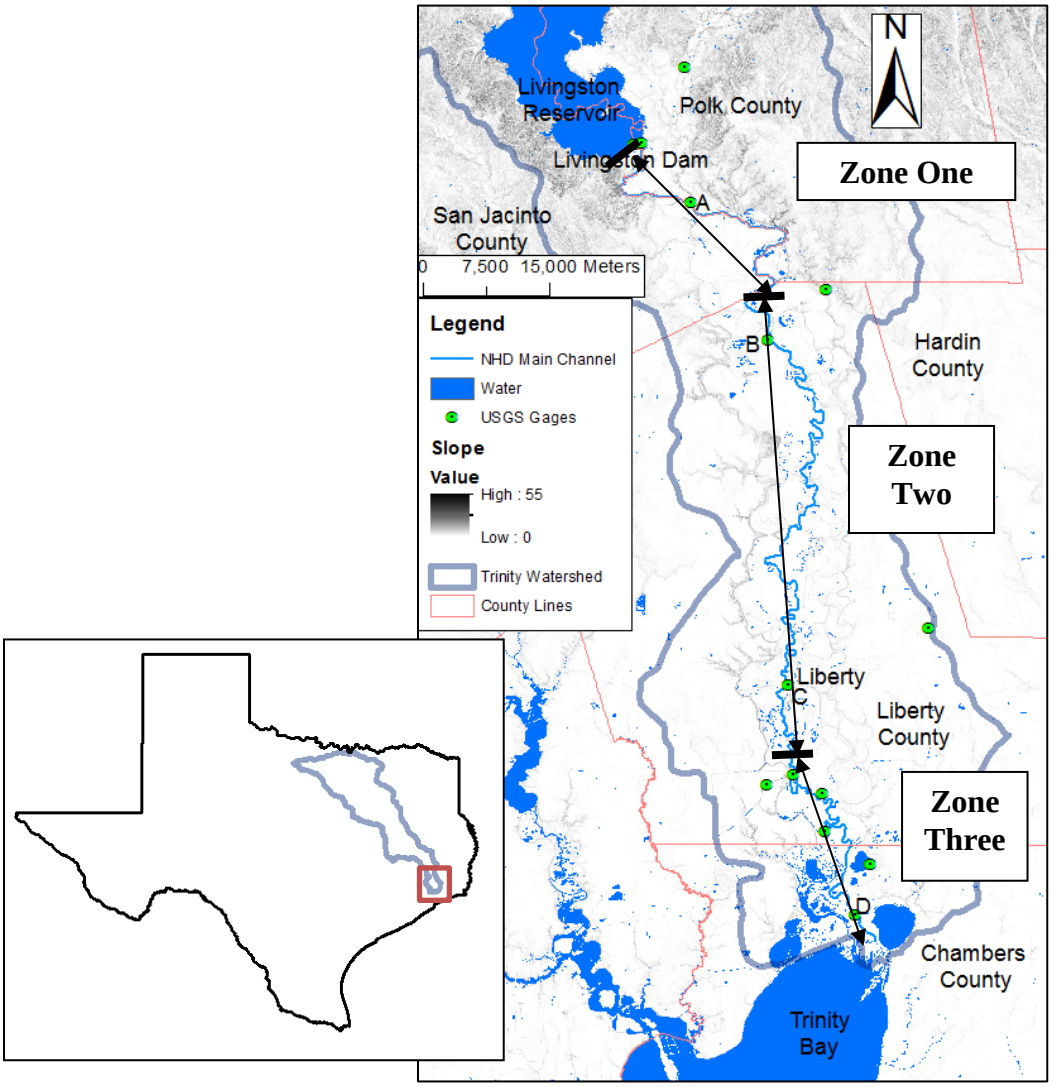


Figure 1.1: Map of the lower Trinity study. The Trinity watershed within the state of Texas is outlined in blue, running across the eastern portion of the state. The red box marks the section of the watershed that is the study area. The study area is bounded by Livingston Dam to the north and Trinity Bay to the south. On this map the counties are outlined in red. The town of Liberty, TX is labeled near gage C. The green circles mark USGS gages at Goodrich, TX (A; USGS number 08066250), Romayor, TX (B; USGS number 08066500), Liberty, TX (C; USGS number 08067000), and Wallisville, TX gage (D; USGS number 08067252). Zone One is the first 60 kilometers downstream of the Livingston Dam (labeled at the top/north of the map). Zone Two is the middle zone of the river, 100 river kilometers long. The most downstream zone of the river is Zone Three, the final 60 kilometers of the river.

Figure 1.2: Bridge failure on the Trinity River near Goodrich, TX in 2004. The red dash line is the infered elevation of the river botton at the time of bridge construction. The bridge is located approximately 16,000 meters downstream of Livingston Dam.

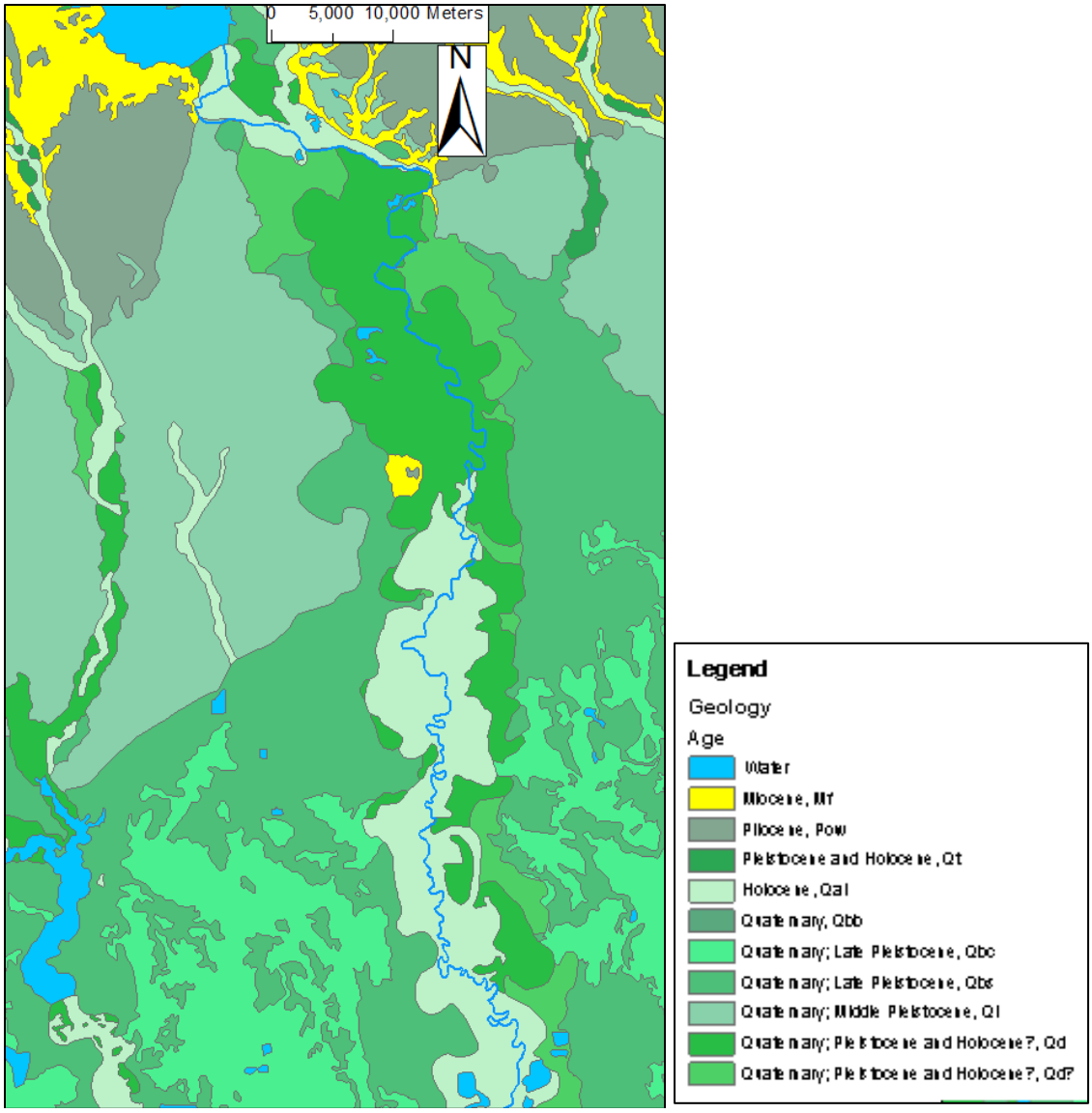


Figure 1.3: Geologic map of the study area. Nearly the entire region is composed of Quaternary deposits shown in green. The blue marks major water bodies for spatial reference. The northern portion of the map has some deposits that are Pliocene and Miocene in age.

**REFERENCES**

Graf, William L., 2005. "Geomorphology and American dams: the scientific, social, and economic context," *Geomorphology,* Vol. 71, p. 3-26.

Hudson, Paul F. and Richard H. Kesel, 2000. "Channel migration and meander-bend curvature in the lower Mississippi River prior to major human modification," *Geology,* Vol. 28, No. 6, p. 531-534.

Ikeda, Syunsuke, Gary Parker and Kenji Sawai, 1981. "Bend theory of river meanders. Part 1. Linear development," *Journal of Fluid Mechanics,* Vol. 112, p. 363-377.

Jerolmack, Douglas J., 2009. "Conceptual framework for assessing the response of delta channel networks to Holocene sea level rise," *Quaternary Science Reviews,* Vol. 28, p. 1786-1800.

Lagasse, P.F. et al., 2004. "Methodology for Predicting Channel Migration," *National Cooperative Highway Research Program Transportation Research Board of the National Academies* Document 67.

Nittrouer, Jeffery, 2010. "Sediment transport dynamics in the lower Mississippi River: Non-uniform water flow and affects on river-channel morphology," Dissertation, University of Texas at Austin.

Parker, Gary and Edmund D. Andrews, 1986. "On the time development of meander bends," *Journal of Fluid Mechanics,* Vol. 162, p. 139-156.

Parker, Gary, Kenji Sawai and Syunsuke Ikeda, 1982. “Bend theory of river meanders. Part 2. Nonlinear deformation of finite-amplitude bends,” *Journal of Fluid Mechanics*, Vol. 115, p. 303-314.

Phillips, Jonathon, Michael Slattery, and Zachary Musselman, 2004. "Dam-to-delta sediment inputs and storage in the lower Trinity River, Texas," *Geomorphology,* Vol. 62, No.1-2, p. 17-34.

Syvitski, et al., 2005. “Impacts of humans on the flux of terrestrial sediment to the global coastal ocean,” *Science* Vol. 308, p. 3376-380.

*The Handbook of Texas: the Trinity River*. Web. 19 Aug. 2010. <http://www.tshaonline.org/handbook/online/articles/TT/rnt2.html>

*Trinity River Audubon Center: home page*. Web. 23 Nov. 2009. <www.trinityriveraudubon.org>.

*Trinity River Basin Master Plan.* Trinity River Authority, 2010.

“Trinity River Bridge, State Highway 105.” *Texas Department of Transportation.* p.1-9. Print.

*USGS Water Data for the Nation*. Web. 20 Aug. 2010. <http://waterdata.usgs.gov/nwis>.

# Chapter 2:
# Dam Influenced Channel Incision


## ABSTRACT

Reservoirs behind dams act as sedimentation sites for the coarsest sediment being transported by rivers. As a result, the water exiting dams is relatively free of sediment and the river flow is well below the transport capacity for bed-material. Because of this, rivers flowing downstream from dams tend to erode into their beds. This occurrence is well documented in gravel-bed rivers, but has not been as completely studied in sand-bed channels such as the lower Trinity River, Texas. The mining of sediment from the bed of a gravel river acts to coarsen the surface layer until the armoring shuts off any further erosion of the bed. This armoring control on the sediment discharge is not effective in a sand bed river. The abundant supply of sediment in a sand bed alluvial river results in a unique response: the river bed is scoured until sediment transport capacity is reached. This process is limited by bed slope, forcing the zone of sediment transport readjustment to lengthen over time. Evidence of this is presented for the lower Trinity River downstream of Livingston Dam. The evidence includes adjustment to the river long profile, grain size, bar size, and cross-sectional shape of the channel.

## INTRODUCTION

Approximately 60 percent of the world's population lives on the coast or within 100 kilometers of the ocean; even though coastal land represents only 10 percent of Earth's land surface. Furthermore, coastal population hubs are often located near the mouths of rivers (*Crossland*, 2005). As a result, coastal rivers frequently support the water resource demands of substantial coastal populations, industry, and productive coastal habitats, such as estuaries and deltas. Coastal rivers in particular play a critical role in delivering sediment to the coastline that can counteract wetland loss associated with relative sea-level rise (*Nicholls,* 2003) and mitigate coastal erosion. Water resource demands require a delicate balance between river and reservoir management affecting this critical delivery of sediment to the coast, as well as river geomorphology and ecology (Lagasse, 2004). The lower Trinity River of Texas is a prime example of an impounded sand-bed river. It supports a large population in the metro-Houston area and serves as the habitat for many species of interest including the American alligator, the alligator gar, and over 400 species of birds, such as the bald eagle and the rosette spoonbill (*Norris and Linam*, 1999). To meet water resource demands, the river has been impounded by Livingston Dam, 180-river kilometers upstream of Trinity Bay. I use this 180-river kilometer reach to study the morphologic adjustments of a sand-bed river in response to impoundment by a coastal dam (Fig. 2.1). Many studies have shown that dam emplacement causes river incision downstream (Williams and Wolman, 1984). This bed erosion alters the channel's form and long profile (*Brandt*, 2000). In coarse-grained rivers an equilibrium bed slope can be achieved through coarsening or bed armoring

(*Kondolf*, 1997). Downstream channel armoring limits the duration and amount of channel scour (*Askoy*, 1971, *Jain and Park*, 1989; *Rzhanitzin et al*., 1971). However, if armoring does not occur, as in the case of sandy rivers, the slope adjustments can be substantial and evolve over decades (*Chein*, 1985; *Petts and Gurnell*, 2003; *Williams and Wolman*, 1984). The Trinity River downstream of Livingston Dam is an excellent site to quantify the persistent channel change associated with a sand-bed river.

The lower Trinity River was impounded in 1968 to create a reservoir, Lake Livingston (Fig. 2.2.1). This reservoir retains most of the sediment delivered from upstream and releases water at the dam with a sediment load far below the transport capacity for the flow. The delta forming from accumulating sediment at the upstream end of Livingston Reservoir is shown in Figure 2.2. Sediment-starved water leaving the dam drives bed and bank erosion as the flow picks up sediment to regain transport capacity (*Mackin*, 1948). Incision of the Trinity River below the dam resulted in failure of a railroad bridge failure in 2004 (Fig. 2.3). Scour around the bridge piers was so great that the bridge became unstable under the weight of a passing train (*Bullet*, 2003).

The lower Trinity River is an ideal site to study river adjustments because of an abundance of historical and present-day data. Aerial photographs provide a geomorphic record of the river dating back to 1952. Collection of river gage data began decades before the dam was impounded and is still ongoing. Surveys of river bathymetry and planform date back to the nineteenth century and in 2007 a comprehensive survey of river-bottom topography was carried out over the entire 180 kilometer reach by Texas Parks and Wildlife. I have assembled all of this information into a large spatial and

temporal database that captures the long term geomorphic response of the channel to the dam. I document the adjustments in the river's profile, the grain size distribution, the bar area, bar shape, the river bend curvature and length, channel cross-sectional shape and rate of lateral migration. I then compared this data against predicted sediment transport and river profile adjustments using a 1-D numerical model developed by Parker (2004). There is also an existing breath of publications concerning the geomorphology of the lower Trinity which have been used as a resource for this work (*Musselman*, 2006; *Musselman*, 2011; *Phillips et al*., 2004; *Phillips et al*, 2005; *Phillips and Slattery*, 2006; *Slattery*, 2007; *Slattery and Phillips*, 2007).

## OBSERVATIONS

### Change in River Hydrology

Livingston Dam has modestly impacted the flow of the lower Trinity River since its closure. Mean daily discharge has increased from 200.7 cubic meters per second during the 44 years preceding dam closure to 238.7 cubic meters per second since 1968 (USGS gage 08066500, Romayor, TX). Figure 2.4 depicts the associated change in flow distribution for two gages in the study area, Liberty and Romayor, TX. Both the highest and lowest discharges have been removed by flow management at the dam. Even though the most extreme values have been lost, the general shape of the distribution is very similar before and after the dam's construction

**Profile Adjustments**

The lower Trinity River has been surveyed several times in the past one hundred and fifty years using a variety of methods. For this study six of these surveys were compared to quantify the morphodynamic changes to the river. The oldest survey used was collected by the U.S. Army Corps of Engineers (USACE) in 1939, roughly 30 years before the impoundment of Livingston Dam. I have digitized their measured long profile for the river using Geographic Information Systems (GIS) and then exported the data to Matlab for analysis. The 1939 profile has a linear trend for the first 120 river kilometer until the channel approaches Trinity Bay where it changes from linear to concave (Fig. 2.5a). The concave shape at the downstream end of the profile is interpreted as a response to the backwater effect of Trinity Bay (e.g., *Nittrouer et al.*, 2012).

A second long profile for the Trinity River was collected in 2007 by the Texas Parks and Wildlife Department (TPWD) (Fig. 2.5b). This data was collected from a small boat using a synched, single-beam depth sounder and GPS unit. To construct a profile comparable to the 1939 survey I reprocessed the topographic data using GIS, grouping the raw data by river kilometer. The solid blue line in Figure 2.5b represents the mean channel-bed elevation in 2007 by river kilometer. The swath surrounding this line of mean elevation defines the 5% to 95% range in channel-bed elevation values per kilometer.

In comparing 1939 and 2007 profiles it is obvious that the channel has experienced significant change in elevation downstream of the dam (Fig. 2.5c). The bed

incision immediately downstream of the dam is five to seven meters. The associated change to the channel bed is a shift from a linear to a convex profile over the zone of incision. Roughly 55 river kilometers downstream from the dam the 2007 profile recovers the linear trend seen since 1939. The most downstream portion of the 2007 profile exhibits a concave shape this is similar to the 1939 profile, but at a slightly higher elevation. This change in this lowermost section of the river is most likely due to the progradation of the Trinity River delta and will not be discussed further here. In this chapter I will only focus on adjustments to the Trinity River profile within 100 river kilometers of the dam. From the 2007 survey this includes both the convex portion of the profile and the transition to the linear long profile with distance downstream.

The transitions from a convex to linear and then linear to a concave profile are even more pronounced when looking at water-surface elevation data (Fig. 2.6). The water surface profiles were calculated using the stage records from the only four gaging stations on the Trinity River within the study area. The stations are located at Goodrich, Romayor, Liberty and Wallisville, TX (USGS number 08066250, 08066500, 08067000, and 08067252). The most recent 20 years of data from these four stations were used to calculate a minimum stage (5% probability), median stage, and maximum stage (95% probability). These river stages are associated with water discharges of 28.1 cubic meters per second, 162 cubic meters per second, and 2381.4 cubic meters per second at the USGS gage at Goodrich, TX. The shape of the water surface profile is a reflection of three distinct geomorphic zones: the convex incisional zone (Zone One), the linear, actively meandering zone (Zone Two), and the concave backwater zone (Zone Three).

Figure 2.7 combines stage data (Fig. 2.6) with the profile of the channel bed and the topographic profiles defining the right and left banks of the river. At high river discharge, water-surface elevations exceed banks elevations at most locations in Zone Two and Zone Three. The same degree of bank inundation is not seen at high river discharge in Zone One (Fig. 2.7). River incision downstream of the dam appears to be in the process of transforming the Zone One flood plain into a terrace substantially elevated above the channel. In the following section I will compare properties of the river in Zone One and Zone Two in order to quantify the geomorphic signature of dam-induced channel incision and to establish the limits of the dam influence.

**Downstream Changes in Channel Cross Sections**

I have evaluated channel response to Livingston Dam by measuring the following variables of cross-sectional geometry as a function of distance downstream: channel relief, elevation of the inner and outer banks, and sidewall slopes of the inner and outer banks. These channel properties were calculated using a digital elevation model (DEM) that combines the 2007 bathymetric survey with land-surface topography based on 1:24000 USGS topographic quadrangles from 1984. Transects perpendicular to the channel centerline were created at a 36 meter downstream spacing. Each transect extended onto the flood plain surface, terminating at the vegetation line mapped on both sides of the channel. Transects were converted to points that were joined to the elevation data of the DEM and then exported to Matlab as channel cross sections which I used to calculate relevant geometric parameters. Figures 2.8 a and b show examples of the steep channel walls that typify of the dam influenced portion of the river; Figure 2.8c shows a

typical cut bank from a downstream section of the river that is not influenced by the dam. The calculated values for channel relief and bank slopes are presented in Figure 2.9. Zone One of the channel is characterized by steeper channel sidewalls and greater channel relief than Zone Two.

**Planform Differences**

In addition to the 1939 and 2007 topographic surveys, this study used four aerial photographic surveys finalized in 1952, 1972, 1996 and 2009 (Texas Natural Resource Information System (TNRIS)). However, the collection date was slightly earlier in some cases (Table 2.1). For the purpose of this study the finalized survey date is reported, but the collection date was used in all temporal calculations. Using GIS, several variables were extracted from these geo-referenced photographs including channel centerline, the vegetation line on each bank, and bar area. Peyret's (2011) Meanders Matlab Program was used to determine the radius of the curvature of the centerline for each set of aerial photographic surveys. The data sampling window was set at 500 meters to optimize the agreement between the positions of calculated and observed channel inflection points on the river. The resulting output was filtered and smoothed to ensure that every inflection point was properly identified with only a small offset due to the spatial averaging aspect of the window size. These points of local maxima in the channel radius of curvature were used to identify every single bend on the river, facilitating the calculation of bend statistics such as bend length, maximum curvature, and sinuosity, and allowing for unambiguous comparison between bends over time.

Values for channel width and lateral migration rate were measured by inputting the digitized centerlines and vegetated bank lines into the GIS Planform Statistics Tool (*Lauer*, 2006). This tool calculates the lengths separating successive centerlines in order to estimate the lateral migration distance for the channel at each transect every 36 meters down the river. The distance between the banks was also calculated at each transect providing an estimate of bankfull width every 36 meters down the river. Figure 2.10 shows how both channel bankfull width and lateral migration rate vary as a function of downstream distance. The width of the river is narrower near the dam and widens as the incision tied to the dam tapers out. The amount of lateral migration of the channel also appears to spatially vary as a function of distance from Livingston Dam (Fig. 2.10b). Like the bankfull width, lateral migration changes with distance away from the dam. Lateral migration is lower near the dam and increases downstream. The observed spatial change in channel width and migration is consistent with the transition from Zone One to Zone Two being located at about river kilometer 55 (Fig. 2.10).

Every bank-attached bar exposed in the 2009 aerial survey was mapped as a GIS polygon. This mapping clearly shows that the bar area increase with distance away from Livingston Dam, but it is an incomplete metric because a significant fraction of all bars extends beneath the water surface and are therefore not visible on the photographs. I corrected for this deficiency by combining the 2007 bathymetric survey with the 2009 aerial survey. The bathymetric data was layered onto the aerial photographs with a partial transparency, allowing for the identification of the full extent of each bar. The

area of each bar was defined by the wooded vegetation line at its top and the break in bed slope within the channel that separates the bar form from the adjacent channel thalweg (Fig. 2.11). The volume of each bar was measured from the bathymetric DEM using GIS tools. The area and volume of each bank-attached bar as a function of downstream distance is shown in Figure 2.12. Clearly the size and volume of bars systematically increases through Zone One into Zone Two. There is a minor exception to this trend found within five river kilometers of Livingston Dam. It appears that the planform of this section of the river was engineered in conjunction with construction of Livingston Dam and stands out as an anomaly and not representative of natural channel adjustment associated with closure of the dam. Maximum and mean bar height are presented in Figure 2.13. Bar height follows the trend observed for size and volume, systematically increasing with distance away from the dam (Fig. 2.14).

**Grain Size Transitions**

The Texas bedrock map shows that the lower Trinity River sits upon a thick section of fluvial deposits, Miocene to Recent in age (Fig. 2.15a). Most of the deposits are Quaternary in age and very weakly to un-cemented (Fig. 2.16a and c). Only a small fraction of the bedrock is Pliocene – Miocene in age and is exclusively found in Zone One of the river (Fig. 2.16b). These deposits are exposed in river cut banks (Fig. 2.8, 16) and a qualitative examination shows them to be weakly to very weakly cemented. The overall lack of intergranular cement has a big impact on how the exposed bedrock is

weathering and on how this substrate is being eroded by river flow. Based on qualitative observations of river-bank exposures through much of Zone One and the Zone – to – Zone Two transition I estimate that approximately 90% of the bedrock almost immediately disaggregates into its constituent grains with even a small amount of movement, while the remaining 10% breaks down into weakly or very weakly cemented sandstone boulders that have a minimum dimension set by a characteristic bed thickness, commonly 20 to 30 centimeters (Fig. 2.16c). These boulders must rapidly break apart with transport because there are no sandstone clasts greater than pebble size are found in bank-attached bars only one river bend downstream of a patch of sandstone boulders

A rough analysis of a comprehensive set cut-bank photographs documenting the entire study reach shows that the Miocene to Recent fluvial deposits are composed of approximately fifty percent mud (silt and clay) and fifty percent coarser material (Fig. 2.8, 16). I estimate that greater than ninety percent of this coarse fraction is sand with the remainder being gravel that is up to cobble size. Most of sandy and gravelly deposits quickly disaggregate into their constituent grains so that gravel deposited in the Quaternary – Miocene is reintroduced to the modern river system (Fig. 2.17). These recycled gravels develop extensive armor surfaces on a number of bar surfaces in Zone One (Fig. 2.14a and 18). The composition of this gravel is primarily chert with lesser amounts of sedimentary-rock clasts, and petrified wood (Fig. 2.19) and bone (Fig. 2.20). The surprisingly abundant amount of petrified wood and bone found on bars in Zone One is important because it indicates that the Pliocene and Miocene bedrock is being actively eroded by the Trinity River and that some considerable amount of this bedrock has been

eroded to produce the volume of petrified wood and bone clasts observed on the Zone One bars.

In June 2012 I carried out a grain size sampling campaign of bank attached bars throughout most of the 180,000 river meter study area. The seven bars sampled in Zone One and the Zone One – Zone Two transition are shown in Figure 2.21. Six sediment samples were collected from each bar. Three grain size samples were taken from the water's edge and three from the vegetation line. The samples were taken 60 paces apart in the centerline direction starting near the upstream end of the bar and ending near the midstream portion of the bar. Each sample was collected exactly at the point of sixty paces to ensure that bias was not introduced into our sediment sampling. The size of the samples varied slightly, averaging $5.56 \times 10^{-5}$ cubic meters. All of these samples were large enough to ensure that the coarsest grains are accurately represented (*Wolman,* 1954). The largest grain in any sample constituted less than one one-thousandth of the total sample volume. Grain size was measured using a Retsch Technology CamSizer that uses image analysis of falling grains captured by two high-speed digital cameras to determine both particle size and shape. The results of this analysis for the bars in Zone One and the Zone One – Zone Two transition are summarized in Figure 2.21b.

The measured trend in median grain size of bars in Zone One and the Zone One – Zone Two transition is noisy and not well developed (Fig. 2.21b). The measured downstream variability in grain size is consistent with the observed spatial variability in gravel distribution within the bedrock. The variability in grain size with distance downstream is also compounded by the introduction of sediment to the Trinity River

from minor tributaries. The landscape surrounding the river is primarily wetland, forest or pasture (Fig. 2.15b) so there is very little anthropogenic influence on sediment yield, but a few small tributaries deliver roughly 12395 cubic meters of sediment to Zone One of the Trinity River per year (*Slattery and Phillips*, 2007; Table 2.2). An example of an internal delta deposited at a tributary confluence is shown in Figure 2.22. Sampling showed that this sediment deposit is somewhat finer grained ($D_{50}$ = 0.26mm) than adjacent bank-attached bars in the main river. Figure 2.22 also shows that these deltas are transient deposits that are eroded by the river over time. The Zone One bar shown in Figure 2.23 is positioned immediately downstream of a contributing tributary and is particularly sand rich relative to other bars in Zone One (Fig. 2.14a and 18). All bars in Zone One contained some fraction of gravel, but this gravel fraction was also much less than fifty percent of the bars by volume. As a result, the gravel has never been seen to stabilize a large section of a bar or segment of the channel bottom.

Lateral movement of the channel in Zone One (Fig. 2.10b) results in a net addition of sediment to the Trinity River. Between 1996 and 2009 an average of 21116 cubic meters of sediment was added to the river transport per year (Table 2.2). This addition of sediment is due to the unequal height of the outer versus inner banks of channel bends (Fig. 2.9c). The greater height of cut banks relative to the bank-attached bars leads to more sediment being eroded from the outer banks than is being deposited on inner banks. I estimated the net addition of sediment to the river in Zone One via cut-bank erosion using the methodology described by Lauer and Parker (2007). The volume of sediment that was eroded from the outer banks and the amount deposited on the inner banks was directly measured using the aerial photographs from 1996 and 2009 to define change in bank positions and the merged bathymetric plus land-based DEM to define

bank heights. Given the very weakly to uncemented character of most bank deposits it is perhaps surprising that the observed rates of bank erosion and lateral migration are not higher (Fig. 2.10b). These rates are limited by the accumulation of large woody debris at the base of cut bank, fallen trees and bushes that baffle the cut bank from the eroding river flow. Examples of this baffling vegetation are presented in Figure 2.24. The slumped trees and other vegetation acts to protect the outer banks from runaway erosion (*Parker et al.*, 2011).

## ANALYSIS

### Analysis of Observations

It is well known that dams have downstream impacts on rivers. However, the means in which the sediment transport mechanics are altered by dams is not fully understood. Figures 2.10, 2.13, and 2.21 summarize changes in river geomorphology tied to Livingston Dam's influence. The spatial adjustments in channel width, rate of lateral channel migration and bar size also define the transition between the dam affected and unaffected portion of the lower Trinity River. As the dam's influence tapers off, the shape of the river changes, as does the geomorphology. In this section I will investigate how these physical changes between Zone One and Zone Two are connected to a spatial change in the sediment transport describe a change in the sediment transport dynamics and fluid mechanics.

The most dramatic evidence of change is found in the adjustment of the elevation profile for the river (Fig. 2.5) caused by dam influenced incision. Figures 2.19 and 2.20 show images of petrified wood and fossilized bone deposited as gravel on the tops of a bar in Zone One. These specimens must have been excavated from the substrate as the channel incised its bed. On several of the bars downstream of the dam petrified bones and rocks covered much of the bar top. While gravel composed of petrified wood and bone were common on the tops of bars in Zone One, no evidence of these gravel types were found on the bars in Zone Two (Figure 2.14b).

Dam related channel incision has led to systematic changes in the channel cross-sectional geometry. Figure 2.9 shows how as the river transitions from Zone One to Zone Two the channel relief and the bank slopes decrease. Immediately downstream of the dam, the channel relief is the greatest (Fig. 2.9a) and it decreases until the as the dam's influence ends. This same trend is seen in the case with the bank slopes (Fig. 2.9b). Like channel relief, the slopes of the banks are steepest immediately downstream of the dam and decrease in steepness as the dam's influence dissipates.

Measurements from the Trinity River presented in Figure 2.10b clearly show that the channel is narrowing in response to dam-influenced bed incision. This incision is consistent with the numerical and experimental results of Cantelli et al. (2007) but is inconsistent with the proposed adjustment by Brandt (2000) and observations on the Trinity River itself by Phillips et al. (2005). The discrepancy with Brandt (2000) is important because it highlights a potential pitfall of using data from only gravel-bed rivers to generalize the response for all rivers to dam impoundment. The results of

Phillips et al. (2004) highlight the need to observe data from many sections along the river. Their conclusion is based on a limited number of cross sections collected exclusively at bridge crossings. The analysis described here found bridge crossings to be connected with geomorphic anomalies.

My analysis also reveals a systematic change in the bar area, volume and height (Fig. 2.12 and 13). The bars in Zone One have a low height (Fig. 2.13, 14), that I interpret to be connected with sediment starvation due to the dam (*Podolak*, 2012). As the dam influence decreases and the bed-material load increases due to mining of the channel bottom, bar size and relief increase (Fig. 2.5, 12 and 13). I interpret the increases in these three variables as a signal of dissipation of the dam's influence and a return to sediment-transport capacity.

The small relative size of bars in Zone One appears to minimize the degree of topographic steering of the flow towards the outer banks of bends. As a result, the lateral migration rates measured in Zone One are significantly less than those found in Zone Two (Fig. 2.10a). In fact, the migration that does occur downstream of Livingston Dam is due to the straightening of the channel. Between years 1952, 1972, 1996, and 2009 the total number of bends in Zone One decreased from 53 to 47 to 45 to 43, and the average bend length increased from 1046 meters to 1166 meters to 1213 meters to 1280 meters (Fig. 2.25).

**Computational Analysis**

In alluvial rivers like the lower Trinity, bed-load is typically only a few percent of the total sediment flux (*Collins and Dunne*, 1990, *Slattery and Phillips*, 2007). However, bed-load is responsible for shaping much of its channel and bed topography (*Kondolf and Wolman*, 1993). The bed-load transport is governed by the boundary shear stress, which in turn is controlled by the flow of the river. This is a continuous cycle as the flow of the river is controlled by the morphology of the channel (*Dietrich and Gallinatti*, 1991).

For geomorphologic analysis of this system I had to determine the values for several characteristic variables describing the physical environmental. The characteristic channel width, *B*, is 134 meters, the average bankfull width for the length of the river. The length of the river modeled was 121 kilometers, the distance from Livingston Dam to the point where the average bed elevation reaches sea level. The slope, $S = 0.00017$, was calculated using the linear portion of the river profile. The mean grain size, $D_{50}$, used was 0.74mm (taken from bar samples collected between Goodrich and Romayor). *R* is the submerged specific gravity of the sediment (1.65). Sediment input was set to zero at the origin to represent the relatively sediment-free water exiting Livingston Dam. The discharge was calculated using gage data from the Romayor, TX USGS gage (number 8066500) from the past 20 years.

I have used a one-dimensional morphodynamics model developed by Parker (2004) to model the adjusting river profile. This numerical model applies the Meyer-Peter Muller equation (1948) to estimate sediment transport. This equation (Eqn. 1) is

based on a simple rule that if the dimensionless bed shear stress ($\tau^*$) is greater than the dimensionless critical shear stress ($\tau_c^*$) there is sediment transport. The amount of sediment being transported is a function of the difference between the $\tau^*$ and the $\tau_c^*$. The greater the positive difference between $\tau^*$ and $\tau c^*$ the more sediment is transported. In Equation 1, $q^*$ is the dimensionless sediment transport, $\alpha_t$ is the sediment transport coefficient, $n_t$ is sediment transport exponent, and $\varphi_s$ is the fraction of bed shear stress that is skin friction.

$$q^* = \begin{cases} \alpha_t(\varphi_s\tau^* - \tau_c^*)^{n_t}, & \tau^* > \tau_c^* \\ 0, & \tau^* \leq \tau_c^* \end{cases} \qquad (Eqn.1)$$

The input variables of the model were set to match the lower Trinity River. A 75% discharge value (intermittency = 0.25), 322.8 cubic meters per second, was used in the model based on discharge data from the Romayor gage. Equation 2 was used to calculated the particle Reynolds number ($Re_*$) of 44.7. Using this number and the Shield's diagram, $\tau_c^*$ was estimated to be 0.039. Within the model $\tau^*$ was calculated using Equation 3.

$$Re_* = \frac{U_* D_{50}}{v} = \frac{\sqrt{\frac{\tau_b}{\rho_w}} D_{50}}{v} = \frac{\sqrt{gHS} D_{50}}{v} = \frac{(0.0588)(0.00076)}{1\times10^{-6}} = 44.7 \qquad (Eqn.2)$$

$$\tau^* = \frac{HR}{SD_{50}} \qquad (Eqn.3)$$

In order to accurately apply the Meyer-Peter Muller equation to the sandy bed of the Trinity River required alteration. The value for $\alpha_t$ was changed from the constant of eight (*Meyer-Peter and Muller*, 1948) to twelve, a value that is representative of high rates of sand transport (*Wilson*, 1966*; Wiberg and Smith*, 1989). The fraction of bed shear stress that is skin friction, $\varphi_s$, was calculated using Equations 4, 5, 6, 7 and 10. The Gauckler-Manning coefficient, calculated in Equation 4 was used to calculate the Chezy coefficient in Equation 5. The Chezy coefficient was used to estimate the composite roughness height, $k_c$. The grain roughness, $k_s$, is calculated using an equation found by Van Rijn, 1984. Equation 8 shows the relationship between $k_c$ and $k_s$ to $\tau^*$ and $\tau_{sk}{}^*$ (*Wright and Parker*, 2004). The flow depth, *H*, was initially estimated to be 2 meters. Once $k_c$ was calculated the flow depth was recalculated using Equation 9 (*Parker*, 1990). In this equation the coefficient in Manning-Strickler resistance relation, $\alpha_r$, was set to 8.1 (*Parker*, 2004). The model using Equation 9 returned a flow depth of 3.55 meters. The value for $\varphi_s$ was assumed to be 1 and $n_t$ was set to 1.5 based on the original work of Meyer-Peter and Muller (1948; *Wiberg and Smith*, 1989; *Wilson*, 1960).

$$n = \frac{k}{U}\left(H^{2/3}\right)\left(S^{1/2}\right) = 0.0171\ \frac{s}{m^{1/3}} \qquad (Eqn.4)$$

$$C_z = \frac{1}{n}H^{\frac{1}{6}} = 72.26\frac{m^{1/2}}{s} \qquad (Eqn.5)$$

$$k_c = \frac{11H}{e^{kC_z}} = 0.00627m \qquad (Eqn.6)$$

$$k_s = 3D_{90} = 0.00717m \qquad (Eqn.7)$$

$$\frac{k_c}{k_s} = \left(\frac{\tau^*}{\tau^*_{sk}}\right)^4 \qquad (Eqn.8)$$

$$H = \left(\frac{Q^2\left(\frac{k_c}{1000}\right)^{1/3}}{\alpha_r^2 g S B^2}\right)^{3/10} = 3.35m \qquad (Eqn.\ 9)$$

The model ran for 60 years, representing a period sixteen years longer than the present impoundment by the dam. An elevation and sediment transport value were calculated for each spatial and temporal node. The model results reproduced the erosion of the lower Trinity River well, as can be seen in Figures 2.26 and 22.7. Figure 2.26 shows model results in twenty year intervals, starting with year zero or 1968. Year zero shows a slope nearly identical to that of the 1939 profile, excluding the backwater zone. The linear trend of both profiles represents a channel that is near or at geomorphic equilibrium. The channel shows no signs of aggradation or incision. After twenty years the model shows an incising river immediately downstream from the position of the dam. There is a small convex portion to the profile. By the fortieth year iteration of the model, the incision had increased and propagated further downstream. The incision continues to increase and propagate further downstream as is seen in the 60 year iteration of the model. The model results show the same shape as changes in the surveys from 1939 to 2007, but the incision is under predicted.

A sensitivity analysis of the model was done by systematically altering one model variable at a time. The results of this analysis are shown in Figure 2.28. This analysis shows that the model is most sensitive to choice of characteristic grain size, and is less sensitive to change in channel width or choice of appropriate discharge. The model

shown in Figures 2.26 and 2.27 used the $D_{50}$ grain size from bars around Romayor. This is likely an over estimate of the grain size. This $D_{50}$ value is only representative of the sample being deposited on the bar. The finest materials being mined from the bed are actually being transported downstream. Therefore, the $D_{50}$ of the bed is likely finer than what was used. This is likely an explanation for the under prediction of the model in Figure 2.26.

## DISCUSSION

Most existing models for sediment transport are based on assumptions of constant sediment exchange and storage rates (*Lauer and Parker*, 2008). This assumption does not hold true downstream of a dam influenced portion of a river. The upstream sediment retention due to dam created sediment transport disequilibrium that causes sediment on the bed to be mined downstream of the dam. The mining of sediment forces the channel adjustment and must be accounted for the when quantitatively describing the physical mechanics of river reaches downstream of a dam (*Graf*, 2006).

The convex shape of the Zone One profile is strong evidence of considerable channel incision. Like the model suggest, it is likely that the length of the scoured Zone One is increasing with time. As the slope of the bed becomes less efficient, the scour propagates forward downstream. The sediment deficiency tapers out 50,000 to 60,000

river meters from the dam the channel profile transitions to its initial constant slope (Fig. 2.26).

A similar trend of downstream propagation can be seen in the predicted spatial change in the sediment transport by the model (Fig. 2.27). The model shows that sediment transport starts at zero and continues to increase until it reaches a constant 0.00012 cubic meters per second. The longer the model runs a greater downstream distance is required to obtain sediment transport capacity. The distance associated with the river reaching 90% of the sediment transport capacity is nearly the same as the re-equilibration point on the 2007 channel profile, approximately 50,000 river meters from the dam.

The model results between 40 and 60 years to show a relatively similar profile to that measured in 2007 (Fig. 2.26). The length of the scour, or length of dam influence agrees with the observational data, but the depth of the scour depicted in the model is less than what has occurred since the impoundment of the dam. A major cause for these differences is due to the empirical values used in the model. Figure 2.28 shows the model is most sensitive to a change in grain size. The model was run with the $D_{50}$ taken from the bar samples, not the substrate of the bed. The bedrock is roughly 50% mud and 50% material that would contribute to the bed-material load of the river. If roughly 50% of the eroded sediment is fine enough to travel down the river fully suspended or as washload. The finest grains are transported downstream, leaving behind the very largest grains to compose the bars. As a result, the grain size being used to run the model is likely an over prediction of the median grain size of the substrate. Use of a lower critical

shear stress (Eqn. 1) would produce is consistent with a finer overall grain size for the substrate and would lead to a greater amount of incision than we predict using only bar material. Our findings match previous work by Phillips et al. (2005) that suggested that the dam's influence extends 60 river kilometers downstream of the dam. As the channel profile transitions from dam influenced to non-dam-influenced around 50 river kilometers there is also a transition in the cross sectional geometry of the channel. Zone One is characterized by steeper channel walls with higher relief (Fig. 2.8 and 9). These decrease as the river transitions into Zone Two and the dam influenced incision decreases. In Zone One the channel cuts down into the bed the floodplain above the channel has become higher than the flood water surface elevation (Fig. 2.7). The floodplain is no longer impacted by the high flows of the lower Trinity. The Zone Two floodplain still interacts with high flows.

The bankfull width of the channel is also less in Zone One (Fig. 2.10a). This is correlated with a reduction of bar size (Fig. 2.12 and 13). As the water flows from the dam and regains its transport capacity, it is scouring sediment from the bed of channel. The below sediment transport capacity flow in Zone One corresponds with smaller bar sizes. The net downstream motion of sediment alters the meander migration mechanics (Fig. 2.10b). The small bars do not topographically steer the water toward the cutbank, like the larger bars of Zone Two. This allows the river to straighten.

## CONCLUSIONS

Much of the existing work on channels responding to dams has focused on gravel rivers. In these studies, bed armoring limits channel bed incision and sediment flux to the coast (*Skvyitski,* 2005). The sandy nature of the lower Trinity River alters its downstream response to Livingston Dam. Unlike gravel rivers, the lower Trinity is continuing to adjust to the dam's influence several decades after impoundment, and will continue to adjust for decades into the future. The abundant source of sandy sediment hinders the development of bed armoring that is commonly seen to develop in response to dams (*Jain and Park*, 1989). Through time, the length of the zone of influence will continue to increase to optimize the recovery of the river's sediment transport capacity, not altering the volume of sediment being delivered to the coast.

The impoundment of Livingston Dam has resulted in downstream scour due to sediment retention in the reservoir. Responding to the upstream removal of bed-material load, the channel has incised approximately five to seven meters. The means and methods by which the channel has adjusted can be accurately reproduced using an adjusted version of Parker's (2004) one-dimensional river morphodynamics model. The model predicts bed elevation adjustments that are a close match to the observed evolution of the lower Trinity River. The removal of bed-material load by the dam has transformed the linear channel profile into a convex profile. Currently, the dam's influence extends approximately 50 river kilometer downstream of Livingston Dam.

The sediment depletion in Zone One can be seen not only in the channel profile, but also in the development of pronounced channel walls, sediment starved point bars and a narrower channel width. The alterations to the geometry of the channel result in an alteration to the channel morphology in Zone One. The small point bars are unable to topographically steer the flow towards the cutbank, as in Zone Two. As a result migration in Zone One is lower and the river has straightened.

.

**NOTATION**

$C_z$ = Chezy coefficient

$D_{50}$ = Mean grain size

$D_{90}$ =grain size in the 90%

$g$ = gravity (9.81 $m^2/s$)

$H$ = depth

$k$ = von Karman Constant (0.41)

$k_c$ = composite roughness height

$k_s$ = grain roughness

$n$ = Gauckler-Manning coefficient

$n_t$ = exponent of the sediment transport relation

$q^*$ = dimensionless sediment transport

$R$ = submerged specific gravity of sediment

$Re_*$ = boundary Reynolds number

$S$ = slope

$U$ = average velocity

$U_*$ = shear velocity

$\alpha_t$ = sediment transport relation

$\rho_w$ = density of water (1000 $kg/m^3$)

$\tau^*$ = dimensionless shear stress

$\tau_c^*$ = dimensionless critical shear stress

$\tau_{sk}^*$ = Shields stress due to skin friction

$\upsilon$ = kinematic viscosity

$\varphi_s$ = fraction of bed shear stress that is skin friction

**FIGURES**

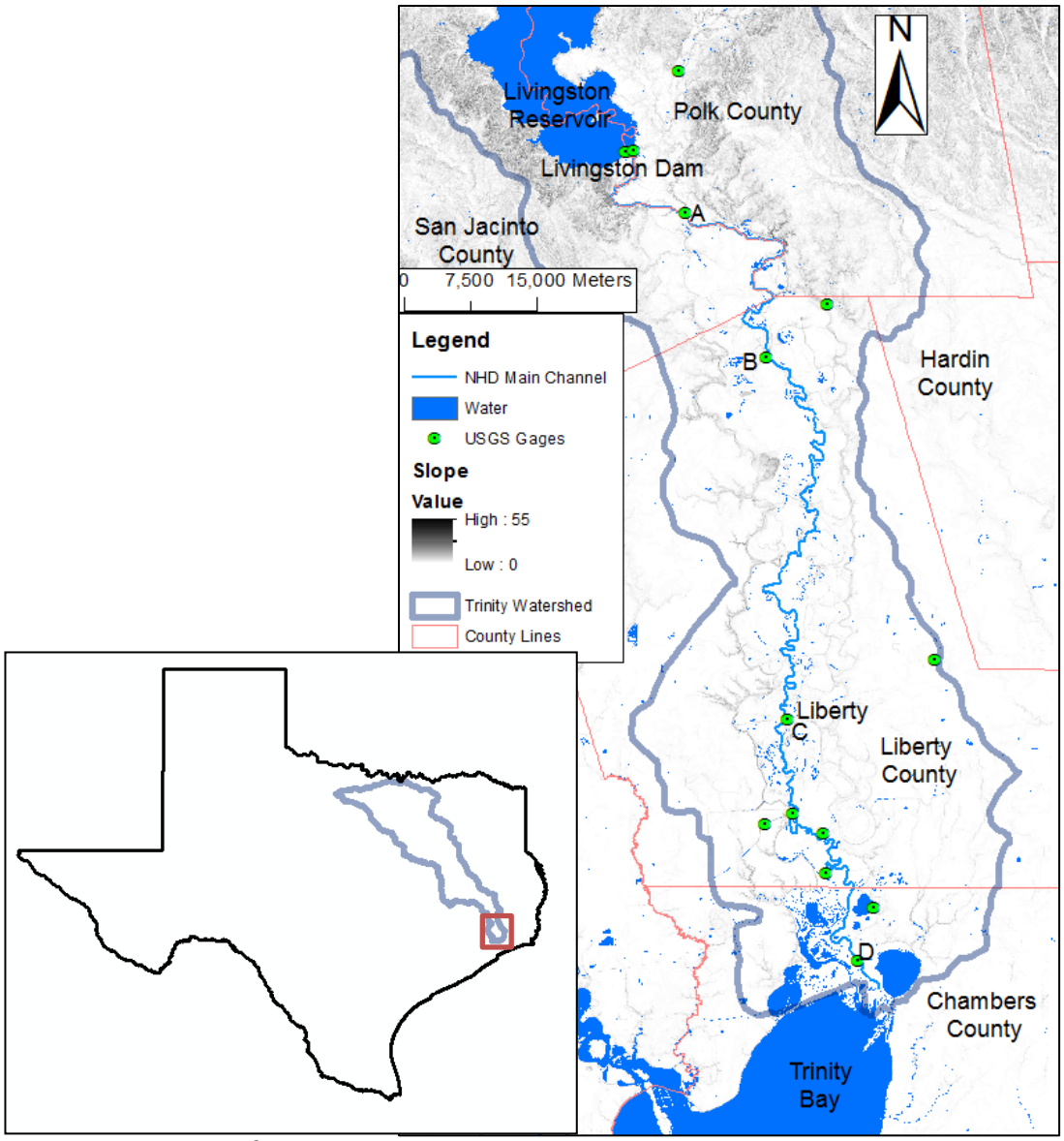


Figure 2.1: Map of the lower Trinity study. The Trinity watershed within the state of Texas is outlined in blue, running across the eastern portion of the state. The red box marks the section of the watershed that is the study area. The study area is bounded by Livingston Dam to the north and Trinity Bay to the south. On this map the counties are outlined in red. The town of Liberty, TX is labeled near gage C. The green circles mark USGS gages at Goodrich, TX (A; USGS number 08066250), Romayor, TX (B; USGS number 08066500), Liberty, TX (C; USGS number 08067000), and Wallisville, TX gage (D; USGS number 08067252).

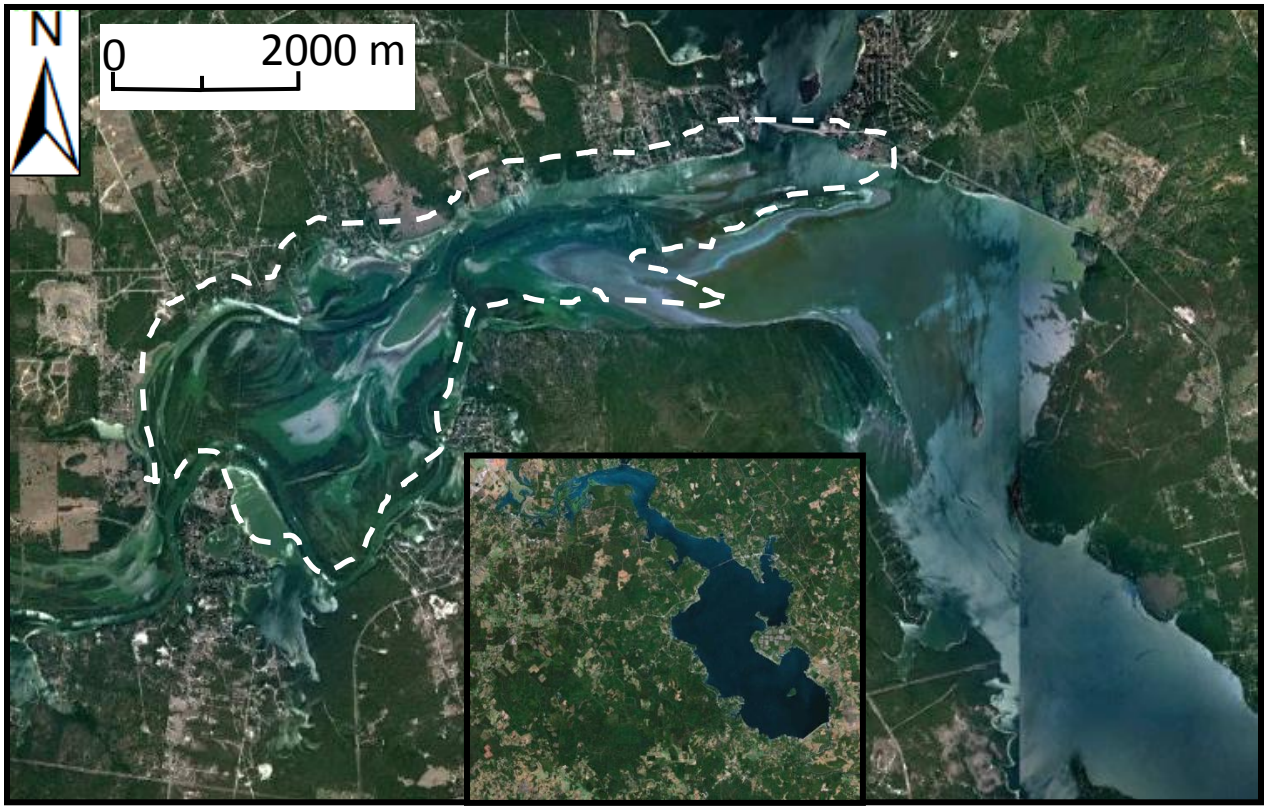

Figure 2.2: The growing delta at the upstream end of Lake Livingston (Fig. 2.1). Stress on sediment decreases as the water flows into the Reservoir. The sub-aerial portion of the delta built from river-deposited sediment is marked by the dashed line.

Figure 2.3: Bridge failure on the Trinity River near Goodrich, TX in 2004. The red dash line is the infered elevation of the river botton at the time of bridge construction. The bridge is located approximately 16,000 meters downstream of Livingston Dam.

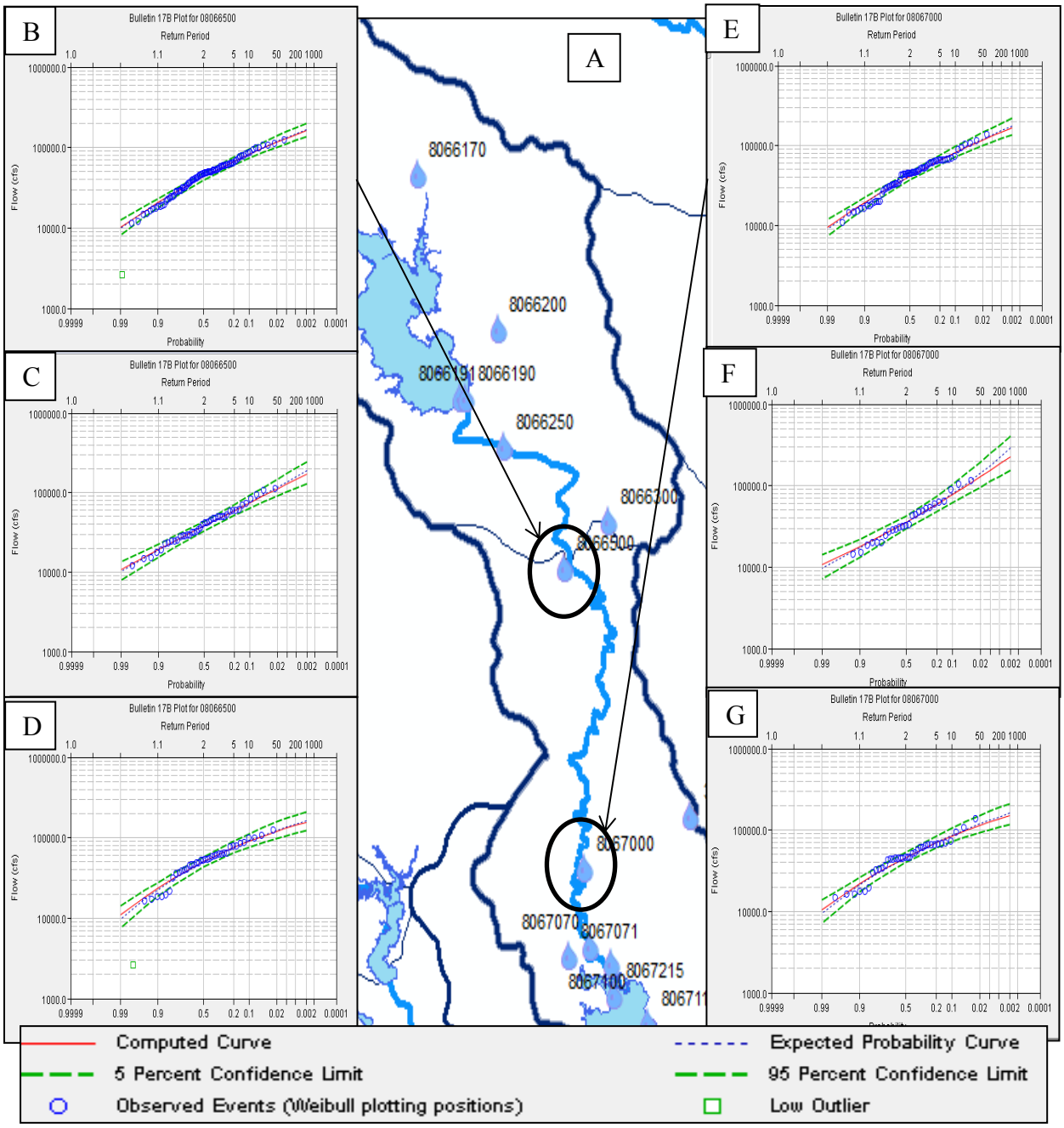


Figure 2.4: (A) shows the locations of two USGS river gages at Romayor and Liberty, TX. The upper gage is Romayor, TX and the lower gage is Liberty, TX, associated with the 17B Bulletins shown in images B-D. Images E-G show the outputs from the 17B Bulletin for Liberty, TX, the lower gage. The two top graphs, B and E, show the flow distribution prior to the dam impoundment. Graphs C and F show the flow distribution after the dam impoundment. The lowest graphs, D and G, show the distribution of flow for the entire record of flow.

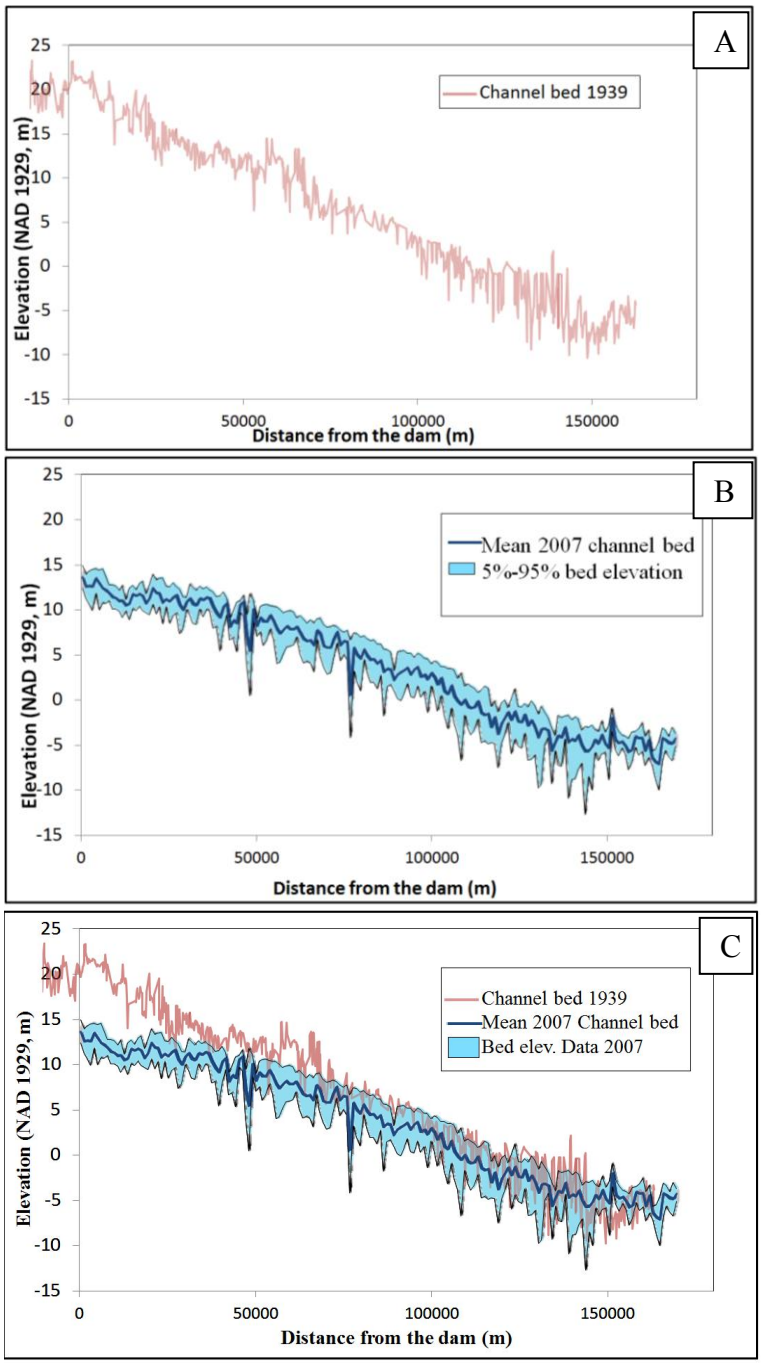


Figure 2.5: (A) Measured river channel profile in 1939. This data was collected by the U.S. Army Corps of Engineers. (B) Measured river channel profile in 2007. This data was collected by the Texas Parks and Wildlife Department. (C) super-imposed channel profiles shows the two profiles together. There has been six to seven meters of incision since dam impoundment. The channel re-establishes a linear profile similar to 1939 form at 50,000-60,000 meters downstream of the dam.

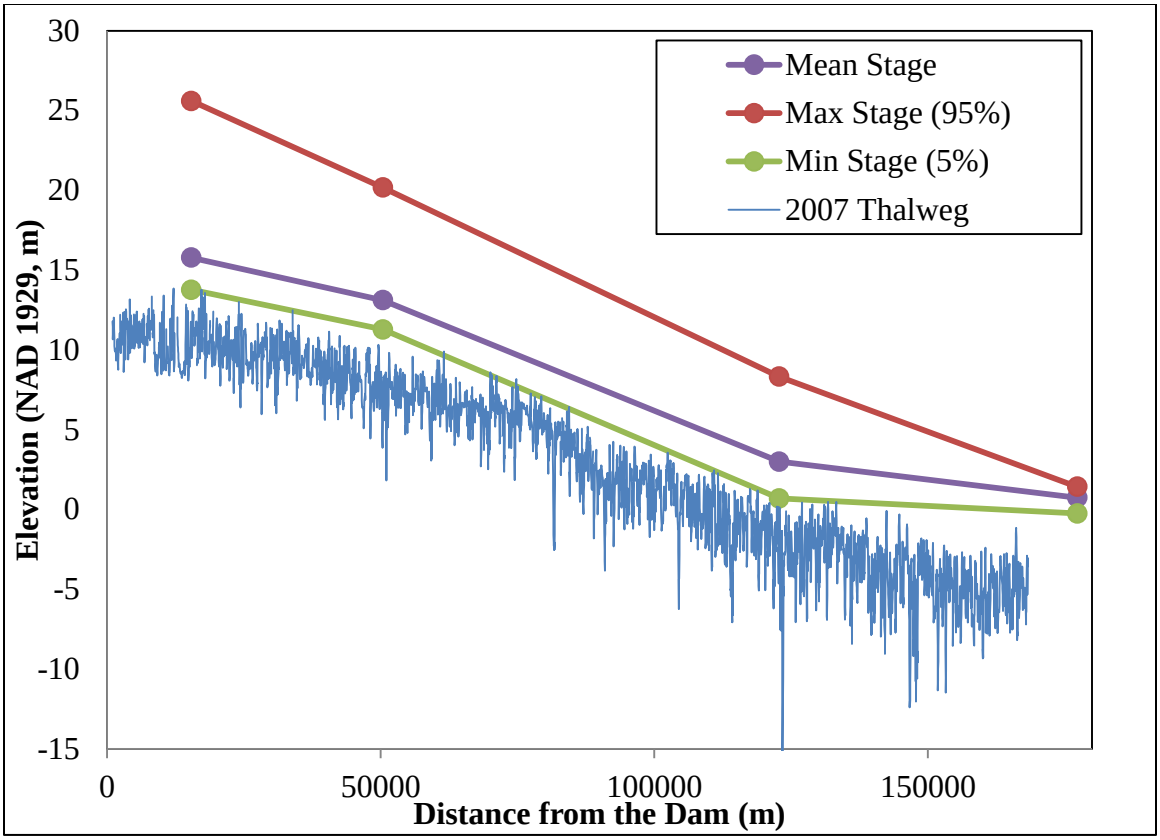


Figure 2.6: The three water surface profiles were created from the USGS gages stations along the lower Trinity River, and the 2007 channel bottom profile. The water surface profiles are based on 20 years of USGS stage gage data from four USGS river gages. The mean value represents the mean stage value for 20 years. The minium is the 5% probability stage (28 cubic meters per second at Goodrich, TX), the mean stage is the 50% probability (162 cubic meters per second at Goodrich, TX) and the maximum is the 95% probability stage (2381 cubic meters per second at Goodrich, TX). The stage values are from USGS gages at Goodrich (USGS gage number 08066250), Romayor (USGS gage number 08066500), Liberty (USGS gage number 08067000) and Wallisville (USGSgage number 08067252). Several of the extreme thalweg values represent bridges; such as, Romayor, TX near river meter 50,000, Farm Rd. 787 at river meter 80,000, a rail bridge at river meter 110,000, and Liberty, TX near river meter 120,000.

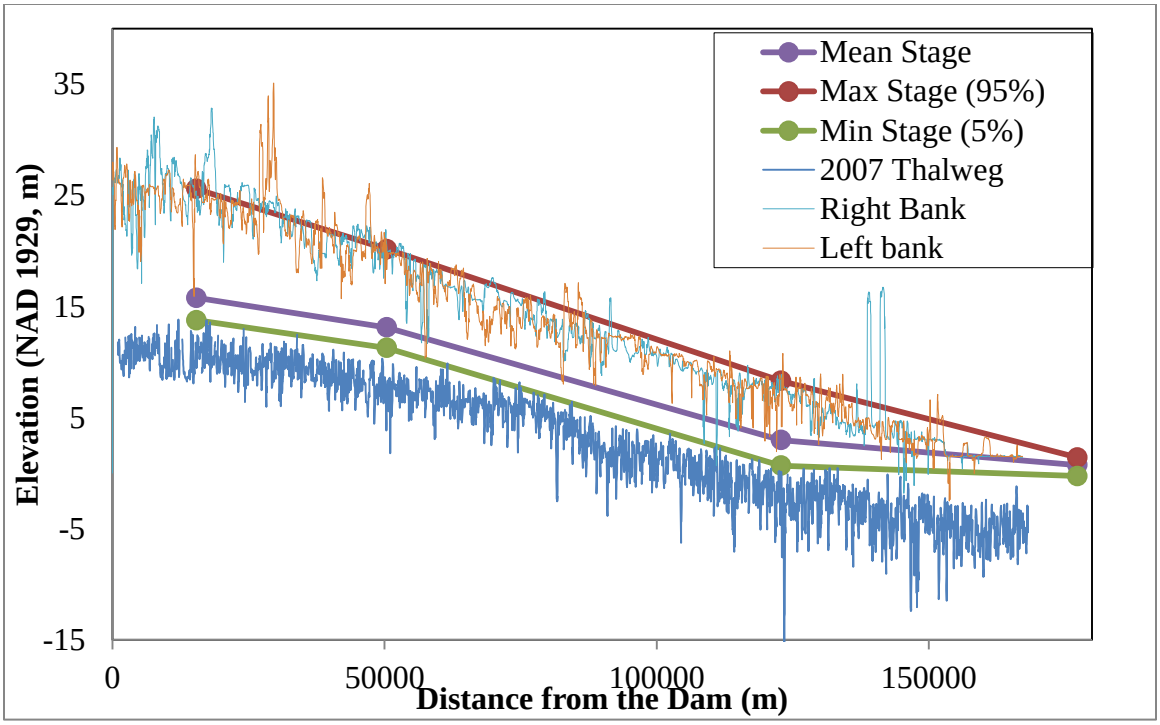


Figure 2.7: Long profile for the study reach of the Trinity River, TX, that includes elevations for the right and left river bank. These elevations for the vegetated alluvial surface were taken from the DEM built from the 1984 USGS 1:24,000 topographic quadrangles.The water surface profiles are based on 20 years of USGS stage gage data from four USGS river gages at Goodrich (USGS gage number 08066250), Romayor (USGS gage number 08066500), Liberty (USGS gage number 08067000) and Wallisville (USGS gage number 08067252).. The mean values is 184 cubic meters per second at Romayor. The minium is the 5% probability stage (22 cubic meters per second at Romayor) and the maximum is the 95% probability stage (2690 cubic meters per second at Romayor). Notice the maximum discharge inundates the river banks between 50,000-180,000 river meters. Only a small function of the bankline is inundated between 0-50,000 river meters.

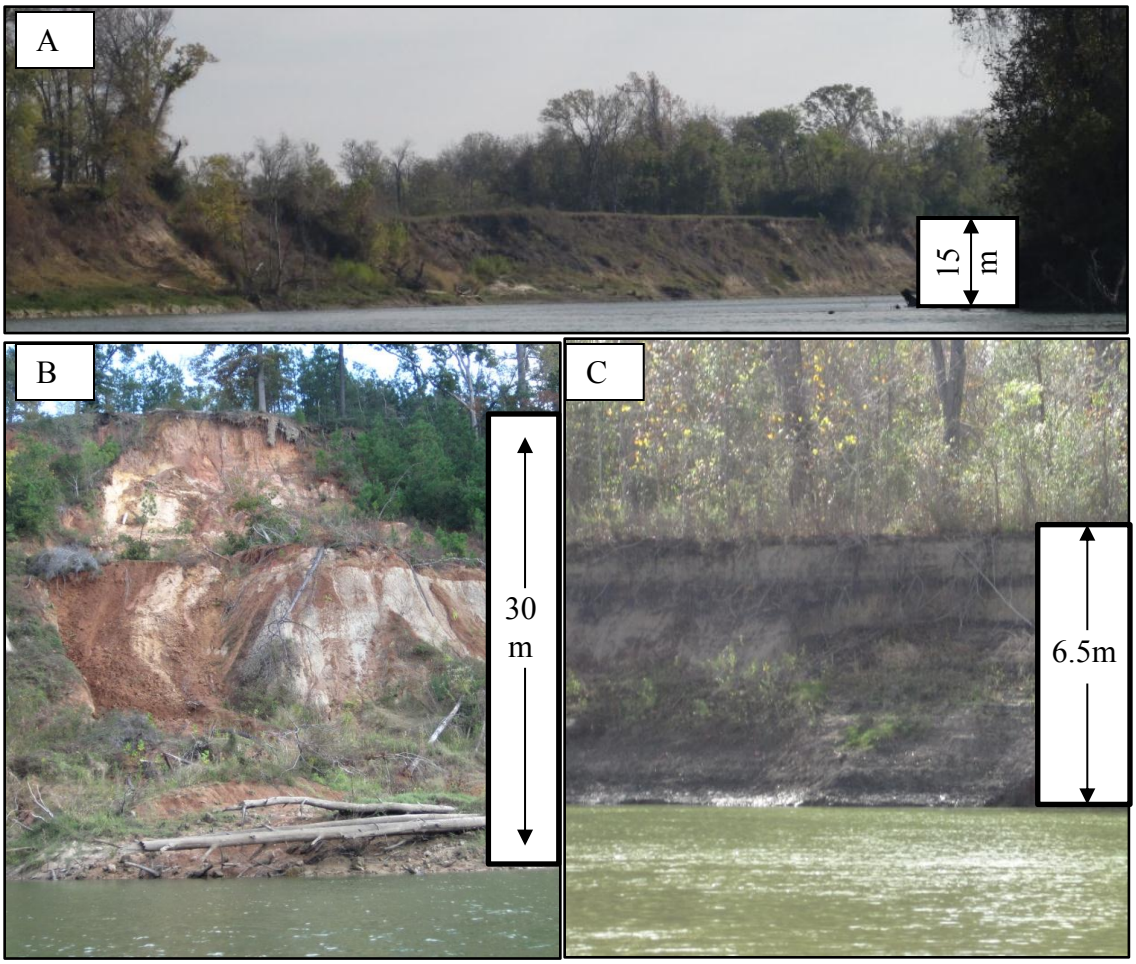

Figure 2.8: Photos of representative cut banks in the Zone One and Zone Two of the lower Trinity River. (A) and (B) show the steep high banks of Zone One. Image A is at river kilometer 23 and image B is at river kilometer 30. (C) Cut bank in Zone Two, at river kilometer 117. The cut banks in (A) and (C) are composed of Quaternary strata. The river banks in (B) expose Miocene deposits.

| Survey Dates | |
|---|---|
| Posted Date | Observed Dates |
| 1952 | 10/18/1952<br>11/12/1952 |
| 1972 | 11/4/1968<br>1/14/1972 |
| 1996 | 9/13/1995<br>1/19/1995 |
| 2009 | 1/23/2008<br>2/1/2008 |

Table 2.1: aerial photographs collected by the Texas Natural Resource Information System (TNRIS) for the Trinity River over approximately 60 years were used for this study. The surveys were finalized in 1952, 1972, 1996 and 2009. However, the survey date was slightly earlier in some cases.

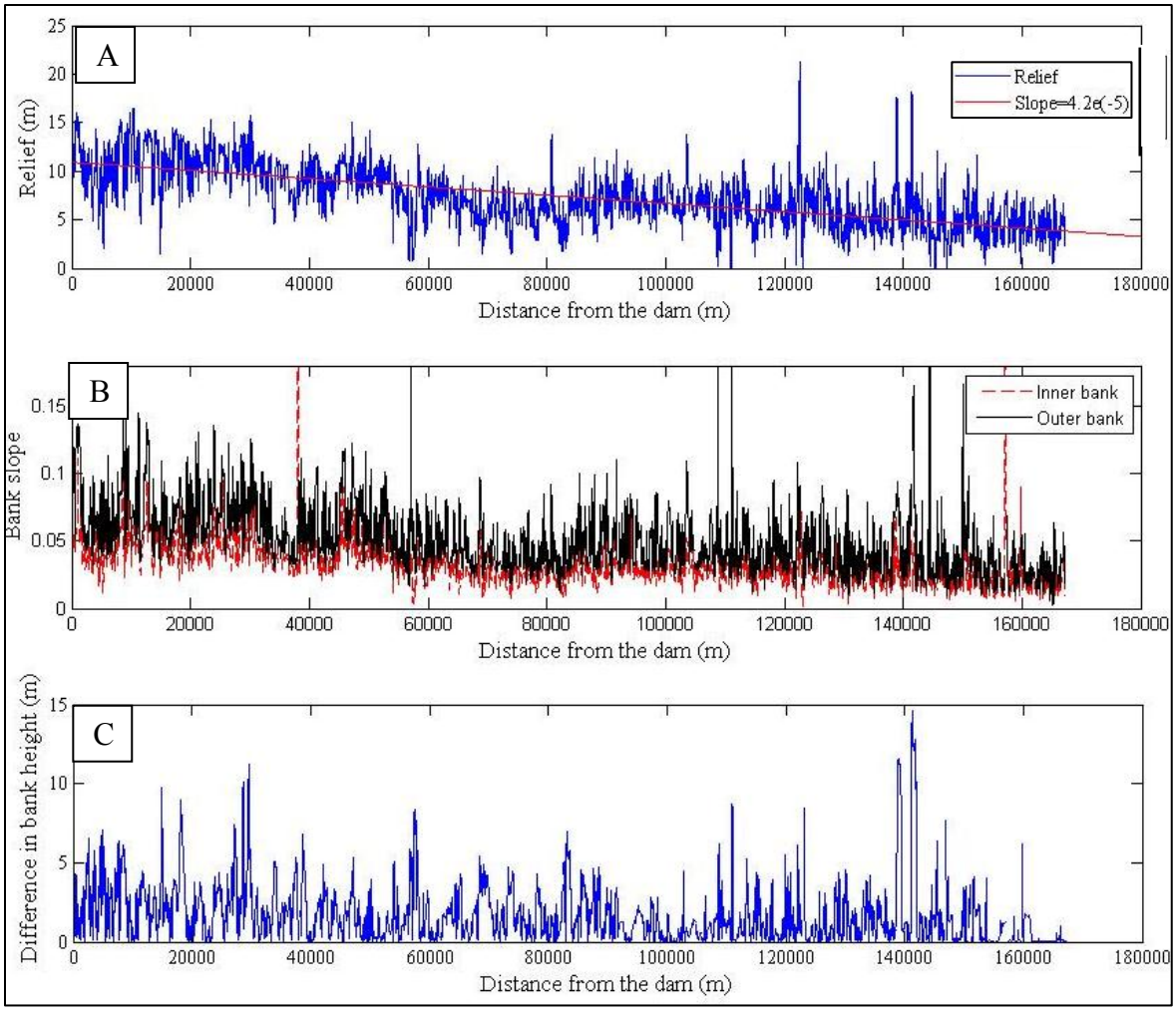


Figure 2.9: (A) Channel relief measured from the 2007 bathymetry data collected by the TPWD and the 1984 USGS DEM. The bathymetry data was converted to a digital elevation model (DEM), which was overlain by a series of transects perpendicular to centerline of the river starting at the left bank flood plain and crossing to the right bank flood plain. 5001 transects were spread over 180,000 river meters. The transects were joined to the elevation data of the DEM, and the relief was calculated for each transect. (B) Sidewall slopes banks for each transect measured from the channel thalweg to the floodplain surface. Several of the extreme values represent bridges; such as, Romayor, TX near river kilometer 50,Farm Rd. 787 at river kilometer 80, a rail bridge at 110, and Liberty, TX near river kilometer 120. The values in the first 5,000 river meters appear to be outliers that are potentially associated with construction due to dam maintenance. (C) The difference in the height of the inner and outer banks.

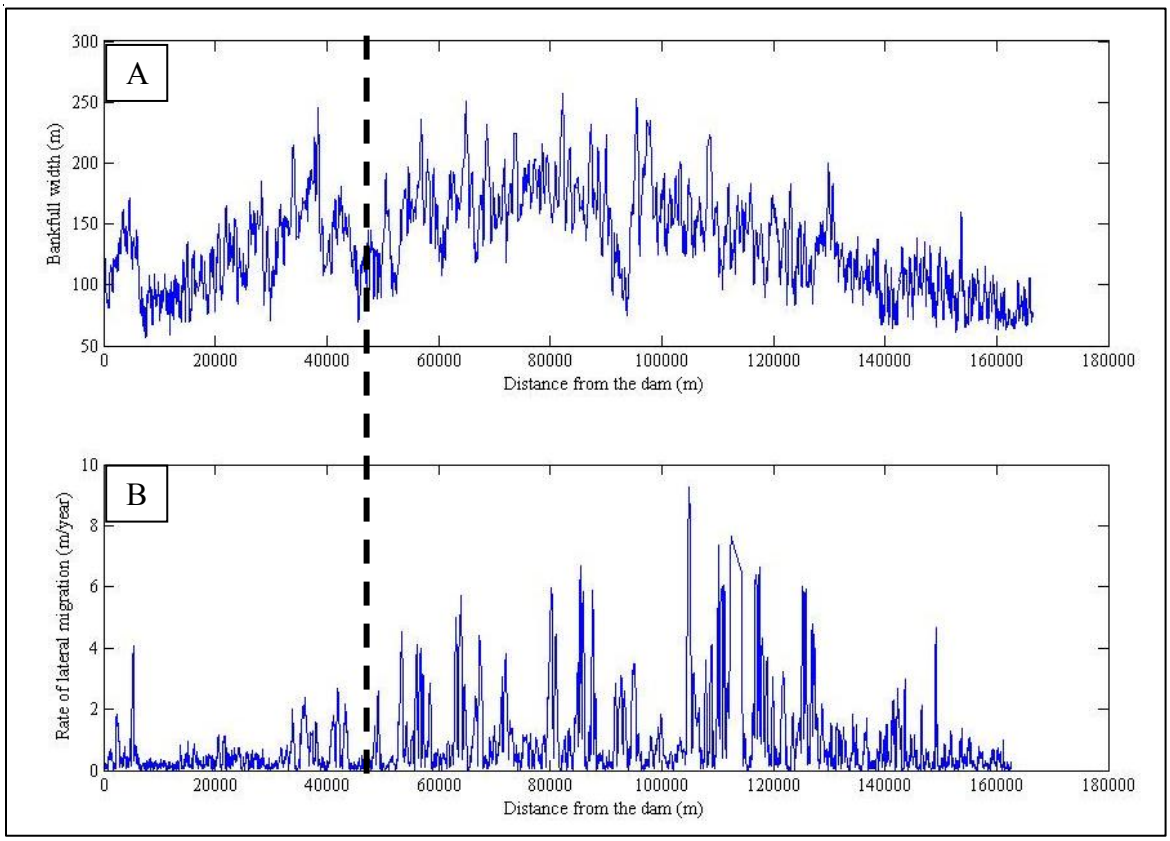


Figure 2.10: (A) Mean outer bank or bankfull width with distance from the dam. These measurements were taken from 2009 aerial photographic survey of the rvier. Channel width was measured between vegetation lines on each channel bank. (B) Lateral channel migration rate from Livingston Dam to Trinity Bay for years 1996 to 2009. The black dashed line shows the approximate location of the transition between Zone One and Zone Two. Several of the extreme values are represent bridges; such as, Romayor, TX near river kilometer 50,Farm Rd. 787 at river kilometer 80, a rail bridge at 110, and Liberty, TX near river kilometer 120. The bar values in the first 5,000 river meters appear to be outliers, that are potentially associated with construction due to dam maintenance.

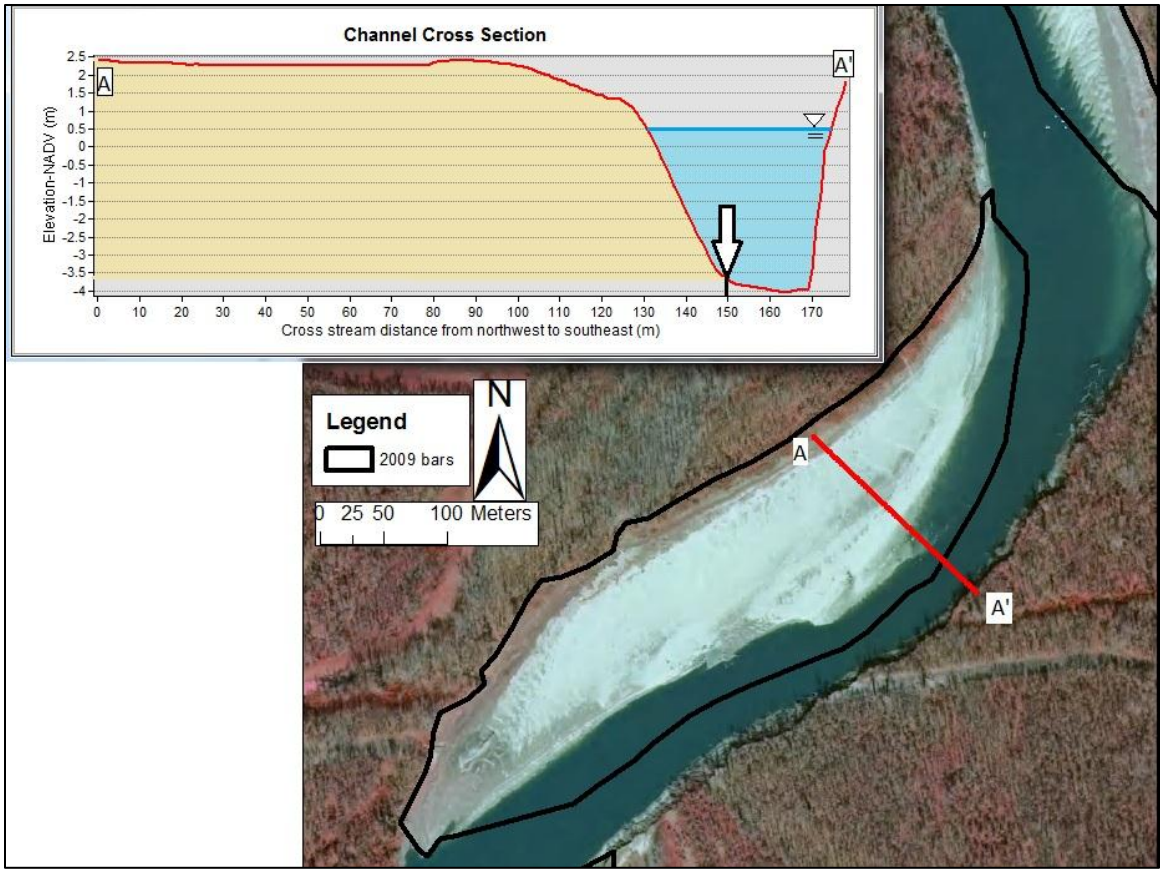


Figure 2.11: A bank-attached bar defined using a combination of the 2009 aerial photographs and the 2007 bathymetric survey. The extent of the bar is marked by the thick black line. The transect in red corresponds to the channel cross section graph. The bar area, in yellow, extends into the channel until there is a slope break, marked by the arrow. The blue line defines the water surface shown in the aerial photograph

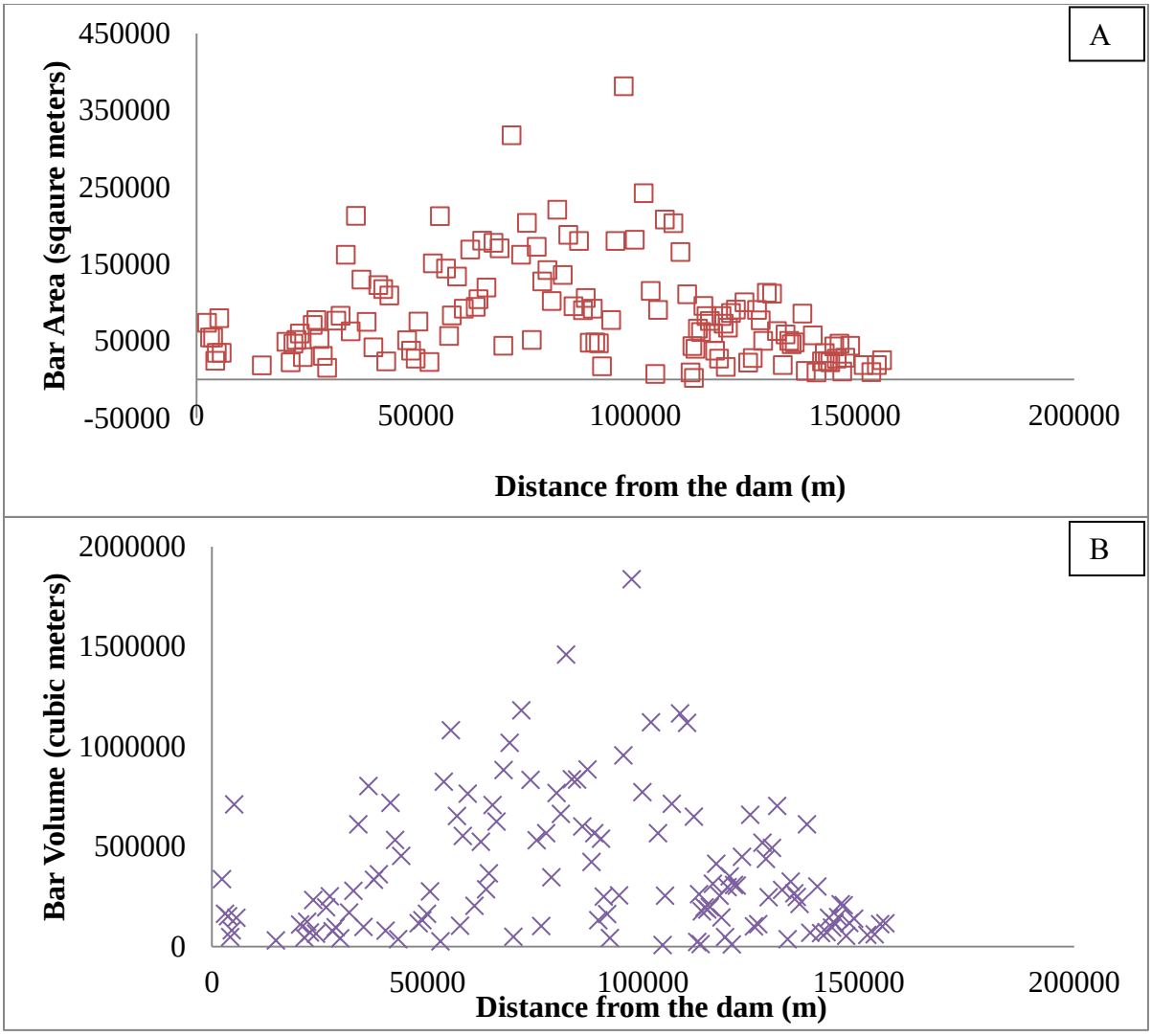


Figure 2.12: (A) Area of each bank-attached bar on the lower Trinity River. Area was measured using both the 2009 aerial photographs and 2007 bathymetric DEM to insure both the exposed and subaqueous portions of the bars are included. (B) Volume of each bar calculated using the 2007 bathymetery data. The area and volume of bars increases from Zone One to Zone Two and then decreases from Zone Two to Zone Three. The bar values in the first 5,000 river meters appear to be outlier, that are potentially associated with construction due to dam maintenance.

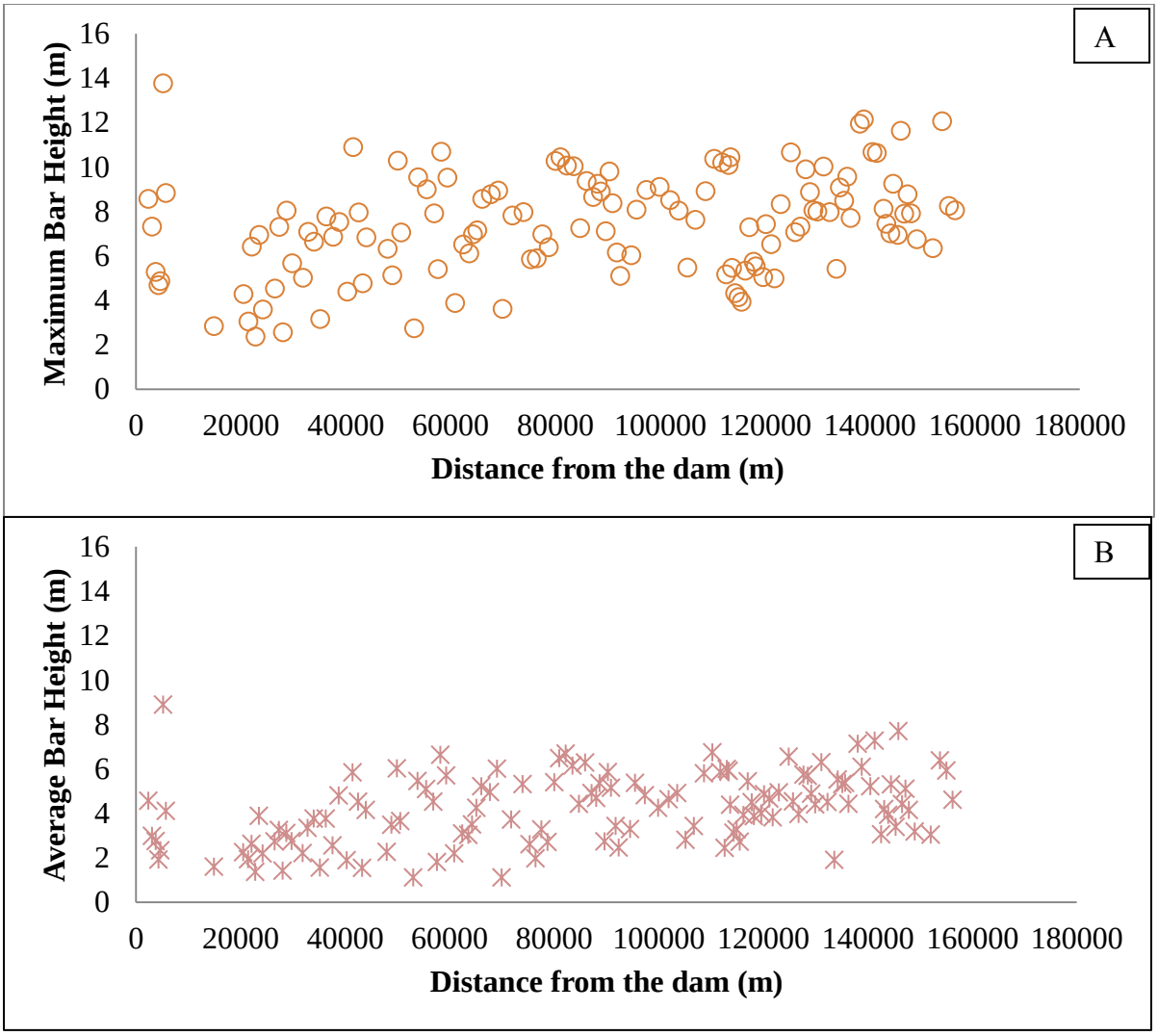


Figure 2.13: (A) Maximum of height of each point bar in the study area. Maximum bar height is equal to the difference between the highest and lowest elevations on each bar taken from the 2007 bathymetric survey. (B) Average height of each bar calculated as the mean value for all measures of elevation difference on the mapped bar surface. These data are also from the 2007 bathymetric survey. The height of bars increase systemically with distance from the dam and toward the coast. The bar values in the first 5,000 river meters appear to be outlier, that are potentially associated with construction due to dam maintenance.

Figure 2.14: (A) Bar from Zone One, approximately 20,000 river meters from Livingston Dam. (B) Bar from Zone Two, approximate 117,000 river meters from Livingston Dam. The bar in (A) is flat and topped with gravel, as is typical in Zone One. The bar in (B) has a much more pronounced in topography.

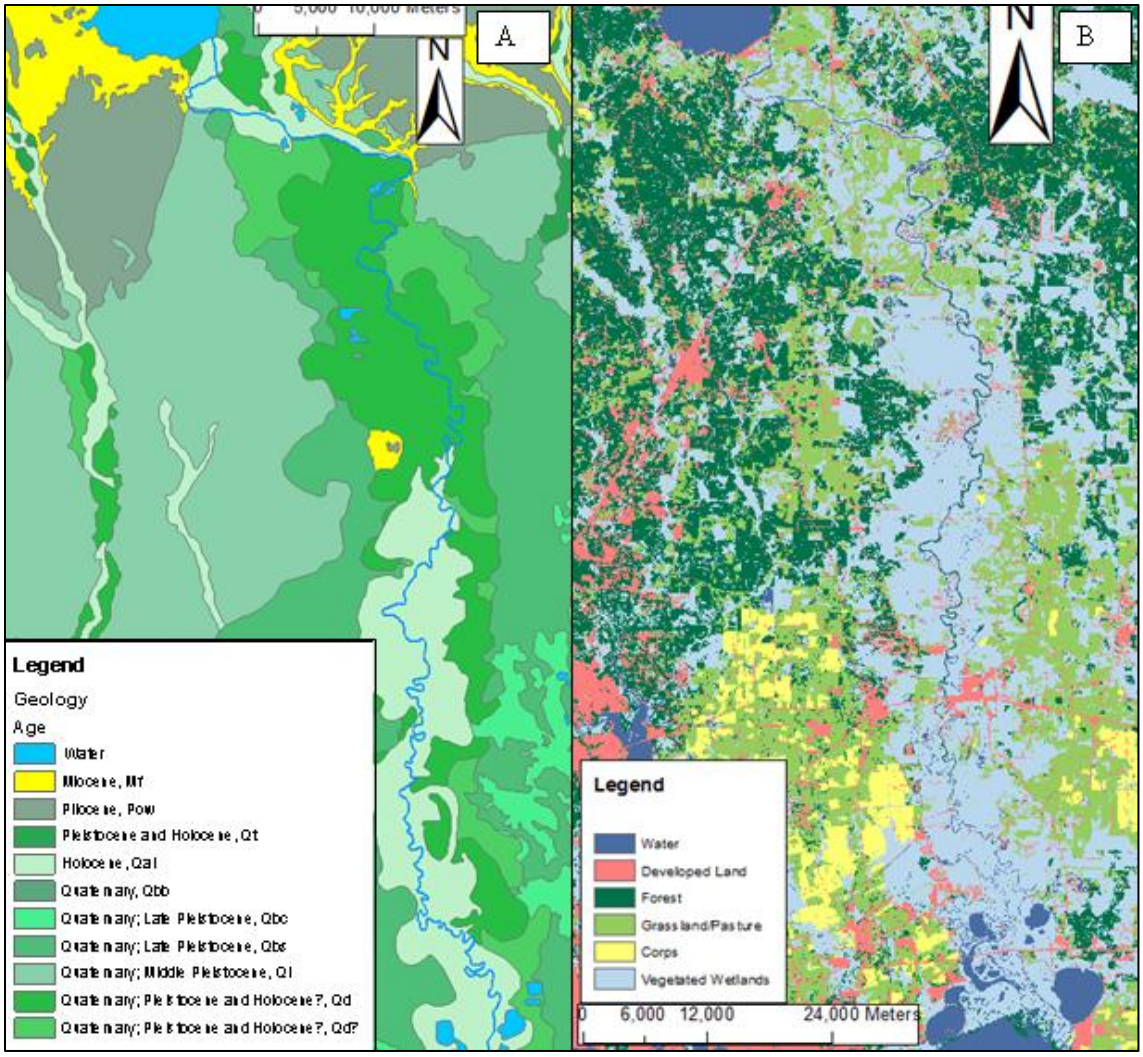


Figure 2.15: (A) Geologic map of the study area. Nearly the entire region is composed of Quaternary deposits shown in green. The blue marks major water bodies for spatial reference. The northern portion of the map has some deposits that are Pliocene and Miocene in age. (B) Map of land cover for the study area. Area adjacent to the channel is comprised primarily of forests, wetlands and pastures.

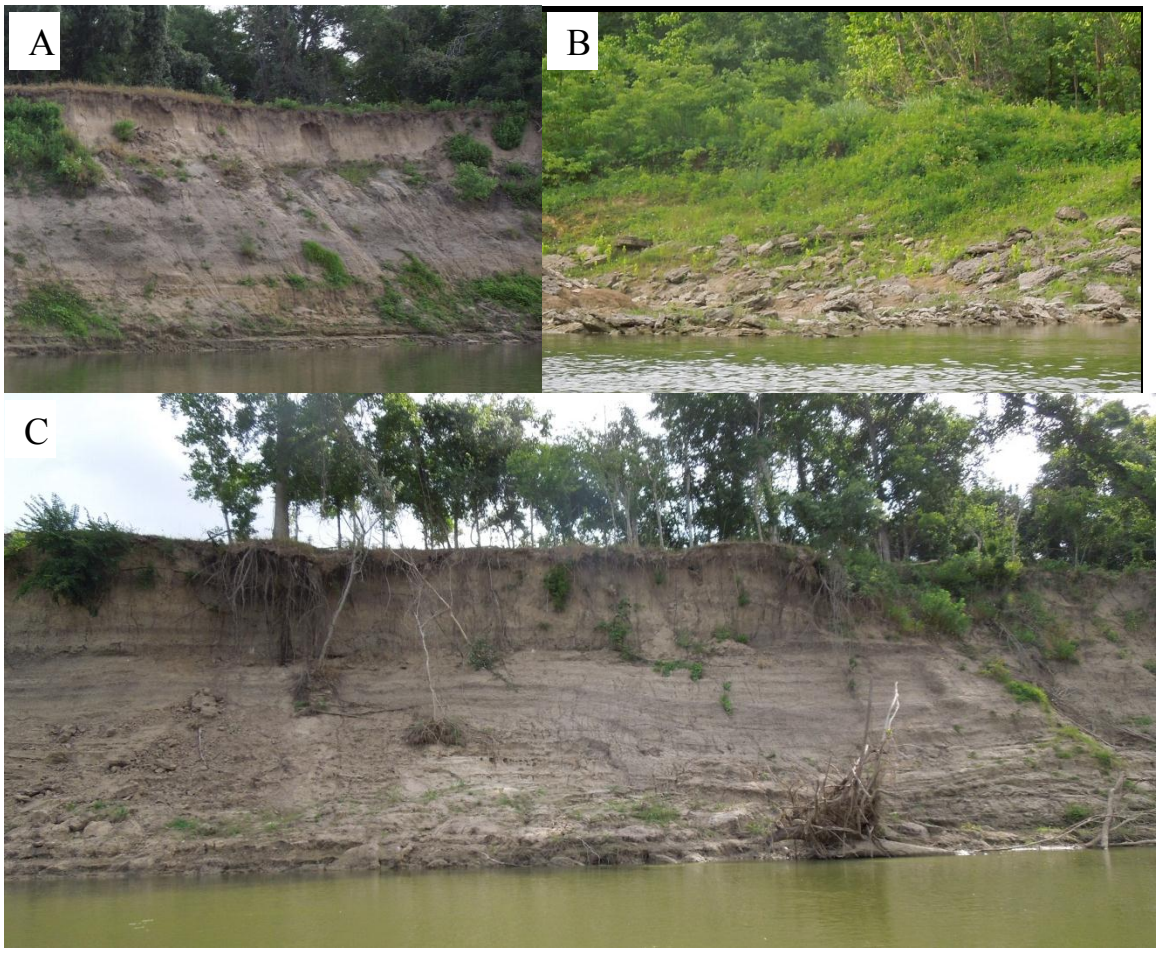

Figure 2.16: Examples of geologic substrate exposed in the channel banks between Goodrich to Romayor, TX, Zone One into the Zone One—Zone Two transition. (A) and (C) very weakly cemented to uncemented Quaternary fluvial deposits. (B) Weakly to very weakly cemented sandstone beds in Miocene fluvial deposits.

Figure 2.17: Weakly cemented conglomerate with a hand and arm for scale. The red box in the lower left corner of (A) corresponds with the box in (B). The conglomerate acts as a source for gravel in the river as it appears to rapidly disintegrate into its constituent grains when eroded from the channel banks and bed. This outcrop of the conglomerate is located about 55,000 meters downstream of Livingston Dam.

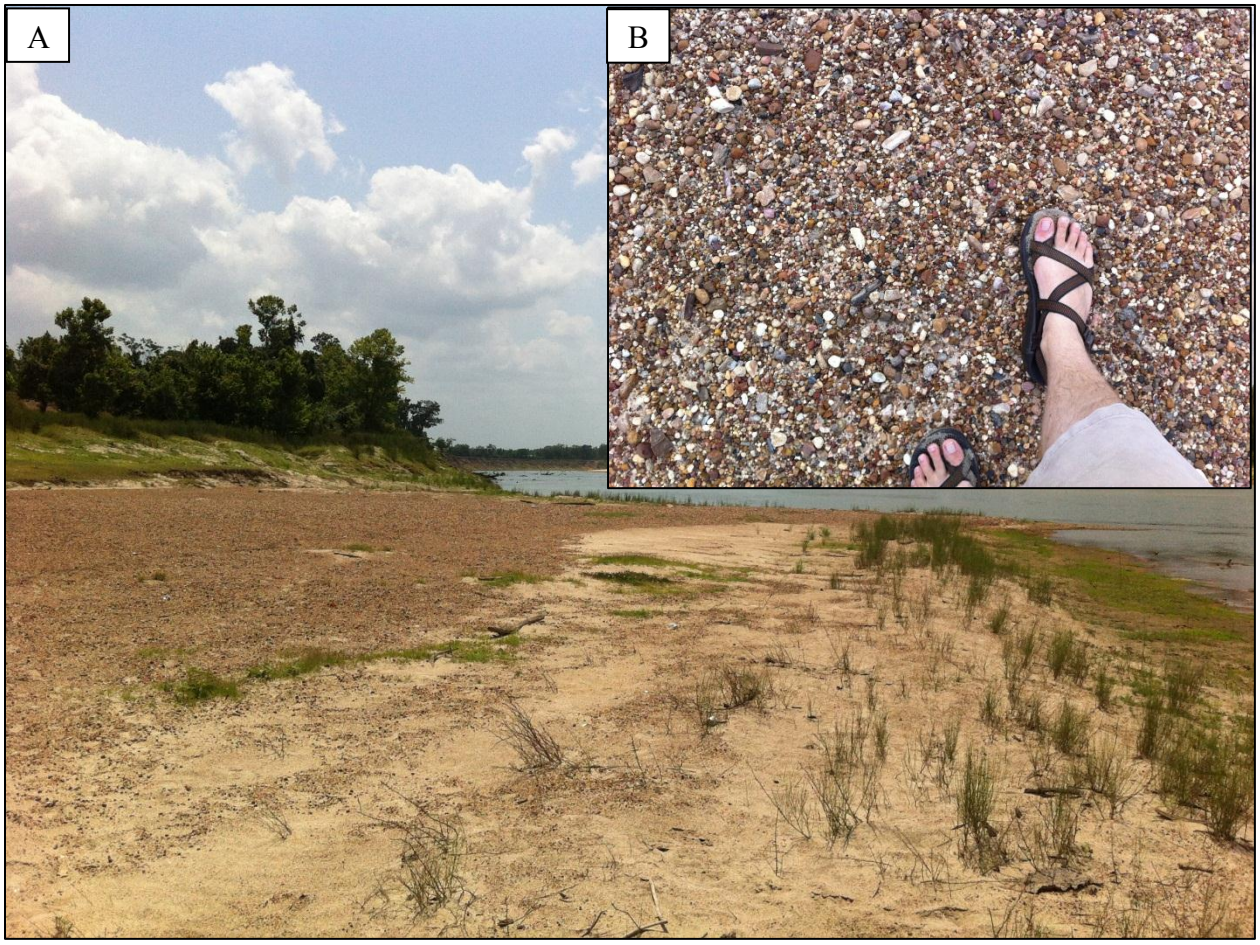


Figure 2.18: Bar-top gravel lags, such as this one, occur throughout the study area, but are far more common in Zone One. (A) shows the upstream end of a bar in Zone One located approximately 21,500 meters from Livingston Dam. The gravel on top of the bar contained an abundance of chert and sedimentary rock clasts, as well as petrified wood and bone. (B) is a close-up view of the gravel lag.

Figure 19: Examples of petrified wood found on Bar Three in Zone One (Fig. 2.14a). The wood is most likely excavated from the Miocene. Samples such as these were only found in upper Zone One.

Figure 2.20: Pieces of petrified bone were found on Bar Three in Zone One (Fig. 2.14). The bone is most likely from a mastodon or woolly mammoth (Dr. Julia Clarke and Dr. Ernie Lundelius, personal communication). Samples such as these were only found in Zone One.

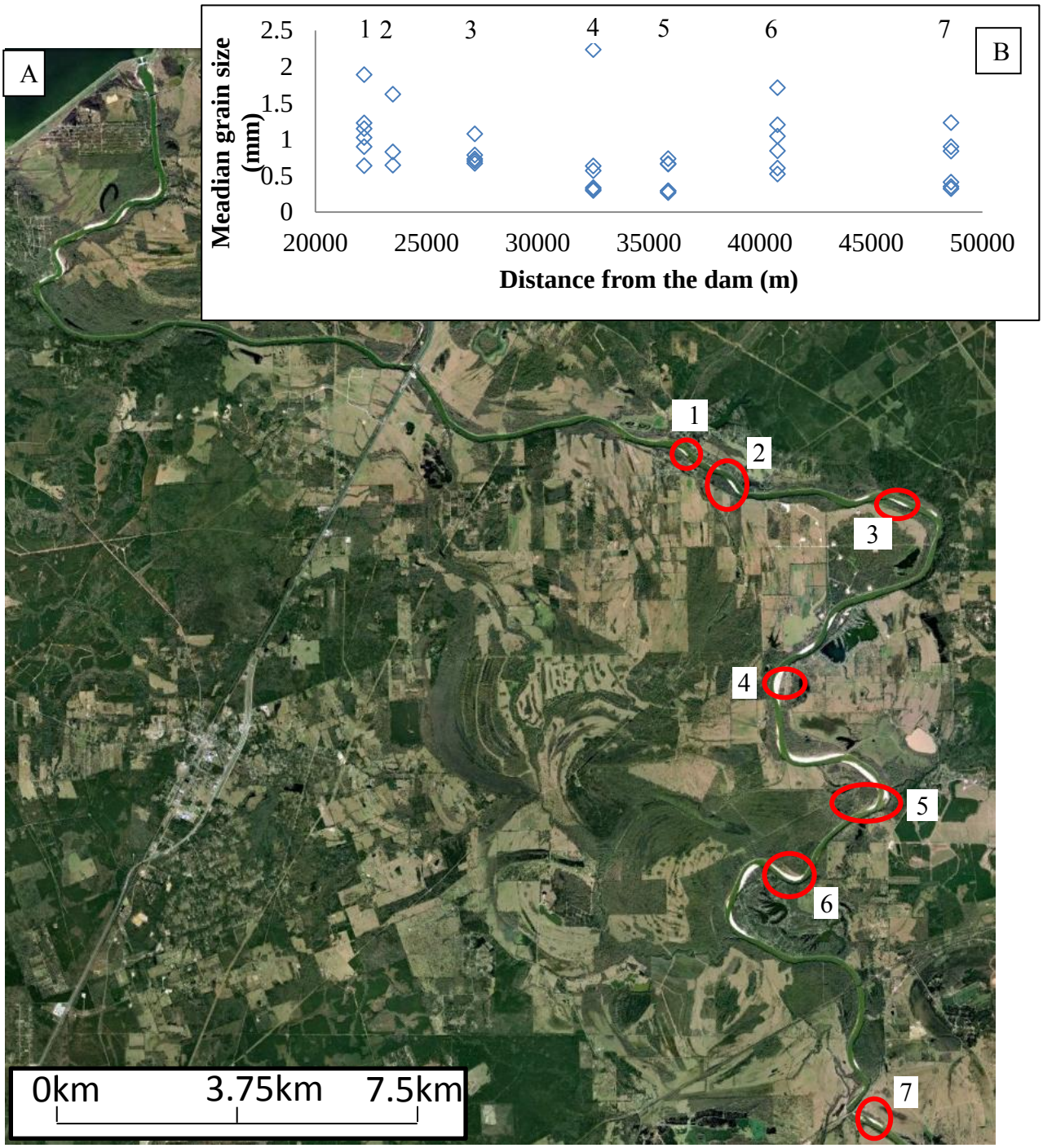


Figure 2.21: (A) Aerial photograph of Zone One and beginning of Zone Two on the lower Trinity River, TX. Livingston Dam can be seen in the upper left-hand corner of the photograph. The red ellipses mark seven bars where sediment samples were collected for size analysis. Six samples of were collected from each bar. The median grain diameter measured for each sample is shown in (B). The transition between Zone One and Zone Two occurs between 50,000 to 60,000 meters downstream of Livingston Dam.

| Sediment Sources in Zone 1 | | |
|---|---|---|
| | **$m^3$/year** | **Volume contribution (%)** |
| Channel Banks | 21116 | 4.6 |
| Tributaries | 12395 | 2.7 |
| Channel Bed | 427910 | 92.7 |
| **Total** | **461421** | |

Table 2.2: Sources of sediment load in Zone One of the lower Trinity River, TX. Contribution from channel banks occurs because volume eroded from cut bank is greater than volume deposited at inner banks. The net sediment contribution is calculated following the method described in Lauer and Parker (2007). The sediment contribution from the small number of entering tributaries has been estimated by Slattery and Phillips (2007). The volume eroded from the channel bed is calculated using the method Parker (2004).

Figure 2.22: Deposits of an internal delta developing at a tributary junction located 29,500 meters downstream of Livingston Dam. This delta provides clear evidence of tributaries delivering bed-material load to the lower Trinity River. Sediment samples from the delta had a $D_{50}$ of 260 micrometers.

Figure 2.23:  Photograph of a sandy bar in Zone One, located approximately 30,000 meters from Livingston Dam. The bar is noteworthy for its relative lack of gravel. It is positioned just downstream of a tributary that contributes sand to the river.

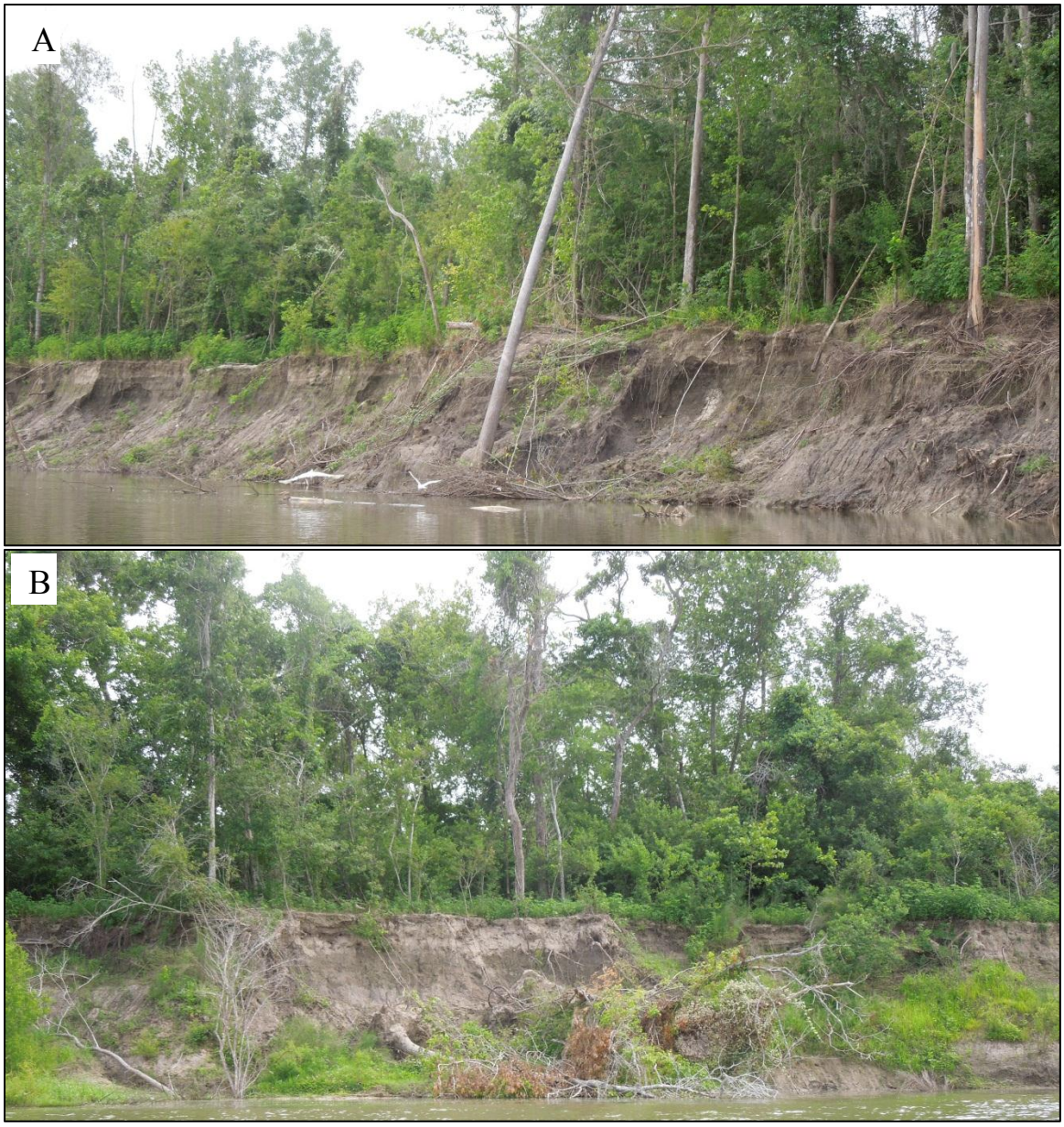


Figure 2.24: Vegetation caught up in erosion of the outer banks of channel bends. (A) Example of an entire tree that has slid down the cut bank. (B) A thick assemblage of fallen trees and bushes maintaining the cut bank. The large amount of material acts to strengthen the bank, inhibiting run-away erosion of the weakly to uncemented Quaternary deposits.

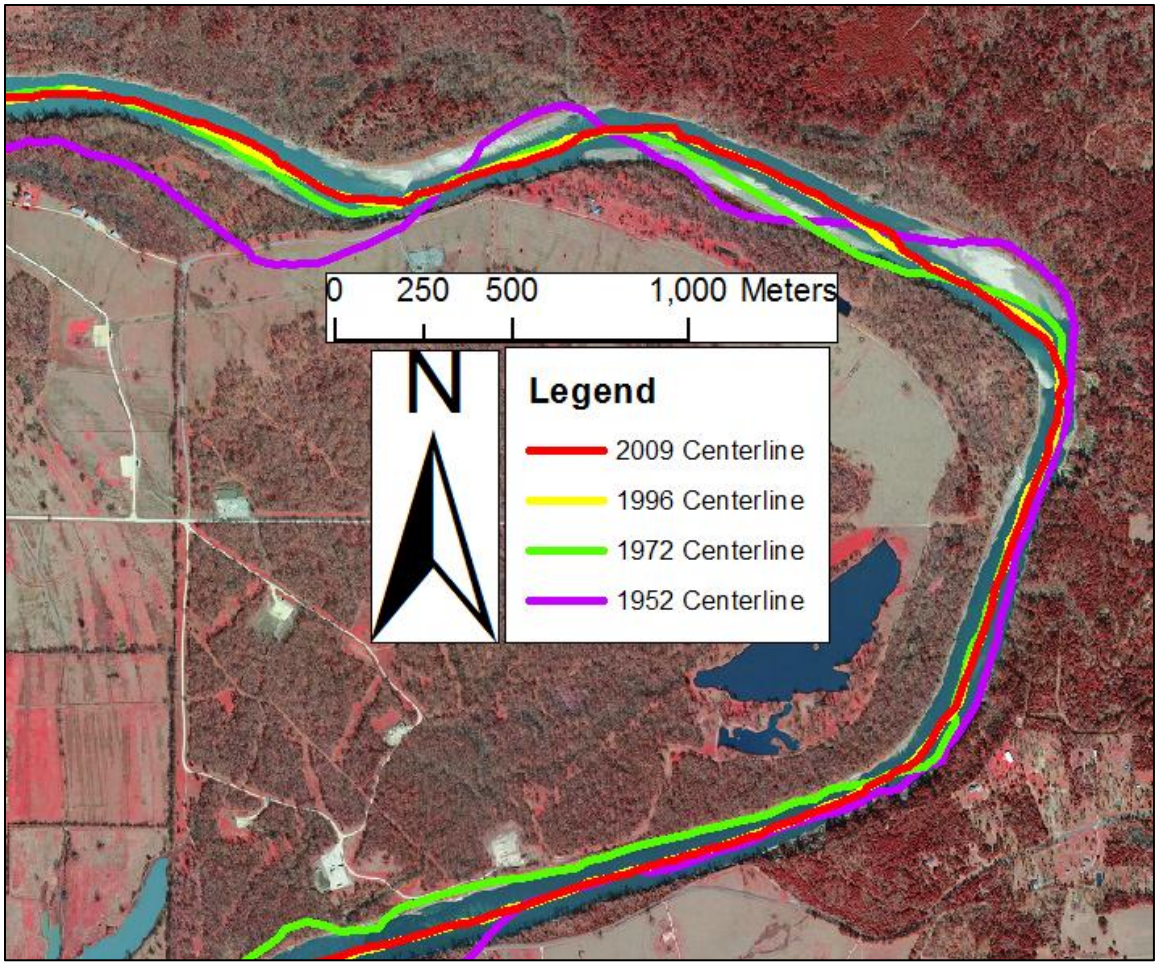


Figure 2.25: The bends in Zone One have straightened since the impoundment of Livingston Dam. The progessive straighten of the river in Zone One has reduced the number of bends, causing the remaining bends to increase in length over time.

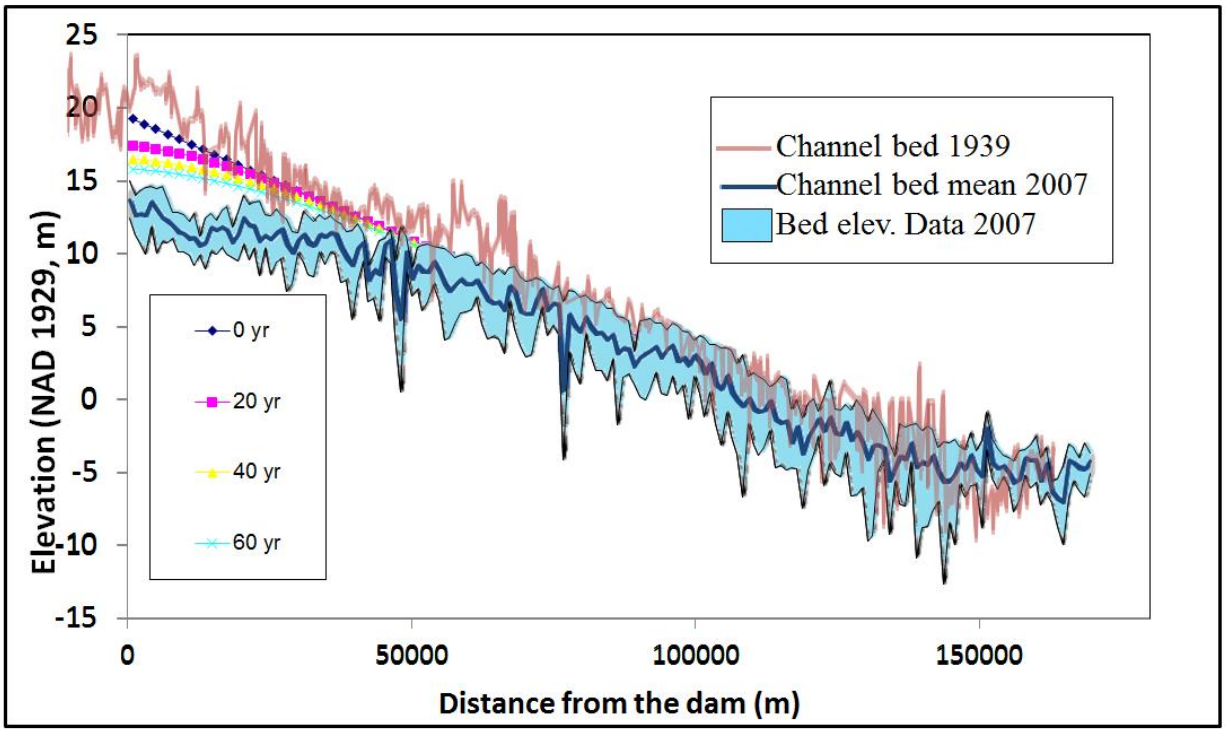


Figure 2.26**:** Data from Figure 5 superimposed results of long profile adjustment model of Parker (2004). Livingston Dam was closed in 1969 so the difference between the 1939 and 2007 profiles is interpreted to the byproduct of 38 years of sediment impoundment behind Livingston Dam. Model results assume a median grain size of 760 micrometers, an effective water discharge of 322.8 cubic meters per second, and a channel width of 125 meters. The model calculates bed stress using equation 3. The model also assumes no bed material load entering the system at the dam and predicts sediment transport with equations 1and 4-9. Model results do good jobs of estimating the location of the transition between Zone One and Zone Two as it is defined by other properties of the system including grain size, width and discharge. The absolute amount of incision at the dam is under predicted by about 50%. We hypothesize that this discrepancy is the product of the substrate being composed of only 50% grains of bed-material load caliber, while the model assumes 100% of the eroded substrate goes into bed-material load.

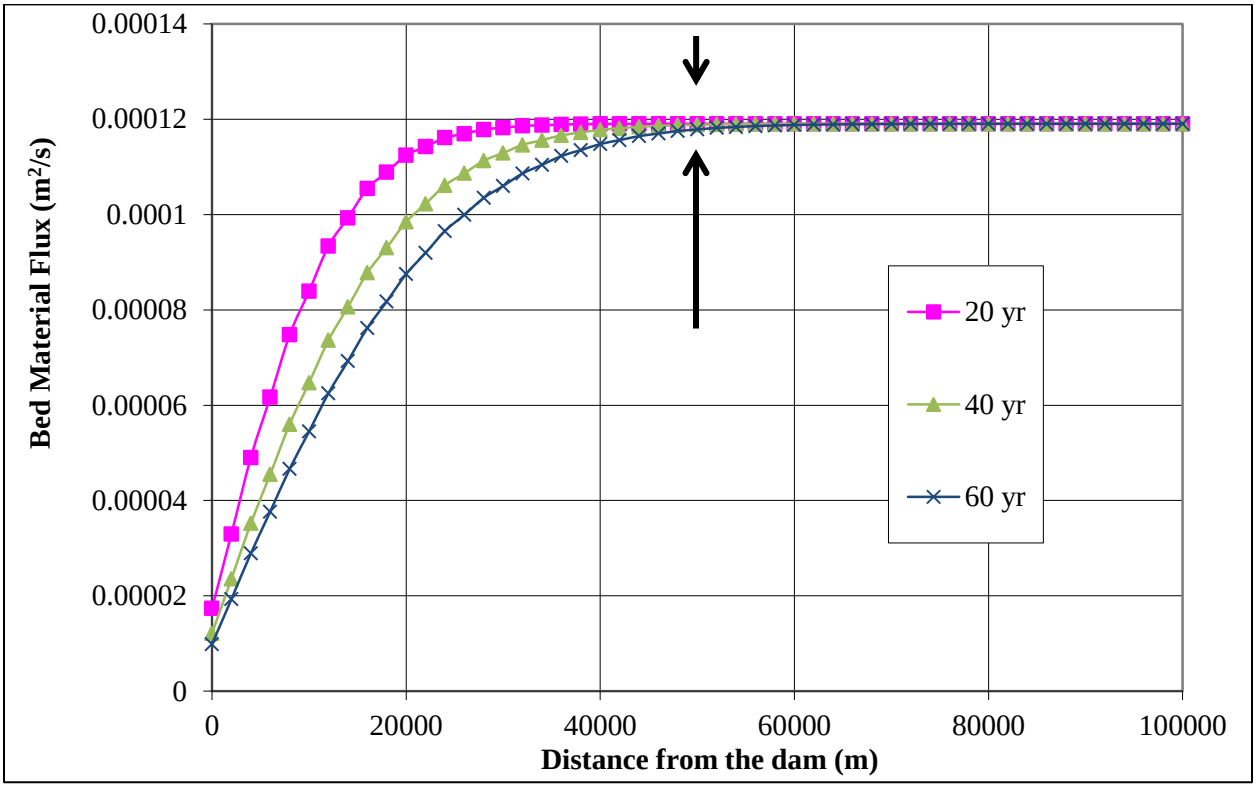


Figure 2.27: Model results showing the river sediment transport adjustment in both time and space downstream of the sediment-retaining Livingston Dam. The model intervals are 20 years apart. The sediment transport regains 90% of its capacity 50, 000 meters downstream of Livingston Dam.

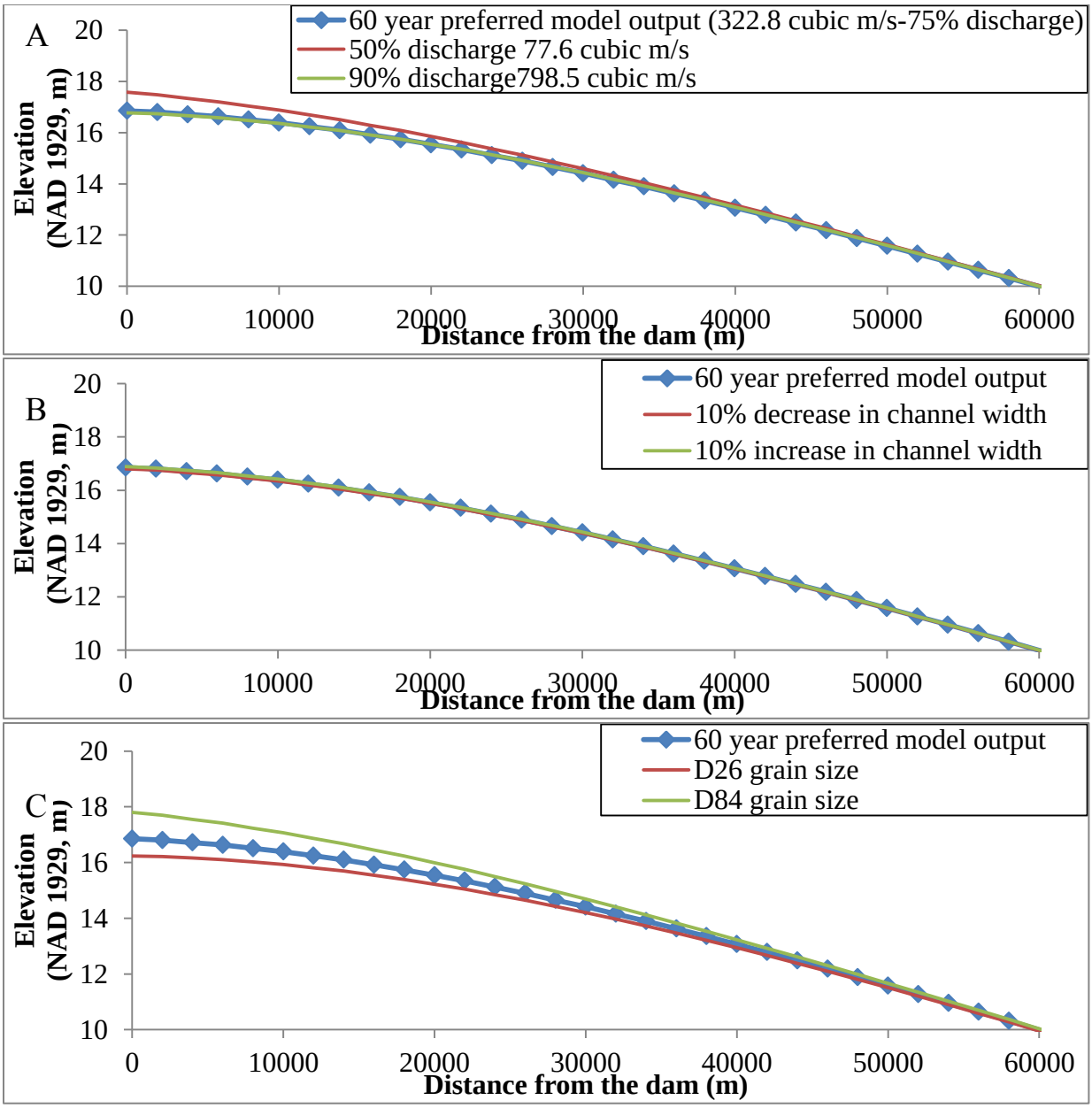


Figure 2.28: Results of a model sensitivity analysis (A) varying discharge, (B) channel width and (C) grain size. The discharge measure show the original model run, at 75% discharge and 25% intermittency, 90% discharge with 10% intermittency, and 50%, or mean discharge value constant intermitancy of one. The channel width was increased and decrease 10% in each direction (B). Changing the width on the channel response to the dam. The grain size was varied by one standard deviation in each direction (C). As the grain size increased incision and propagation decreased. As grain size decreased the response to the dam increased.

**REFERENCES**

Aksoy, S., 1971. "River-bed degradation downstream of dams." *Proceedings of the 14th Congress*, IAHR, Paris, France, Vol. 3, No. C33, p. 275-282.

Brandt, S.A., 2000. "Classification of geomorphological effects downstream of dams," *Catena*, Vol.40, p. 375–401.

Bullet, Bob. "Feb 20th, 2004 Trinity River Bridge Collapse W/Train on Bridge."*Webshots!* Webshots!, 09 May 2003. Web. 29 Aug. 2012. <http://rides.webshots.com/album/72572243DSKXLk>.

Cantelli, A., M. Wong, G. Parker, and C. Paola, 2007. "Numerical model linking bed and bank evolution of incisional channel created by dam removal," *Water Resources Research*, vol. 43.

Chien, Ning, "Changes in river regime after the construction if upstream reservoirs." *Earth Surface Processes and Landforms*, vol. 10, p. 143-159, 1985.

Collins, B. and T. Dunne, 1990. "Fluvial geomorphology and river gravel mining: A guide for planners, case studies included," California Division of Mines and Geology Special Publication 98. Sacramento, California.

Crossland, Christopher J., Hartwig H. Kremer, Han J. Lindeboom, Janet I. Marshall Crossland, Martin D.A. Le Tissier, 2005. "Costal Fluxes in the Anthropocene: The land-ocean interactions in the coastal zone project of the International Geosphere-Biosphere Programme," Global Change, IGBD Series, Springer Publishing, Berlin.

Dietrich, William E. and John D. Gallinatti, 1991. "Chapter 5: Fluvial geomorphology." *Field Experiments and Measurement Programs in Geomorphology*. University of British Columbia Press, Vancouver, Ed. O. Slaymaker.

Engelund, F., and E. Hansen, 1967. "A monograph on Sediment Transport in Alluvial Streams," Technisk, Vorlag, Copenhagen, Denmark.

Graf, William L., 2005. "Geomorphology and American dams: the scientific, social, and economic context," *Geomorphology*, Vol. 71, p. 3-26.

Graf, William L., 2006. "Downstream hydrologic and geomorphic effects of large dams on American rivers," *Geomorphology*, Vol. 79, p. 336-360.

Kondolf, G. Mathis, 1997. "Hungry Water: Effects of dams and gravel mining on river channels." *Environmental Management*, Vol. 21, No. 4, p. 533-551.

Kondolf, G.M. and M.G. Wolman, 1993. "The sizes of salmonid spawning gravels," *Water Resources Research*, Vol. 29, No. 7, p:2275-2285.

Jain, Subhash C., and Inbo Park, 1989. "Guide for estimating riverbed degradation," *Journal of Hydraulic Engineering*, Vol. 115, No. 3, p. 356-366.

Lagasse, P.F. et al., 2004. "Methodology for Predicting Channel Migration," *National Cooperative Highway Research Program Transportation Research Board of the National Academies* Document 67.

Lauer, J Wesley and Gary Parker, 2007. "Net local removal of floodplain sediment by river meander migration," *Geomorphology* Vol. 96, p.123-144.

Lauer, J Wesley and Gary Parker, 2008. "Modeling framework for sediment deposition storage, and evacuation in the floodplain of a meandering river: Theory," *Water Resources Research*, Vol. 44.

Mackin, J. Hoover, 1948. "Concept of the Graded River," Bulletin of the Geological Society of America, Vol. 59, p: 463-512.

Meyer-Petter, E., and R. Muller, 1948. "Formulas for bed load transport," Report on second meeting of international association for Hydraulics Research, Stockholm, Sweden, p. 39-64.

Musselman, Zachary A., 2006. "Tributary response to the Lake Livingston impoundment—the Lower Trinity River, Texas," Doctoral Dissertation, University of Kentucky.

Musselman, Zachary A., 2011. “The localized role of base level lowering on channel adjustment of tributary streams in the Trinity River basin downstream of Livingston Dam, Texas, USA,” *Geomorphology,* Vol. 128, p.42-56.

Nicholls, Robert J., 2003. “Coastal flooding and wetlands loss in the 21st century: changes under the SRES climate and socio-economic scenarios,” *Global Environmental Change,* Vol. 14, No. 1, p. 69-86.

Norris, Chad W., and Gordon W. Linam. 1999. "Ecologically Significant River and Stream Segments - Region H." *TPWD: Ecologically Significant River/Stream Segments of Region H, Regional Water Planning Area*. Texas Parks and Wildlife Department, n.d.

Nittrouer, Jeffery, 2010. “Sediment transport dynamics in the lower Mississippi River: Non-uniform water flow and affects on river-channel morphology,” Dissertation, University of Texas at Austin.

Norris, Chad W., and Gordon W. Linam. 2012 "Ecologically Significant River and Stream Segments - Region H." *TPWD: Ecologically Significant River/Stream Segments of Region H, Regional Water Planning Area*. Texas Parks and Wildlife Department, n.d. Web. 23 Sept. 2012. <http://www.tpwd.state.tx.us/publications/pwdpubs/pwd_rp_t3200_1059c/index.phtml>

Parker, Gary, 1990. “Surface-based bedload transport relation for gravel rivers,” *Journal of Hydraulic Research,* Vol. 28, No. 4, p. 417-436.

Parker, Gary (2004). “1D Sediment Transport Morphodynamics with Applications to Rivers and Turbidity Currents: E-book.” St. Anthony Falls Laboratory, University of Minnesota, Minneapolis, http://vtchl.uiuc.edu/people/parkerg/morphodynamics_e-book.htm, August 20, 2010.

Parker, G., Y. Shimizu, G.V. Wilkerson, J.D. Abad, J.W. Lauer, C. Paola, W.E. Dietrich, and V.R. Voller, 2011. “A new framework for modeling the migration of meandering rivers,” *Earth Surface Processes and Landforms*, vol. 36, no. 1, p. 70-86.Petts, Geoffrey E. and Angela M. Gurnell, 2005. “Dam and geomorphology: Research progress and future directions.” *Geomorphology*, Vol. 71, p. 27-47.

Peyret, Aymeric-Pierre B., 2011. “Morphodynamics and geometry of channels, turbidites and bedforms,” Dissertation, the University of Texas at Austin.

Phillips, Jonathans and Michael Slattery, 2007. “Downstream trends in discharge, slope, and stream power in a lower coastal plain river," *Journal of Hydrology*, Vol. 334, p. 290-303.

Phillips, Jonathans, Michael Slattery, and Zachary Musselman, 2004. "Dam-to-delta sediment inputs and storage in the lower Trinity River, Texas," *Geomorphology*, Vol. 62, No.1-2, p. 17-34.

Phillips, Jonathans, Michael Slattery, and Zachary Musselman, 2005. "Channel adjustments of the lower Trinity River, Texas, downstream of Livingston Dam," *Earth Surface Processes and Landforms,* Vol. 20, No.11, p. 1419-1439.

Podolak, Charles Joseph Pena, 2012. "Channel bed response to an increased sediment supply," Dissertation, Johns Hopkins University.

Rzhanitzin, N.A., E.K. Rabkovam, P.A. Artemiev, 1971. "Deformation of alluvial channel downstream from large hydro-projects," *Proceedings of the 14th Congress,* IAHR, Paris, France, Vol. 3, No. C32, p. 265-274.

Slattery, Michael, 2007. "Sediment budgeting in the upper and middle basins of the Brazos and Trinity Rivers, TX: An assessment of methods and directions for future work," Jun. 2007, Texas Water Development Board.

Slattery, Michael C. and Jonathan D. Phillips, 2007. "Sediment monitoring in Galveston Bay – Final Phase," *Final Report,* Texas Water Development Board.

Syvitski, et al., 2005. "Impacts of humans on the flux of terrestrial sediment to the global coastal ocean," *Science* Vol. 308, p. 3376-380.

Van Rijn, Leo C., 1984. "Sediment transport, Part III: Bed forms and alluvial roughness," *Journal of Hydraulic Engineering,* Vol.110, No.10, p. 1431-1456.

Wiberg, P. L. and Smith, J. D., 1989. “Model for calculating bedload transport of sediment,” *Jounral Hydraulic. Engineering,* Vol. 115, No. 1, p.101-123.

Williams, G.P. and M.G. Wolman, 1984. “Downstream effects of dams on alluvial rivers,” Geological Survey Professional Paper 1286, U.S. Government Printing Office, Washington, DC, Vol. 83, p. 1-60.

Wilson, K. C., 1966. “Bed load transport at high shear stresses,” *Journal of Hydraulic Engineering,* Vol, 92, No. 6, p. 49-59.

Wolman, M. Gordon, 1954. “A method of sampling coarse river-bed material,” *Transactiona of the American Geophyscial Union,* Vol. 35, No. 6, p. 951-956.

Wright, Scott and Gary Parker, 2004. “Flow resistance and suspended load in sand-bed rivers: Simplified stratification model,” *Journal of Hydraulic Engineering,* Vol. 130, No. 8, p. 796-805.

# Chapter 3: Meander Mechanics


## ABSTRACT

Like many sandy coastal rivers, the lower Trinity is geomorphically active. From Livingston Dam to Trinity Bay the river meanders for 180 kilometers, through 177 bends. The river exhibits three styles of channel geometry and kinematic behavior that have been characterized using aerial photographs spanning the past 60 years, as well as bathymetric and field surveys of the entire channel. The three geomorphic zones of the channel correspond to spatial change in sediment transport properties. The upstream zone exhibits straightening and is defined by channel-bed incision, small bars, and relatively slow rates of lateral channel migration linked to sand retention behind Livingston Dam. Eventually the channel flow scours enough sediment from the channel bed to reestablish a transport capacity for sand in the river, marking the transition to the central zone. This second section is defined by fully developed point bars and a high rate of lateral channel migration. The second zone continues until the sediment transport is influenced by the backwater effect of Trinity Bay, defining a third segment. This backwater zone is characterized by very small point bars, steep channel walls, and lower channel migration rates. Migration in this segment is primarily translation with very little lengthening or shortening of bends. There are no cutoffs or rapid straightening events. To analyze the difference between the three zones a database with a myriad of physical variables describing the river was created to categorize the rivers shape as a function of

downstream distance, by individual channel bend, and by bar. Studying connections between channel geometry, migration dynamics, sediment transport and fluid mechanics in each zone provides us with a more complete understanding of the relationships between channel shape and the mechanics at play.

## INTRODUCTION

There is an expanse of work contributing to the comprehension of meandering river bends. Since the early 20$^{th}$ century, scientists and engineers have observed geometric patterns in meandering rivers (*Jefferson,* 1902). As the community has endeavored to understand the relationship between the channel flow and the physical parameters of meandering bends, numerous numerical and physical models have been produced to describe flow in a meandering river. Much of the work can be summarized by two landmark publications in 1974 and 1981. In 1974 Engelund developed a theory for flow in a channel bend. A few years later this theory was applied to lateral migration by both Hasegawa and Ikeda separately (*Engelund,* 1974; *Hasegawa,* 1977; *Ikeda et al.*, 1981; *Parker et al.,* 2011). The developments of this work resulted in a simple equation to describe lateral migration:

$$\dot{\eta} = E\,\Delta U \qquad (Eqn.\ 1)$$

where $\dot{\eta}$ is positive migration rate in the normal stream direction, $E$ is the coefficient of bank erosion and $\Delta U$ is half the mean stream-wise velocity. This equation served as a basis to further the development of meander theory by explaining meander characteristics; such as meander wavelengths, asymmetric meander loops, meander growth rates, and downstream migration rates (*Parker et al*., 1982; *Smith and McLean*, 1984; *Parker and Andrews*, 1986; *Deitrich*, 1987; *Whiting and Dietrich*, 1993 a, b, c; *Murray and Paola*, 1994; *Sun et al.*, 2001; *Parker et al*., 2006; and *Parker et al*., 2011).

Eqn. 1 provides a straightforward method to estimate rates of bank movement; however, diverse meander shapes and migration rates suggest that many other variables impact meander dynamics. The community is still seeking to fully understand the additional variables impacting river migration and bend evolution. The majority of this work has been done through computational models and flume experiments. Few large scale field surveys focusing on the mechanism controlling fluvial migration exist due to the difficulty of large scale data and subaqueous data collection.

My study is based on several large scale field studies spanning 70 years. The data was collected along the lowest 180 river kilometers of the lower Trinity River, TX and was digitized. The surveys consisted of a 1939 survey of the transects of the river, four aerial photographic surveys from 1952, 1972, 1996 and 2009, a bathymetric survey from 2007, and a grain size survey from 2012. Figure 3.1 shows a slope map of the study area overlain with river centerlines from each aerial survey. The three map subsets are examples from the three distinct geomorphic zones: a dam influenced zone, an actively meandering zone, and a backwater zone. By examining the kinematic and geometric

variability of the three zones in both space and time, we can understand more about the channel flow and sediment transport in these three types of meandering river environments. Ultimately, this allows us to create linkages between the fluid mechanics, sediment transport and channel geometry.

## PREVIOUS WORK

Over a century of scientific work has vastly increased our knowledge of how river meanders develop and evolve *(Inglis*, 1937; *Bates*, 1939; and *Leopold and Wolman*, 1957). Some of the earliest work sought patterns of statistical significance in river meander frequency (*Jefferson*, 1902*)*. As the science developed, researchers were able to describe and develop linkages between the channel geometry, fluid mechanics and sediment transport (*Leliavsky*, 1955; *Ikeda et al.*, 1981; and *Smith and McLean*, 1984). Previous work has shown that flow within a bend is stratified cross-sectionally. The velocity of the flow at the outer bank is higher than the velocity of the flow at the inner bank. Through time the high velocity flow at the outer edge of the bend erodes the outer bank. The reduced velocity near the inner bank allows for sediment deposition from the flow. As a result, the bend migrates in an outward and downstream direction (*Hickin*, 1974; *Whiting and Dietrich*, 1993, a, b and c; *Hooke*, 2007). Bars aid in bend growth by topographically steering the channel towards the outer bank of the bend (*Nelson*, 1989). The evolution of the meander bend is also dependent on local erodibility of the river banks, which can be a function of soil strength, bank protection due to slumping of

vegetated blocks of bank material, coarse debris deposits, or anthropogenic bank protection efforts (*Leopold and Wolman*, 1957; *Hooke*, 2007; *Brauderick*, 2009; *Parker et al.*, 2011).

The general shape and description of flow of an individual meander bend can be seen in Figure 3.2. The presence or absence of meanders has been attributed to many causes. Meanders are a natural occurrence and the shape, frequency, and curvature may be a function of sediment supply, slope and discharge. The presence of bends is more common in nature than long straight channel reaches. Leopold and Wolman (1960) suggest that it is atypical for channels to be straight more than ten channel widths. Additionally, existing investigations suggest that meanders can be the product of a channel adjusting to landscape elevation changes (*Schumm*, 1993).

Channel straightening has been linked to a change in the river discharge and sediment transport (*Graf*, 2006). These types of changes may be attributed to dams, as dams function as highly efficient sediment traps (*Brune*, 1953). The result is a greatly reduced sediment load leaving the reservoir. As discussed in the previous chapter, the sediment-free water scours channels downstream of dams until a relative equilibrium is achieved in the transport of sediment. Dams can affect channel slope, discharge and sediment load, and have been linked to river straightening. While this has been observed in several papers, to the authors' knowledge, a complete mechanistic explanation for this phenomenon is still missing (*Brandt*, 1999; *Williams and Wolman*, 1984).

Sediment transport and hydraulics are also altered by backwater effects. Concepts of backwater influenced river mechanics have long been established by geologists and engineers, yet the breadth of work on this topic is relatively narrow, primarily focused on hydraulics and not on the corresponding change in sediment transport and connected change in river-channel geometry and kinematics. A backwater condition always occurs where a river enters a standing body of water, such as a bay. As the river adjusts to the standing surface elevation, the channel depth upstream increases, illustrated in Figure 3.3. The mechanical changes associated with channel deepening also propagate upstream (*Chow*, 1988; *Dingman*, 1991). The length of backwater influence can be estimated using the backwater length equation:

$$L_b = \frac{H}{S} \qquad (Eqn.\ 2)$$

where $L_b$ is the backwater influence length, *H* is the average channel depth and *S* is the average slope of the water surface (e.g., *Paola and Mohrig*, 1996). Based on an *H* of 6 meters and *S* of 0.00001(*Phillips et al.*, 2005), the average $L_b$ for the lower Trinity River is approximately 60000 meters. In the backwater length of a river the boundary shear stress is no longer accurately estimated using the depth-slope product:

$$\tau_b = \rho g H S \qquad (Eqn.\ 3)$$

Instead the boundary shear stress is best estimated using the full backwater equation:

$$\frac{\partial U}{\partial t} + U\frac{\partial U}{\partial x} = -g\frac{\partial H}{\partial x} - g\frac{\partial \eta}{\partial x} - \frac{\tau_b}{\rho H} \qquad (Eqn.\ 4)$$

$$\tau_b = \rho C_f U^2 \qquad (Eqn.\ 5)$$

Recent work has shown the effects of the backwater on the sediment transport dynamics (*Parker et al.*, 2008, *Nittrouer et al.*, 2012). Studies on the Mississippi suggest a correlation between reduced lateral migration and backwater influence in the lower Mississippi River (*Jerolmack*, 2009; *Hudson and Kesel*, 2000) due to a reduction in sediment transport (*Nittrouer*, 2010). Like the lower Mississippi River, the lower Trinity River undergoes a decrease in lateral migration in the backwater influenced segment of the river. A primary goal of this study is to define what geometric properties of the river are connected to this reduction in channel migration rate.

Most of the published studies investigating river migration have focused on rivers at normal flow. Existing models for the planform evolution of channels have difficulty predicting several nonlinear meander characteristics (*Sun et al.*, 1996; *Ikeda et al.*, 1981). While Eqn. 1 has successfully propelled meander theory, the powerful but simple equation does not address all variables influencing meandering channels. This is particularly true for locally influential variables such as bank interactions, bank cohesion and total strength. Targeted experimental work and more complicated numerical models have advanced our understanding of the physics of flow and sediment transport in a meander bend (*Whiting and Dietrich,* 1993 a, b, c). It is now clear that local aspects, such as bank erosion coefficient or the presence of gravel lags on the bar tops, must be field calibrated. The degree of cohesion within bank soils is not consistent in a natural environment (*Hooke*, 2007; *Leopold and Wolman*, 1960; *Murray and Paola*, 1994; *Parker et al.*, 2011; *Sun et al.*, 1996). Additionally, the concept of constant channel

width continues to elude scientists. While models described by Hasegawa (1977) and Ikeda et al. (1981) also assume that meandering river banks maintain a constant bankfull width, the physics of the bank relationship necessary to maintain bankfull width in a river has not yet been fully explained (*Parker et al*., 2011).

The physics at play in the dynamics of the river are reflected in its geomorphology. Many studies have tied meander evolution to the geometry of the channel. The earliest papers were based on observations of rivers in nature (*Jefferson*, 1902; *Leopold and Wolman*, 1960). Later work focused on channel geometry relationships, such as width and radius of curvature (*Leopold and Wolman*, 1960; *Blondeaux and Seminara*, 1985). Further investigations linked channel geometry and channel mechanics (*Dietrich and Whiting*, 1993 a, b, and c). These connections were propelled by the understanding of the helical flow within the bends (*Purs-Chacinski*, 1954; *Leliavsky*, 1955; *Leopold and Wolman*, 1960; *Smith and McLean*, 1984; *Dietrich*, 1987).

Many fluvial geomorphic studies have looked to the bend radius of curvature to model bend evolution. The radius of curvature of a bend impacts the flow structure within a bend, changes the erosion of the cut bank and affects the rate and style of point bar construction. The relationship between channel width and radius of curvature has been linked to bend migration (*Whiting and Dietrich*, 1993 a, b and c; *Carson and Lapointe*, 1983; *Blondeaux and Seminara*, 1985; *Williams*, 1986; *Furbish*, 1988; *Biedenharn et al.*, 1989; *Nelson*, 1990; *Petts et al.*, 1989; *Hudson and Kesel*, 2000; *MacDonald et al.*, 1991; *Hooke*, 2003; *Begin*, 2003). Several published sets of

observations and models have reproduced a relationship between width and radius of curvature similar to that shown Figure 3.4 (*Hooke*, 2003). Many of these studies investigating this and other river characteristics were limited by two major obstacles. First, there are surprisingly few large databases for rivers. Second, until recently there have been no automated methods for calculating the radius of curvature, making quantitative comparative analyses difficult (*Peyret*, 2011).

Another variable of interest to fluvial geomorphologists is bend length. Parker and Andrews (1986) concluded that freely meandering bends exceeding a threshold minimum length grew in amplitude until there was a cutoff. Bends that were not able to establish themselves beyond the threshold length experienced straightening—or self-obliteration. Other papers have linked bend growth to migration. The length of a channel bend affects bed stability, or lack thereof, resulting in bend migration (*Blondeaux and Seminara*, 1985). The instability of the channel bed causes the construction of alternate bars (*Leopold and Wolman*, 1957; *Lewin*, 1976). Nelson (1990) noted that small bends migrated less. As bends increased in size, migration rate increased to a threshold; after a certain length, migration rate decreased.

As bends grow and evolve their alteration often impacts the development of neighboring bends. Howard and Knutson (1984) suggested that evolving bends influenced the flow in neighboring bends, both upstream and downstream; a concept that was later developed into a spatial autoregressive model for meandering rivers (Furbish, 1991). This is seen most dramatically in bends where there has been a recent neck or chute cutoff (*Larsen and Shen*, 1989). As a cutoff occurs, the change in channel

planform forces other bends to absorb the changes in the flow. This has been documented in several investigations (*Hooke,* 1995; *Lagasse et al*., 2004). Bends can also impact each other in less dramatic ways. Simply by growing, bends can become compound bends (*Brice*, 1974; *Parker and Andrews*, 1986). Fully understanding these interactions has been limited by lack of large spatial datasets.

Computer technology has allowed for improvements in modeling and data analysis, aiding the community's understanding of the elements governing meandering rivers. By developing computational models the physical variables impacting bend evolution could be tested. Computer models, based on the early work of Ikeda et al.(1981) have enabled theory testing for long-term river behavior (*Sun et al*., 1996), combining and testing multiple subsequent developments to the meander theory (*Sun et al.*, 2001). In 2004 the National Academy of Sciences commissioned a report, *Methodology for Predicting Channel Migration for the Transportation Research Board*, which presents various physical and computational models of lateral river migration. Many of these models were compiled to create a GIS tool for measuring and predicting river morphology (*Lagasse et al*., 2004).

## STUDY AREA

The Trinity River of Texas begins northwest of Fort Worth, Texas and flows into to Trinity Bay on the Gulf Coast of Texas. It is the largest river fully contained within the state and supports over half of the water needs for the state's populations, as it flows through the population hubs Fort Worth and Dallas. The lower most dam on the river creates a reservoir, Lake Livingston, which provides water to metro Houston. The area of this study focuses on the river downstream of Livingston Dam to the coast. From Livingston Dam the Trinity flows 180 river-kilometers to Trinity Bay (Fig. 3.1a). This portion of the lower Trinity River is an active, sandy meandering channel that can be divided into three geomorphic zones. For the purpose of this paper I will refer to them as Zone One, Zone Two and Zone Three. The dashed lines depict the approximate positions of the transitions between zones. The colored lines shown in the subset images mark the positions of the river centerlines in 1952, 1972, 1996 and 2009. Zone One (Fig. 3.1b) is just downstream of the dam and is strongly influenced by it. The dam influence persists approximately 60 kilometers downstream until tapering out. Zone Two begins where the noticeable dam influence ends. Zone Two (Fig. 3.1c) has approximately relative equilibrium sediment transport and a highly active migration rate. It is the longest zone, approximately 100 river kilometers in length. Eventually, Zone Three, the backwater zone, begins when the Trinity Bay influences the river's geomorphology, 60 kilometers upstream the river outlet (Fig. 3.1d).

The channel bottom and walls of the lower Trinity River are primarily composed of Quaternary fluvial deposits. Figure 3.5 shows a geologic map of the region,

dominated by Quaternary Period fluvial deposits, with some Miocene Period outcrops. Strata of paleo-channel surfaces are frequently exposed in the side walls of the channel, particularly in the actively meandering Zone Two. Figure 3.6 is an example of previous channel surfaces, outlined by dark lines. In essence, the fluvial deposits provide an abundant sediment supply. As the river migrates it continually reworks its own previous sediment deposits.

While the Quaternary deposits dominate the local geology the Miocene rocks also have a role in the system's evolution. Along the river there are areas of the channel wall and bed that contain older harder Miocene rock, shown in yellow in Figure 3.5. An example of these types of deposits can be seen in Figure 3.7, taken approximately 55 kilometers downstream of Livingston Dam. This deposit and others are the source for the larger gravel clasts in the system. Fine sediment is provided to the system through bed and bank erosion as well as tributaries.

## METHODOLOGY

The lower Trinity River served as an excellent study area due to the geomorphic nature, an abundance of available data, and an extensive breath of existing publication about the river (*Musselman*, 2006; *Musselman*, 2011; *Phillips et al*., 2004; *Phillips et al*, 2005; *Phillips and Slattery*, 2006; *Slattery*, 2007; *Slattery and Phillips*, 2007); all of which proved very useful for this project. The lower Trinity River has been surveyed

several times in the past 150 years using a variety of methods. For this study, many of these surveys were integrated to quantify the morphodynamic changes. The oldest used in this study was a 1939 survey from the U.S. Army Corps of Engineers (USACE). I digitized the river profile from the survey using a Geographic Information Systems (GIS) in the program Arc GIS and then exported to Matlab for analysis. Figure 3.9 shows the channel profile from 1939 for the study area depicted as a red line. This was approximately 31 years before the river impoundment of Livingston Dam. The second super-imposed profile in Figure 3.9, in blue, shows both the mean and total range of channel-bed elevations for the same portion of the Trinity River in 2007. I created this profile from data collected by the Texas Parks and Wildlife Department (TPWD) and re-processed it in Arc GIS and Matlab. This data was collected using an integrated, single head depth sounder and GPS device. The elevation data was tested and processed in Matlab to create a mean elevation profile of channel. The stage during the days when this data was collected was at or near (within a few centimeters) of 16 meters and a discharge of 855 cubic meters per second at the USGS Romayor gage (number 08066500), sufficient flow to top the sandy bar deposits of the river.

The transitions from a convex to linear and then linear to a concave profile are even more pronounced when looking at water-surface elevation data (Fig. 3.10). The gaging stations are located at Goodrich, Romayor, Liberty and Wallisville, TX (USGS number 08066250, 08066500, 08067000, and 08067252). The most recent 20 years of data from these four stations were used to calculate a minimum stage (5% probability), median stage, and maximum stage (95% probability). These river stages are associated with water discharges of 28.1 cubic meters per second, 162 cubic meters per second, and 2381.4 cubic meters per second respectively at the USGS gage at Goodrich, TX. The

shape of the water surface profile is a reflection of three distinct geomorphic zones: the convex incisional zone (Zone One), the linear, actively meandering zone (Zone Two), and the concave backwater zone (Zone Three). A convex, linear, and concave segment in the water-surface profile from upstream to downstream is well defined by the stage data. These three segments with different patterns of curvature in the water-surface elevation are tied to the three distinct morphodynamic segments of the channel.

A suite of aerial photographs collected by the Texas Natural Resource Information System (TNRIS) for the Trinity River over approximately 60 years were used for this study. The surveys were finalized in 1952, 1972, 1996 and 2009. However, the survey date was slightly earlier in some cases (Table 3.1). For the purpose of this study the survey date was used for all temporal calculations. The photographs were imported to ArcGIS as images and geo-referenced using historical infrastructure such as bridges, railroad tracks and roads (shapefiles were obtained from TNRIS). The banks, vegetation lines, water's edge, centerlines and bar deposits (from grassy edge to water's edge) were then traced using GIS tools for the length of the river for each of the four surveys. Once the banks and centerlines were translated into GIS features, as points, lines and polygons, the planform geometry of the river was quantitatively analyzed comprehensively for the entire length of the river downstream of Livingston Dam for the 60 year span. Using GIS tools, various variables for the river were calculated, such as bankfull width, bar area, bar volume, bar centroid, river width, lateral river migration, river translation and change in bar area. Values for channel width and migration were found using the GIS Planform Statistics Tool (*Lauer*, 2006). Once the variables were

calculated for each of the aerial surveys and they were spatially joined to the centerline shapefile for that survey and exported to Matlab as a function of distance from the dam.

Further analysis was done in MatLab. To compare data in a similar context, I clipped each of the datasets in order to represent the same length of the river, starting at Livingston Dam and running 170 river-kilometers, ending just upstream of the Wallisville Project. The data was then interpolated along the centerline to create a point every 36 meters. In Matlab the variables were tested against each other to identify spatial correlations and trends.

Peyret's (2011) Meanders Matlab program was used to determine the radius of the curvature of the river for each set of aerial photographs *(Peyret*, 2011). After testing several window sample sizes, the sampling window used to calculate the radius of curvature was set to meters. This sampling window was chosen because the calculated inflection points were a best fit to the observed inflection points. There was a slight offset due to the spatial averaging aspect of the window size. To accommodate for this issue the points were filtered and smoothed to remove the outlying inflection points.

Using the maximum radius of curvature values as inflection points allowed for the identification of individual bends. This facilitated the calculation of bend statistics; such as bend length, curvature, and sinuosity, as well as temporal dynamics. Creating a quantitative method for isolating bends facilitated identifying correlations between bend morphology and physical variables impacting the bend mechanics. Isolation of the variables and analysis of how they change through time allowed me to test factors impacting bend evolution; such as bend length, curvature, width, and bend interaction.

I used ArcGIS to create a digital elevation model (DEM) by combing the TPWD data and the 1984 USGS land surface survey. Transects, perpendicular to the centerline of the channel, every 36 meters were created extending 500 meters from the left flood plain to the right flood plain (Fig. 3.12). These were used to extract elevation data for cross sectional analysis. Each transect was converted to spatial points that were joined to the elevation data from the DEM of the 2007 channel. Using these transects, elevation data was extracted from the DEM to create a set of channel cross sections. Channel transects were used to calculate the channel-bottom relief, bankfull (vegetation line to vegetation line on the right and left banks of the channel) channel relief, channel wall slopes and channel symmetry. The GIS work flow associated with making these calculations is presented in Figure 3.11.

I used the aerial photographs and the combined surveys DEM to calculate the bar shapes. The bathymetric data from the 2007 was laid over the aerial photographs with a partial transparency. This allowed the bars visible in the photographs to be seen. The bars extend well into the channel. The survey data allowed for the identification of the extent of the bar. For the purpose of this study, the bars were defined as the area from the wooded vegetation line into the channel, where there is a slope break (Fig. 3.13). The area of the bars was calculated using GIS tools. The relief was found by extracting the highest and lowest elevation values from the 2007 bathymetric DEM with in the bar shape. The volume was found by using raster math to subtract the minimum elevation value from the bar shape extracted DEM. These values were then summed and multiplied by the area.

I completed several targeted field campaigns on the river between 2009 and 2012 to compliment the regional images and surveys. This field work included the collection

of bathymetry data (not discussed here), sampling bars for grain size, surveying bars (not discussed here), and photographing over several portions of the study area. One field survey of the grain composition of the bars was done of the zone transitions. This study was completed in June 2012 (Fig. 3.13 and 14). Seven point bars were sampled from Goodrich, TX to Romayor, TX, across the transition from Zone One to Zone Two (Fig. 3.13a). Nine point bars were sampled between Liberty, TX and Moss Bluff, TX, crossing the transition zone between Zone Two and Three (Fig. 3.14a). Six sediment samples were collected from each bar. Three grain-size samples were taken from the water's edge and three from the vegetation line. The samples were taken 60 paces apart in the centerline direction starting near the upstream end of the bar and ending near the midstream portion of the bar. Each sample was collected exactly at the point of sixty paces to ensure that bias was not introduced into our sediment sampling. The size of the samples varied slightly, averaging $5.56 \times 10^{-5}$ cubic meters. All of these samples were large enough to ensure that the coarsest grains are accurately represented (*Wolman*, 1954). The largest grain in any sample constituted less than one one-thousandth of the total sample volume. Grain size was measured using a Retsch Technology CamSizer that uses image analysis of falling grains captured by two high-speed digital cameras to determine both particle size and shape. The results of this analysis for the bars in Zone One and the Zone One – Zone Two transition are summarized in Figures 3.13b and 3.14b.

## OBSERVATIONS

### Profile Adjustments

The profile of the lower Trinity River is shown in Figure 3.9; the 1939 pre-dam profile (in red) and 2007 profile (in blue). The river and profile can be divided into three geomorphic zones, shown in (Fig. 3.1). In comparing the two profiles, there is a distinct difference—the most upstream portion of the profile has changed. In 1939 the profile exhibited a linear trend, but by 2007, the first 60 river kilometers of the profile morphed into a convex shape. As described in chapter two, this is a function of dam induced scour.

Between river-kilometer 50 to 60 the 2007 channel profile transitions from convex up shape to linear profile, like the 1939 profile. The linear trend in the river's profile represents the second zone of the river, the freely meandering zone. This portion of the river shows no evidence of major channel evolution. The profile data shows the channel bed did not aggraded or incised between 1939 and 2007 (Fig. 3.9).

The linear profile morphs into a concave profile around river-kilometer 130. The change is due to the backwater effect as the river flows into Trinity Bay (Fig. 3.3). In the case of the Trinity River, the backwater length corresponds to a distance of approximately 60000 meters (see *Previous Work* for calculation details). The backwater length in both 1939 and 2007 begin at about the same downstream distance, approximately when the channel bottom reaches sea level, around river kilometer 130. The downstream portion of the 2007 profile exhibits a similar concave shape as the 1939 data, but with a higher elevation. The 1939 data shows a dip in the profile around river kilometer 150, while the 2007 profile does not.

**Grain Size Trends**

The grain samples taken from the 2012 river survey are shown in Figures 3.13b and 14b. The locations of the transitions from one zone to the next are difficult to identify because as they do not occur abruptly, defined by a single location, but rather happen over a length of the channel. It is also difficult to identify the transition between zones by studying the grain sizes present on the bars across the transition. An analysis of the grain sizes of the bars across the deposit also showed that while there is a general downstream trend in the grain sizes of the bars, the grain-size can be highly variable from bar to bar. In the case of the Lower Trinity, the transition from Zone Two to Zone Three is easier to identify by grain size than the Zone One to Zone Two transition. In Zone One the bars are enriched in gravel fraction relative to the other two zones. The samples from the Zone One-Zone Two transition, shown in Figure 3.13b, range from 0.27 millimeters to 2.24 millimeters, with a mean of 0.82 millimeters. As can be seen in Figure 3.13b the transition between the zones is gradational and noisy.

The transition between Zone Two and Three is slightly more dramatic, although still very noisy (Fig. 3.14 a and b). A majority of the bars in Zone Three are composed of entirely of sand; however, there are exceptions due to a local supply of course sediment from older channel deposits exposed in the modern banks. The samples from the Zone Two-Zone Three transition, shown in Figure 3.14b, range from 0.32 millimeters to 1.63 millimeters, with a mean of 0.82 millimeters.

The variation in the trend shows the influence of the local geology, particularly the introduction of heterogeneous bank material into the channel (Fig. 3.7 and15). To gain a deeper understanding of gravel enrichment the samples were separated into sand

and gravel portions for analysis. Sediment is being supplied to the river from erosion of the bed, banks, and tributaries. No samples of the channel substrate were taken. I hypothesize the channel bed to be composed of a combination of sand, mud and lithified sandstone. The basis for this estimate is observations from the channel walls. In the Zone One to the Zone One-Zone Two transition a qualitative observation of the channel suggested that approximately 85% of the material was composed of unlithified material, 50% mud and 50% sand. The remaining 15% was composed of the sheets of sandstone, no thicker than 20 to 30 centimeters. Examples of from the channel are shown in Figure 3.16.

From the tributaries observed, the sediment being supplied is predominantly medium sand. Samples from the mouths of the tributaries, processed using the Retsch Technology CamSizer, showed the incoming sediment had $D_{50}$ equal 0.26 millimeters. An example of the mouth of a tributary can be seen in Figure 3.15, which was taken approximately 31kilometers downstream of Livingston Dam. Most of the observed tributaries were hanging and appear to function primarily during high flow. During high flow these sediment sources input an abundant amount of sediment into the system, influencing sediment load and the local morphology of the river.

**Cross Sectional Differences**

The lower Trinity River is incised into sedimentary fill of a paleo-river valley, almost entirely composed of sandy fluvial deposits (Fig. 3.1 and 5). Between Livingston Dam and the coast, the river is cut into the valley fill to the degree that the tops of most of the cut banks and the vegetation lines bounding tops of point bars join at the terraced flood plain. The modern flood plain and the Quaternary Terrace are approximately one

in the same. Examples of this can be seen for each photo in Figure 3.17. Image 3.17a and b show the banks and floodplain in Zone One. Images 3.17c shows a cut bank in Zone Two, and Image 3.17d shows river banks in Zone Three. The flood plain terrace is persistent down the course of the river. The height of the flood plain relative to the river varies by morphodynamic zone, decreasing in the downstream direction. Although the Zone One and Zone Two cut bank slopes are steep they are naturally protected. Along the entire length of the study area, particularly in Zone One and Zone Two, trees and vegetation slumping helps to protect the cut banks from runaway erosion (*Parker et al.*, 2011). Examples of this are shown in Figure 3.18.

The downstream lowering of the floodplain can be seen in the plot of the cross sectional relief (from floodplain terrace to thalweg), shown in Figure 3.19. The channel relief is calculated from the thalweg to the top of the bank as a function of downstream distance. Figure 3.20 shows the height of the banks relative to the water surface and bed elevation. At 95 percent flow (discharge of 2381 cubic meters per second at Goodrich, Texas) almost all of banks in Zone Two and Zone Three are overtopped, but only some of the banks in Zone One.

In Zone One the channel profile has responded sand retention behind Livingston Dam by incising its bed since the dam was closed over 50 years ago. This bed incision is disconnecting the channel from its flood plain which is changing elevation at a much slower rate (Fig. 3.17a and b). This results in the Zone One floodplain being elevated well above the normal water surface compared to the rest of the study area (Figure 3.20). As the river transitions from Zone One to Zone Two the relief decreases and then maintains a constant elevation (Fig. 3.17c and 20). Between Zone Two and Zone Three, the relief of the channel decreases again (Fig. 3.17d and 20) as the total dynamic range of

water surface elevations drops as a function of the backwater influence. Even during high flow the river stage never raises much above the mean stage, maintaining low channel banks. These trends are highlighted by the difference between the minimum and maximum water surface profiles shown in Figure 3.8.

The total channel relief (Fig. 3.19) measured from the flood plain to channel bottom decreases as a function of downstream distance. The flow depth at moderate discharges does not show this same trend. Figure 3.21 shows the channel depth measured during a high flow event, (discharge at Romayor was 855 cubic meters per second). Zone Three is the deepest, due to the effect of the backwater (Nittrouer et al., 2011, 2012). However, this is not the case for the width to depth ration (Fig. 3.22). Like channel depth and width the ratio increases from Zone One to Two and decreases into Zone Three, suggesting that Zone Two has the highest propensity for migration (*Parker*, 1976).

It should be noted that the depth trend is not maintained during flood events. Figure 3.23 shows the change in depth and cross sectional area of the channel from 75% flow (322 cubic meters per second at Romayor) to the 95% flow event (2690 cubic meters per second at Romayor). During flood events the depth becomes higher in Zone One and Zone Two, but not in the backwater zone, Zone Three. The cross sectional geometry shows a similar trend and high flow reversal.

Figure 3.24 and 25 describe the asymmetry of the channel. Figure 3.24 uses only the 2007 channel bathymetry data collected by the TPWD. The data represents the underwater portion of the channel during the survey (the stage at the Romayor USGS gage was 16 meters). The symmetry of each cross section was calculated by taking the

absolute value of the differences between the right and left bank slopes of the channel divided by the mean slope (Eqn. 6). This was done for 5001 transects evenly spaced along the centerline, then averaged by kilometer. A larger difference between the relative slopes is representative of a greater cross-sectional asymmetry. The trend shown in Figure 3.24 suggests the channel is more symmetrical, u-shaped, in Zone One and Zone Three. In Zone Two, the highly migrating portion of the river, the channel is highly asymmetrical. Here the bar width becomes more dominant within the channel in Zone Two. Figure 3.26 shows a plot of the ratio of bar width to river width.

$$\frac{|S_{left\ bank} - S_{right\ bank}|}{S_{mean}} \qquad (Eqn.\ 6)$$

Figure 3.25 shows bank slope as a function of distance from the dam, showing the asymmetry of the channel between the right top of bank to the left top of bank. The bank slopes were found using the cross sections created from the TWPD 2007 survey and the TNRIS DEM, as it represents the entire cross-sectional length of the channel, from the top of the right bank to the top of the left bank (Fig. 3.10). The slope difference values were calculated by finding the slope from the thalweg to the top of the bank on either side of the river, and taking the difference between them. Figure 3.25 shows a trend similar to the channel relief (Fig. 3.19). The highly incised banks of Zone One result in steeper slopes, leading to a greater asymmetry. The low slopes in the backwater show the banks are fairly symmetrical.

**Downstream Changes in Bars**

The graphs in Figures 3.27 and 3.28 describe the sizes of the bars as a function of downstream distance. In Zone One the bars are small (Fig. 3.27a and b). This generally corresponds with the trends in Figures 3.28a and b, which show the heights of the bars as a function of downstream distance, resulting in a change in bar slope (Fig. 3.29).

The bars in Zone One have relatively small areas and low heights (Fig. 3.27 and 3.28). As the channel approaches Zone Two, the heights of the bars increase, as do the bar area and bar volume. As the channel transitions into the backwater zone at around river-kilometer 120, the bar area and bar volume decrease while bar height continues to increase. The bars in Zone Three are small and steep. It should be noted that immediately downstream of the dam there is a chain of bars that are anomalies, potentially due to dam related channel maintenance.

To gain a deeper understanding of the geometric trends within the channel the bar surfaces were measured. Slopes of the bars were extracted from the TWPD 2007 channel survey. Figure 3.29 shows a graph of bar surface slopes measured orthogonal to the direction of the channel centerline, crossing the bars in the local cross-stream direction. The blue dots represent all transects on every bar. The red line is a plot of the surface slope at the apexes of all bars. The cross-stream surface slopes for bars in Zone One and Zone Two are more similar than different. The significant increase in bar slopes begins at the downstream end of Zone Two and into the transition to Zone Three. Zone Three has the steepest slopes.

Examples of the bars in each zone are shown in Figures 3.30, 3.31 and 3.32. The bars in Zone One show a low relief topped with gravel (Fig. 3.30). The bars in Figure

3.31, located in Zone Two, are robust in their topography and composed primarily of sand. Figure 3.32 shows bars from Zone Three, which all have small areas and steep cross-stream surface slopes (Fig. 3.27 and 3.29).

**Downstream Change in Channel Planform**

Figure 3.33 shows the distribution of four planform variables as a function of downstream distance along the river: width (A), lateral migration (B), bar area (C), bar volume (D). The width and lateral migration of the river was measured in GIS using the Planform Statistics Tool and banks extracted from 2009 aerial photographs (*Lauer*, 2006). For this analysis the width was measured from the vegetation edge, near the cut bank, to the vegetation edge bounding the outer edge of the point bar. The bars are the same as those in Figure 3.27 and 28. Downstream of the dam the channel width is narrow, migration rate is low, and bar size is small. As the dam influence tapers out in the transition between Zone One and Zone Two the channel widens, migration increases and bars become larger. As the channel descends into Zone Three the channel narrows, migration decreases, and bar areas diminish again.

A description of the planform geometry is incomplete without considering the river curvature (Fig. 3.34). The low radius of curvature values represent the apices of the bends, where the radii of curvature are smallest the bends are tightest. The high values represent inflection points between the bends where the channel is straightest. There is a general downstream trend that shows the bends in Zone One have larger radius of curvature, meaning that the bends are straighter. As the river transitions into Zone Two the radius of curvature values decrease, indicating tighter bends. Between Zone Two and

Zone Three there is no notable difference in the channel radii of curvature (Fig. 3.34) even though bar shape and size change considerably (Fig. 3.27 and 28).

**Lateral Migration Rates of Channel Bends**

The lateral migration rates for the lower Trinity River vary by zone. The measured rates of lateral migration are summarized in Table 3.2 and Figure 3.33b. Zone Two's migration rate is roughly twice as large as zone's one and three. The migration rate is low near the dam and increases with distance downstream. The rates remain consistently high through Zone Two. The migration rates decrease again as the river approaches Trinity Bay. A comparison of the graphs in Figure 3.30 shows how the spatial change in migration rates (Fig. 3.33b) corresponds with spatial change the channel planform geometry. Where bars have small areas (Fig. 3.33c) and volumes (Fig. 3.33d), the river's bankfull width is narrow (Fig. 3.33a) and the channel migration rate is lower.

Zone Two displays two different styles of channel migration: persistent outward and downstream translation, and abrupt response to an upstream channel cutoff. Bend translation occurs as sediment is eroded from the outer bank of a bend and sediment is deposited on the inner bank of a bend. As a bend translates downstream the amplitude grows until it eventually experiences a cutoff (*Brice*, 1974; *Hooke*, 2003). The cutoff straightens the river, altering the momentum of the water and introducing additional sediment into the system causing downstream migration to accelerate in response (*Zinger et al.*, 2011).

Zone One and Zone Three exhibit only the translation style of migration. Zone One and Zone Three migrate substantially less per year (Table 3.2). The Zone One portion of the river migrates approximately 2.1 meters per year and shows signs of

straightening. In Zone Three, the river migrates approximately 1.5 meters per year. Figure 3.1 provides examples of the time series centerlines from each zone's highlighting the different rates of migration. The centerlines in Zone One (Fig. 3.1b) and Zone Three (Fig. 3.1d) do not show significant change channel location over the 60 years that were surveyed. The centerlines from Zone Two (Fig. 3.1c) show an abundant amount of lateral migration.

## ANALYSIS

Trends in the river's physical characteristics are well defined the by observational data. Distinct trends are present the river profile, grain-size, cross sections, geometry, and lateral motion. The three zones of the river could be identified through graphs of the profile (Fig. 3.8 and 9), grain-size (Fig. 3.13 and 14), channel relief, symmetry and depth (Fig. 3.19, 21, 22, 23, 24, 25, and 26), bar size and slope (Fig. 3.27, 28 and 29), channel width (Fig.33), channel curvature (Fig. 3.34), and migration rate (Fig. 3.33). The three geomorphic zones impacted the trends in these variables are the result of three styles of sediment transport.

In Zone One, downstream of the dam the sediment transport is well below capacity creation and erosional system. Approximately 50 to 60 river kilometers from the dam sediment transport capacity is regained, marking the start of Zone Two. In this zone the sediment transport is at relative equilibrium. The aerial photographs show over 60 years the width of the channel has remained relatively constant through Zone Two.

These consistencies suggest the sediment flux entering this zone is relatively equal to the sediment flux exiting this zone. From a mass balance prospective, the amount of sediment entering the system is equal to the amount of sediment leaving the system. In Zone Three sediment transport decreases, in coordination with a greater flow depth in the backwater zone. To gain insight into the trends seen along the course of the river, data was partitioned and analyzed in two fashions: by bends and by bars.

**Bends**

I propose that the bends in each of the three zones function differently due to a variation in the local sediment transport. Isolating the bends allowed me to study their temporal evolution. Figure 3.34 shows the radius of curvature as of the channel as a function of downstream distance calculated by the Meanders Code (*Peyret*, 2011). The minimum points of radius of curvature show the apices of the bends. The maximum radiuses of curvature values represent the points of inflection. When the inflection points were identified the bends were isolated for further analysis of the geometric and mechanical relationships. Once the bends were isolated several trends became obvious; such as, the profile, planimetric, cross-sectional and granular observations each zone displayed unique bend characteristics relating to the local river mechanics.

Since the dam's construction the upstream portion of the river has straightened, causing a loss of bends and an increase in the length of remaining bends (Fig. 3.35). The number of bends in Zone One decreased from 53 bends to 43 bends between 1965 and 2009, nearly a 20% decrease in bend number (Fig. 3.36). An example of the straightening occurring in Zone One is shown in Figure 3.37. This image of the channel centerlines was taken approximately 34 river kilometers from Livingston Dam. Prior to

the Dam impoundment, in 1952 (purple centerline) there were seven bends along this stretch of the river. In 2009, shown in red, there were five bends.

Figure 3.35a also shows an increase in the length of bends in Zone Two. This is due to naturally occurring bend cutoffs and the resulting straightening of the channel. When a cutoff occurred, the straightened portion of the river that was produced was excluded from the dataset to simplify the analysis, as it was difficult to identify new bends within a recently cutoff reach of the river. Evidence of this is given in Figure 3.35b. Unlike Zone One, the change of bend lengths in Zone Two is often associated with major events (cutoffs are represented with high spikes in the change in length), instead of the evenly distributed trends seen in Zone One and Three.

In both Figure 3.35a and b there is very little change in the length of bends in Zone Three. This portion of the river migrates, although less than Zone Two. Figure 3.38 shows the change in the median radius of curvature per bend between each of the four surveys. Like Zone One and Zone Two, Zone Three bends are changing shape. The style of morphology of Zone Three bends is unique relative to the other zones in that the bends are not changing length; instead they experience a fairly steady, relatively slow migration, with no major cutoff events or major straightening. An example of this is shown in Figure 3.39. The location of this image is 146 river kilometers downstream of Livingston Dam. Each survey centerline shows migration, however, it is a steady marching style of migration best characterized as translation.

Many studies have suggested a correlation between bend radius of curvature and channel migration (*Furbish*, 1988 and 1991; *Havery*, 1989; *Hooke*, 2003; *Lagasse et al*., 2004). When considering the entire study area, it is difficult to see a correlation between

radius of curvature and migration (Fig. 3.40). If only Zone Two is considered, and abnormal bends are removed (i.e. bends that are being influenced by bridges or tributaries), the correlation becomes better defined. Figure 3.41 shows the logarithmic relationship between minimum radius of curvature within a bend and the median lateral migration. When the bends are tighter, the migration rate is higher.

It has also been shown that width can play an influential role in the rate of channel migration (*Hooke*, 2003; *Lagasse et al*., 2004; Fig. 3.4). Figure 3.42 shows a positive correlation between width and migration. Based on the width and migration trends shown in Figure 3.33, this correlation is expected. In Zone Two, shown in blue in Figure 3.42, the migration rate and width are highest. Close observation of the three colors/shapes representing the various zones show that the relationship between width and migration varies with each zone.

The sediment transport varies within each zone, resulting in different relationships between the geometric variables. These differences are represented in the variation of the trends in each zone. Figure 3.43 and 44 show the relationships between radius of curvature and channel width. In Zone One there is a positive correlation between channel width and radius of curvature, meaning that the river is wider where the channel is straight, or at the point of bend inflection (Fig. 3.43a). There are two small areas in Zone Two that also have a positive radius of curvature to width correlation; these locations are where bridges cross the river. In Zone Two and Three the correlation between channel width and radius of curvature is negative, meaning that channel is widest at the bend apex (Fig. 3.44). The relationship prevalent in Zone Two and Zone Three is consistent with the typical style of migration depicted in Figure 3.2 and the trends shown in Figure 3.33.

Figure 3.45 shows the relationship between median migration (between 1996 and 2009) and the minimum radius of curvature divided by median width for each bend in Zone Two. Compared with Figure 3.41, migration has a better correlation to radius of curvature over width, than just width alone. Migration is generally greatest when the radius of curvature is small (the bend is tight) and the width of the channel is large (there is likely a bar).

Figure 3.46a shows the same data plotted within an envelope. The shape of the data envelope is very similar to the data presented by previous studies (Fig. 3.4). However, the Trinity River data suggests that envelope represents a maximum migration amount, not a predictive value. Figure 3.46b shows the same results calculated for each of the transects along the entire study area.

Local influences, such as neighboring bends and geologic anomalies, lead to a range in migration rate for bends with the same radius of curvature. Wide tight bends may have a higher potential for migration, but additional influences can limit a bends ability to migrate. In Figure 3.47 there are several bends with high radii of curvature. The most upstream bends shown are migrating rapidly, while the subsequent bends, with comparable radii of curvature and width are migrating more slowly. This section of the river is located 125 kilometers downstream of Livingston Dam. This shows migration is not solely function of the radius of curvature, but rather the radius of curvature characterizes the migration potential for a bend.

Figure 3.48 presents the same data from Zone Two as a probability plot for migration at different values for radius of curvature divided by channel width. The envelope clearly defines an upper limit to all of the possible migration rates. Bends with

a small radius of curvature to width relationship have a greater range of potential lateral migration distances than bends with large values for radius of curvature to width. Bends with a large radius of curvature to width relationship will only migrate within a small window of lateral migration distances. The darker the color in Figure 3.48, the higher the probability is for that migration-radius of curvature-width combination.

Figure 3.49 shows bend migration as a function of radius of curvature divided by width for all three zones. Each zone exhibits a unique envelope to its measured values that I propose is linked to the sediment transport dynamics for that portion of the river. The bends in Zone One and Three do not have the same migration potential as those in Zone Two. The radius of curvature to width relationship for Zone One is different that the relationship in Zone Two and Three (Fig. 3.43 and 44), which is the cause for the unique shape of the envelope in Zone One.

An additional analysis was done to compare radius of curvature and downstream radius of curvature. While it is understood that bends interact, influencing the other migration rates of bends upstream and downstream, I was unable to capture that in this data analysis. The image in Figure 3.50 shows the radius of curvature plus a change in the radius of curvature plotted against migration, described in Eqn 7. In this equation radius of curvature, *Rc*, is added to the change in *Rc* in the downstream direction over centerline length between bends, *Cl*. Althought it is widely believed that bends impact upstream and downstream migration rates (*Furbish*, 1991) there is no discernible trend.

$$\eta = aRc + b\left(\frac{\partial Rc}{\partial Cl}\right) \qquad \textit{(Eq. 7)}$$

**Bars**

I propose that the size and shape of the bars is tied to the style of sediment transport occurring in each zone. The sediment transport is also linked to the grain-size distribution. The survey of grain samples across the zone transitions showed a general fining trend in the downstream direction. While the bar sizes changes from Zone One to Zone Two and Zone Two to Zone Three, the grain sizes composing the bars also change (Fig. 3.13 and 14).

The coarser grains of the bar surfaces in Zone One are connected with net bed erosion of this section of river. Water leaving the dam is below sediment transport capacity. The flow scours sediment from the channel to reestablish sediment transport capacity, incising the channel and deflating the bars. While sediment is being provided from the channel walls and tributaries the vast majority is sourced from the bed (Table 3.2). The finest sediment are quickly transported downstream and larger gravels and rocks are left behind on the bar surfaces. In extreme case the bars were topped with petrified wood and fossilized bone. In Zone Two the point bars are connected with capacity transport of sand.

As the river flows into the backwater zone the channel deepens to adjust to the sea level (Fig. 3.3). The deepening of the channel results in a change in the shear stress transporting sediment along the channel (see *Previous Work* section of this chapter). The larger grains fall out of transport and only the finest grains are transported downstream. Zone Three has the steepest slopes, suggesting a change in the process of bar construction in the backwater-dominated zone.

There appears to be a fundamental grain-size distribution for sand in bars that remains fairly constant through the course of the river. Figures 3.51a, b and c show the grain-size distribution of sand and gravel on a bar from Zone One, Two and Three from the 2012 grain sample survey. In each case the sand, shown in blue, has the same distribution. This sand distribution can therefore be subtracted from each bar sample to estimate the coarse fraction present at that location on that bar. The difference between the red line (gravel) and the blue line (sand) represent the amount of gravel enrichment. Bar Four is approximately 33 river kilometers from Livingston Dam. The samples from this bar contained a substantial amount of larger grains (2% at 7mm). Bar Nine is located 130 river kilometers from Livingston Dam. This bar had a higher percentage of gravel than Bar Four, but the gravel size is finer. Finally, Bar Sixteen was the most downstream sampled bar, 145 river kilometers from Livingston Dam. This bar was nearly all sand. By this distance downstream the gravel has largely been removed from the transport system.

With further analysis it became evident that the trend is not simply captured by a central moment of the grain-size distributions bar surfaces (i.e., mean, median). The distributions are effectively bimodel, containing both a sand and coarse fraction. Figure 3.52a shows the fraction of gravel on a bar as a function of downstream distance. There is a general downstream trend of decreasing gravel content with outliers that are likely due to local sediment inputs from gravel deposits mined from the cut banks (Fig. 3.7). Bars with abnormally high percentages of gravel also contained larger clasts (Fig. 3.52b). The red line shows the mean grain-size of the gravel. The blue area surrounding the red line represents one standard deviation of the gravel size. The spikes in the gravel grain-size distribution correspond with peaks in the sample percentage of gravel distribution

(Fig. 3.52a). The bars laden with gravel also contain larger gravel clasts. Notice that the transition to Zone Three is marked by bars containing no gravel. The coarsest sediment is being selectively removed from the flow as the river approaches the coast.

Additionally, the bars sizes play a critical role in determining migration rate. Channel width is linked to the rate of channel-bend migration in the Trinity River because local width captures size of point bars which effect bend migration (Fig. 3.33). Point bars form where the width of the channel is greatest (Fig. 3.26). This trend is evident when comparing the portion of the river channel occupied by the point bar. When the bars occupy a greater ratio of the river cross section, the migration rate is higher. The larger bars of Zone Two topographically steer the flow of the channel towards the outer bank aiding in the channel migration. Figure 3.53 shows the positive correlation between bar area and lateral migration. As the bar area increases there is an increase in the lateral migration.

## DISCUSSION

### ZONE 1 – Dam Influenced

Since the impoundment of Livingston Dam the upstream zone of the study area has incised at least five to seven meters (Fig. 3.8). Livingston Reservoir impounds sand and gravel and as a result the water leaving the Dam is sediment starved. This condition leads to incision of the channel bed downstream of the dam until the flow regains sediment capacity. The bars in this zone are topographically deflated and enriched in gravel (Fig. 3.13, 28, 51, and 52). The sediment disequilibrium results in

erosion of the bed, but also creates other physical changes in the cross sections of channel. The volume and area of the bars decreases (Fig. 3.27 and 28), the channel is narrowing (Fig. 3.33), and the channel is straightening through the disappearance of bends through time (Fig. 3.35a). Sediment is being transported downstream, but is not being replenished by an equal influx of sediment. As the bars become less pronounced the bends become less asymmetric (Fig. 3.24). Through the data displayed in Figure 3.26 we know that the bars in Zone One take up less of the river cross sectional width than in Zone Two. The deflation of the bars changes the mechanics within the bends by decreasing the topographic steering and reducing lateral channel migration (Fig. 3.33b and 53).

As the number of channel bends decrease the length of the existing bends increases. Graphs in Figure 3.35b and 36 show the changes in bend length for the entire Lower Trinity River. Figure 3.35b shows the average length per bend by zone for each of the surveys. The graph shows a clear increase for the length of bends in Zone One and Two. The bends in Zone One increase by about 231 meters per bend. The increase in Zone Two is misleading. The length increase is largely due to cutoffs along the channel. As cutoffs occurred the new bends were not able to be incorporated into this particular analysis. By not including the resultant bends of cutoffs in the analysis the bend length in Zone Two remained fairly constant. This is shown in Figure 3.32b through a plot of the change in the length of individual bends. This graph shows the change in bend length between every survey plotted as a function of downstream distance. The small scatter in Zone One is due to straightening of the river by the dam. The extreme scatter in Zone Two is due to migration and river cutoffs. In Zone three there is very little change in bend length.

In analyzing the observations there is a group of bends and bars, less than 10 river kilometers from the Dam, that do not follow these trends. These anomalous bars are not likely naturally occurring. It is more likely that this group of bars is the byproduct of river alterations near the Dam.

**ZONE 3 – Bay Influenced**

As the river approaches the Trinity Bay the channel physically changes. The effects of the backwater hydraulics alter the river profile (Fig. 3.8) and the surface water profile (Fig. 3.9 and 10). The channel deepens to adjust to flowing into the Trinity Bay (Fig. 3.3 21 and 23). Like Zone One, the bankfull width of the channel narrows, the migration rate recedes (Fig. 3.38), the bar area and volume decrease (Fig. 3.27 and 28), the channel becomes more symmetrical (Fig. 3.24 and 25), and the bars make up a smaller percentage of the cross channel width (Fig. 3.26). However, the unlike Zone One the channel banks lower (Fig. 3.19), the depth of the channel increases (Fig. 3.21) and the river does not straighten over time. In Zone Three the bend lengths change very little (Fig. 3.35). The mechanics driving these changes differ from those in Zone One. Zone One's morphology is driven by a depletion of sediment, while the changes that occur in Zone Three are driven by the effect of the Bay and an associated change in sediment transport in this zone. As a result, the bars are steeper, yet smaller and finer-grained than bars in Zone 2 (Fig. 3.14b, 27, 28, 29 and 51).

Although the sediment transport is greatly reduced during mean flow in the backwater zone (Nittrouer et al., 2011, 2012), some channel migration is still occurs through time. With the change in the style of sediment transport the channel migration is limited to slow marching general translation. Cutoffs and straightenings generally do not

occur in this zone. This is evident from Figures 3.35b and 36. Figure 3.35b shows no major changes in bend length, suggesting no major morphological events. In Figure 3.39 there is an example of a chain of three bends slowly migrating. This example was taken from river kilometer 146, well into Zone Three.

The change in channel depth in Zone Three results in an increase in the cross sectional area of the channel (Fig. 3.23). Assuming a relatively constant discharge along the profile of the river during regular flow, the depth and cross sectional area are greater in the downstream reach of the river. The constant discharge and higher cross sectional area suggest that the velocity would be lowest where the cross sectional area is greatest—in the backwater zone. At flood stage the depth and cross sectional area are lowest in the backwater zone. Again assuming the discharge of the river is fairly constant from upstream to downstream, the decrease in cross sectional area suggests an increase in flow velocity. The distribution of the flow along the profile of the river reverses during high flow. This matches the findings in the lower Mississippi River, and may describe a general property of backwater systems (*Nittrouer et al.*, 2012).

Additionally, it should be noted that there has been aggradation and the filling in of a substantial dip in this zone between 1939 and 2007 (Fig. 3.8). This difference can potentially be explained by several scenarios. Around 1939 the Army Corps of Engineers, partnering with other State level organizations, attempted to convert the Trinity River into a canal system to Dallas (Fig. 3.53). The project never came to fruition due to the active river bed and lack of funding halted the project. However, dredging of the channel may have created the dip anomaly in the survey. Additionally, since 1939, a water outtake has been constructed near river kilometer 140. The water is sold to the Neches River basin for irrigation. This outtake could influence the morphology of the

profile. Finally, the difference in the two profiles in Zone Three could be tied to progradation of the Trinity River delta.

**ZONE 2 – Freely Meandering**

In Zone Two there is no influence from the Bay or the Dam, the river has normal flow conditions. The river is able to meander freely, cutting through predominately Quaternary fluvial deposits (Fig. 3.5). This zone is characterized by a linear channel profile (Fig. 3.8), large bars (Fig. 3.27, 28 and 31), a wider channel outer bank to outer bank (Fig. 3.33a), and a higher rate of migration (Fig. 3.33b).

I propose that bars help to drive the river migration by forcing high velocity core of the flow toward the outer bank of a bend. Less bar area means less bar-induced topographic steering within a bend, resulting in a lower migration rate. The large bars fill a greater portion of the channel compared to other zones (Fig. 3.26) and they create a strongly asymmetric channel (Fig. 3.24). The large bars route the flow around the bends and towards the outer banks, aiding the rapid migration rate of this portion of the river.

Predicting future channel migration patterns is difficult due a myriad of factors driving and influencing channel adjustments, as well as measuring the channel adjustments on an appropriate timescale to capture the lateral shifting without significant deformation of each bend. Several previous studies have investigated the relationship between channel migration and radius of curvature, and channel migration and radius of curvature divided by the channel width. When comparing migration to the channel radius of curvature for the entire channel, from Livingston Dam to Trinity Bay, there is no desirable trend (Fig. 3.40). When the same comparison is made for only Zone Two a

weak trend emerges (Fig 41). When width of the channel (vegetation line to vegetation line) was accounted for in this comparison the relationship showed an even better correlation. Figure 3.45 shows migration as a function of minimum radius of curvature over channel width within Zone Two. The plot shows a negative correlation, suggesting that with the channel has a smaller radius of curvature to width relationship the channel has a greater migration rate. The envelope of the data (Fig. 3.46) has a shape similar to those found in previous studies (Fig. 3.4); however, the majority of the data does not lie on the envelope boundary. This envelope varies by river zone (Fig. 3.49). Figure 3.47 shows examples of bends in Zone Two with similar radii of curvature-to-widths, but very different migration rates. The envelope in migration rate defines the total possible range of observed rates for any given value of channel radius of curvature divided by channel width (Fig. 3.48 ).

## CONCLUSIONS

Through the 180 river kilometers of the study area the Lower Trinity River meanders through 177 bends. These bends were characterized using aerial photographs spanning the past 60 years, as well as bathymetric and field surveys of the entire channel. In analyzing the river data it became obvious that the river exhibits three styles of channel geometry and behavior. The three channel zones correspond to spatial change in sediment transport properties.

The upstream zone exhibits straightening and is defined by channel-bed incision, small bars, and relatively slows rates of lateral channel migration. The characteristics of

this portion of the channel are linked to sand retention behind Livingston Dam. Eventually the channel flow scours enough sediment from the channel bed to reestablish a transport capacity for sand in the river, marking the transition to the central zone. This second section is defined by fully developed point bars and a high rate of lateral channel migration. The second zone continues until the sediment transport is influenced by the backwater effect of Trinity Bay, a third segment. This backwater zone is characterized by very small point bars, steep channel walls, and low channel migration rates. Migration in this zone is gradual, with no cutoffs or rapid straightening.

**NOTATION**

$C_f$ = General non-dimensional friction factor

$D_{16}$ =grain size in the 16%

$D_{50}$ = Mean grain size

$D_{84}$ =grain size in the 84%

$E$ = coefficient of bank erosion

$g$ = gravity (9.81 $m^2/s$)

$H$ = depth

$L_b$ = backwater length

$\eta$= positive migration, normal to stream direction$\dot{\eta}$= positive migration rate, normal to stream direction

$S$ = slope

$U$ = Cross-sectionally averaged flow velocity

$\Delta U$ = half the mean streamwise velocity

$\rho$ = density of water (1000 $kg/m^3$)

$\tau_b$ = shear stress

**FIGURES**

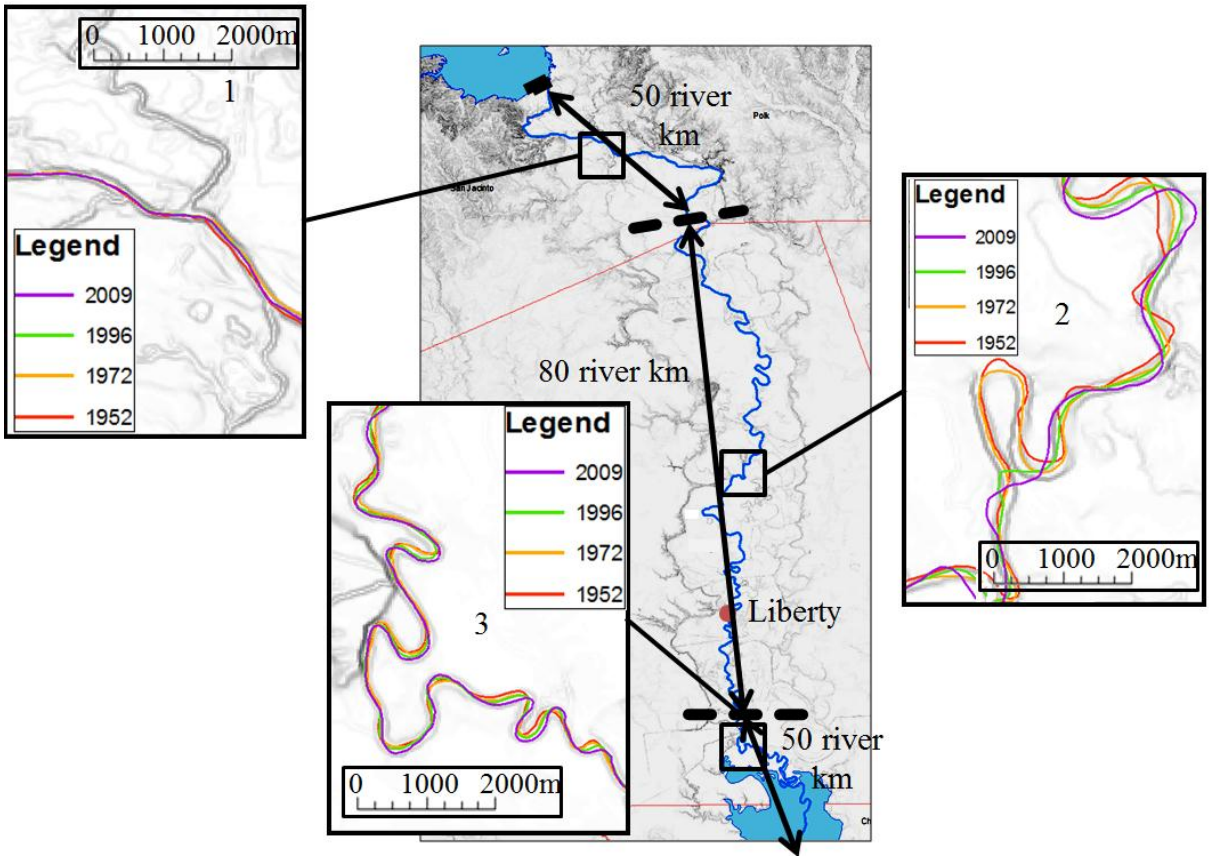


Figure 3.1: (A) Map of the entire study area of the lower Trinity River. The river is shown in blue on top of a slope map of the surrounding area. The red dashed lines are rough estimates of the gradual transitions between the three geomorphic zones. (B) A smaller scale portion of the first flow regime, downstream of the dam, Zone One. (C) A smaller scale portion of the second flow regime, the laterally migrating portion of the lower Trinity, Zone Two. (D) Smaller scale portion of the third flow regime, the backwater influenced Zone Three. The colored lines show the river's centerlines traced from 1952, 1972, 1996, and 2009 aerial photographs.

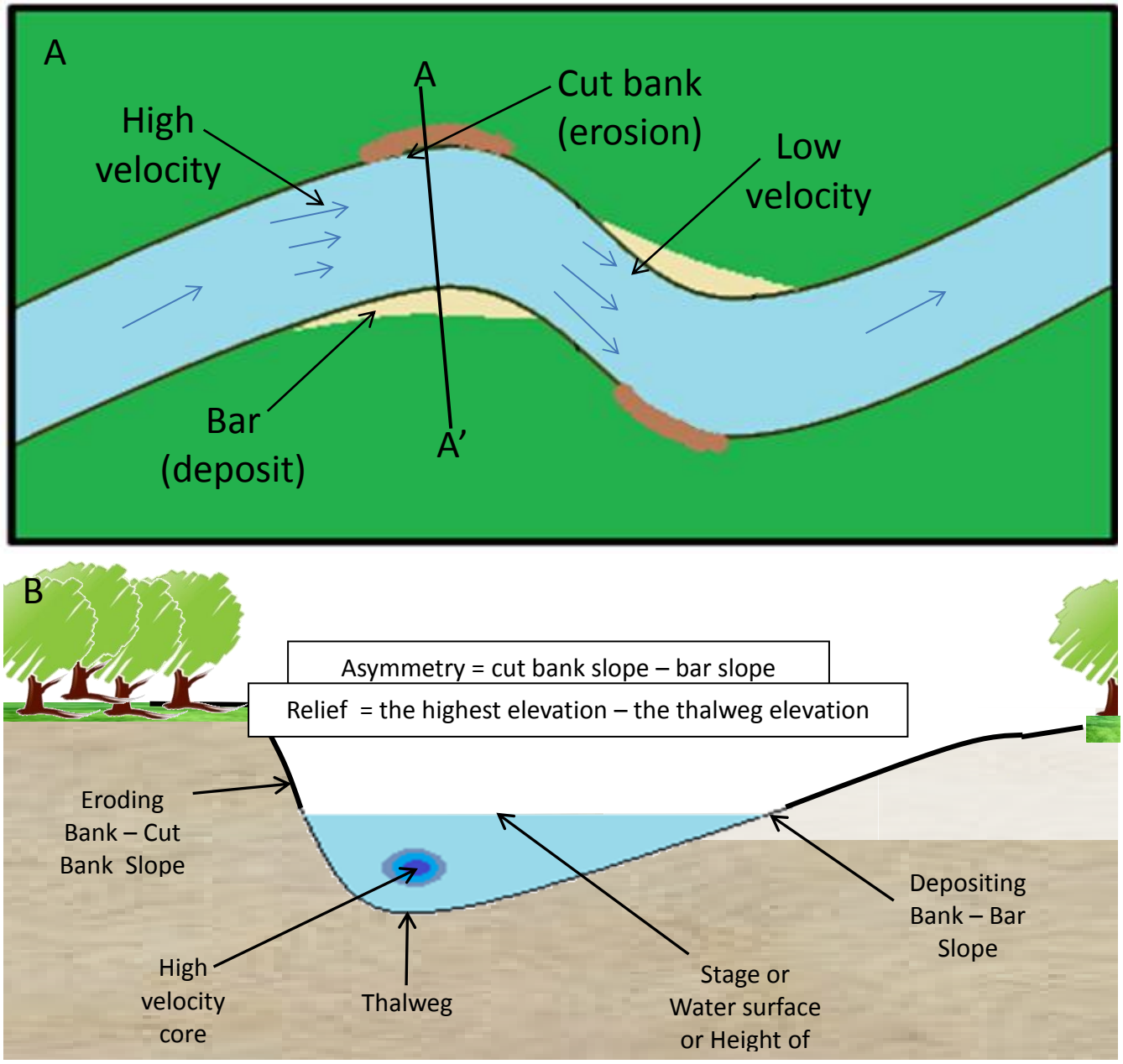


Figure 3.2: (A) A river flowing from left to right through two bends. The features of the bend are labeled. Across the center of the first bend is a transect labeled A-A'. (B) corresponding transect looking downstream. The images show the planform and cross-sectional geometric relationship present in a laterally migrating river bend.

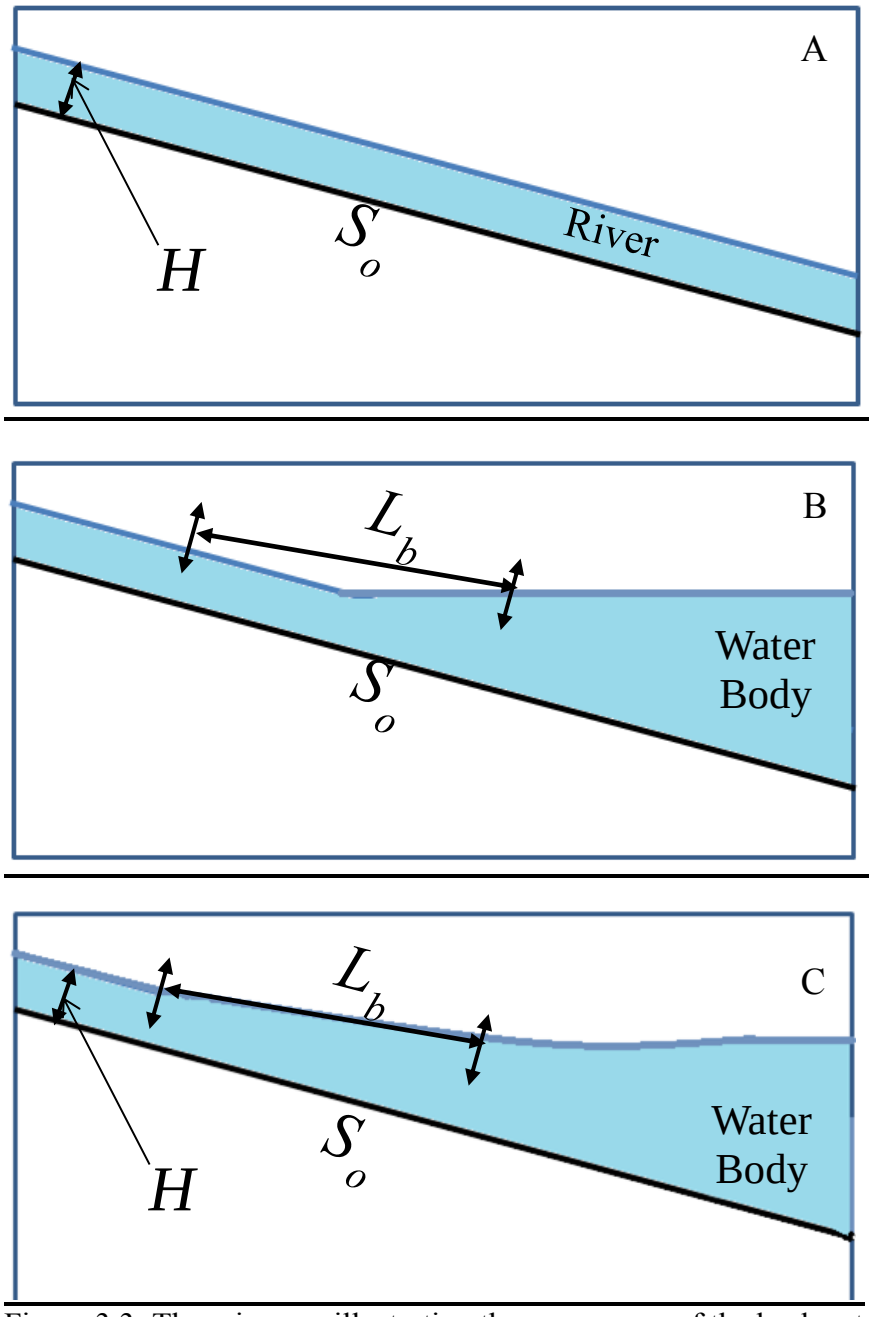


Figure 3.3: Three images illustrating the occurrence of the backwater length. (A)Normal flow where the river bed slope and the water surface slope are parallel. (B) As the river flows into a standing water body (C). The zone of hydraulic adjustment between conditions of normal flow and the standing body of water is the backwater zone. The length of the zone is $L_b$.

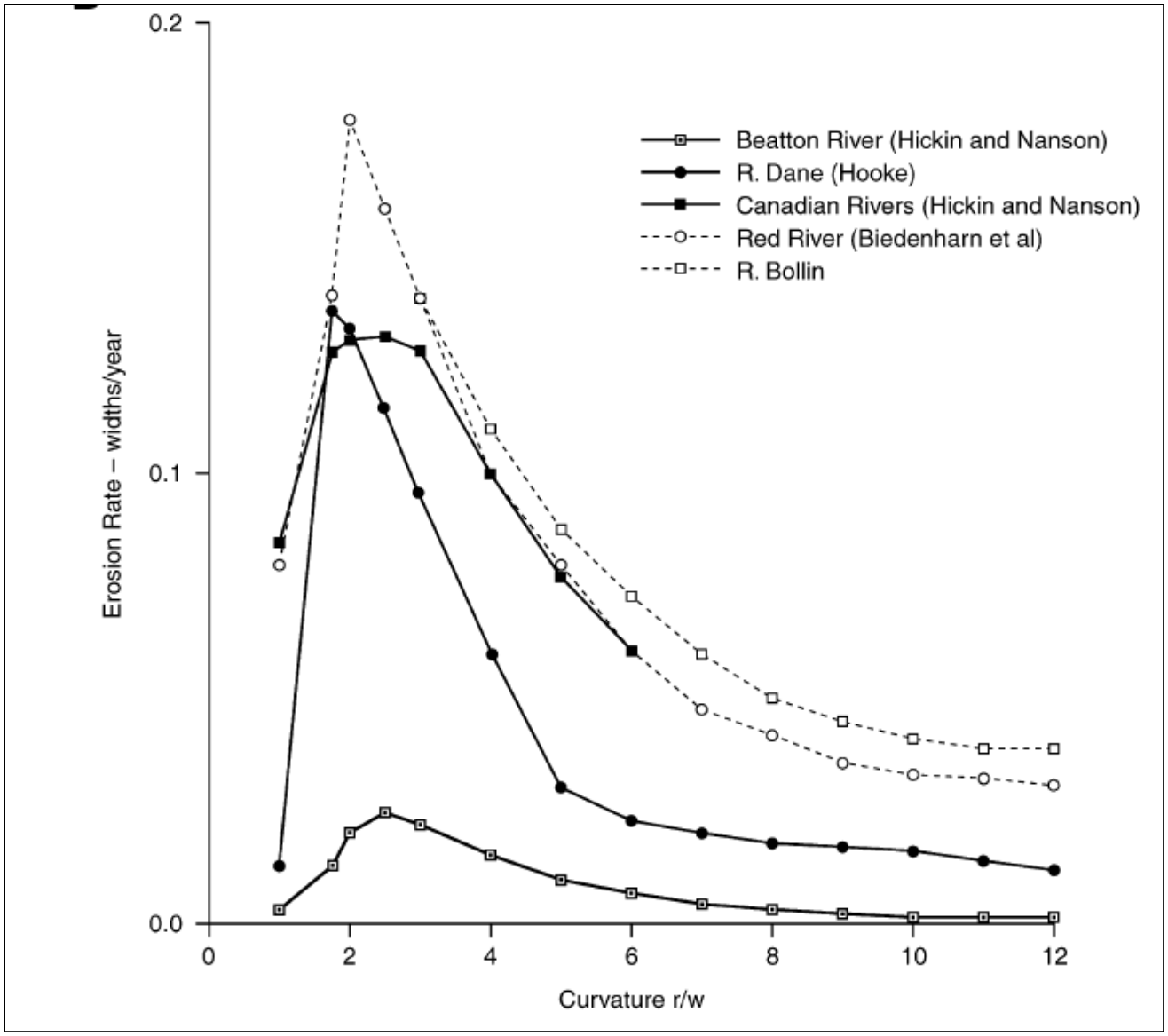


Figure 3.4: Relationship between channel bank erosion rate as a function of channel curvature divided by channel width (*Hooke*, 2007).

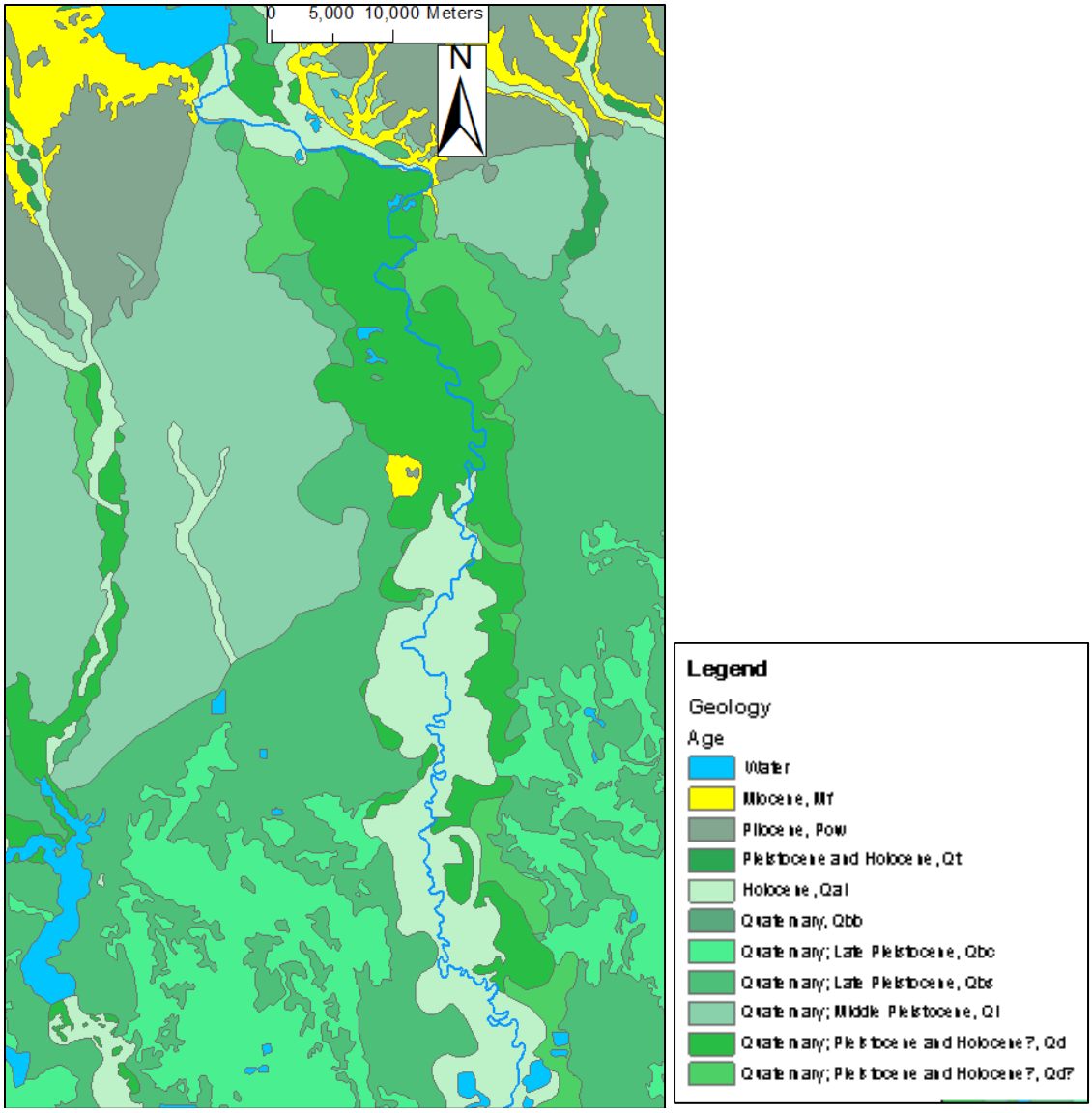


Figure 3.5: Geologic map of the study area. Nearly the entire region is composed of Quaternary deposits shown in green. The blue marks major water bodies for spatial reference. The northern portion of the map has some deposits that are Pliocene and Miocene in age.

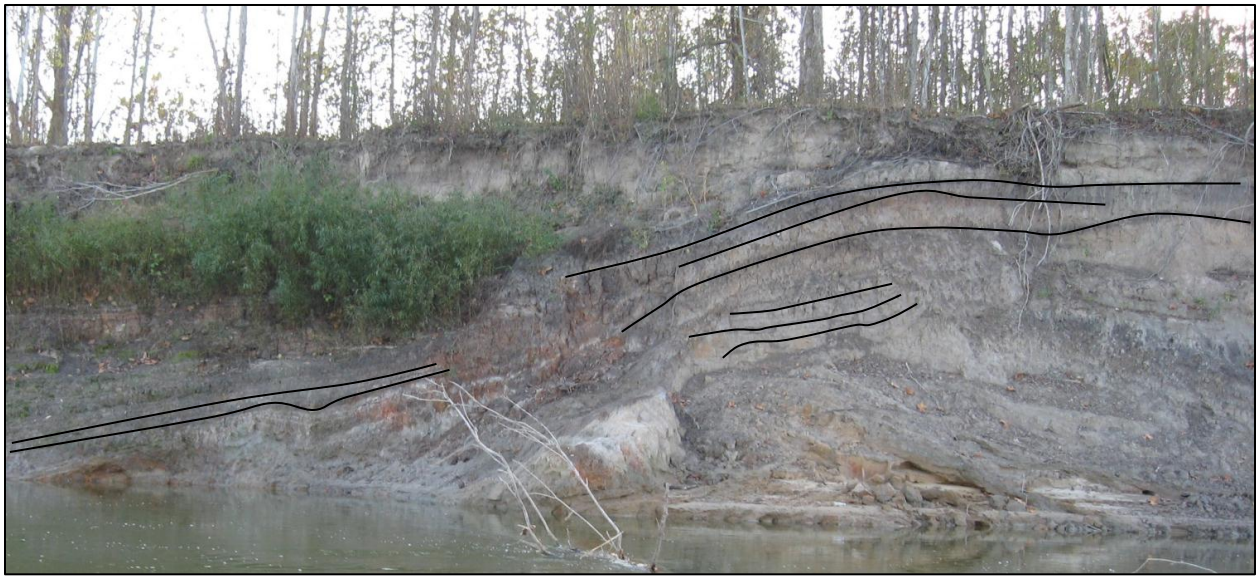

Figure3. 6: A cutbank in Zone Two, approximately 118,000 river meters from Livingston Dam. The height of the bank is approximately 6.5 meters. The black lines highlight strata from previous channel deposits.

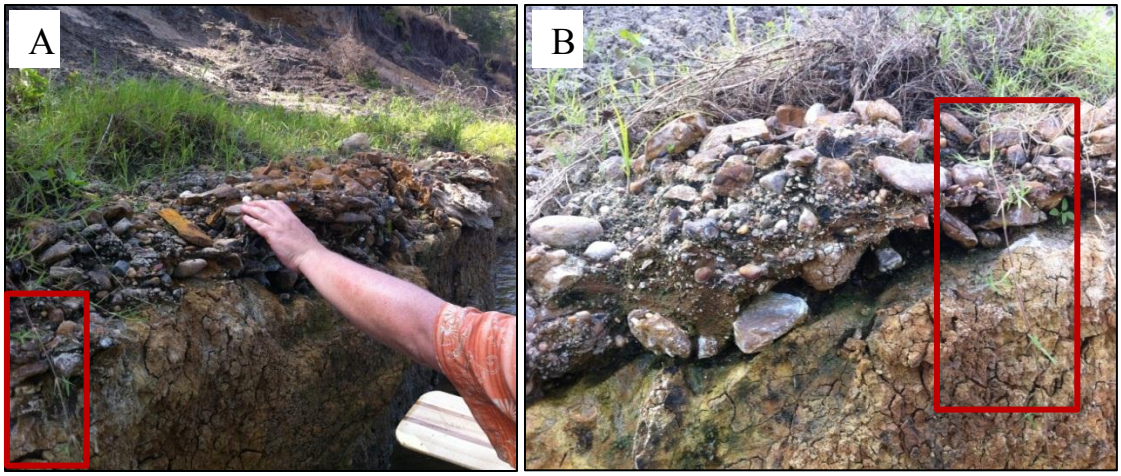


Figure 3.7: Weakly cemented conglomerate with a hand and arm for scale. The red box in the lower left corner of (A) corresponds with the box in (B). The conglomerate acts as a source for gravel in the river as it appears to rapidly disintegrate into its constituent grains when eroded from the channel banks and bed. This outcrop of the conglomerate is located about 55,000 meters downstream of Livingston Dam.

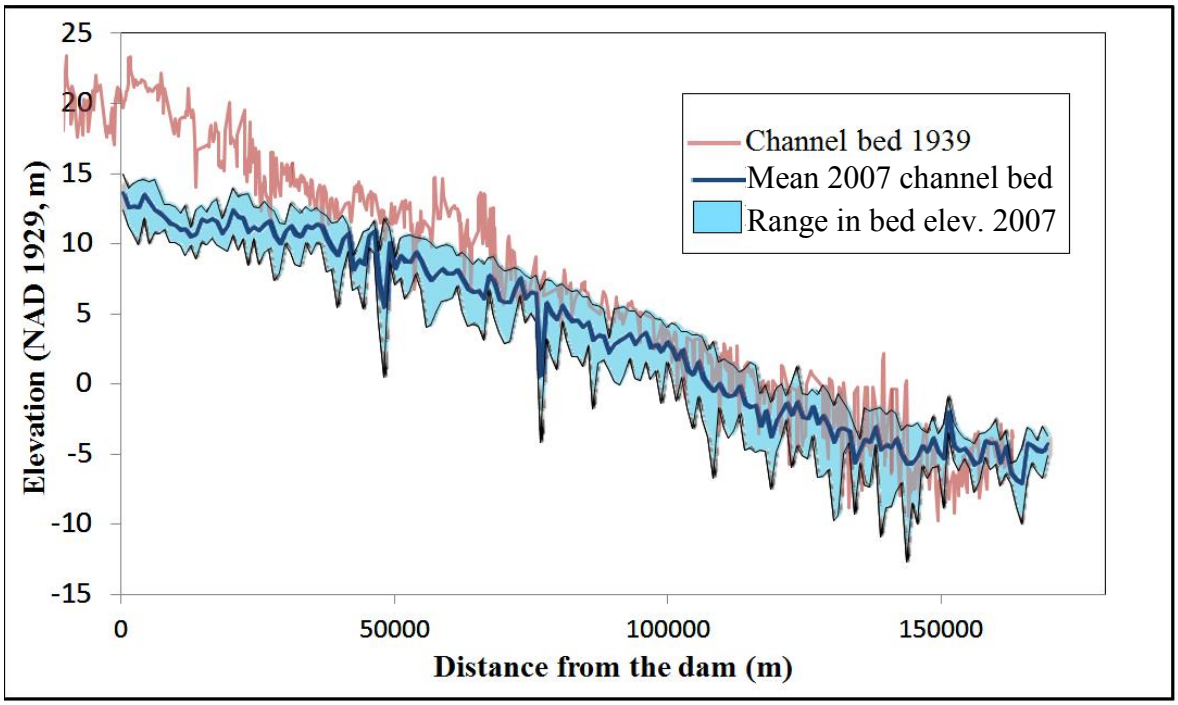


Figure 3.8: Super-imposed channel profiles shows the two profiles together. The red line marks the measured river channel profile in 1939. This data was collected by the U.S. Army Corps of Engineers. The blue line marks the measured river channel profile in 2007. This data was collected by the Texas Parks and Wildlife Department. There has been six to seven meters of incision since dam impoundment. The channel re-establishes a linear profile similar to 1939 form at 50,000-60,000 meters downstream of the dam.

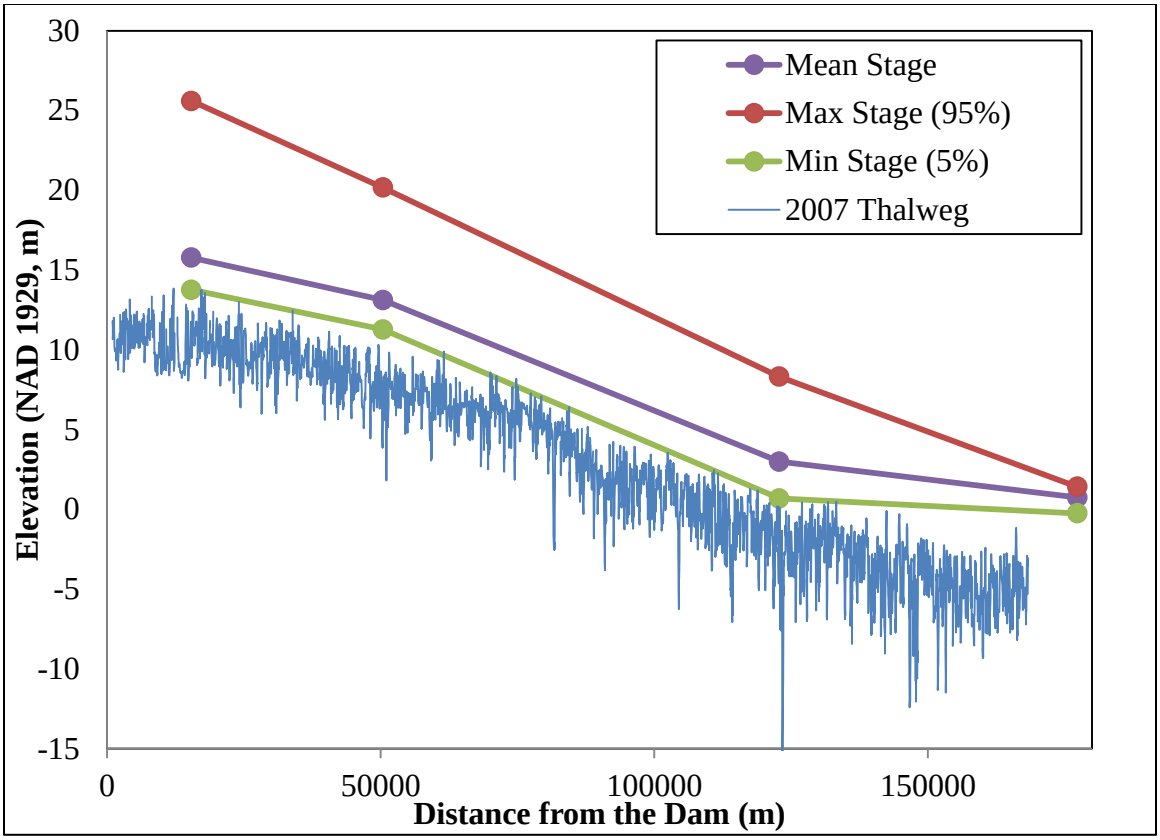


Figure 3.9: The three water surface profiles were created from the USGS gages stations along the lower Trinity River, and the 2007 channel bottom profile. The water surface profiles are based on 20 years of USGS stage gage data from four USGS river gages. The mean value represents the mean stage value for 20 years. The minium is the 5% probability stage (28 cubic meters per second at Goodrich, TX), the mean stage is the 50% probability (162 cubic meters per second at Goodrich, TX) and the maximum is the 95% probability stage (2381 cubic meters per second at Goodrich, TX). The stage values are from USGS gages at Goodrich (USGS gage number 08066250), Romayor (USGS gage number 08066500), Liberty (USGS gage number 08067000) and Wallisville (USGSgage number 08067252). Several of the extreme thalweg values represent bridges; such as, Romayor, TX near river meter 50,000, Farm Rd. 787 at river meter 80,000, a rail bridge at river meter 110,000, and Liberty, TX near river meter 120,000.

| Survey Dates | |
|---|---|
| Posted Date | Observed Dates |
| 1952 | 10/18/1952<br>11/12/1952 |
| 1972 | 11/4/1968<br>1/14/1972 |
| 1996 | 9/13/1995<br>1/19/1995 |
| 2009 | 1/23/2008<br>2/1/2008 |

Table 3.1: aerial photographs collected by the Texas Natural Resource Information System (TNRIS) for the Trinity River over approximately 60 years were used for this study. The surveys were finalized in 1952, 1972, 1996 and 2009. However, the survey date was slightly earlier in some cases.

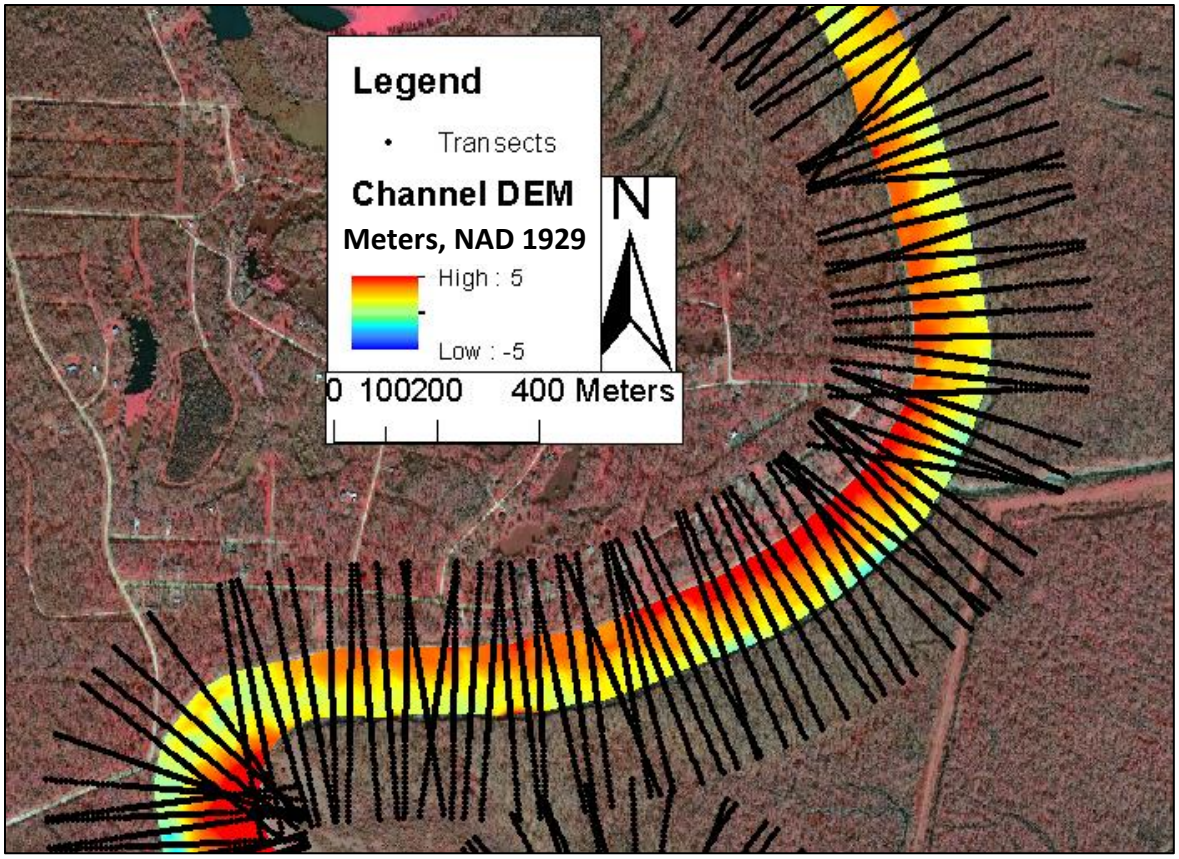

Figure 3.10: The transect points overlain on the DEM were used to produce cross sections of the river. The example of the transects shown above are located approximately 112,000 river meters from Livingston Dam.

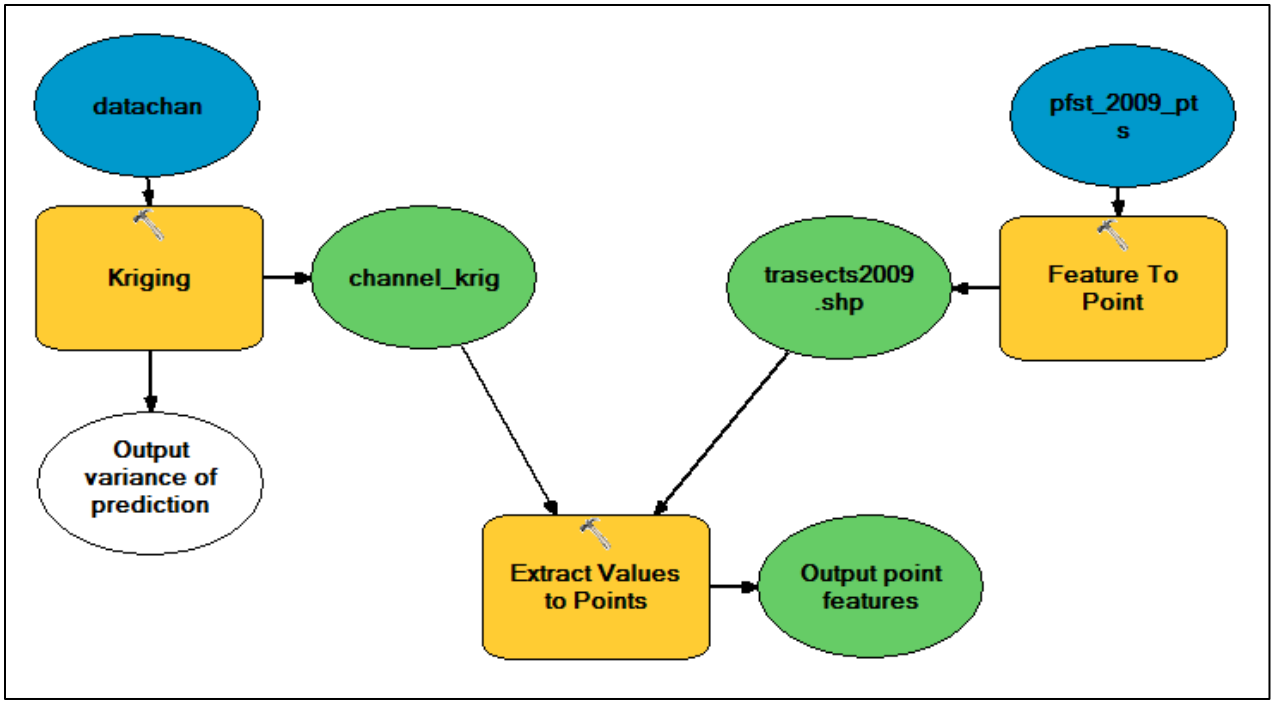


Figure 3.11: The work flow for creating transects of the river using in ArcGIS. Starting at the upper, a raster surface of the channel was created by applying a Kriging spatial average to the bathymetry data of the channel. On the upper right, 5001perpendicularly oriented channel cross sections were turned into points. The points were then used to extract the values from the channel raster. The transect points were labeled by cross sectional distance and a unique line number for analysis.

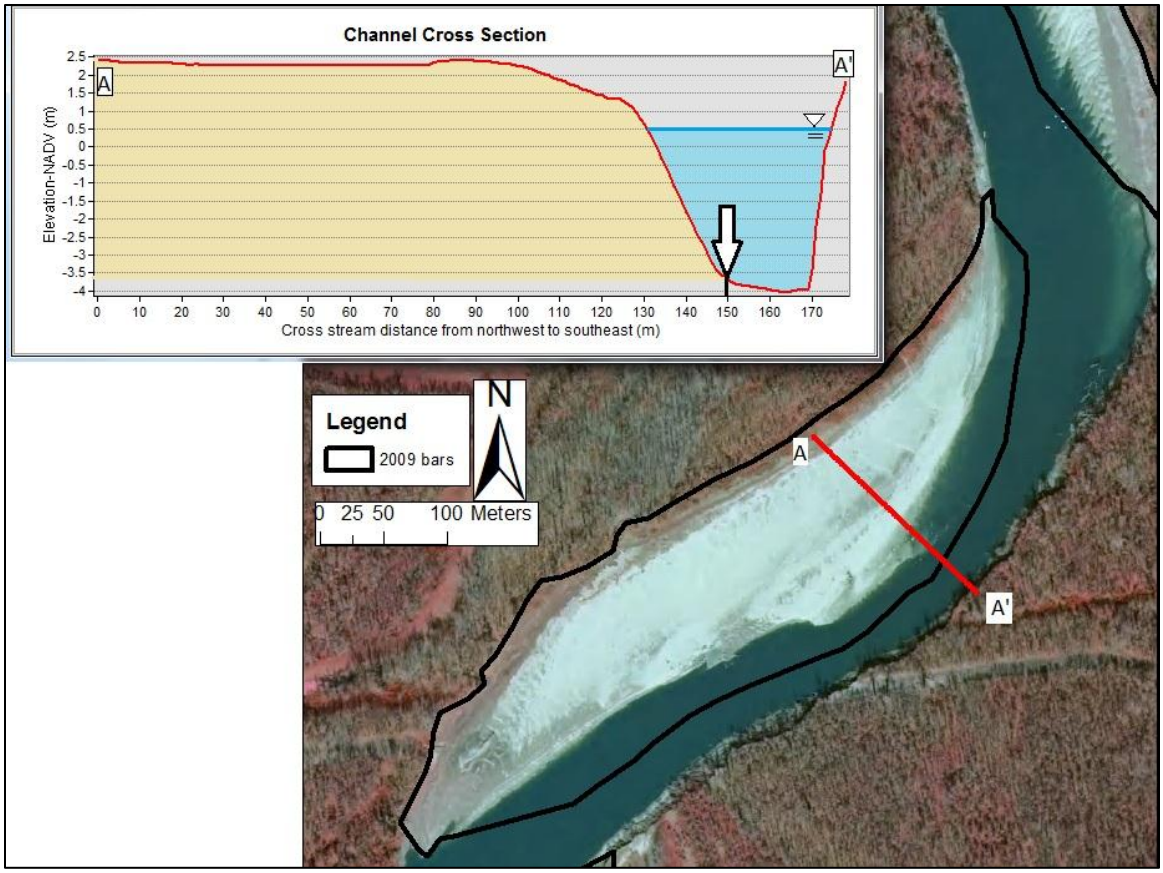


Figure 3.12: A bank-attached bar defined using a combination of the 2009 aerial photographs and the 2007 bathymetric survey. The extent of the bar is marked by the thick black line. The transect in red corresponds to the channel cross section graph. The bar area, in yellow, extends into the channel until there is a slope break, marked by the arrow. The blue line defines the water surface shown in the aerial photograph.

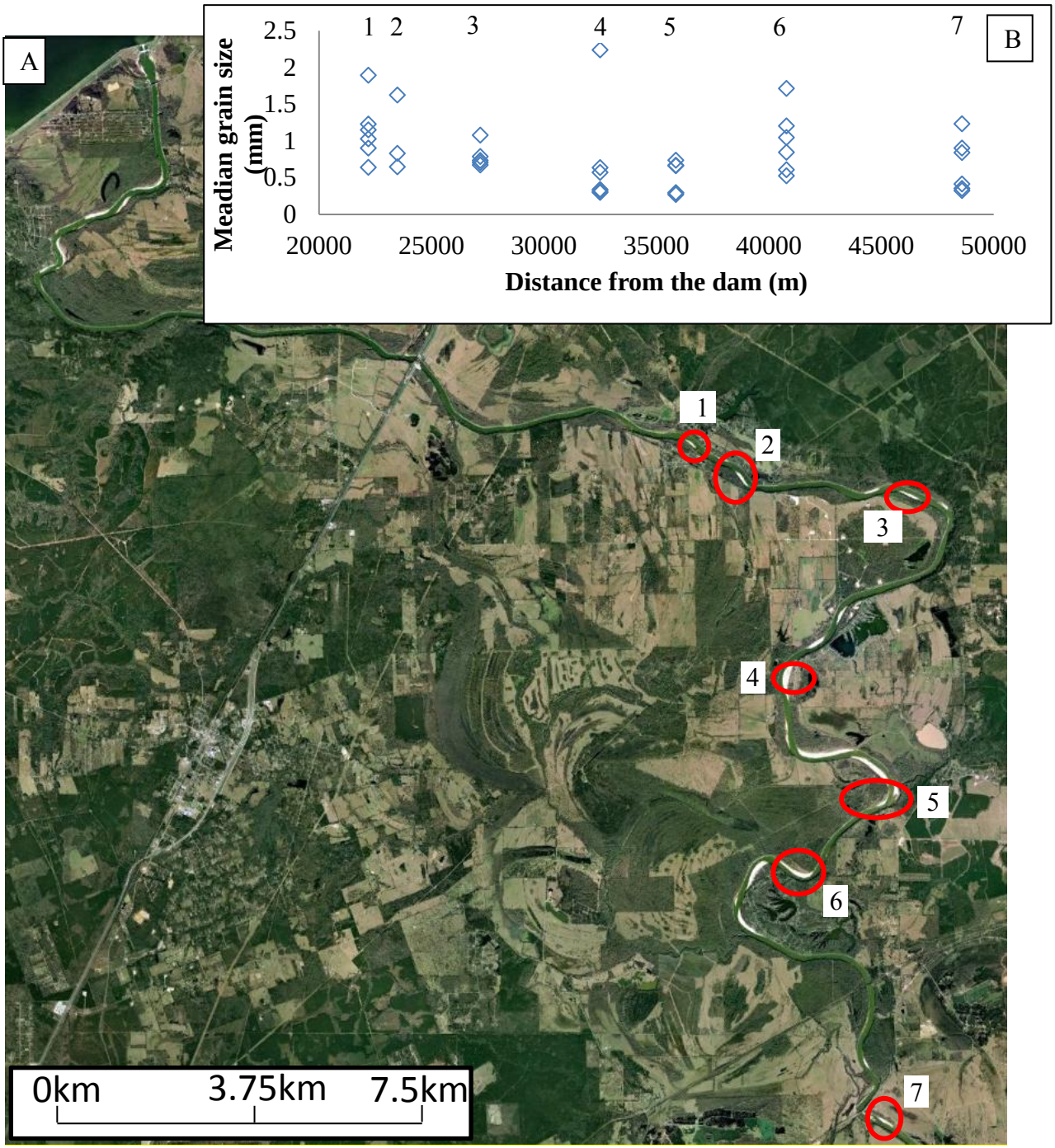


Figure 3.13: (A) Aerial photograph of Zone One and beginning of Zone Two on the lower Trinity River, TX. Livingston Dam can be seen in the upper left-hand corner of the photograph. The red ellipses mark seven bars where sediment samples were collected for size analysis. Six samples of were collected from each bar. The median grain diameter measured for each sample is shown in (B). The transition between Zone One and Zone Two occurs between 50,000 to 60,000 meters downstream of Livingston Dam.

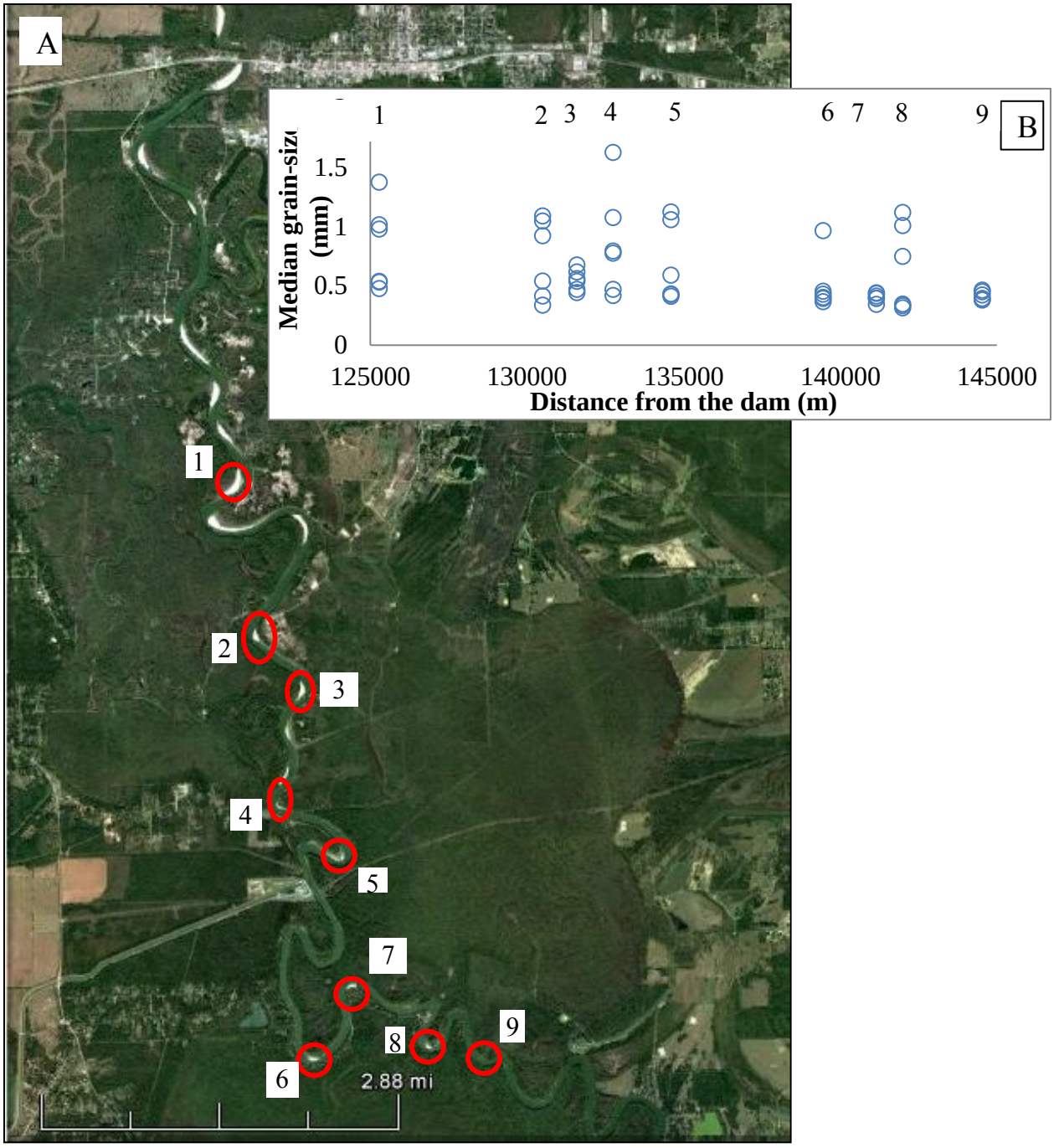


Figure 3.14: (A) Aerial photograph of Zone Two and beginning of Zone Three on the lower Trinity River, TX. The red ellipses mark nine bars where sediment samples were collected for size analysis. Six samples of were collected from each bar. The median grain diameter measured for each same is shown in (B). The transition between Zone Two and Zone Three occurs between 130,000 to 140,000 meters downstream of Livingston Dam.

Figure 3.15: Deposits of an internal delta developing at a tributary junction located 29,500 meters downstream of Livingston Dam. This delta provides clear evidence of tributaries delivering bed-material load to the lower Trinity River. Sediment samples from the delta had a $D_{50}$ of 260 micrometers.

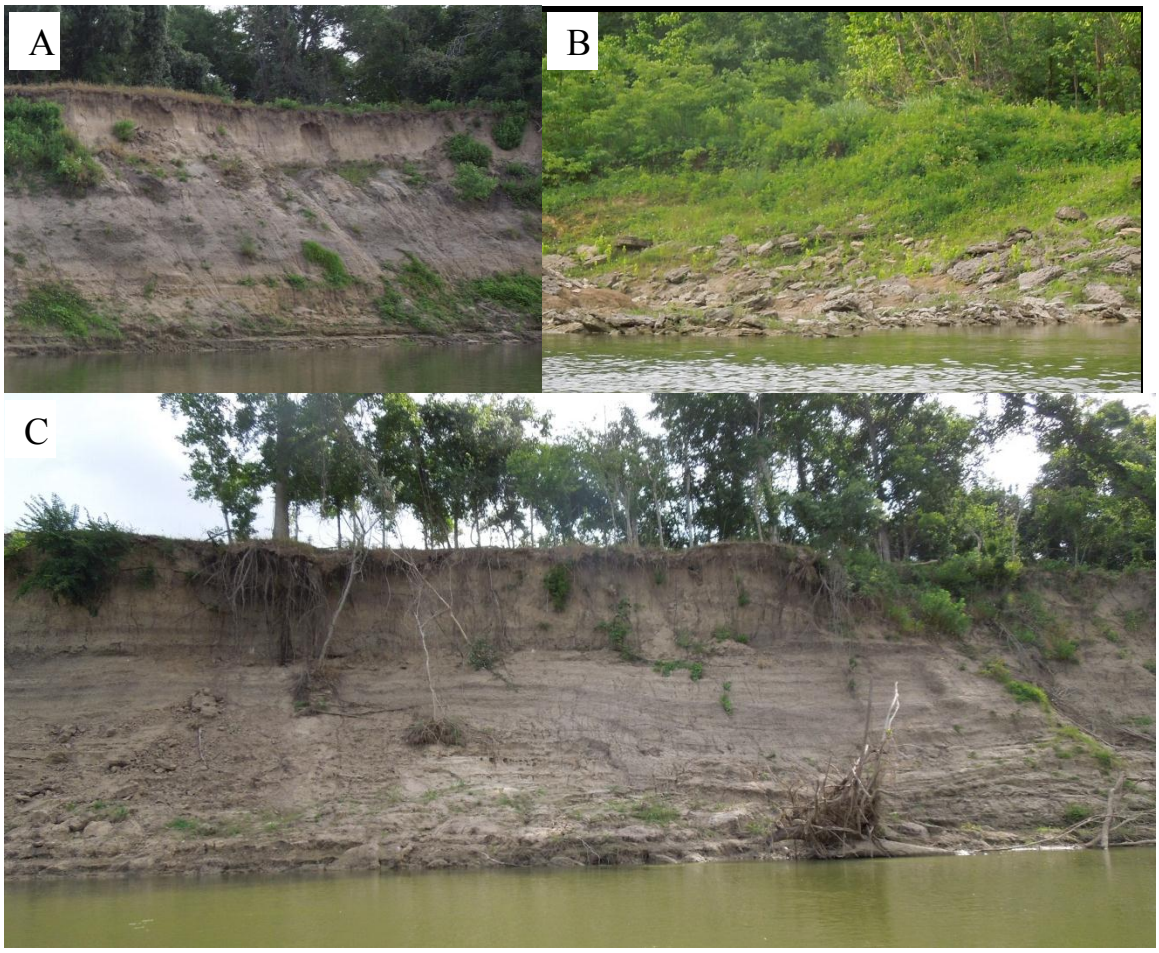

Figure 3.16: Examples of geologic substrate exposed in the channel banks between Goodrich to Romayor, TX, Zone One into the Zone One—Zone Two transition. (A) and (C) very weakly cemented to uncemented Quaternary fluvial deposits. (B) Weakly to very weakly cemented sandstone beds in Miocene fluvial deposits.

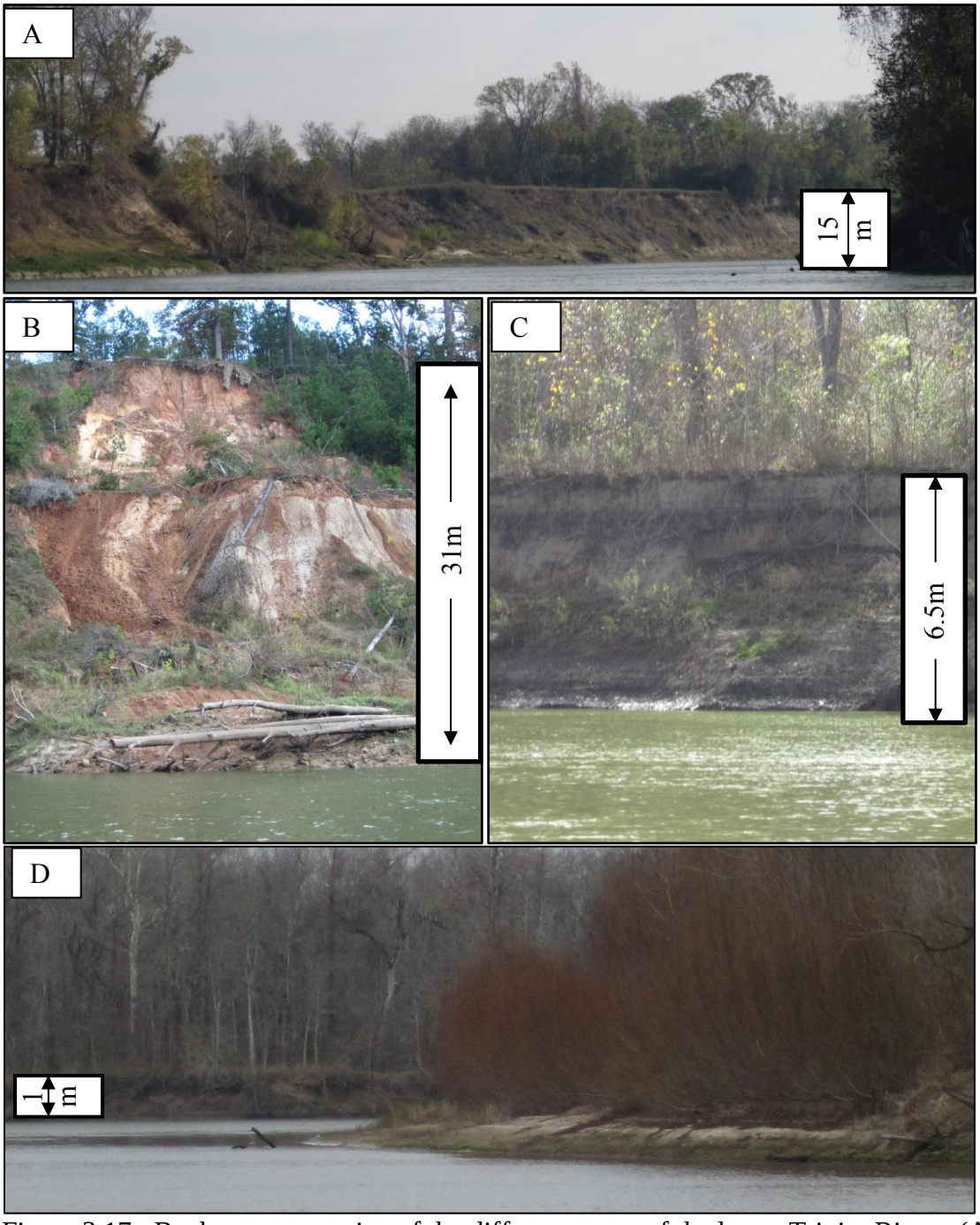

Figure 3.17: Banks representative of the different zones of the lower Trinity River. (A) and (B) Steep high banks of Zone One. (A) Quaternary deposit located at river meter 23,000. (B) Miocene deposits located at river meter 31,000. (C) Cut bank Quaternary deposits of Zone Two located at river meter 117,000. (D) Low banks characteristic of Zone Three at river meter 149,000.

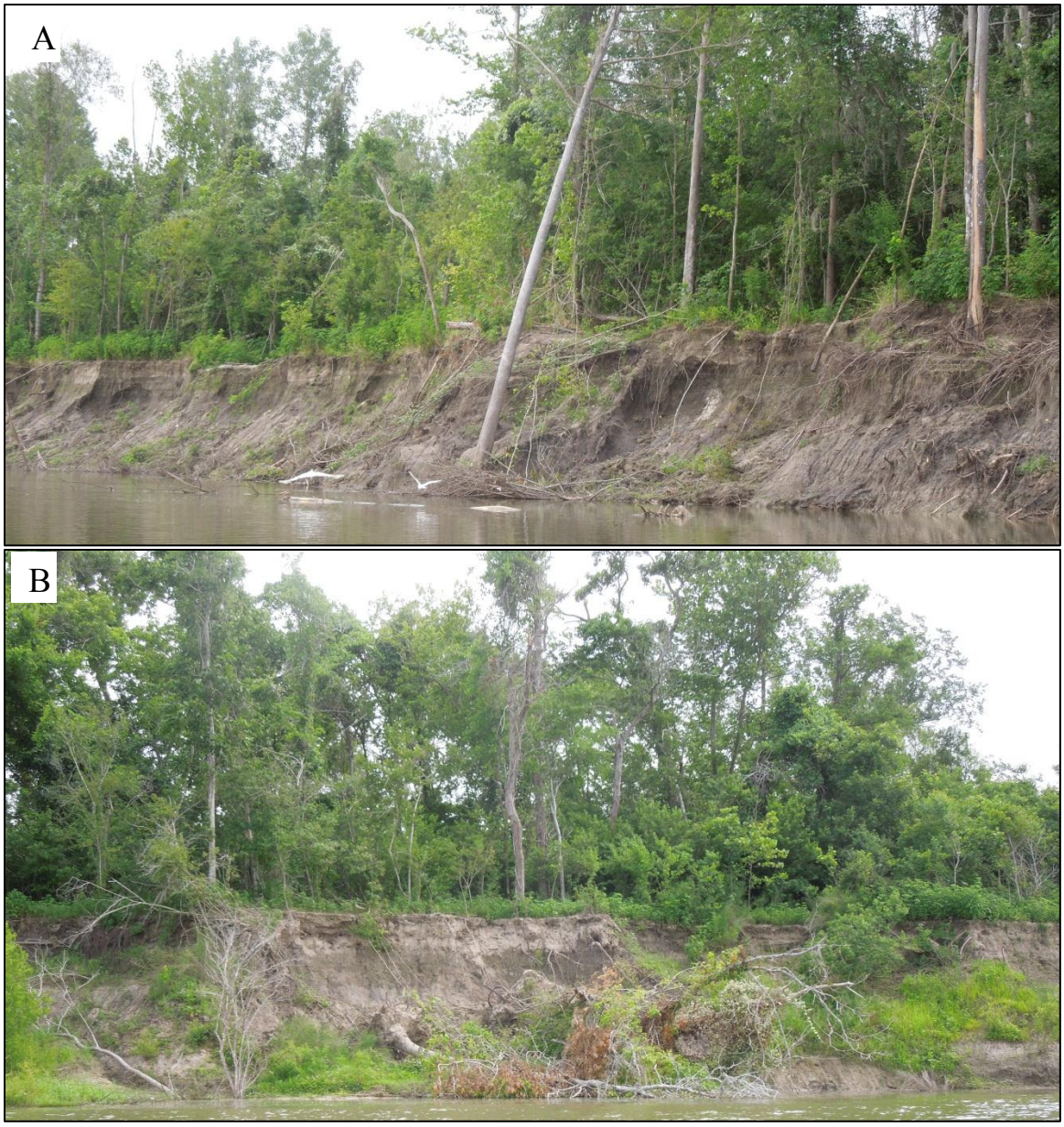

Figure 3.18: (A) and (B) Examples of slumped trees and brush acting to baffle runaway erosion of very weakly to uncemented outer banks on the lower Trinity River, TX.

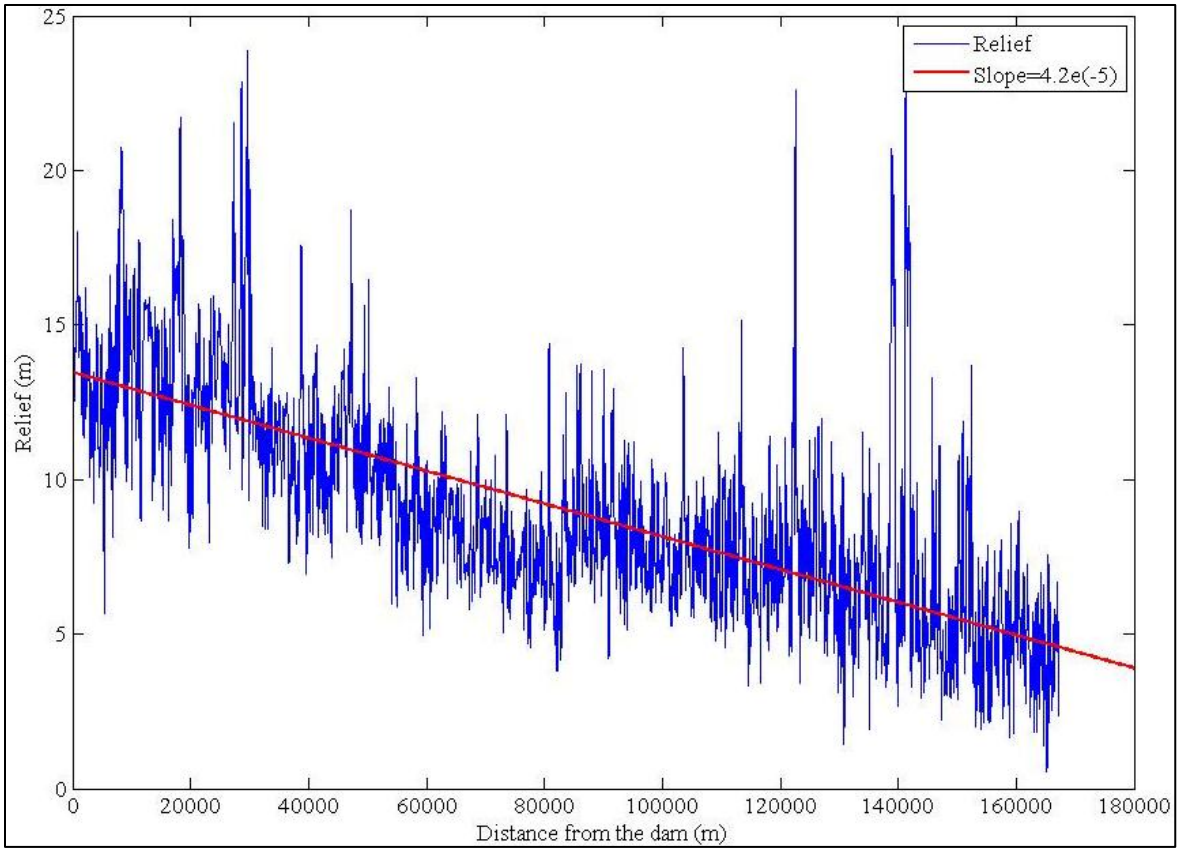


Figure 3.19: Channel relief measured by combining the 2007 bathymetry data collected by the TPWD and the 1984 USGS DEM. The bathymetry data was converted to a digital elevation model (DEM), which was overlain by a series of transects oriented perpendicular to centerline of the river that ran from the vegetated left bank to the vegetated right bank. 5001 transects were spread over 180,000 river meters. The transects were joined to the elevation data of the DEM (Fig. 3.12), and the relief was calculated for each transect by subtracting the thalweg elevation from the lower of the two banks.

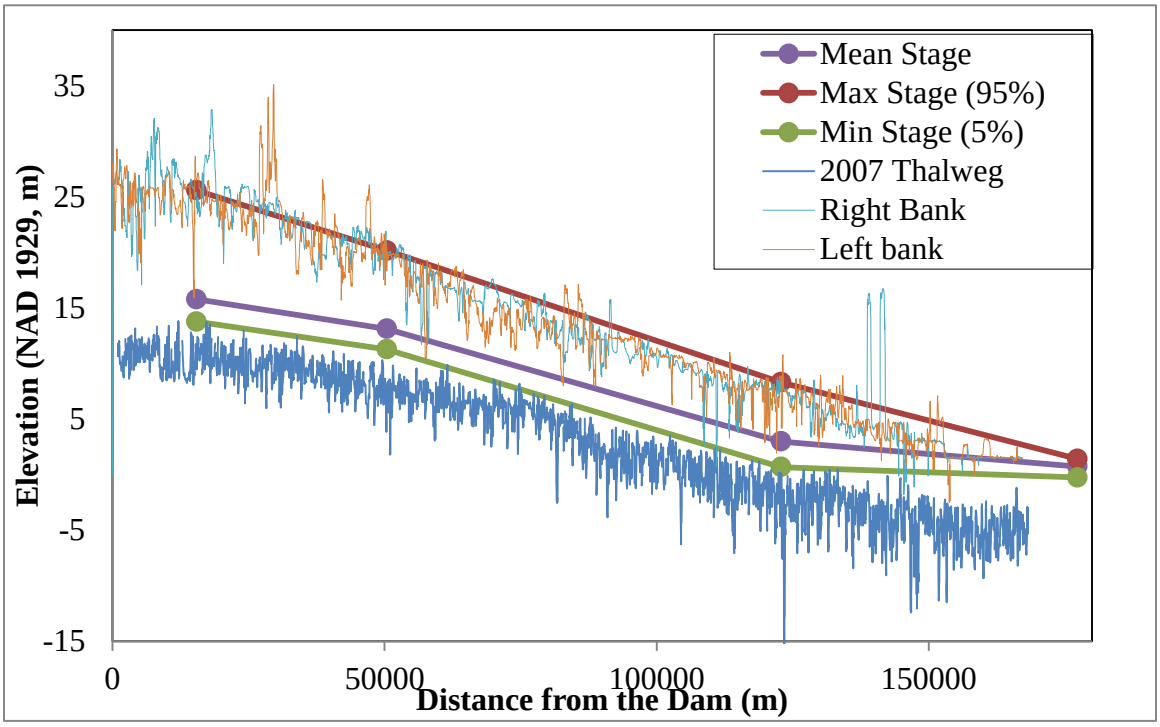


Figure 3.20: Long profile for the study reach of the Trinity River, TX, that includes elevations for the right and left river bank. These elevations for the vegetated alluvial surface were taken from the DEM built from the 1984 USGS 1:24,000 topographic quadrangles. The water surface profiles are based on 20 years of USGS stage gage data from four USGS river gages at Goodrich (USGS gage number 08066250), Romayor (USGS gage number 08066500), Liberty (USGS gage number 08067000) and Wallisville (USGS gage number 08067252).. The mean values is 184 cubic meters per second at Romayor. The minium is the 5% probability stage (22 cubic meters per second at Romayor) and the maximum is the 95% probability stage (2690 cubic meters per second at Romayor). Notice the maximum discharge inundates the river banks between 50,000-180,000 river meters. Only a small function of the bankline is inundated between 0-50,000 river meters.

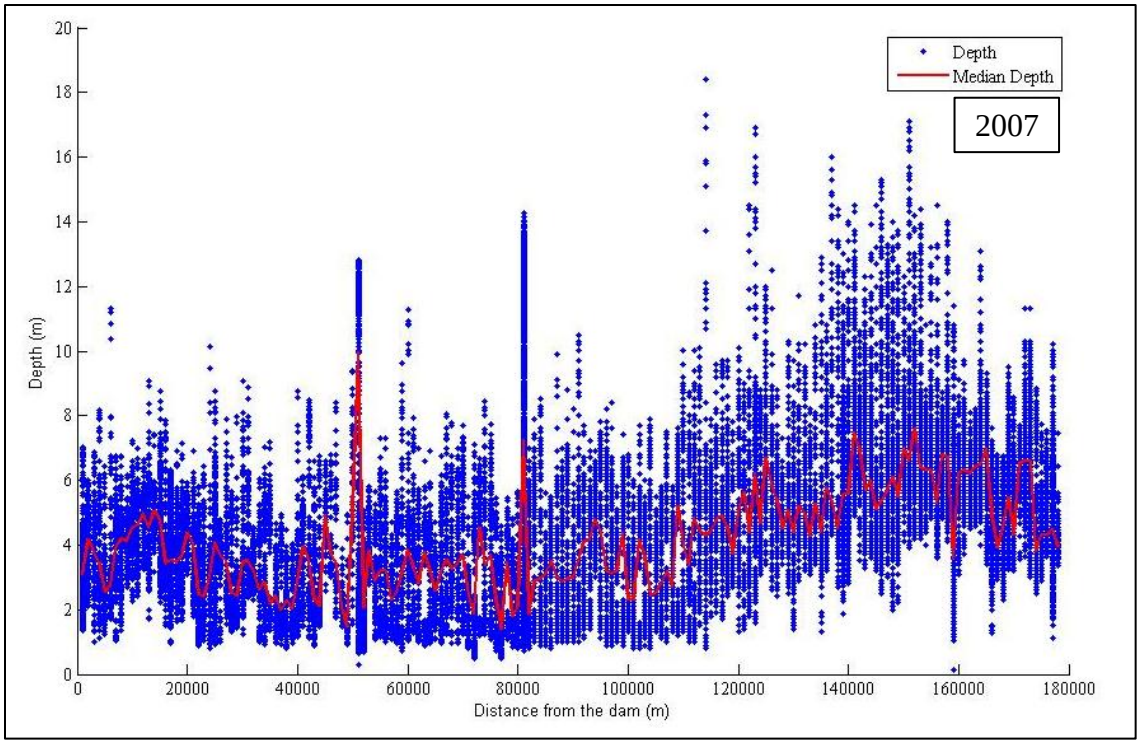


Figure 3.21: Depth data from the 2007 TWPD survey of the lower Trinity River (stage during survey was 855 cubic meters per second measured at Goodrich). The blue points represent the average water depth for data binned by kilometer. The median depth, by kilometer, is plotted in red. Notice that at this river discharge the flow depth increases into Zone Three. The surveys discharge is equal to the 92% probability stage.

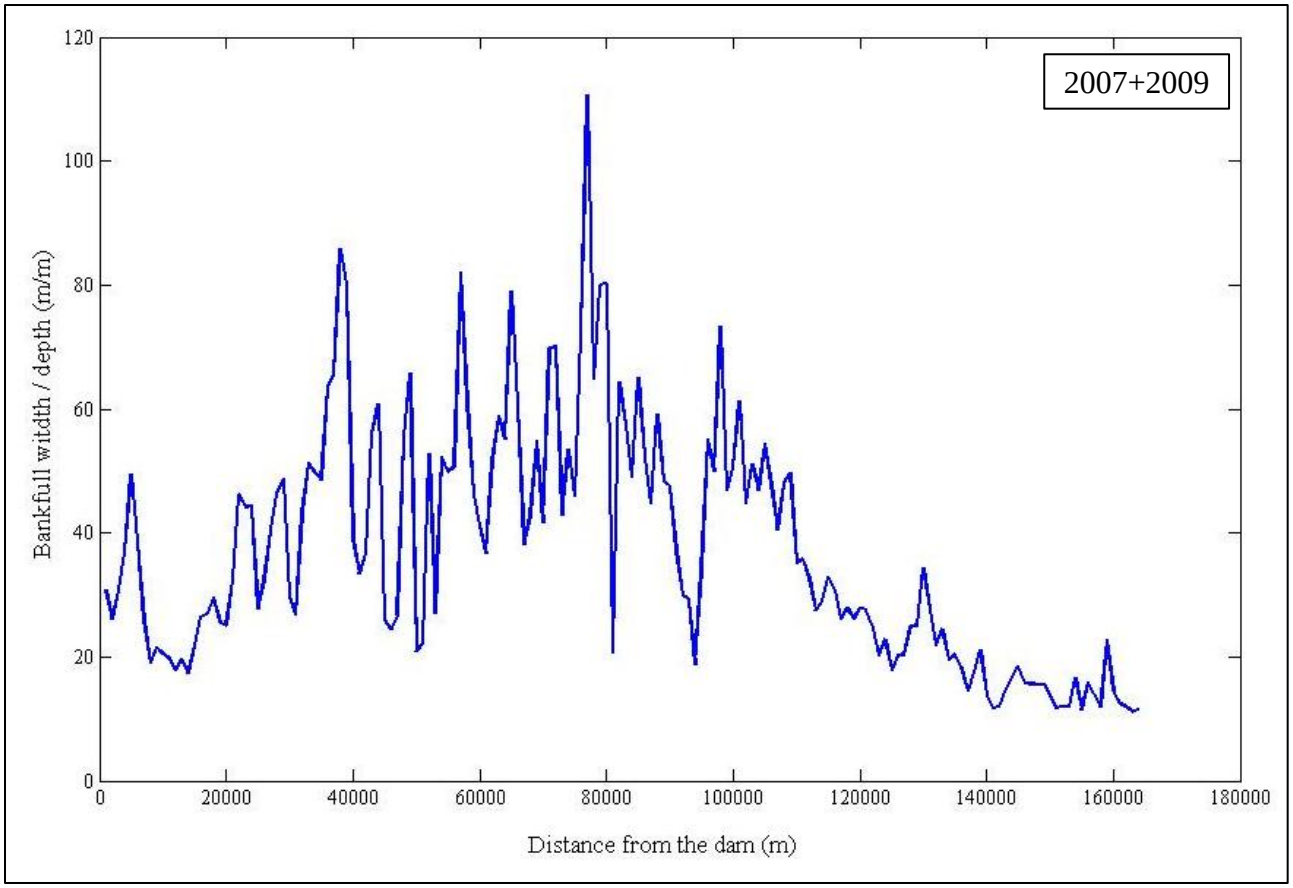

Figure 3.22: Width to depth ratio for the channel through the study area. The width and depth values are the average width and depth values for each river kilometer. The width to depth ratio increases into Zone Two and decreases into Zone Three.

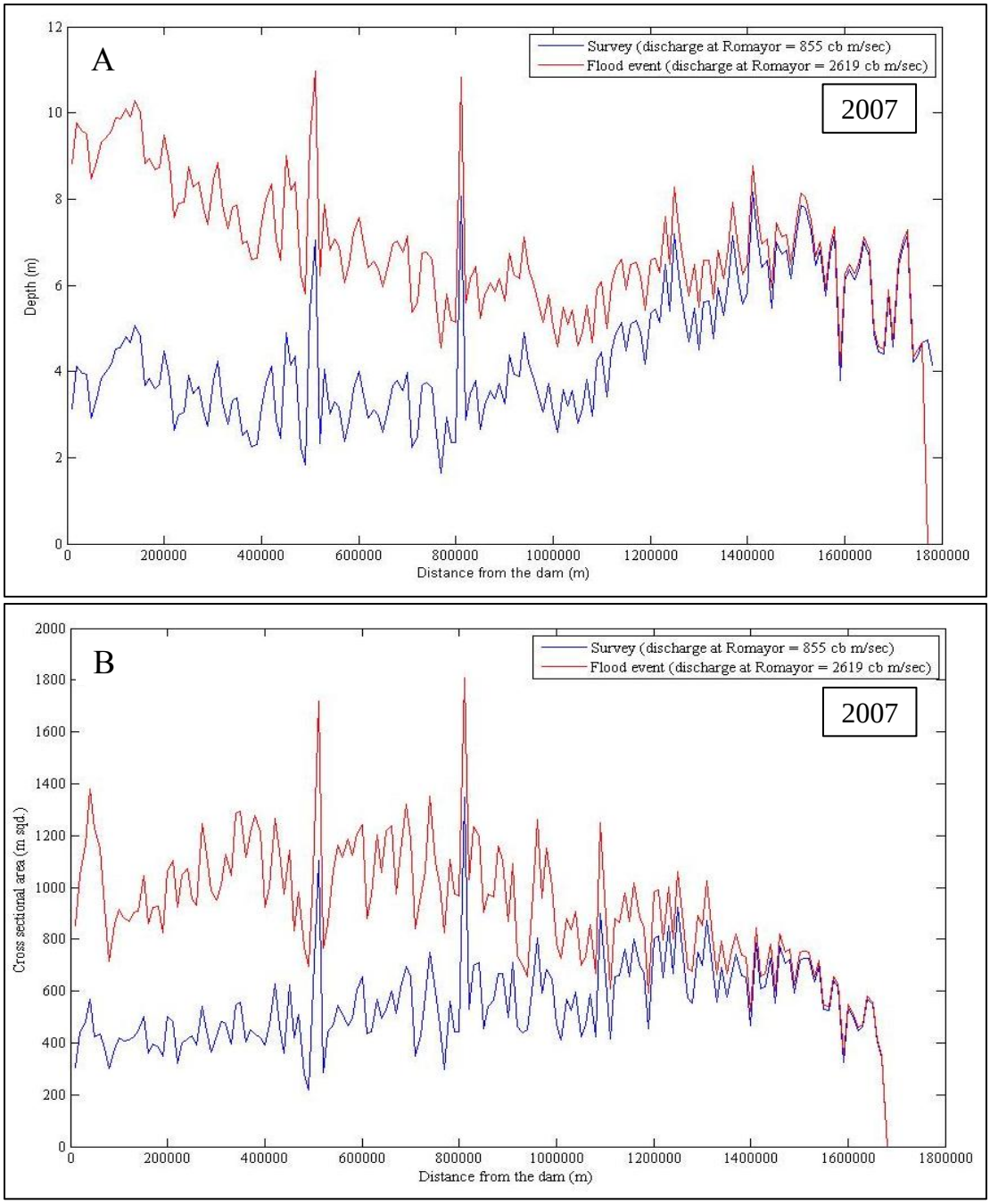


Figure 3.23: Water depth (A) and wetted cross sectional area (B) as a function of distance downstream and channel discharge. At high flow Zone Three has the greatest water depth and wetted cross sectional area, but at flood stage Zone One has the greatest depth and cross sectional and both decrease with distance downstream towards Trinity Bay.

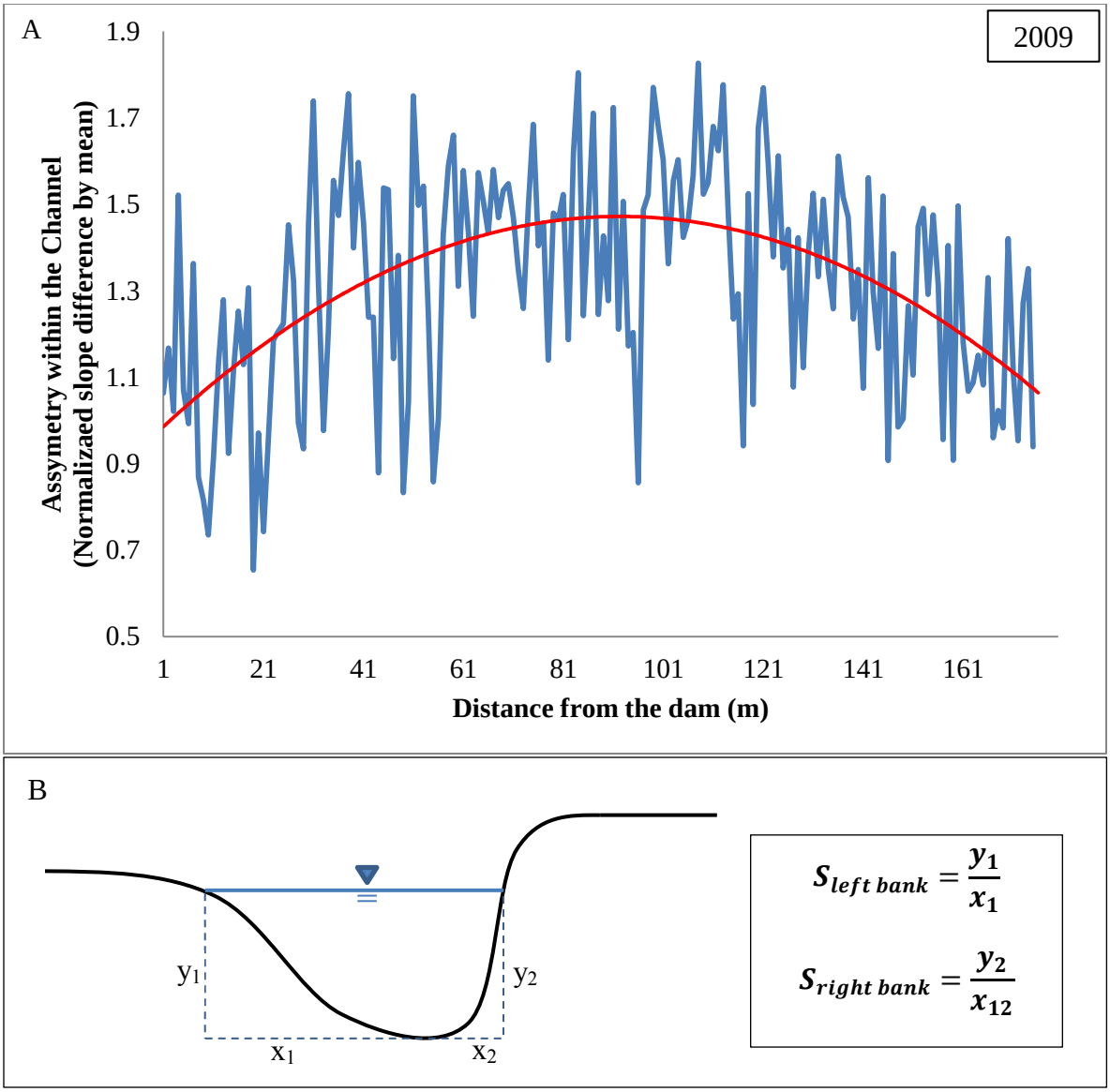


Figure 3.24: (A) Channel asymmetry calculated using the 2007 channel bathymetry DEM transects (Fig. 3.10). (B) The slopes were calculated for the right and left channel wall for each transect. The differences were taken between the slopes and divided by the mean slope to normalize the data.

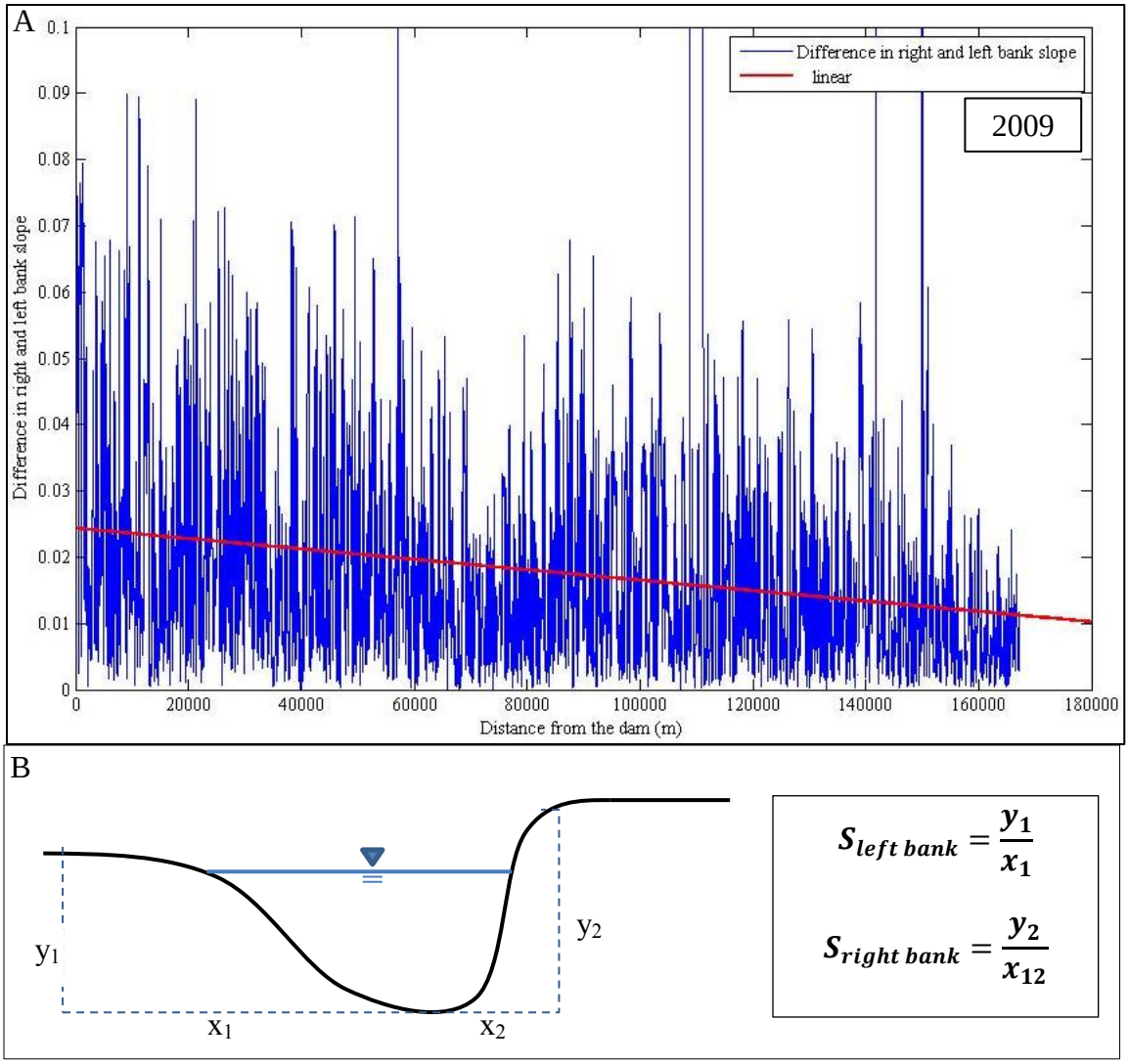


Figure 3.25: (A) Asymmetry of the channel is calculated up to the flood plain using the combined data that was also used to calculate channel relief in Figure 3.19 (the USGS DEM and the 2007 bathymetric survey DEM). (B) Slopes were calculated for either side of the thalweg at each transect (Fig. 3.10), and the difference was taken between the wall slopes and the plotted as an absolute value.

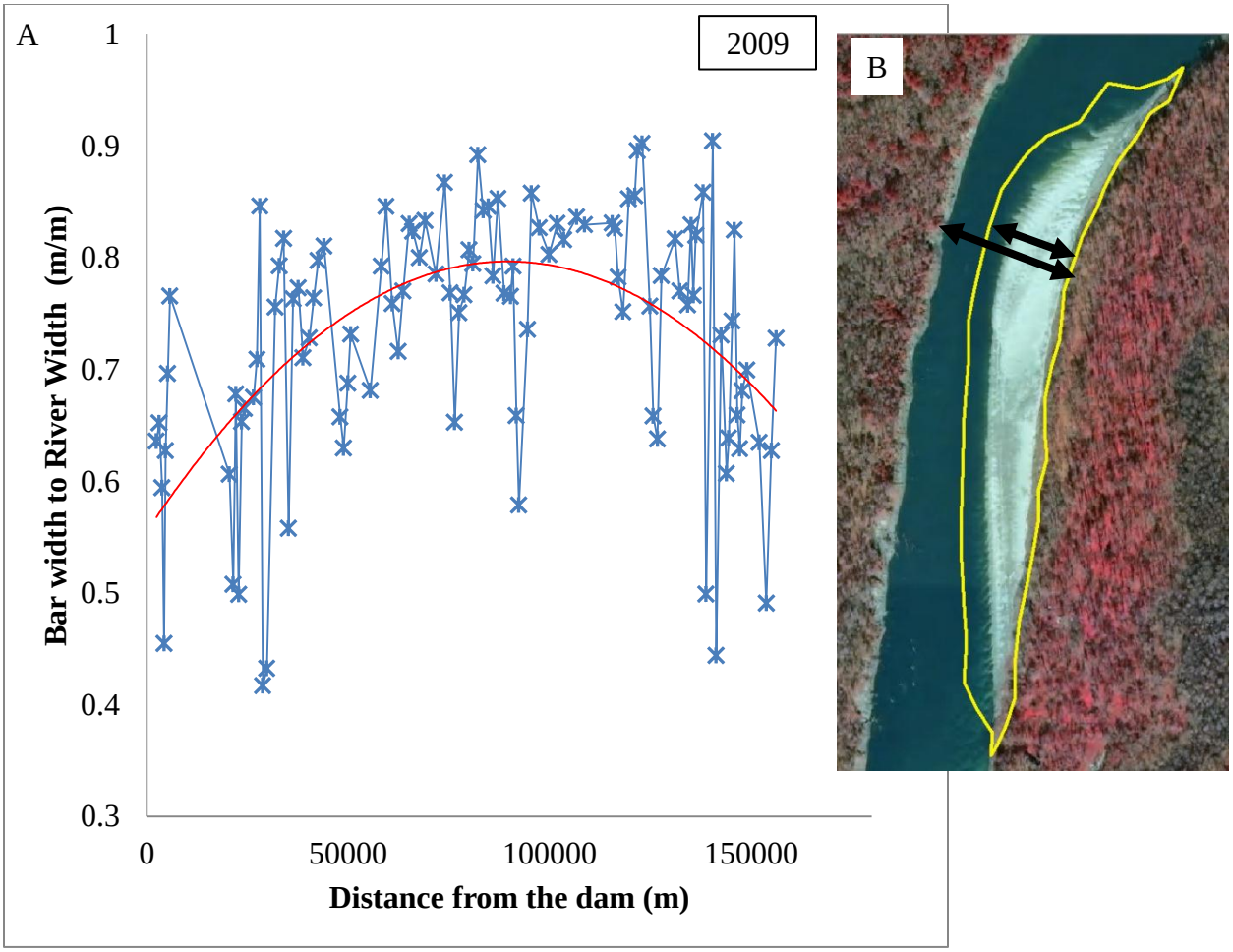


Figure 3.26: (A) Ratio of bar width to river width at widest point on each bar. (B) Bars and river were measured at the widest point of the bar. The bar areas were defined as the area between the wooded vegetation line and where the slope of the bar breaks within the channel (Fig. 3.12). In Zone Two the bars make up the largest fraction of the channel cross section.

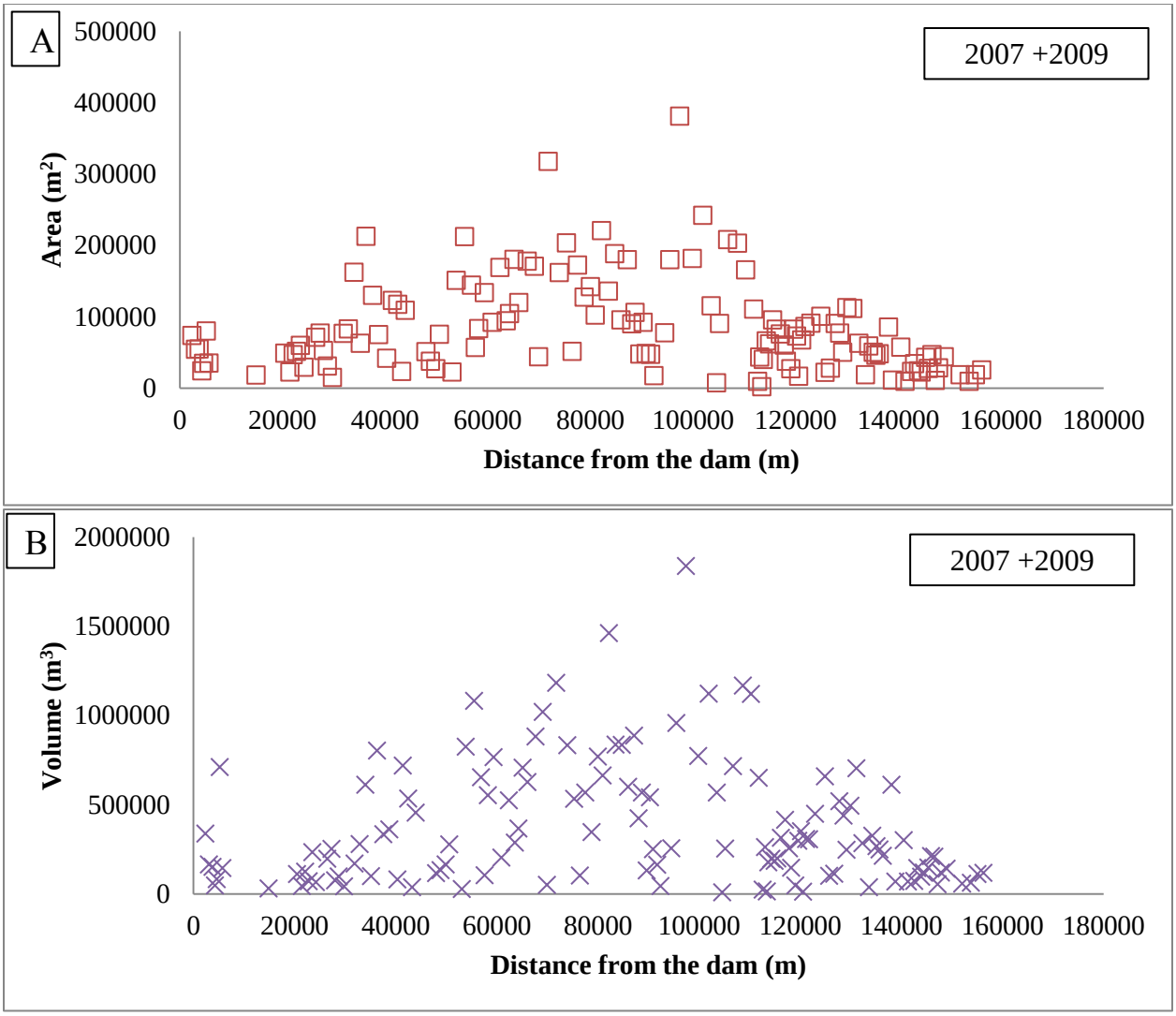


Figure 3.27: (A) Area of each bank-attached bar on the lower Trinity River. Area was measured using both the 2009 aerial photographs and 2007 bathymetric DEM to insure both the exposed and subaqueous portions of the bars are included. (B) Volume of each bar calculated using the 2007 bathymetery data. The area and volume of bars increases from Zone One to Zone Two and then decreases from Zone Two to Zone Three. The bar values in the first 5,000 river meters appear to be outlier, that are potentially associated with construction due to dam maintenance.

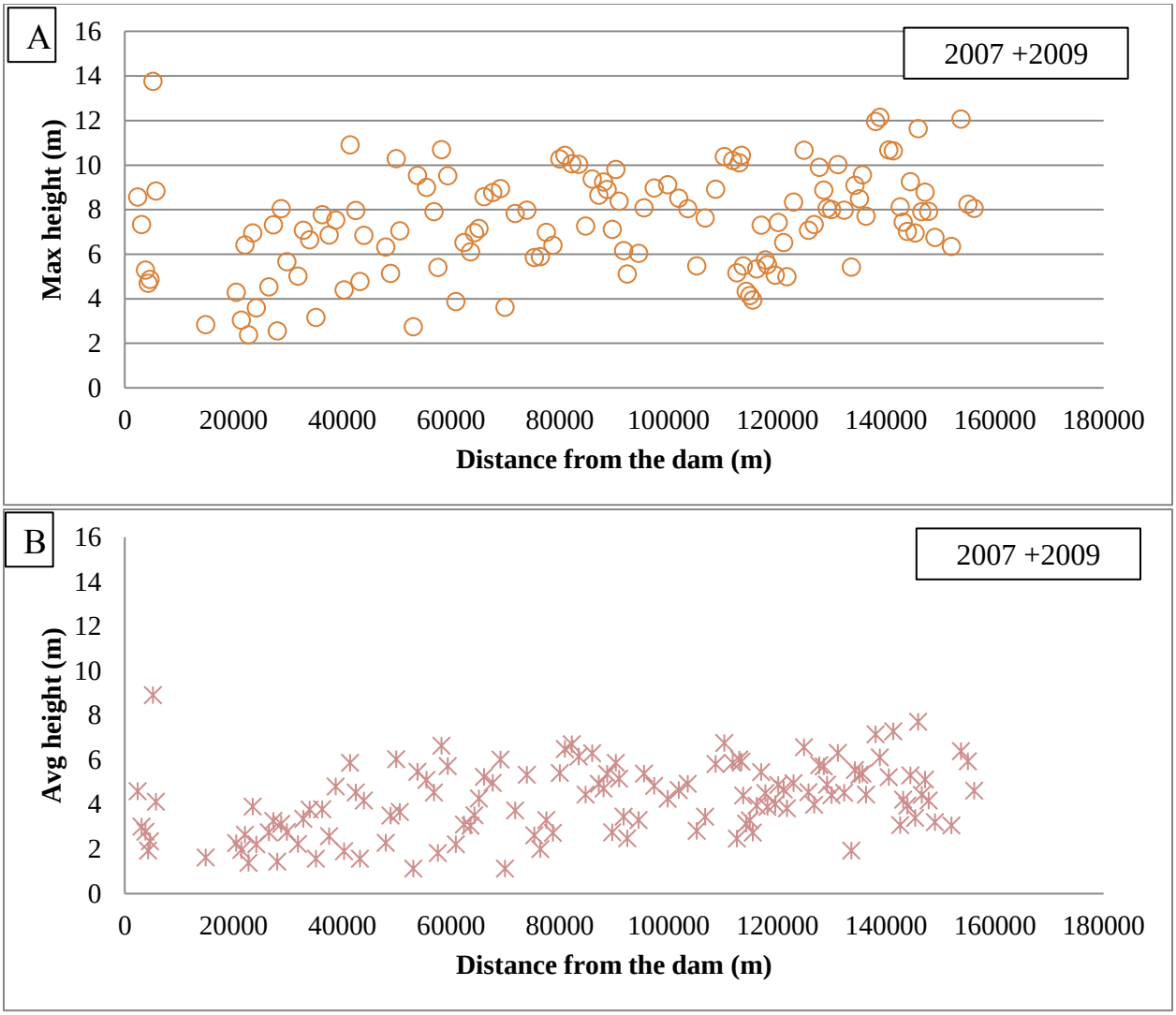


Figure 3.28: (A) Maximum of height of each point bar in the study area. Maximum bar height is equal to the difference between the highest and lowest elevations on each bar taken from the 2007 bathymetric survey. (B) Average height of each bar calculated as the mean value for all measures of elevation difference on the mapped bar surface. These data are also from the 2007 bathymetric survey. The height of bars increase systemically with distance from the dam and toward the coast. The bar values in the first 5,000 river meters appear to be outlier, that are potentially associated with construction due to dam maintenance.

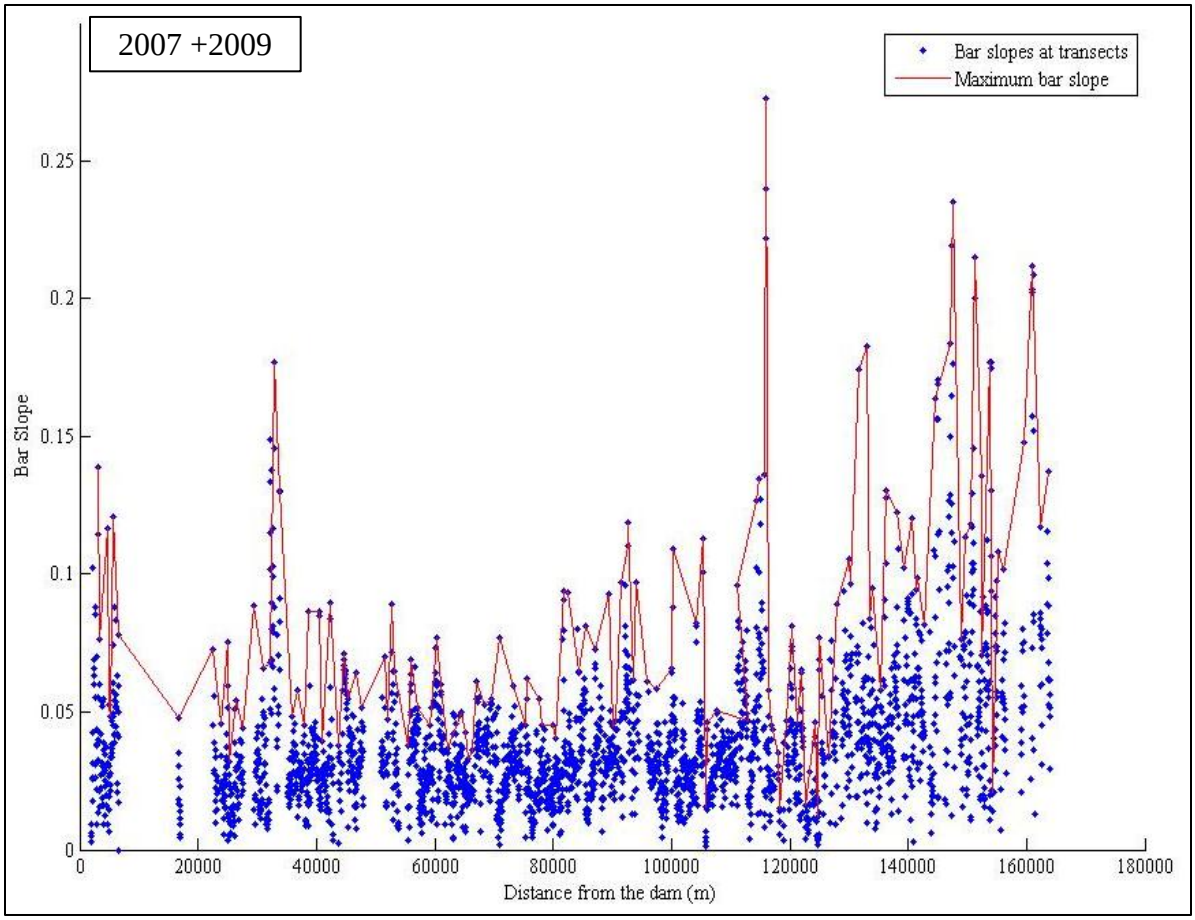


Figure 3.29: The lateral slope of bank-attached bar in the lower Trinity River. The slopes were measured using the depth data from the 2007 TWPD survey of the Lower Trinity River. Transects points with the elevation data (Fig. 3.12) were clipped to the bar shapes. The clipped transect points were then used to calculate the bar surface slopes (shown in blue). The largest slope for each bar is plotted in red.

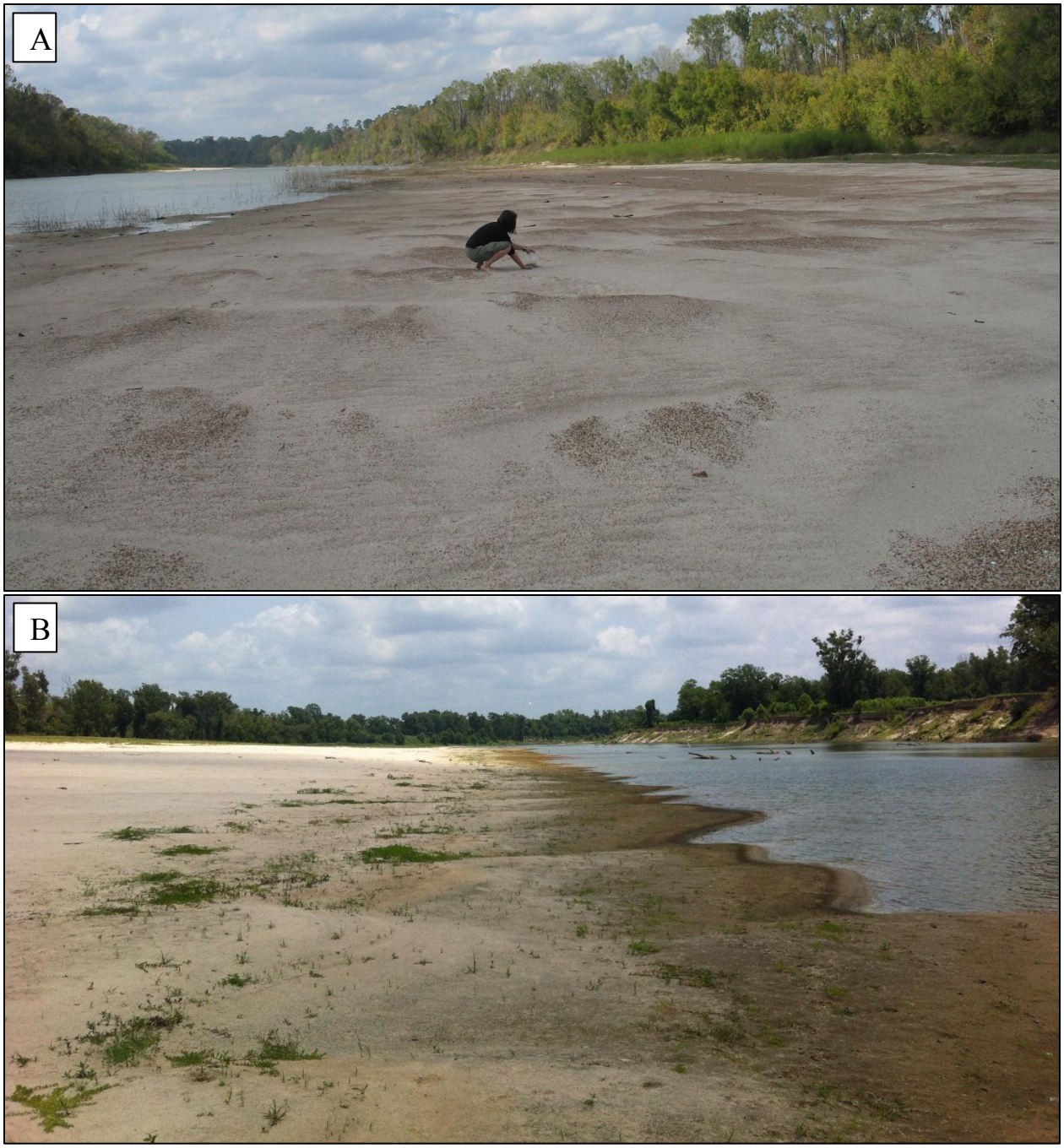


Figure 3.30: (A) Bar in Zone One, approximately 20,000 river meters from Livingston Dam. (B) Bar in Zone One, approximate 29,000 river meters from Livingston Dam. The bar in (A) is flat and topped with gravel, as is typical in Zone One. Both bars have a distinctly flat topography.


Figure 3.31: (A) Bar in Zone Two, approximately 117,000 river meters from Livingston Dam. (B) Bar in Zone Two, approximate 126,000 river meters from Livingston Dam. Both bars exhibit contain large volumes of sand.

Figure 3.32: (A) Bar from Zone Three, approximately 137,000 river meters from Livingston Dam. (B) Bar from Zone Three, approximate 130,000 river meters from Livingston Dam. As is typical with bars in Zone Three, both bars are small in area, with steep surface slopes.

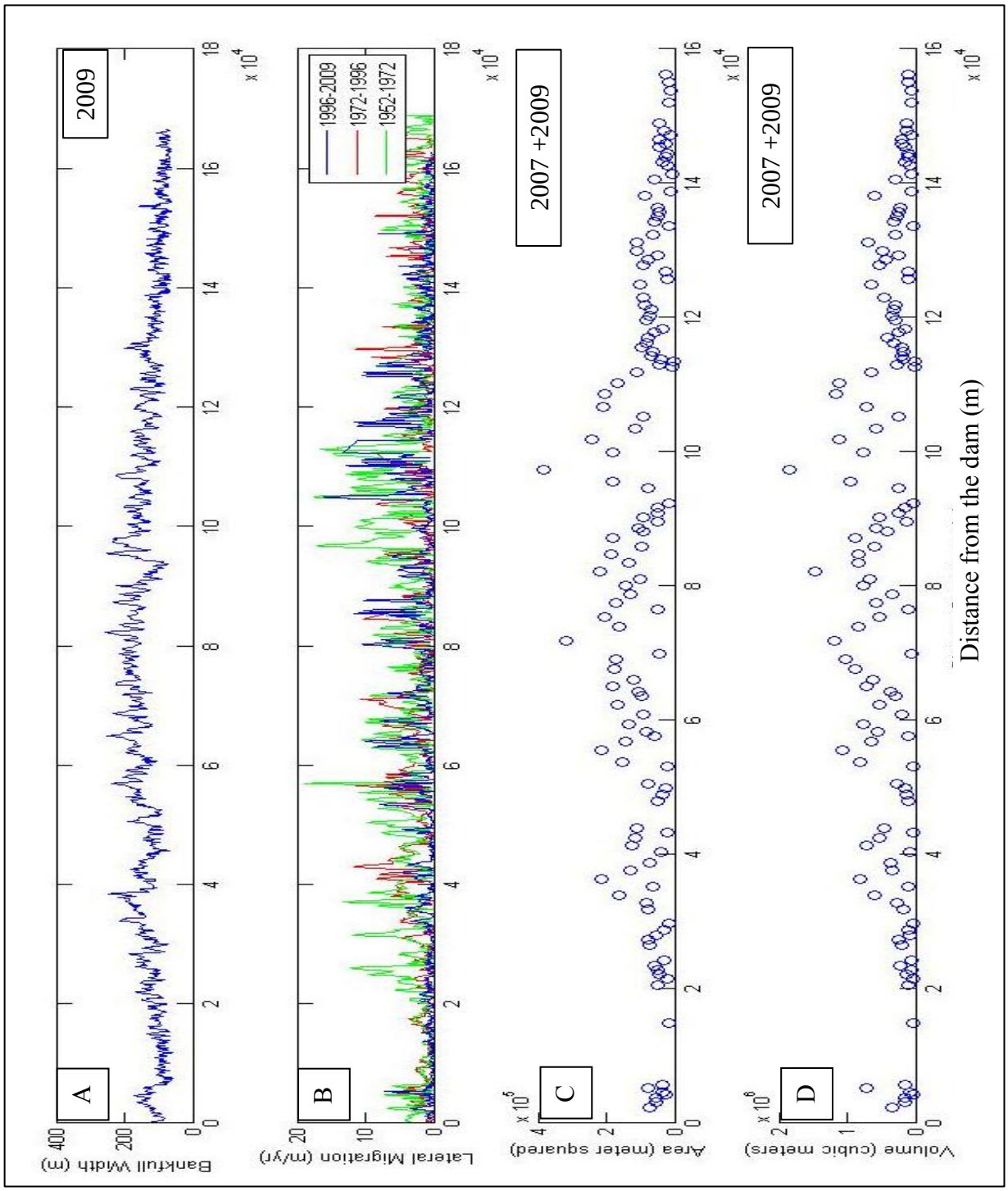


Figure 3.33: Bankfull width (A), lateral migration rate (B), bar area (C), and bar volume (D) from Livingston Dam to Trinity Bay. Notice that the similar shape to all of these curves.

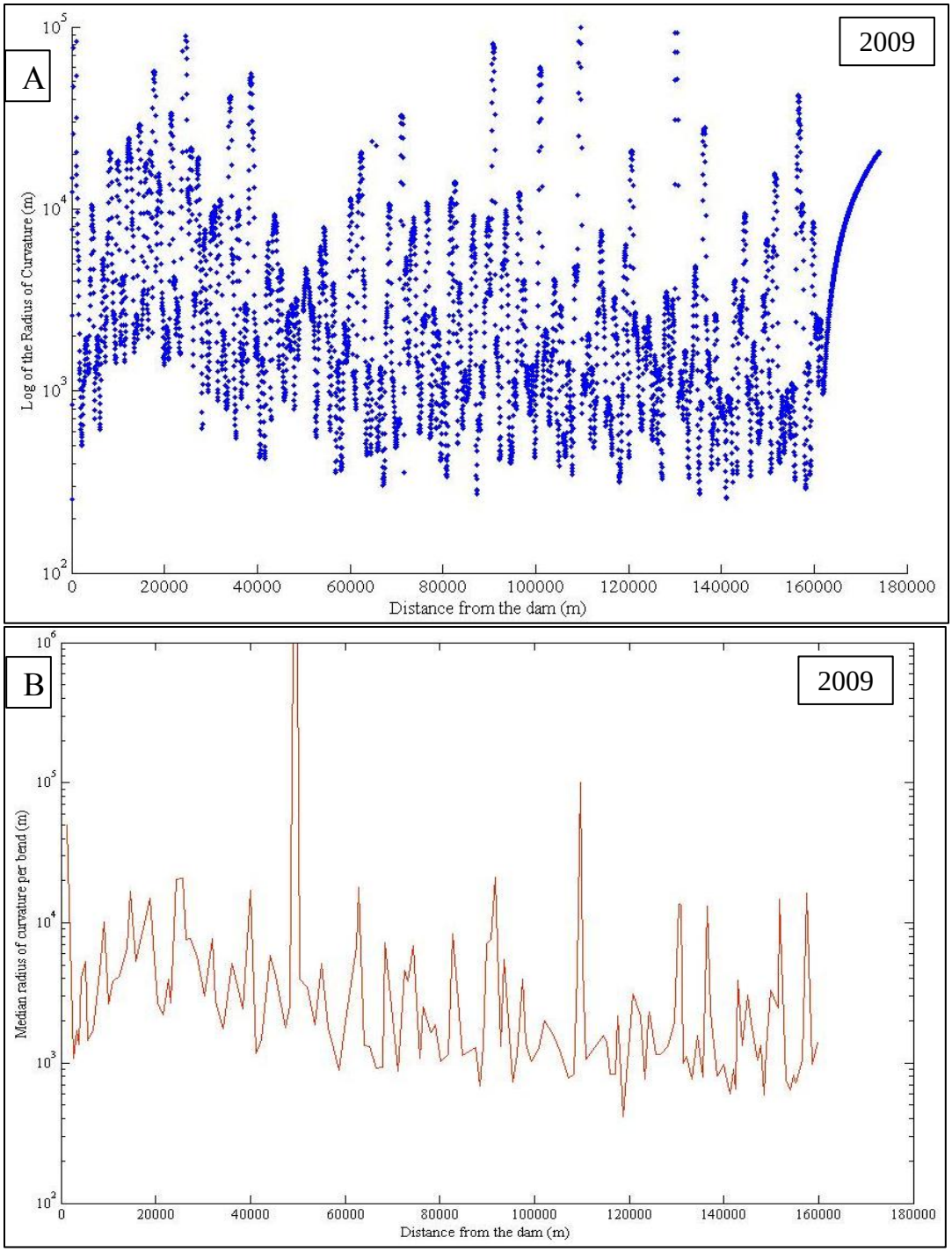


Figure 3.34: (A) Channel Radius of curvature as a function of downstream distance. These values were measured using the digitized centerline from the 2009 aerial survey. Radius of cuvature was measured every 36 meters along the centerline. (B) Median radius of curvature for each bend in red. All values were calculated using the Meanders Program (*Peyret.*, 2011).

| | Rate (m/year) | | | |
|---|---|---|---|---|
| | 1952-1972 | 1972-1996 | 1996-2009 | Average |
| Zone 1 | 2.88 | 2.06 | 1.09 | 2.01 |
| Zone 2 | 3.69 | 4.41 | 4.52 | 4.21 |
| Zone 3 | 1.58 | 1.33 | 1.80 | 1.57 |

Table 3.2: The channel migration rates based on digitized channel centerlines from aerial photographs and the GIS Planform Stastics Tool. Zone One is the most upstream reach, and Zone Three is the most downstream reach.

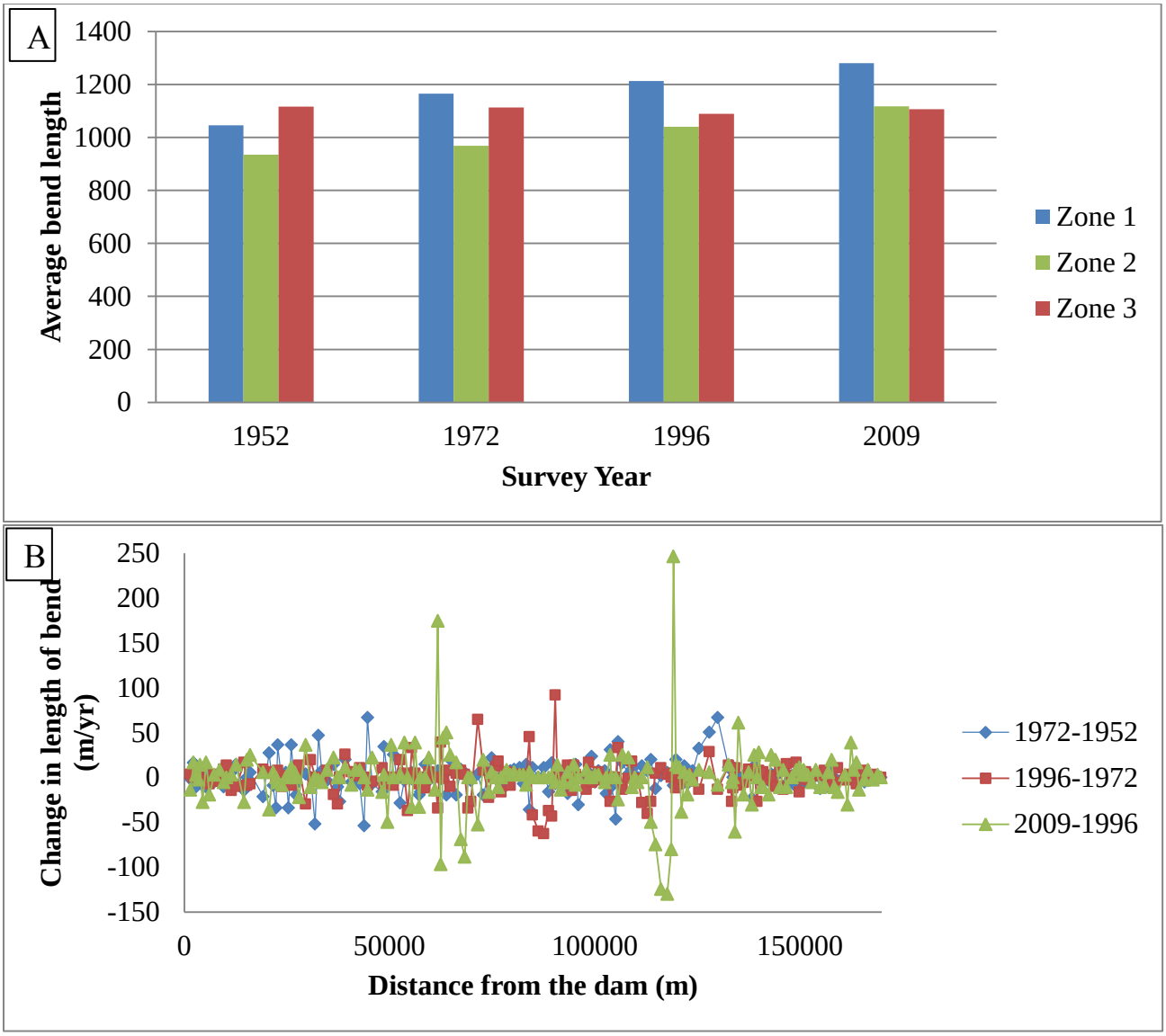


Figure 3.35: (A) The average bend length for each zone, measured for each survey. The bends in Zone One are getting progressively bigger. The bends in Zone Two appear to be increasing in length, but this is actually due to cut offs. (B) Change in bend length as a function of downstream distance. The difference was calculated between each survey. Change in Zone One is due to straightening. The change in Zone Two is due to migration. Zone Three changes very little.

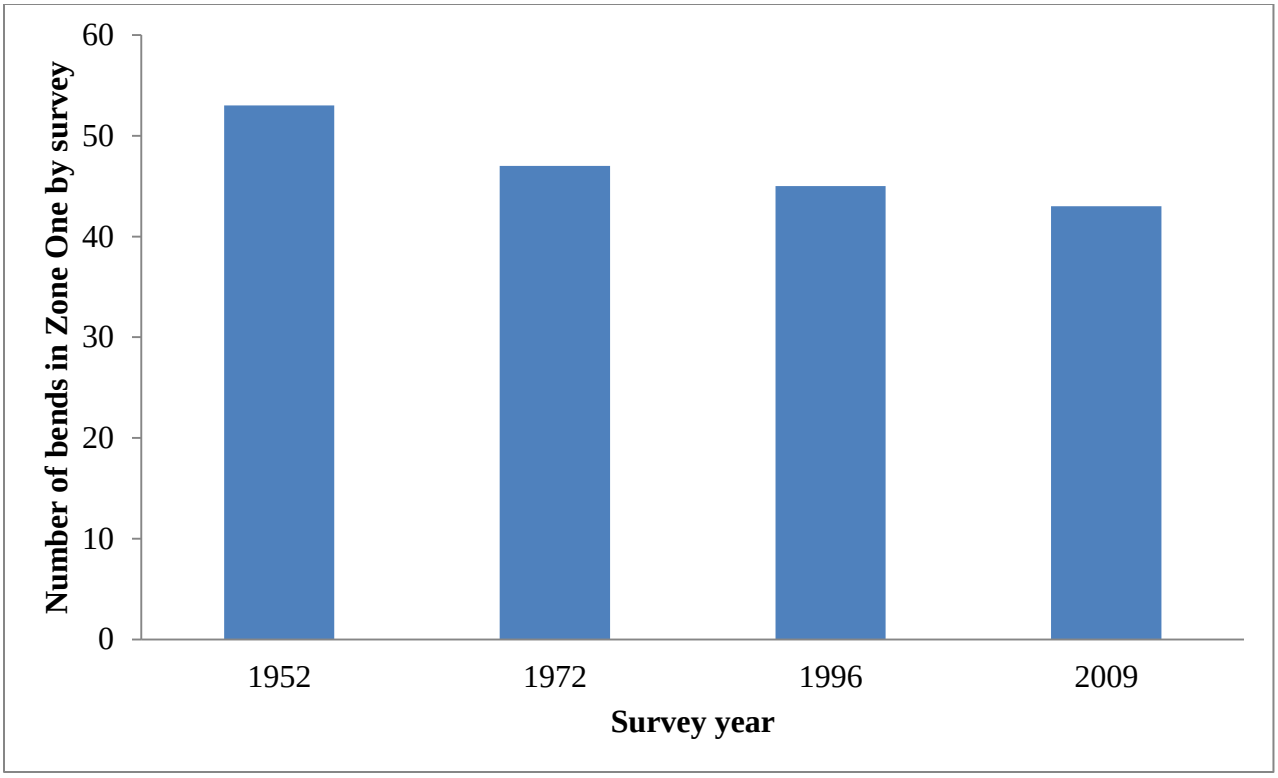


Figure 3.36: The number of bends present in Zone One, the first 55 river kilometers, during each of the aerial photograph surveys. The number of bends decreases with every survey. Between 1952 and 2009 the number of bends was reduced from 53 to 43, a 20% decrease.

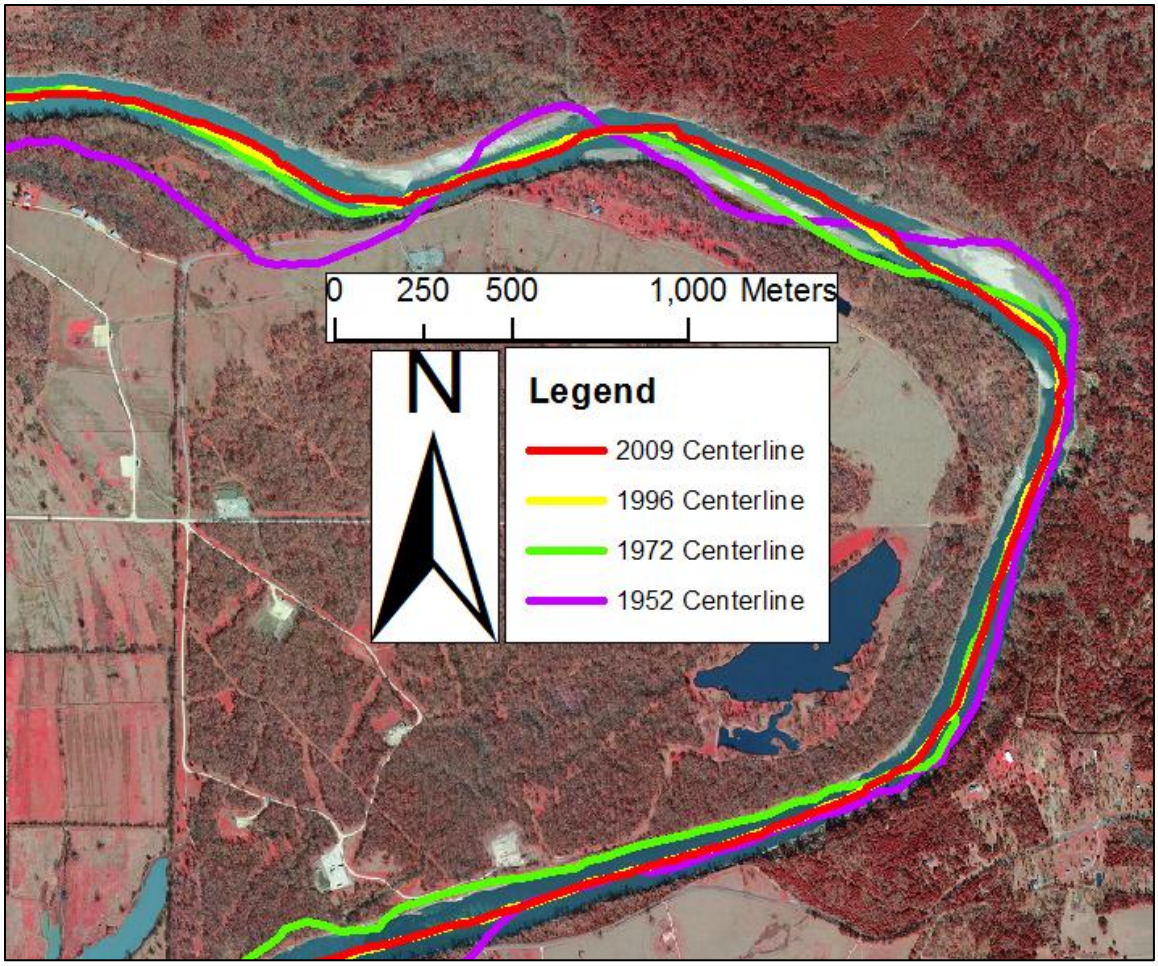


Figure 3.37: The bends in Zone One have straightened since the impoundment of Livingston Dam. As a result, the bends lengthen (Fig. 3.31a) and the number of bends is reduced (Fig. 3.32).

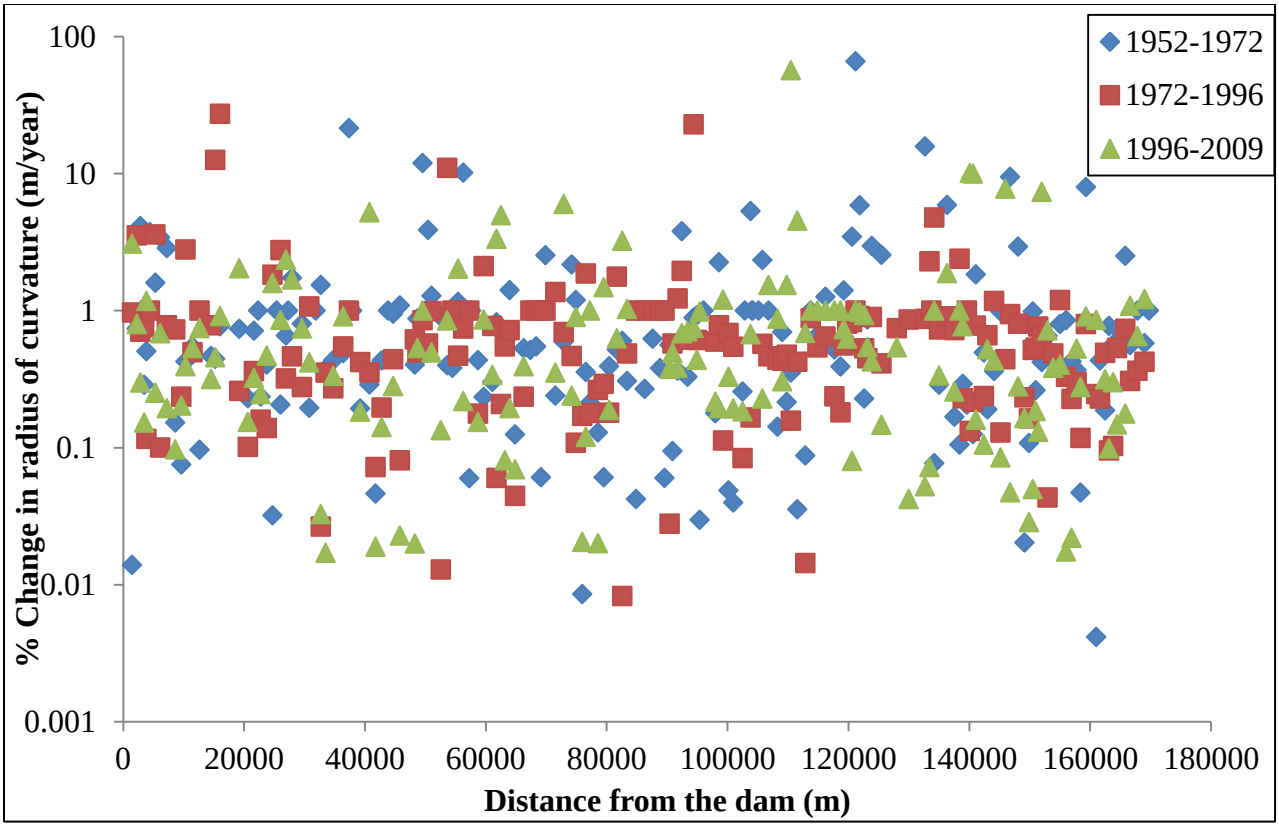


Figure 3.38: Precent change in radius of channel curvature overtime as a function of downstream distance. The change was measured between each of the four surveys.

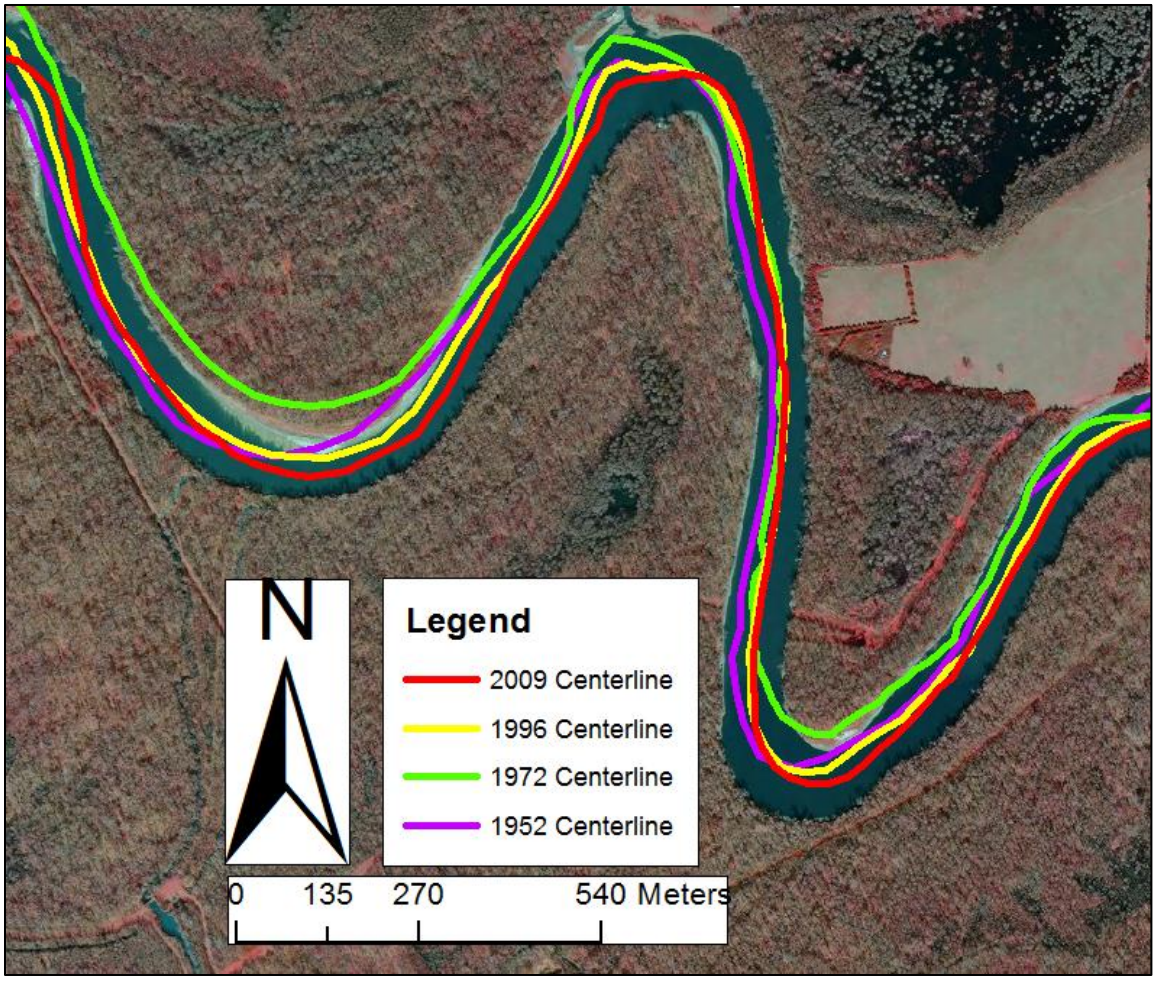

Figure 3.39: The bends in Zone Three migrate, but do not change in length. Therelatively constant lengths are evident in Figures 3.31a and b. The varying radius of curvature is shown Figure 3.38.

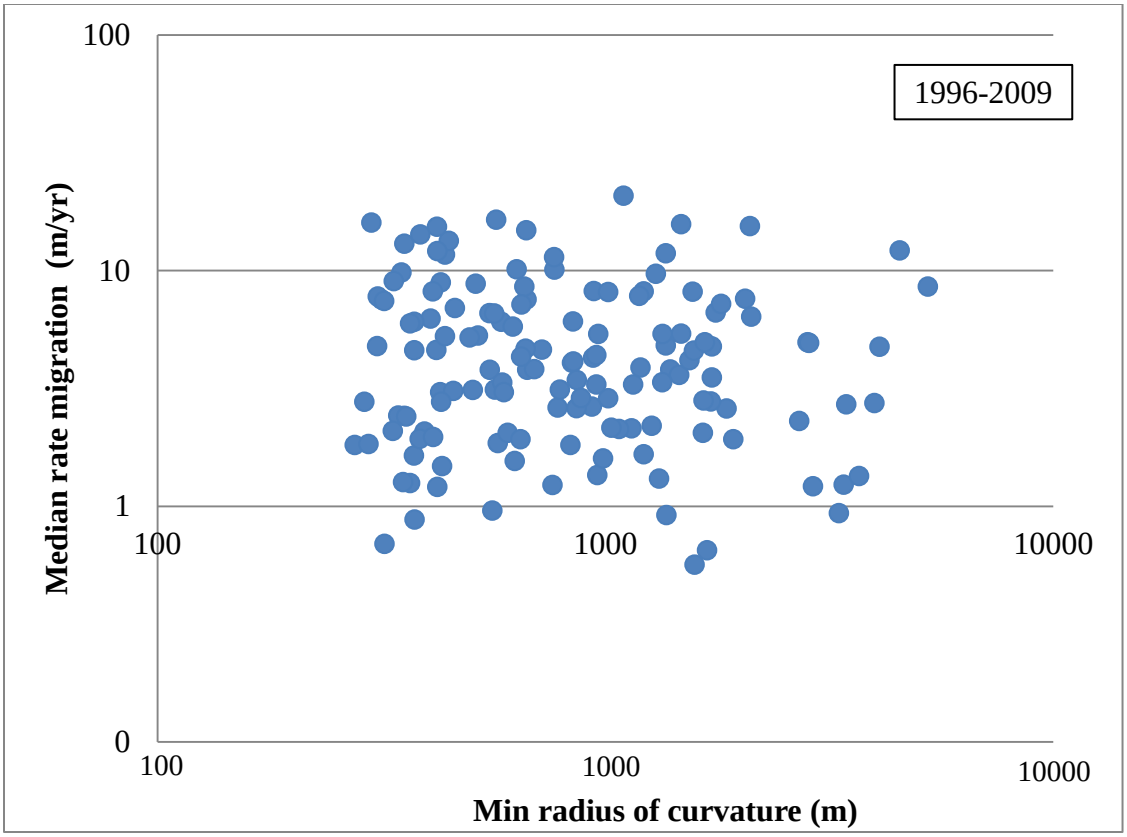


Figure 3.40: median migration rate for each channel bend as a function of the minimum radius of curvature for that bend. The minimum radius of curvature represents the tightest point in the bend, or the apex of the bend.

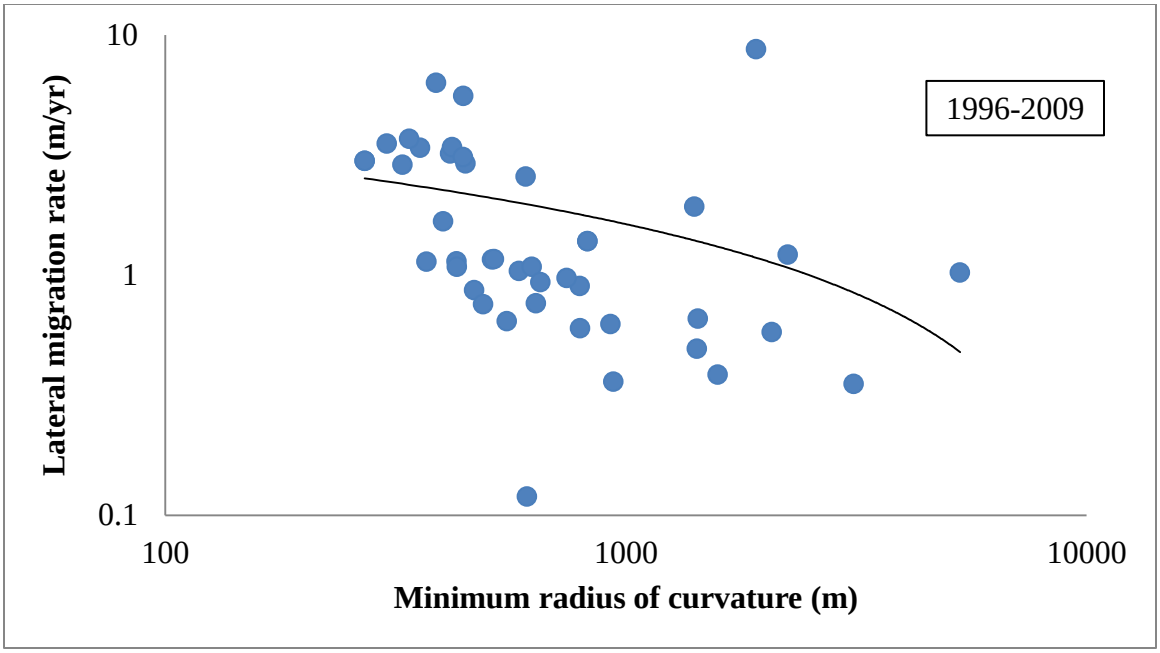


Figure 3.41: Relationship between lateral migration and minimum radius of curvature in Zone Two. The data used in these plots have been filtered and abnormal bends removed; such as bends with tributaries building deltas and bends with bridges. Unlike Figure 3.40 there is a definate trend in the migraton–radius curvature relationship.

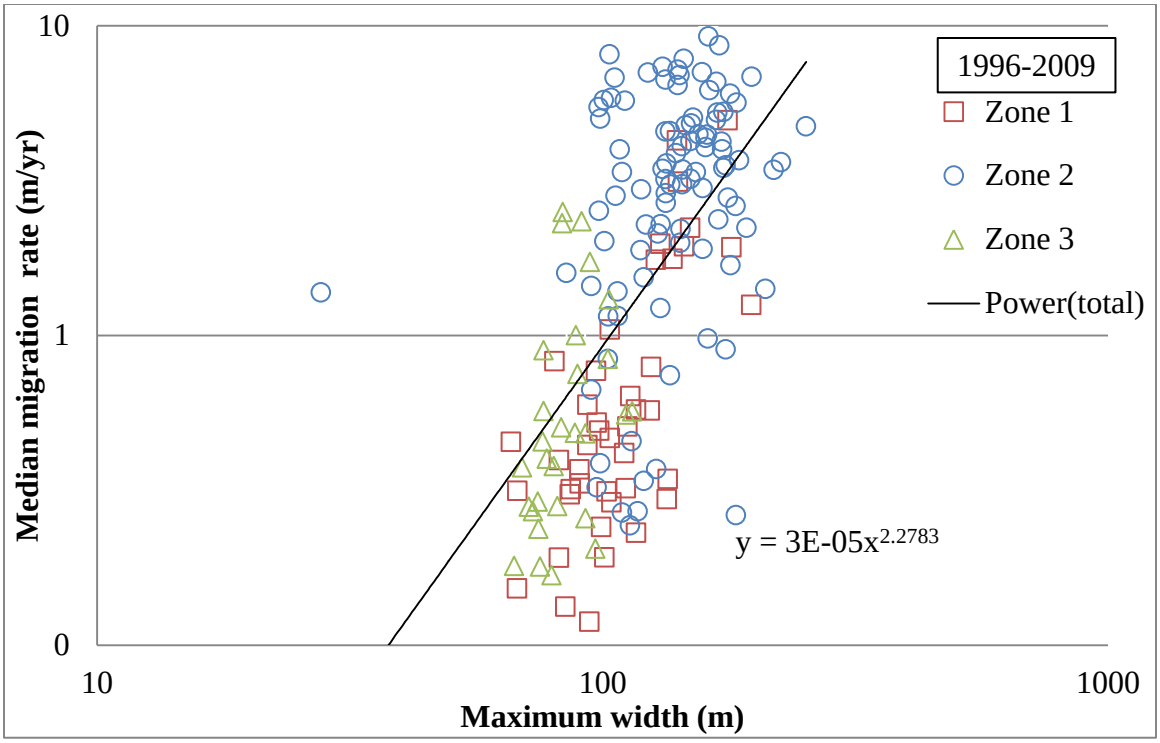


Figure 3.42: Median bend migration rate as a function of the maximum value for channel width in that bend. Each zone has a slightly different migration to width relationship. Zone One is shown with red squares, Zone Two is shown with blue circles, and Zone Three is shown with green triangles.

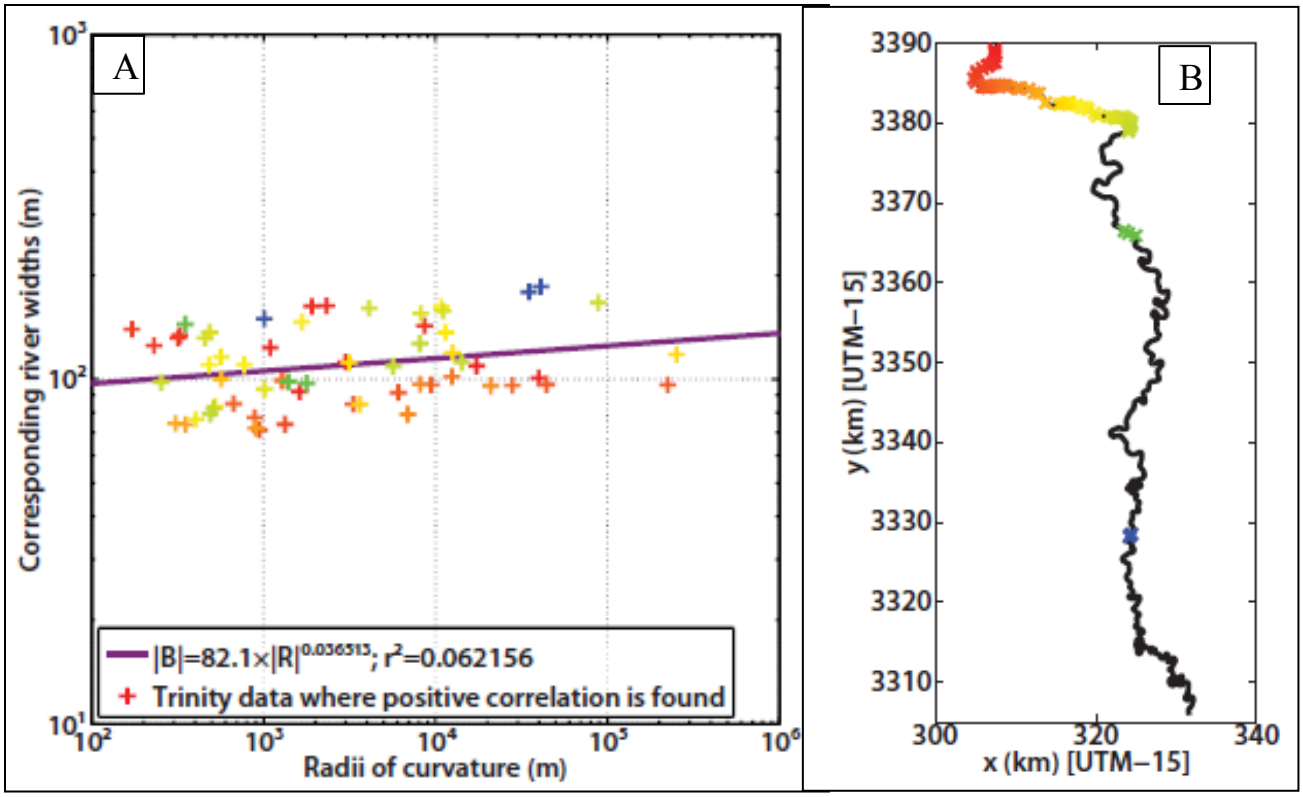


Figure 3.43: (A) Local bankfull river width as a function of local radius of channel curvature for Zone One. When the channel is wider the bend is straighter and when the channel is narrower the bend is tighter. The colors in (A) correspond with the locations shown on the map of the study area (B). The two areas that are exceptions in Zone Two are located at bridge crossings.

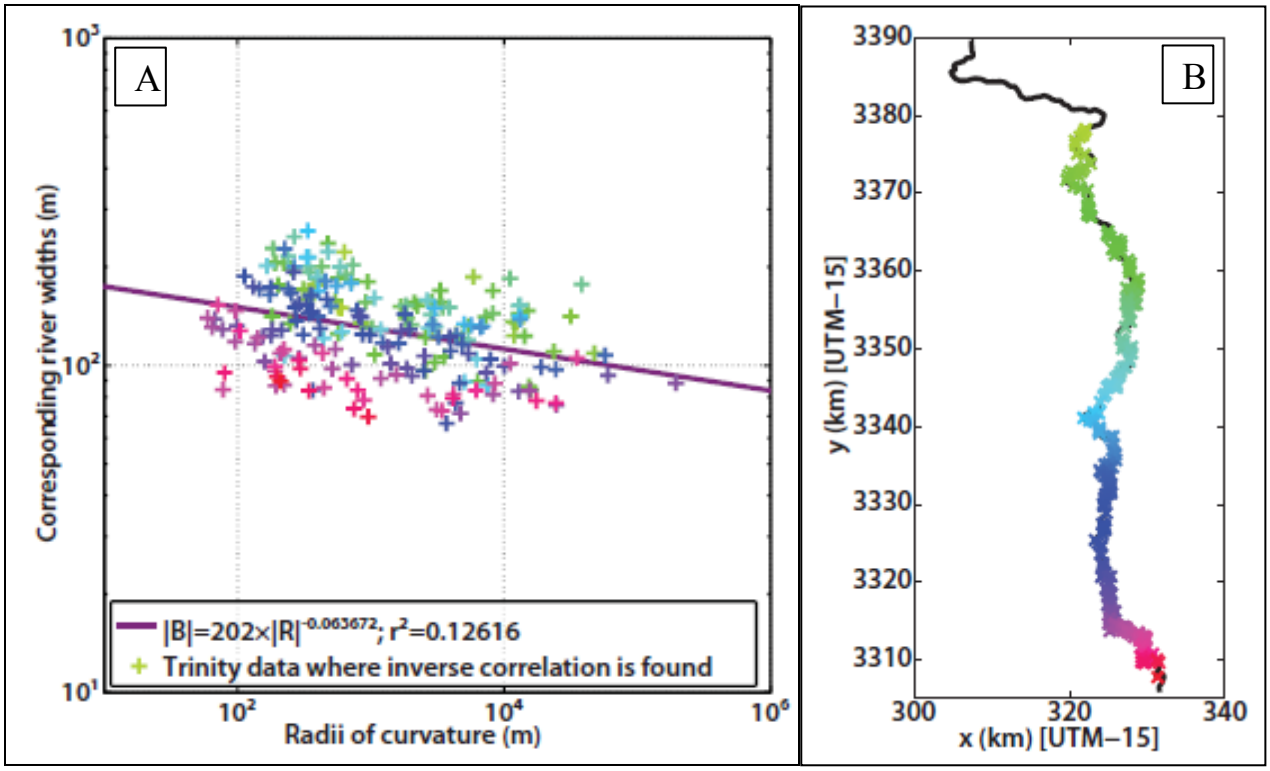


Figure 3.44: **(A)** Local bankfull river width as a function of local radius of channel curvature for Zone Two and Zone Three. When the channel is wider the bend is tighter and when the channel is narrower the bend is straighter. The colors in (A) correspond with the locations on the map of the study area (B).

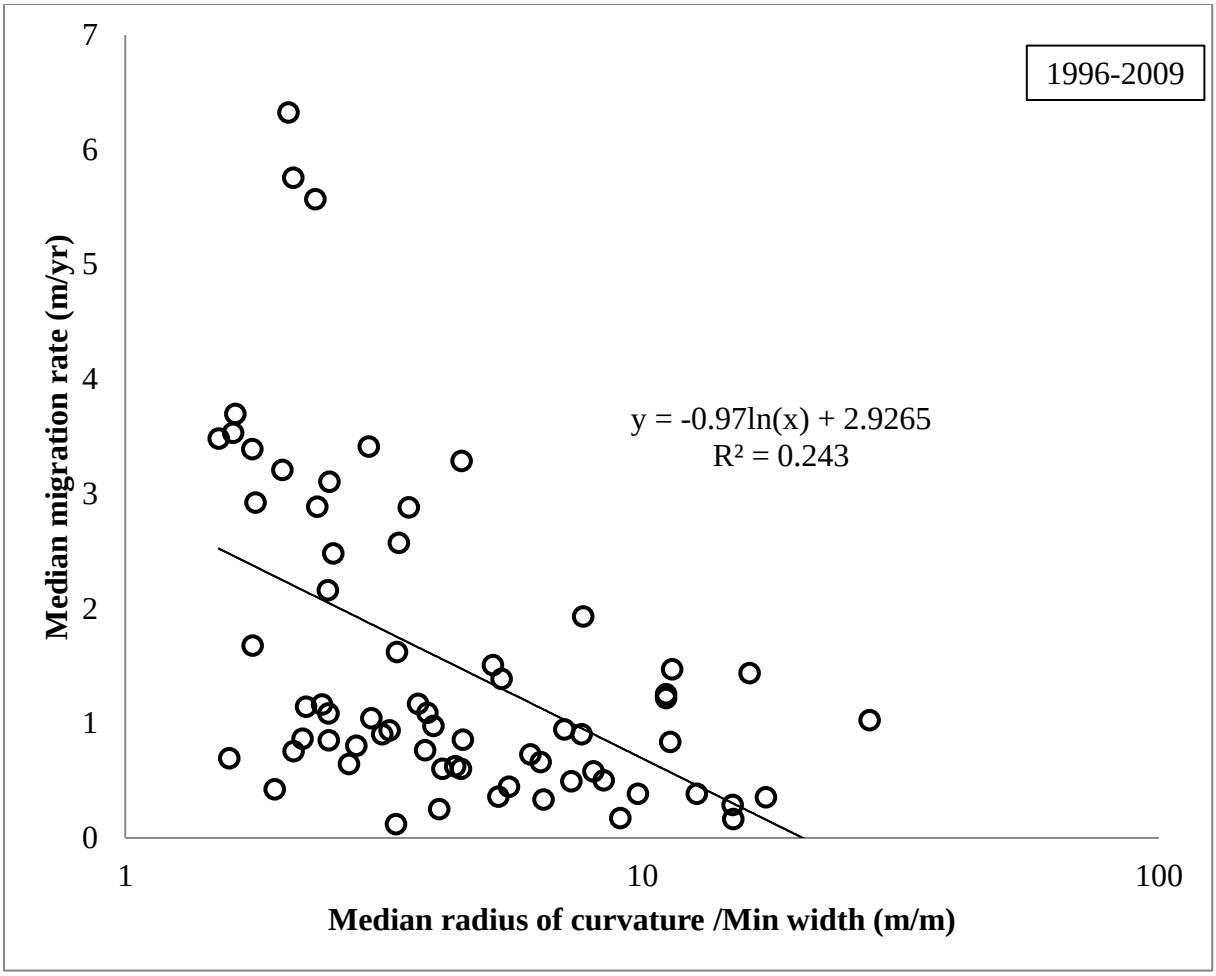


Figure 3.45: Median value for lateral migration rate as a function ofminum radius of curvature normalized by the maximum channel width for each bend Zone Two.

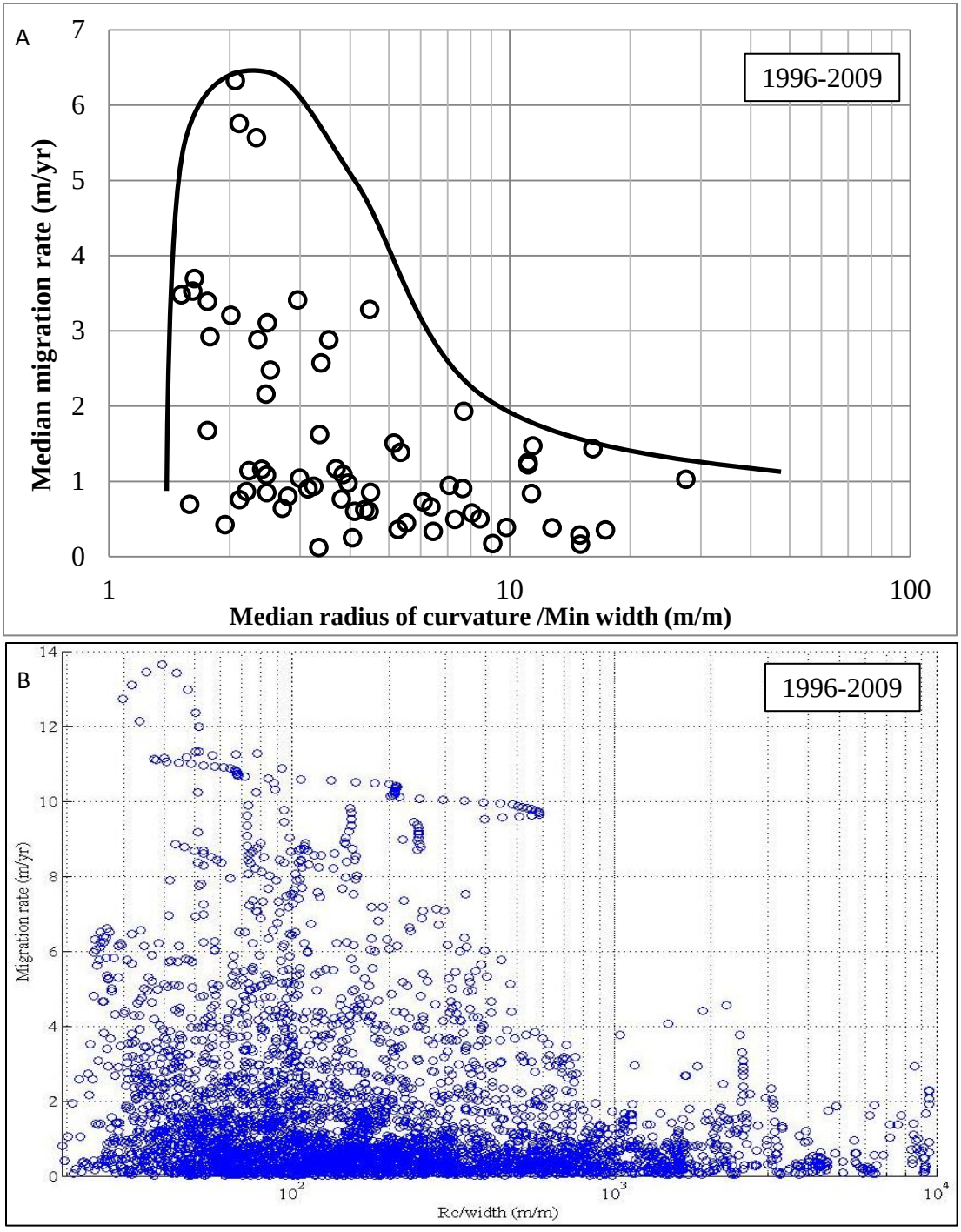


Figure 3.46: The black line marks an envelope containing the data for bends from Zone Two. The shape of the envelope is similar to the shape of the graphs from previous studies (Fig. 3.4). The bends plotted in the graph do not include bends containing tributary mouths or bridges. (B) The lateral migration versus width normalized radius of curvature for every transect along the river (Fig. 3.10).

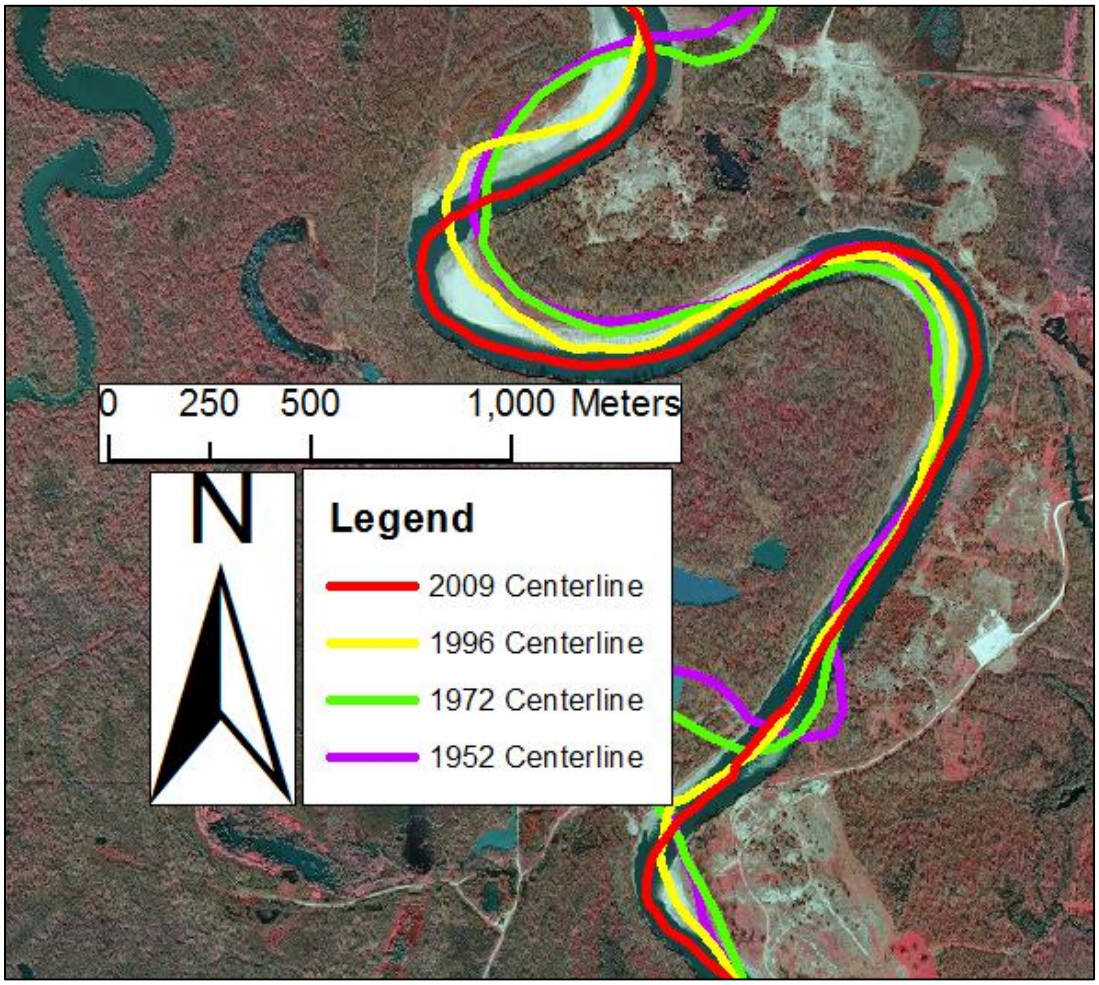

Figure 3.47: Several bends in Zone Two, the normal flow portion of the river. Two of the bends near the center of the image have similar curvatures, but very diffreent rates of migration. This location is roughly 125 river kilometers from the Livingston Dam.

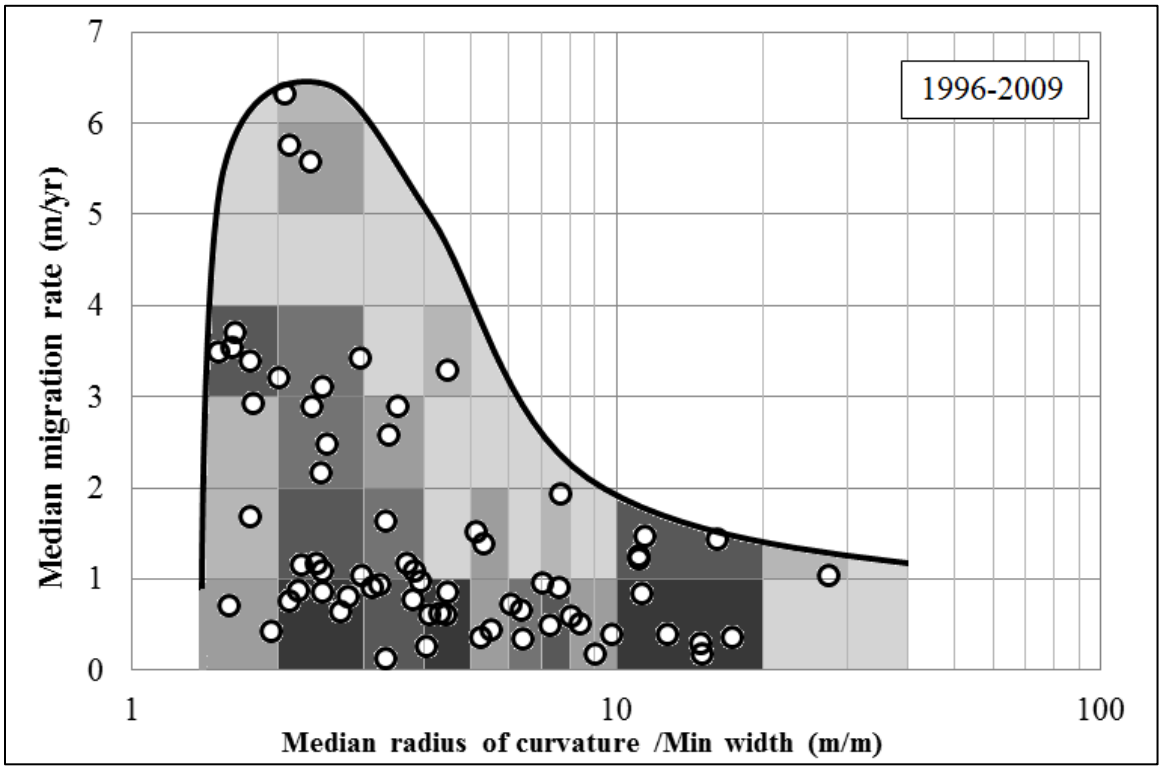


Figure 3.48: The envelope containing the data from the bends in Zone Two. The shades if grey in represent the probability of occurrence for any particular migration rate at a given normalized radius of curvature. The darker the color the higher the probability, the lighter colors show lower probability of occurence. This data points represent bends in Zone Two of the river.

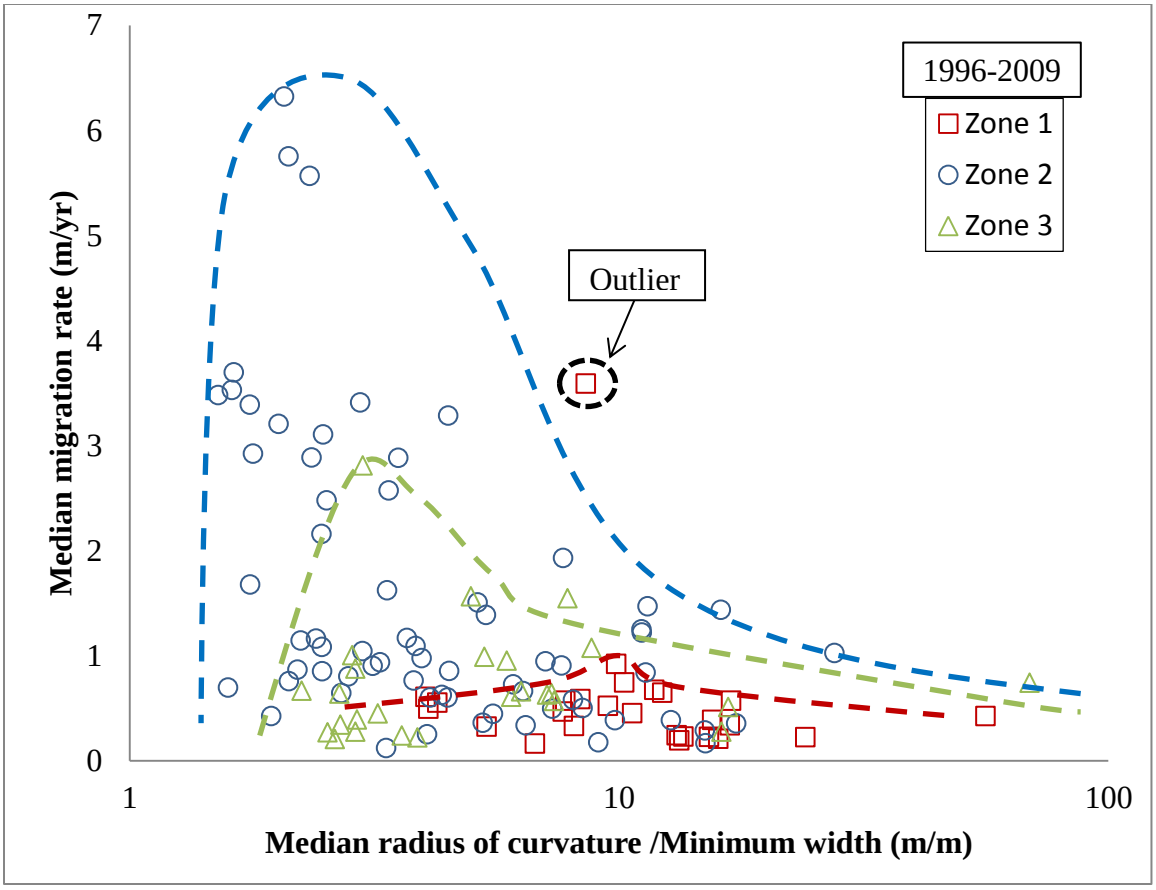


Figure 3.49: Three datasets represent the three geomorphic zones of the river. The dashed lines represent the envelope of each dataset. For Zone Two and Zone Three the envelopes closes resemble the graphs from previous studies (Fig. 3.4). Zone One shows a different pattern. This is due to an inconsistence in the radius of curvature to width relationship in Zone One (Fig. 3.42). There is one outlying point shown in Zone One. This point does exist, but is likely due to construction near the dam.

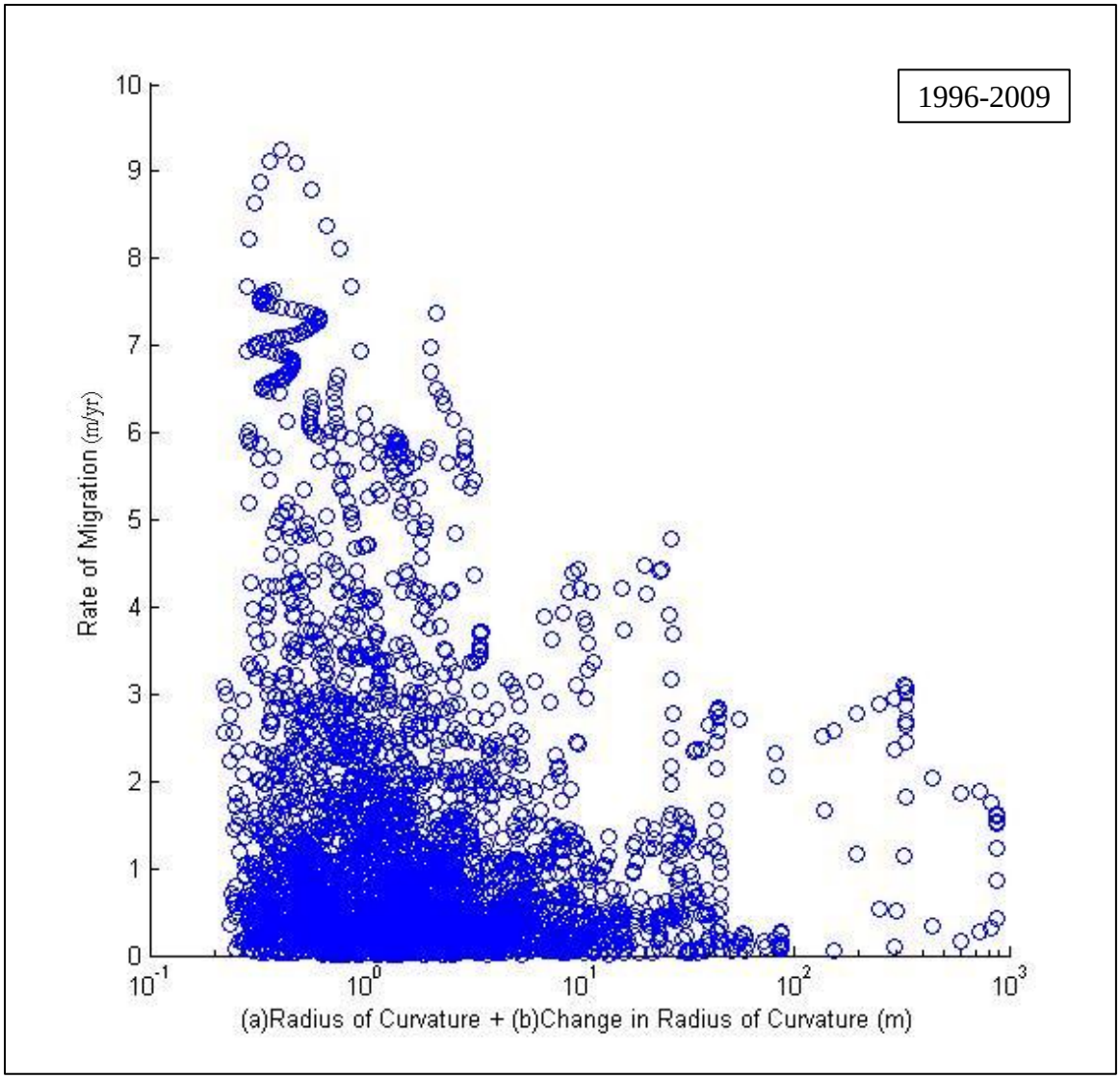


Figure 3.50: While it is understood that bends interact, influencing the migration rates of bends upstream and downstream I was unable to capture that in this data analysis. This graph shows the radius of curvature plus a change in the radius of curvature plotted against migration. There is no discernible improvement over the data reported in Figure 3.45.

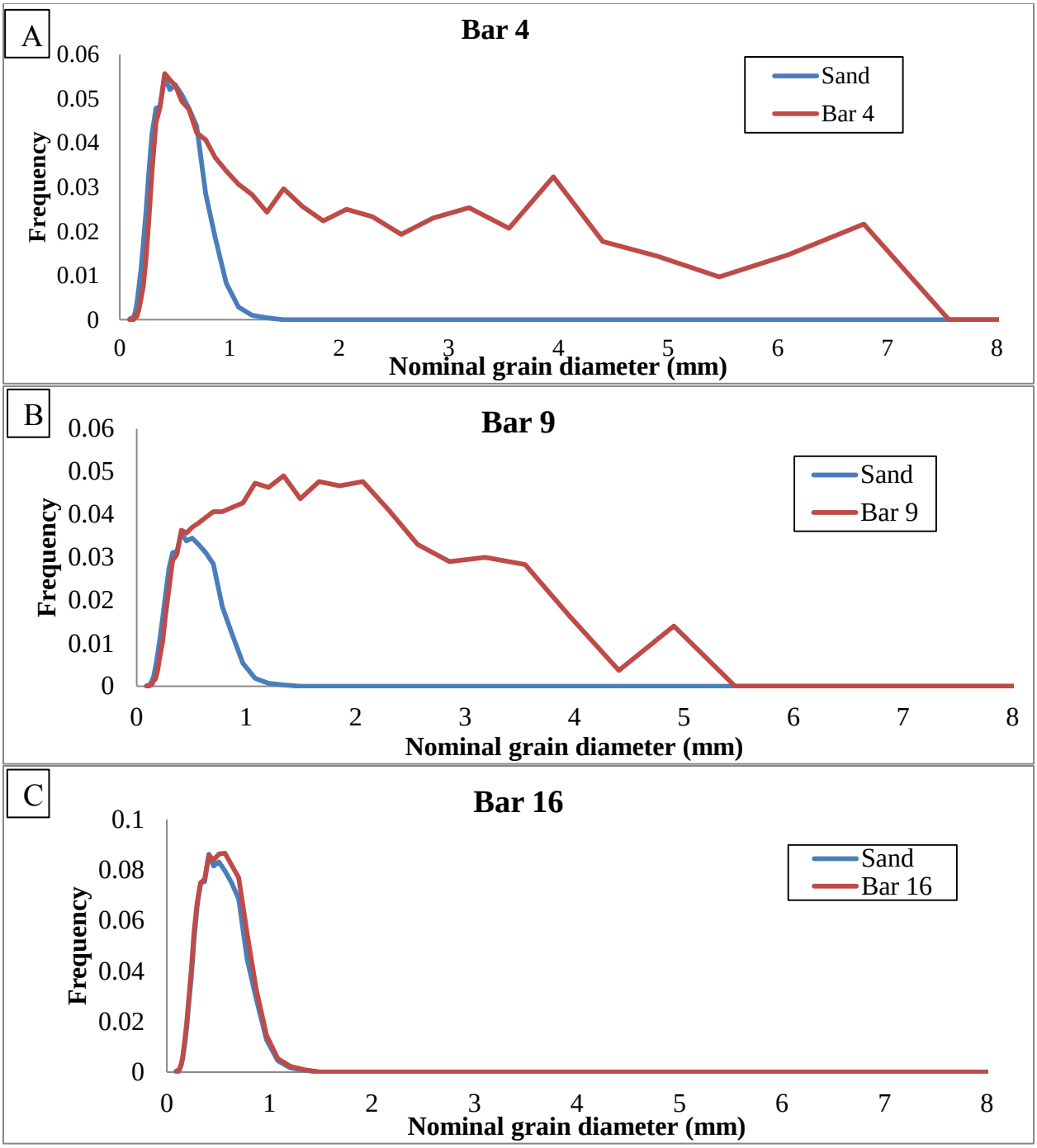


Figure 3.51: The blue line above shows the distribution for sand that remains approximately constant through the system (Fig. 3.13 and 3.14). The red line shows the distribution for all of the grains on a bar (A). Bar Four is roughtly 33 river kilometers from Livingston Dam. This bar has a greater precentage of large grains than most bars. (B) Bar Nine approximately 128 river kilometers from the dam. (C) Bar Sixteen is the most downstream bar sampled for grain size and is nearly exclusively sand.

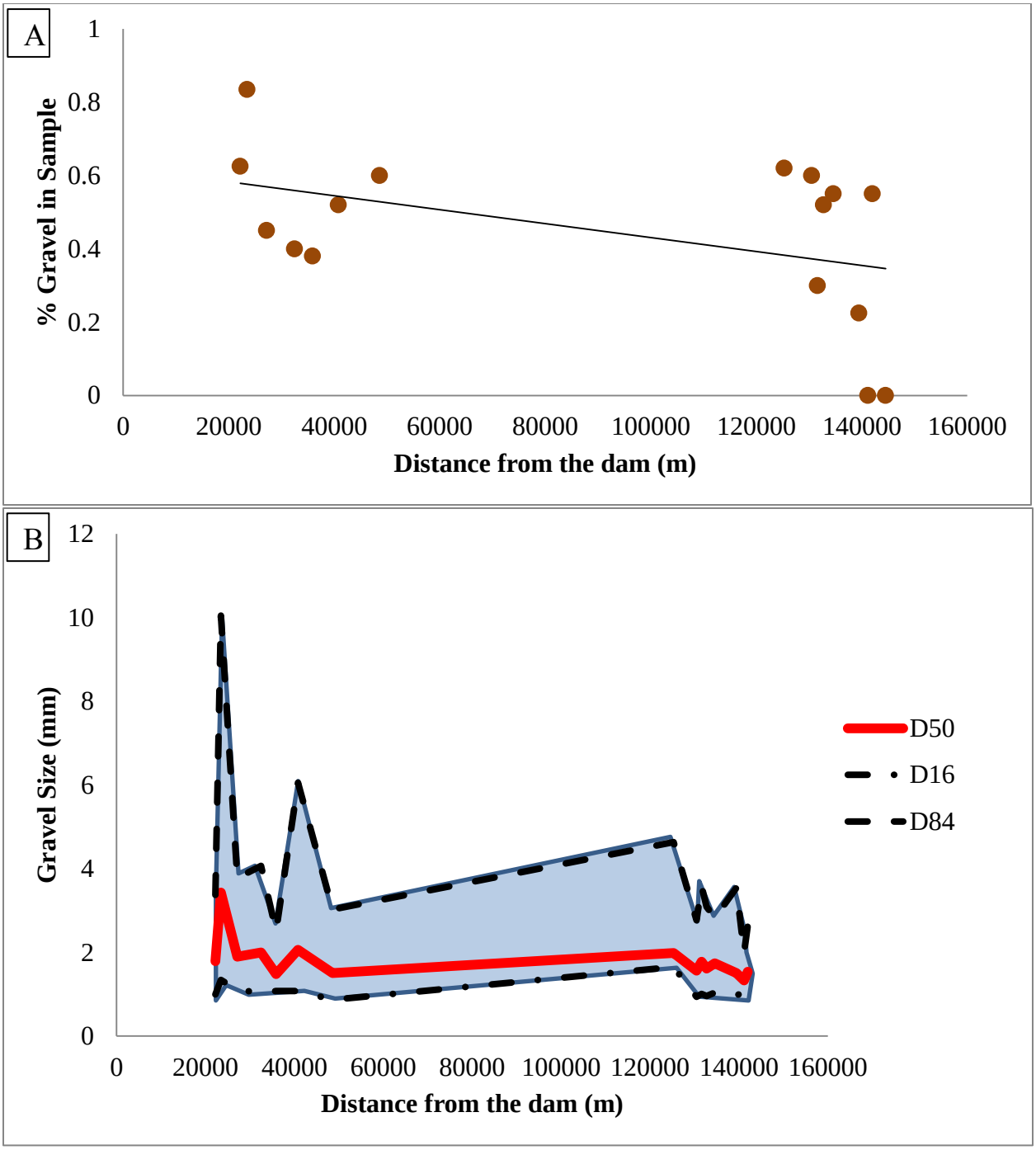


Figure 3.52: (A) and (B) Downstream gravel transition. (A) General trend in volume percent gravel with downstream distance. (B) Median gravel size is shown in red and and the standard deviation is shown around it in light blue. Median gravel size decreases with distance downstream.

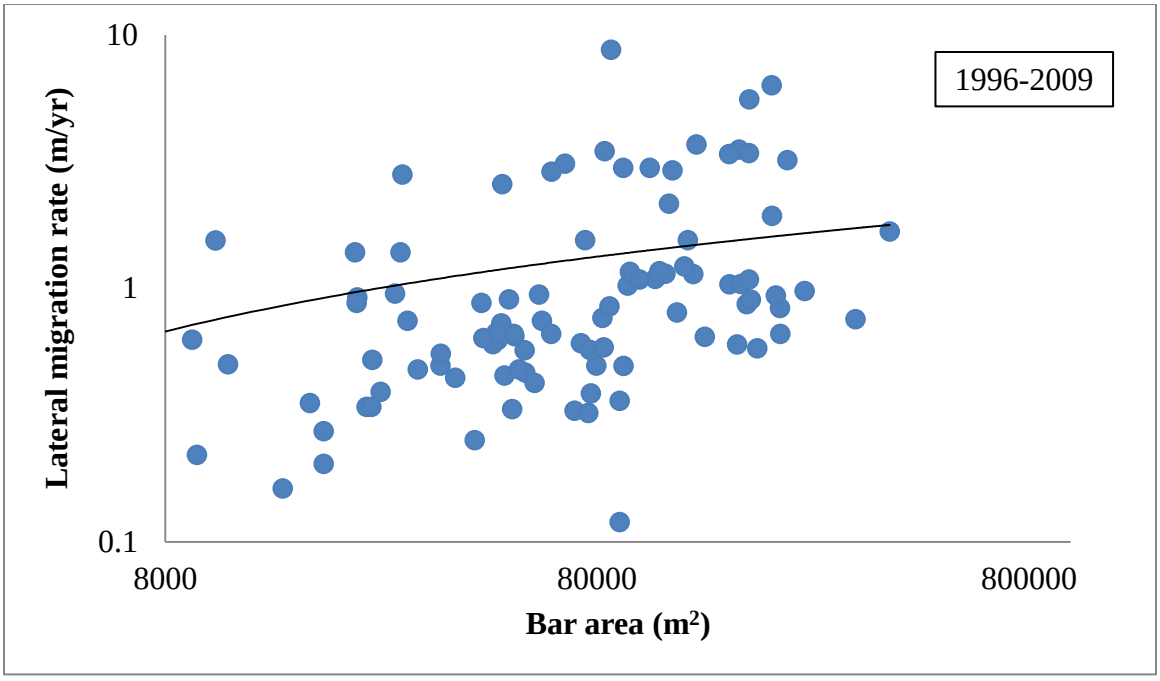


Figure 3.53: Median value for bend migration rate as a function of area for the bar attached to the inner bank of that bend. As bar area increases the lateral migration of the river increases. This matches the trends seen in Figure 32. The data above represents all of the bars in the study area (Zone One, Zone Two and Zone Three).

Figure 3.54: Historic image shows workers on the lower Trinity River. The image does not have an exact data, but was a product of the 1939 U.S. Army Corps of Engineers survey of the river. Around this time there were attempts to transform the river into a shipping canal from the Gulf of Mexico to Dallas and Fort Worth.

**REFERENCES**

Bates, R.E., 1939. "Geomorphic history of the Kickappo Region," *Geological Society of America Bulletin*, Vol. 50, p. 819-879.

Begin, Z.B., Stream curvature and bank erosion: a model based on the momentum equation, *The Journal of* Geology, vol. 89, no. 4, p. 497-504, 1981.

Biedenharn, D., N. Raphett, and C. Montague, 1989. "Long-term stability of the Ouchita River," In: C.M. Elliot (ed.), River Meandering, *Proceedings of the Conference Rivers'83,* New Orleans, LA, p.126-137.

Blondeaux , P., and G. Seminara, 1985. "A unified bar-bend theory of river meanders," *Journal of Fluid Mechanics*, vol. 157, p. 449-470.

Brandt, S.A., 2000. "Classification of geomorphological effects downstream of dams," *Catena,* Vol.40, p. 375–401.

Braudrick, Christian A., William E. Dietrich, Glen T. Leverich and Leonard D. Sklar, 2009. "Experimental evidence for the conditions necessary to sustain meandering in coarse-bedded rivers," Proceedings of the National AcaDEMy of Sciences of the United States of America, Vol. 106, no. 40, p. 16936-16941.

Brice, J.C., 1974. "Evolution of Meander Loops," *Geological Society of America Bulletin,* Vol. 85, p.581-586.

Brune, Gunnar M., 1953. “Trap Efficiency of Reservoirs,” *Transactions,* American Geophysical Union, Vol. 34, No. 3, p.407-418.

Carson, M.A. and M.F. Lapoionte, 1983. “The inherent asymmetry of river meander planform,’ *Journal of Geology,* vol. 91, no. 1, p. 41-55.

Chow, Ven Te, David Maidment and Larry Mays, 1988. Applied Hydrology, McGraw, New York, p. 281.

Dietrich, William E., 1987. "Chapter 8: Mechanics of Flow and Sediment Transport in River Bends." *River Channels: Environment and Process: Institute of British Geographics Special Series*. Ed. K. Richards. Vol. 18, p. 179-227.

Dietrich, William E., and Peter Whiting, 1989. "Boundary shear stress and sediment transport in river meanders of sand and gravel." *American Geophysical Union*, p. 1-50.

Dingman, S. Lawrence, 1991. Fluvial Hydrology, W.H. Freeman and Company, New York, p. 184-193.

Engelund, F., 1974. “Flow and bed topography in channel bends,” *Journal of Hydraulics*, Vol. 100, 1631-1648.

Furbish, D.J., 1988. “River-bend curvature and migration: How are they related?”, *Geology*, vol. 16, p. 752-755.

Furbish, D.J, 1991. “Spatial autoregressive structure in meander evolution”, *Geological Society of America Bulletin*, vol. 103, p. 1576-1589.

Graf, William L., 2006. “Downstream hydrologic and geomorphic effects of large dams on American rivers,” *Geomorphology*, Vol. 79, p. 336-360.

Harvey, Michael D., 1989. “Meanderbelt dynamics of the Sacramento River, CA,” *USDA Forest Service Gen. Tech. Rep.*, PSW-110, p.54-59.

Hickin, E.J., 1974. “The Development of Meanders in Natural River-channels”, *the American Journal of Science*, vol. 274.

Hooke, J.M., 1995. “Processes of channel planform change on meandering channels in the U.K.”, In: Gurnell, A and Petts, G. (eds), Changing River Channels, John Wiley and Sons Chichester, U.K., p. 87-115.

Hooke, J.M., 2003. “River meander behavior and instability: a framework for analysis”, *Transactions of the Institute of British Geographers*, vol. 28, no. 2, p. 238-253.

Hooke, J.M., 2007. “Spatial variability, mechanisms and propagation of change in an active meandering river,” *Geomorphology*, vol. 84, p. 277-296.

Howard, A.D. and T.R. Knutson, 1984. “Sufficient conditions for river meandering: A simulation approach”, *Water Resource Research*, vol. 20, no. 11, p. 1659-1667.

Hudson, Paul F. and Richard H. Kesel, 2000. “Channel migration and meander-bend curvature in the lower Mississippi River prior to major human modification,” *Geology,* Vol. 28, No. 6, p. 531-534.

Ikeda, Syunsuke, Gary Parker and Kenji Sawai, 1981. “Bend theory of river meanders. Part 1. Linear development,” *Journal of Fluid Mechanics,* Vol. 112, p. 363-377.

Inglis, C.C., 1937. “The relationships between meander belts, distance between meanders on axis of stream, width and discharge of rivers in flood plains and incised rivers: Annual Report,” Central Board of Irrigation (India) 1938-1939, p. 49.

Jefferson, M., 1902, “Limiting width of meander belts,” *National Geographic Magazine*, vol. 13, p. 373-384.

Jerolmack, Douglas J., 2009. “Conceptual framework for assessing the response of delta channel networks to Holocene sea level rise,” *Quaternary Science Reviews,* Vol. 28, p. 1786-1800.

Lagasse, P.F. et al., 2004. “Methodology for Predicting Channel Migration,” *National Cooperative Highway Research Program Transportation Research Board of the National AcaDEMies* Document 67.

Larsen, E. and H.W. Shen, 1989. “The evolution of meander bends of the Mississippi River,” In: Yalin, M.S. (Chair), Hydraulics and the Environment, *Proceedings of the XXIII Congress of the IAHR,* Vol. B, Fluvial Hydraulics, p. B33-B39.

Lauer, J. Wesley and Gary Parker, 2008. “Modeling framework for sediment deposition storage, and evacuation in the floodplain of a meandering river: Theory,” *Water Resources Research* Vol. 44.

Lewin, J., 1978. “Meander bend development and floodplain sedimentation: A case study from mid-Wales,” *Geology Journal,* vol. 13, part 1, p. 25-36.

Leopold, Luna B,and M. Gordon Wolman, “River channel patterns: Braided, meandering and straight,” U.S. Geological Survey Professional Paper 282B, p. 85, 1957.

Leopold, Luna B,and M. Gordon Wolman, 1960. “River Meanders,” *Geological Society of America,* vol. 71, p. 769-794.

Leopold, Luna B., M. Gordon Wolman, and John P. Miller. 1964. *Fluvial Processes in Geomorphology*. San Francisco: W.H. Freeman.

Leliavsky, Serge, 1955. “An introduction to fluvial hydraulics: London”, Constable and Co, p.255.

Lauer, J Wesley and Gary Parker, 2007. “Net local removal of floodplain sediment by river meander migration,” *Geomorphology* Vol. 96, p.123-144.

MacDonald, T.E., G. Parkers, D.P. Leuthe, 1991. “Inventory and analysis of stream meander problems in Minnesota,” St. Anthony Falls Hydraulic Laboratory Project Report No. 321, p. 38.

Murray B, and C. Paola, 2001. “A cellular model of braided rivers,” *Nature,* Vol. 371, p. 54-57.

Musselman, Zachary A., 2006. “Tributary response to the Lake Livingston impoundment—the Lower Trinity River, Texas,” Doctoral Dissertation, University of Kentucky.

Musselman, Zachary A., 2011. “The localized role of base level lowering on channel adjustment of tributary streams in the Trinity River basin downstream of Livingston Dam, Texas, USA,” *Geomorphology*, Vol. 128, p.42-56.

Nelson, J.M. and J.D. Smith, 1989. “Flow in meandering channels with natural topography,” in S. Ikeda and G. Parkers (Eds.), *River Meandering, American Geophysical Union Water Resources Monograph 12*, p. 1-50.

Nelson, J.M., 1990. “The initial instability and finite-amplitude stability of alternate bars in straight channels,” *Earth-Science Reviews*, vol. 29, p. 97-115.

Nittrouer, Jeffery, 2010. “Sediment transport dynamics in the lower Mississippi River: Non-uniform water flow and affects on river-channel morphology,” Dissertation, University of Texas at Austin.

Nittrouer, Jeffery, David Mohrig, and M.A. Allison, 2012. “Punctuated transport of bed materials in the lowermost Mississippi River,” *Journal of Geophysical Research-Earth Surface.*

Nittrouer, Jeffery, John Shaw, Michael Lamb, and David Mohrig, 2012. “Spatial and temporal trends for water-flow velocity and bed-material sediment transport in the lower Mississippi River,” *GSA Bulletin,* Vol. 124, No. ¾, p. 400-414.

Paola, Chris, and David Mohrig, 1996. “Paleohydraulics revisited: Paleoslope estimation incoarse-grained braided river,” *Basin Reservoirs,* Vol. 9, p. 243-254.

Parker, Gary, 1976. “On the cause and characteristic scales of meandering and braiding in rivers,” *Journal of Fluid Mechanics,* Vol. 76, p. 457-480.

Parker, Gary, 2004. “1D Sediment Transport Morphodynamics with Applications to Rivers and Turbidity Currents: E-book.” St. Anthony Falls Laboratory, University of Minnesota, Minneapolis, http://vtchl.uiuc.edu/people/parkerg/morphodynamics_e-book.htm, August 20, 2010.

Parker, Gary and Edmund D. Andrews, 1986. “On the time development of meander bends,” *Journal of Fluid Mechanics,* Vol. 162, p. 139-156.

Parker, G., T. Muto, Y. Akamatsu, W. E. Dietrich, and J. W. Lauer, 2008. "Unravelling the conundrum of river response to rising sea-level from laboratory to field. Part II. The Fly–Strickland River system, Papua New Guinea", *Sedimentology*, Vol. 55, p. 1657–1686.

Parker, Gary, Kenji Sawai and Syunsuke Ikeda, 1982. "Bend theory of river meanders. Part 2. Nonlinear deformation of finite-amplitude bends," *Journal of Fluid Mechanics*, Vol. 115, p. 313-314.

Parker, G., Y. Shimizu, G.V. Wilkerson, J.D. Abad, J.W. Lauer, C. Paola, W.E. Dietrich, and V.R. Voller, 2011. "A new framework for modeling the migration of meandering rivers," *Earth Surface Processes and Landforms*, vol. 36, no. 1, p. 70-86.

Parker, Gary, Tetsuji Muto, Yoshihisa Akamatsu, William E. Dietrich, and J. W. Lauer, 2006. "Unraveling the conundrum of river response to rising sea level from laboratory to field. Part II. The Fly-Strickland River System, Papua New Guinea." MS 2. National Center for Earth-surface Dynamics.

Petts, Geoffrey E. and Angela M. Gurnell, 2005. "Dam and geomorphology: Research progress and future directions." *Geomorphology*, Vol. 71, p. 27-47.

Peyret, Aymeric-Pierre B., 2011. "Morphodynamics and geometry of channels, turbidites and bedforms," Dissertation, the University of Texas at Austin.

Phillips, Jonathans and Michael Slattery, 2007. “Downstream trends in discharge, slope, and stream power in a lower coastal plain river," *Journal of Hydrology*, Vol. 334, p. 290-303.

Phillips, Jonathan, Michael Slattery, and Zachary Musselman, 2005. "Channel adjustments of the Lower Trinity River, Texas downstream of Livingston Dam," *Earth Surface Processes and Landforms,* Vol. 31, p. 1419-1439.

Prus-Chacinski, T.M., 1954. “Patterns of motion in open-channel bends,” *International Association of Hydrology*, pub. 38, vol, 3, p. 311-318.

Schumm, S.A., 1993. “River Response to Baselevel Change: Implications for sequence stratigraphy,” *The Journal of Geology*, Vol. 101, No. 2, p. 279-294.

Slattery, Micheal C. and Jonathan D. Phillips, (2007). “Sediment monitoring in Galveston Bay – Final Phase,” *Final Report,* Texas Water Development Board.

Slattery, Michael C. and Jonathan D. Phillips, 2007. “Sediment monitoring in Galveston Bay – Final Phase,” *Final Report,* Texas Water Development Board.

Smith, J.D. and McLean, 1984. “A Model for meandering rivers,” *Water Resources Research*, Vol. 20, p. 1311-1315.

Sun, Tao, Paul Meakin and Torstein Jossang,, 1996. “A simulation model for meandering rivers,” *Water Resources Research,* Vol. 32, No. 9, p. 2937-2954.

Sun, Tao, Paul Meakin and Torstein Jossang, 2001. “A computer model for meandering rivers with multiple bed-load sediment sizes, 1. Theory,” *Water Resources Research,* Vol. 37, No. 8, p. 2227-2241.

Williams, G.P., 1986. “River Meanders and channel size,” *Journal of Hydrology*, vol. 88, p. 147-164.

Williams, G.P. and M.G. Wolman, 1984. “Downstream effects of dams on alluvial rivers,” Geological Survey Professional Paper 1286, U.S. Government Printing Office, Washington, DC, vol. 83.

Whiting, Peter J and William E. Dietrich, 1993. “Experimental constraints on bar migration through bends: Implications for meander wavelength selection,” *Water Resources Research*, Vol. 29, p.1091-1102.

Whiting, Peter J and William E. Dietrich, 1993. “Experimental studies of bed topography and flow patterns in large-amplitude meanders: 1. Observations,” *Water Resources Research*, Vol. 29, p.3605-3614.

Whiting, Peter J and William E. Dietrich, 1993. “Experimental studies of bed topography and flow patterns in large-amplitude meanders: 2. Mechanisms,” *Water Resources Research*, Vol. 29, p.3615-3622.

Zinger, Jessica A., Bruce L. Rhodes and James L. Best, 2011. “Extreme sediment pulses generated by bend cutoffs along a large meandering river,” *Nature Geoscience,* Vol. 4, P. 675-678.

# Chapter 4:

# Point Bar Construction


## ABSTRACT

Rivers exhibit two general styles of migration: persistent outward and downstream motion of bends and relatively abrupt adjustments in channel length due to bend cutoffs. Persistent lateral migration is primarily driven by the flow mechanics in bends that drive outer bank erosion and sedimentation along the inner bank of a bend. Cutoffs, on the other hand, quickly alter the course of a river, forcing a sequence of more rapid bed and bank adjustments to a set of neighboring channel bends. This chapter investigates the relationship between the two styles of channel motion and the growth of associated point bars by examining two meander bends in the lower Trinity River of Texas. The lower Trinity River is a sandy coastal river with banks that are primarily composed of sandy Quaternary fluvial deposits. One of the studied bars is in a bend that has experienced rapid adjustment in response to an upstream cutoff. This bar is characterized by steep adverse and lateral surface slopes at its upstream end and an associated tear-drop shape in planview. The second bar is situated in a bend undergoing persistent lateral migration over the past 60 years. The bar has smaller adverse and lateral slopes at its upstream end and is crescent-like in plan form. I synthesized time-lapse planimetric maps, high-resolution topographic and bathymetric surveys, and trenching of the two point bars deposits to: 1) evaluate the cause-and-effect relationship between cutoffs and meander

adjustments, and 2) understand the relationship between channel plan form, bar morphology and bar sedimentation.

## INTRODUCTION

To better understand the geomorphology of rivers it is import to comprehend the manner in which they migrate and construct or destruct their channel walls. River migration is typically thought of as a continuous process where the pattern of river migration is fairly consistent from year to year. The cut bank is slowly eroded while a helicoidal flow transports sediment away from the cut bank to the point bar or further downstream (*Deitrich*, 1987) . Eventually this bank erosion may reach a critical point resulting in channel cutoff and straightening.

Bend cutoffs and channel straightening create an abrupt change in the system, disabling the typical pattern of river migration. The occurrence of cutoffs or straightening causes a change in the channel flow, impacting the downstream bends and forcing a more rapid style of bend migration. The physical alteration of the river's course due to these events changes the position of the high-velocity core of the flow entering the downstream bend and changes the location and degree to which this core flow impinges on the outer bank. This in turn modifies the cut bank-point bar relationship.

Both styles of bend motion, steady versus abrupt, can be observed in freely meandering rivers such as the lower Trinity River. The larger study area in this discussion begins upstream at Livingston Dam and flows 180 river kilometers to Trinity

Bay, as described in chapter one. The geomorphic expression of the dam persists for approximately 55 river kilometers downstream before tapering out. The most downstream portion of the river, the last 60 kilometers, is influenced by Trinity Bay. The central portion of the study area, approximately 100 river kilometers between the dam and bay influenced zones is freely meandering and the focus of this particular analysis. These zones are shown in Figure 4.1 and are numbered as follows: Zone One is immediately downstream of the dam, Zone Two is freely meandering and Zone Three is influence by the Bay. The bars in this study are located in Zone Two.

The channel bed and walls of the lower Trinity River are composed of previous fluvial deposits from the river itself. The vast majority of these deposits are Quaternary in age with a minor Miocene component (*Phillips et al.*, 2005; Fig. 4.2). The image in Figure 4.3 shows the channel walls of the lower Trinity River. Strata from paleo-channels are evident in the side walls of the channel. The river continually reworks its previous sediment deposits, providing a large supply of fine grain sediment for the river to erode, transport and deposit. The mean grain size in Zone Two is approximate 0.35mm.

The constant supply of fine grain sediment creates an environment that facilitates very active river migration. Zone Two of the study area averages approximately 4.2 meters per year of lateral movement, reflecting both styles of channel migration: persistent lateral motion (Fig. 4.4) and abrupt bend cutoff. Bends beyond a threshold length will grow outward, translate downstream and increase in curvature through time. As a bend translates downstream, its curvature gets tighter and tighter until it eventually

experiences a cutoff (*Parker and Andrews*, 1986). The cutoff of a bend straightens the river, causing downstream migration to acceleration in response. Each style of channel motion impacts the river differently, producing a different rate of change, channel geometry, and bar architecture. This chapter is designed to highlight the differences in the mechanics of these two types of channel migration by studying their migration patterns and styles of point bar construction.

## PREVIOUS STUDIES

Theory suggests that river meanders tend to migrate downstream through a combination of erosion and deposition (*Leopold et al*., 1964). In a sinuous river, flow enters a meander bend tangentially, having just exited from an upstream meander. As the river bends, the flow is forced towards the outer bank due its inertia and the centrifugal force. The presence of the bars causes a topographic steering of the flow (*Nelson and Smith*, 1989). The force causes the velocity of the flow to become laterally stratified with a high velocity core near the outer bank and lower velocity water near the inner bank. The higher velocity flow near the outer bank of a bend spatially correlates with an increasing basal shear stress that leads to erosion along the cut bank (Fig. 4.4). Decreasing values for basal shear stress in the low velocity zone allows for sediment to be deposited along the inner bank, leading to point bar construction (*Dietrich and Gallinati*, 1991).

The spatial variability in the flow field is reflected in many of the physical parameters of a meander bend. The high velocity flow is associated with a super elevation of water surface near the outer bank, higher shear stresses, and greater sediment transport as recorded in experiments by Whiting and Dietrich (1993) and depicted here as Figure 4.5 (*Whiting and Dietrich*, 1993 a, b, c; *Leeder and Bridges*, 1975).

Typically point bars show a downstream fining in grain size. The sorting of grains within a bend can be attributed to the spatial variability of shear stress, flow velocity, and bed topography. Larger grains are transported via bedload while smaller grains can move in suspension. Generally, the highest stress and velocity area on the bar is near its upstream end and decreases with downstream distance. The grain sizes of the deposits follow this trend, fining in the downstream distance (*Dietrich*, 1987).

In addition to the downstream transport, grains are also being transported in a cross-stream direction. For particles moving as bedload, this cross-stream transport is influenced by both the lateral slope of the bar form and the direction of the near-bed flow. For suspended grains the transport direction is governed by the cross-channel component of the flow field that includes the helicoidal flow (*Bridge*, 1977; *Dietrich*, 1987, *Dietrich and Whiting*, 1989).

The net result is point bars that typically exhibit a crescent shape, wrapping around the apex of the bend. Bends typically evolve through outward and downstream movement matches the depositional and erosional processes (*Carson and Lapointe*, 1983; *Parker and Andrews*, 1986). This shape has been documented in numerous field studies

and reproduced in flume experiments (*Jackson*, 1976; *Dietrich et al.*, 1979; *Whiting and Dietrich*, 1993 a, b, c).

As the bend grows outward the radius of curvature is reduced to maintain a constant wavelength. Eventually the curvature of the bend will reach a critical point where a cutoff occurs (*Gagliano and Howard*, 1984; *Mosely*, 1975). For the purposes of this paper, I refer to these single-bend events as cutoffs and cutoffs involving a chain of bends as a straightening. Cutoffs can occur in one flood event but, more commonly, cutoffs occur through a course of several floods (*Nanson*, 1980).

Cutoff and straightening types of events impact the river by increasing the momentum of the water entering the downstream bend. The gain of momentum associated with an upstream cutoff serves to amplify the downstream migration (*Furbish*, 1988). As the river enters the bend the thalweg is pushed dramatically close to the cut bank and deepened, and the cut bank is rapidly eroded. At the same time, the growth of the cutoff erodes the upstream portion of the inner bank, resulting in a temporal increase in the sediment load present in the channel. The introduction of the additional sediment contributes to the alteration of the geomorphology immediately downstream of the cutoff (*Zinger et al.*, 2011). Unlike the case of the persistent lateral migration, the river does not move in a constant manner. Instead, the downstream river bends rapidly readjust to the upstream changes. Eventually the channel re-stabilizes and returns to the persistent style of migration (*Nanson*, 1980).

## STUDY AREA

Within the freely meandering zone of the lower Trinity River there is a very high rate of migration. This portion of the river experiences continuous motion of bends, as well as frequent bend cutoffs and straightening. This study investigates two bends in Zone Two of the river, shown in Figure 4.7. The first bend, Bend One, shown in image 4.7a, is an example of a bend responding to a recent upstream cutoff. In 2002 there was a river straightening event in the bend immediately upstream (Fig. 4.8). Due to the straightening upstream this meander bend experienced an accelerated migration. The second bend, Bend Two, shown in image 4.7c, has only experienced a slower rate of continuous bend movement (Fig. 4.7b).

The migration history of Bend One can be seen in Figure 4.8a from 1952 to 2007. The various colored lines represent four different aerial photograph surveys from 1952, 1972, 1996 and 2009. As can be seen in this image, the channel experiences a cutoff between 1996 and 2007. After the straightening event, the channel downstream has an accelerated migration rate.

Figure 4.9 shows the cutoff and post-cutoff adjustment at Bend One. In 1995, image 4.9a, Bend One was located downstream of a tight bend. At this point the point bar appears to be atypical, wrapping about the bend apex. By 2002, image 4.9b, the bend experienced a cutoff. After the cutoff occurred the straightening continued and the downstream migration was accelerated. By 2005, image 4.9c, a road on the outer bank,

just upstream, has been washed away. By 2010, image 9f, the upstream end of the point bar has been completely eroded away, so that the bar no longer wrapped around the apex of the bend. At this stage, the bar exhibited a tear-drop shape. After reviewing all of the bars downstream of cutoffs in the four aerial photographic surveys for the entire lower Trinity River I found that bars downstream of recent cutoffs exhibited the teardrop shape, as opposed to the more typical crescent shape. Between 1952 and 2009 there were eight major cutoffs. In each instance the front portion of the bar had been washed away resulting in a teardrop shape. Four examples of teardrop shaped bars downstream of cutoffs are shown in Figure 4.10.

The point bar in Bend Two, exhibits the more common crescent shape, as can be seen in Figure 4.8b. Unlike the first bend, this style of migration never reshaped the bend, but instead pushed it outward and downstream. The image shows that the bend is marching in the direction of the eroding outer bank and the inner bank is being built by sediment deposition. In this image the centerlines are depicted from 1952, 1972, 1996 and 2009. This style of migration maintains a fairly constant rate year to year.

**METHODOLOGY**

A suite of aerial photographs were shot for the Trinity River over several decades. The aerial photographs, taken in 1952, 1972, 1996 and 2009, were imported to GIS as images. The suite of aerial photographs collected by the Texas Natural Resource

Information System (TNRIS) for the Trinity River over approximately 60 years were used for this study. The surveys were finalized in 1952, 1972, 1996 and 2009. However, the collection date was slightly earlier in some cases (Table 4.1). For the purpose of this study the finalized survey date is reported but the collection date was used in all temporal calculations. In GIS, the images were geo-referenced using shapefiles of local infrastructure; such as bridges, railroad tracks and roads (shapefiles from TNRIS). The banks, centerlines and point bars were then traced using GIS tools and made into shapefiles. Once the banks, bars and centerlines were translated into GIS shapefiles (points, lines and polygons) the river was analyzed comprehensively for the entire length of the river, from the Livingston Dam to Trinity Bay.

After digitizing the river features, the Planform Statistics Tool (PST) was used to measure the lateral migration and channel width (*Lauer*, 2006). The tool uses Bezier curves to measure the lateral distance between two lines. The GIS outputs of the analysis include migration rate, channel width, and point bar area. These outputs also allowed us to qualitatively and quantitatively analyze the changing shape of the two bars.

To gain a deeper understanding of the mechanics at play in the bends we, myself and Mohrig research group, surveyed each bend extensively. In early December of 2010 a field survey was done on two point bars in Zone Two of the Trinity River. Three styles of surveys were used: topographic, bathymetric and transects. In addition to these surveys, grain samples and many photographs were taken. The combination of these surveys allowed us to draw a three dimensional image of the bars and the depositional mechanics at play.

The topographic survey was done using a Trimble Total Station and tied into two NetRS GPS antennas. The top of the bar was surveyed in a grid. Lines were surveyed perpendicular and parallel to the centerline of the river. The survey covered the entire bar and continued into the water. By expanding the survey into the water, the topographic and bathymetric surveys could be integrated. The surveys were geographically referenced using NetRS GPS antennas. The antennas were left stationary for one hour, tied into the survey and moved further downstream on the bar. In addition to surveying the entirety of bars, the outer bank was surveyed in Bend One.

The bathymetric survey was accomplished with the use of the River Bandit. The River Bandit, shown in Figure 4.11, is a structure built from extruded aluminum bar and designed to hold bathymetric surveying equipment, transducers, off the sides of the boat. The apparatus holds four hydrophones and two GPS antennas. Two GPS's were position on the center top of the lattice 1.25 m apart. The hydrophones were spaced 1.61 m apart, each 15cm below the water surface. The hydrophones used were single-beam depth sounders, made by SyQwest, Inc. The GPS antennas used there the NetRS GPS antennas. The NetRS data was processed using tools from NASA's Automatic Precise Positioning System (APPS). A custom Matlab code was then used to pair the NetRS data with the hydrophone data. Finally, the data was cleaned using GIS. This survey was then tied into topographic survey.

Figure 4.12a shows the topographic survey for Bar One. Figure 4.13a shows the results of the topographic survey for Bar Two. The colors of the points represent the surface elevation, warm colors being higher elevations and cool colors being lower

elevations. The transects that were dug perpendicular to the centerline of the river across the bar are labeled by number and color in Figures 4.12a and 4.13a. These transects correspond with the elevation profiles shown in Figure 4.12b and 4.13b. The transects and surveys show that Bar One has a greater amount of relief than Bar Two. Bar One has a steep upstream face. Bar Two gently slopes from the tree line to the thalweg.

The surveys were processed in GIS. In GIS a three dimensional surface was created for each bar using a distance weighted averaging method. Lengthwise transects (parallel to the centerline of the river) were taken from this surface, shown in Figure 4.14. Figure 4.14a and b show the location of where the lengthwise transects were sampled. Figure 4.14c shows the elevation of each transect going from upstream to downstream. There are two immediately noticeable differences between the two transects. First, the transects differ greatly in the upstream portion. The front of Bar One is the steepest portion of the bar and has the highest elevation. The front of Bar Two is gentle, one of the lowest slopes of the bar. The peak of the second bar is slightly downstream of its midpoint. A comprehensive view of the elevation distribution of the bars is shown in Figure 4.15. Figure 4.15a and b show DEM for each of the bars.

The transect survey was accomplished though transecting the bars by digging a series of trenches across the bar tops. Three trenches and two pits were dug across Bar One. The trenches were approximately 50 meters long. The pits were much shorter, only a few meters in length. Both the pits and trenches were half a meter to a meter deep. One side of the trench or pit was smoothed using a machete to expose the cross-strata of the point bar. Overlapping pictures were taken these faces along the length of each

trench and pit. Figure 4.16 and 17 show elevation profiles for the transects and sample images from the trenches. Complete mosaics of the photographs from the trenches that were dug across Bar One and Bar Two are available in the appendix.

Grain samples were collected every half meter along each trench. Each sample was labeled with the distance from the water's edge and any descriptive details pertaining to the samples origin location. The majority of these samples were later processed using a Retsch Technology CamSizer. The finest-grain samples were analyzed using a Laser Particle Size Analyzer (LPSA).

**RESULTS**

A compilation of the data revealed differences between the bars' shape and style of construction. While the shapes of the bars differ, the sizes of the bars are relatively the same. Each bar is approximately 650m long. Bar One has a slightly greater width; 152m compared to Bar Two's 102m. Also, the area and volume are slightly larger in Bar One. Bar One's area is 67,477 square meters, and its volume is roughly 306,840 cubic meters. Bar Two's area is 62,817 square meters, and has a volume of 283,470 cubic meters. Bar Two showed a more typical crescent structure, representing construction during consistent migration of the point bar, while Bar One exhibited a teardrop shape. The structure of the first bar represents the physical adjustment occurring due to the upstream

cutoff. Each scenario is mechanically unique, and it is reflected the physical parameters of the bends and bars.

**Planform differences**

Crescent shaped point bars have been documented in numerous field studies and reproduced in flume experiments (*Whiting and Dietrich*, 1993, a, b, c). Like many actively meandering rivers, this shape is commonly found in the lower Trinity River. This shape is clearly depicted by Bar Two (Fig. 4.7c). The bar begins slightly upstream of the apex of the meander bend, on the inner bank. The bar then continues to wrap around the bend, with a slightly asymmetrical placement around the curve. The thalweg of the channel is forced to the outer or cut bank. On the along the inner bank of the bend the flow decelerates relative to the thalweg, producing a lower and spatially decreasing boundary shear stress (Fig. 4.4 and 5). Ultimately this allowed for deposition of sediment on the inner bank, which built up the point bar. As the meander developed the point bars grew in the downstream direction and was somewhat eroded at its upstream end. Together, both the bend and point bar have been translated downstream.

Downstream of recent cutoffs, point bars develop a very different appearance. These point bars, like point Bar One, lack the predominately symmetrical shape. Bar One has been reformed to an asymmetrical shape via the erosion of roughly the upstream third of the bar, producing the characteristic tear-drop shape (Fig. 4.7a, 8a). The upstream straightening of the river forced an increase in downstream migration due to a change in the angle of the incoming flow. The front of the bar was eroded away while

the downstream portion of the bar is still being built by sediment deposition. The rapid shift of the centerline post cutoff implies an increase in the migration rate of the bend.

These trends in bars downstream of cutoffs have been repeated a number of times throughout Zone Two of the lower Trinity River. Eight major cutoffs have occurred since 1952. This has allowed for the examination the channels response to several cutoffs in other locations. In each case, bends responded to upstream cutoffs or straightening events with a change in bar shape and an increase in bend migration rate. Every time there was a bend cutoff the bar immediately downstream morphed from a crescent to a teardrop shape. Four examples of other cutoffs are shown in Figure 4.10. In addition to the unique bar shape, these examples also exhibit accelerated channel migration in response to the upstream cutoff.

**Three dimensional differences**

The topographic and hydrophone surveys showed three dimensional differences between the bars. Changes in the topography reflect the method in which the point bar deposits were made and the direction in which the point bars are growing and the banks are being eroded. Figure 4.12 and 13 show the results of topographic and bathymetric surveys. Several transects were take across this survey. The elevation profiles from these surveys are shown in Figures 4.12b and 4.13b.

Bar One is shown in Figure 4.10. From these images it is evident that the upstream bar slopes dramatically rise up from the thalweg (Transect One). The cross-

stream slopes of the bar are not homogenous. The steepest slope, fifteen degrees, is located upstream at transect one. The bar slope then decreases in the middle of the bar (Transects Two, Three, and Four) before increasing again at the downstream end of the bar. The cross-stream surface slope for Bar One at Transect 5 was nine degrees.

The topography of Bend Two was obliviously different from Bend One. The cross-stream slopes of the transects change very little in the downstream direction. The stream-wise elevation of the point bar was fairly symmetrical, tapering at the upstream and downstream edges of the point bar, transects one and four. The greatest elevations and slopes on Bar Two, while still fairly gentle, are Transects Two and Three.

A three-dimensional bar surface was created from each of the topographic and bathymetric surveys. That surface was sampled to create the stream-wise profiles shown in Figure 4.14. Bar One is distinctly asymmetrical. The lengthwise transect highlights the blunt, topographically high front of this bar. Bar Two is more symmetrical with the point of maximum elevation occurring only slightly downstream from the bar centroid.

The trenches on both bars showed predominately dune cross-strata. This indicates sediment deposition primarily through bed load transport. These deposits were comprised primarily of medium and fine sands. As expected, both bars fine in the downstream direction and upslope toward the tree line. An important exception to the dune stratification was found at the upstream end of Bar One where the bar top is built out of climbing ripple deposits with mud drapes, implying sedimentation from

suspension. These deposits were made of very fine sand. A distribution of the types of deposits observed is shown in Figure 4.18.

The grain data that was sampled from the trenches showed a lot of variability in grain size, particularly for Bar Two. Samples taken from the troughs of the cross strata had larger grains while samples from the tops of dune cross strata were finer. Samples taken from the ripples and mud drapes were the finest. This was unexpected. It was hypothesized that due to downstream fining Bar One should be coarser, as Bar One is upstream of Bar Two. The samples from Bar One had a mean grain size of 0.29mm, and the samples ranged from 0.15mm to 0.41mm. The mean grain size of the samples in Bar Two was 0.44mm. The mean of the samples ranged from 0.24mm to 0.91mm. The grain size results are summarized in Figure 4.19.

## DISCUSSION

Data integration reveals two distinct types of bars. These physical observations imply that there are also distinct differences in the sediment transport associated with each bend.

**Bend One – Response Driven Migration**

Bend One is adjusting to a cutoff that occurred less than 1000 meters upstream of the bend in 2002 (Fig.9). The upstream straightening of the river has changed the tangential angle of the water entering the bend. Flow that had been entering the bend at a low angle is now entering the bend at closer to 90 degrees relative to the orientation of the outer bank (the minimum radius of curvature at this bend is 63 meters). These changes have caused an accelerated erosion of the outer bank and as a result the bend is pushing outwards and downstream rapidly (Fig. 4.8a).

Bar One has a blunt steep upstream nose. The highest point of elevation occurs at the top of the first transect, on the most upstream section of the bar (Fig. 4.14). The slope of the bar then decreases towards its tail. The bar, like the bend itself, is in a state of readjustment. Looking at images from previous aerial surveys shows that the bend and bar did not always exhibit this shape. Previously, the bend and bar exhibited a more typical crescent shape. The current teardrop shape of the bar is a product of the upstream cutoff. The increase in the bend's angle caused the upstream portion of the bar to be eroded. It is likely that prior to the upstream cutoff the bar's upstream slope was much gentler, and that the highest elevation was closer to the centroid of the bar.

Like most bars, Bar One generally fines in the downstream direction. There is also fining from the channel centerline to the tree line (Fig. 4.18a). This is to be expected, however, the bar also exhibited some unexpected trends. Fine grains were found in ripple cross strata in the most upstream bar transect (Fig. 4.16c). The ripple

formations imply that the grains are settling out of suspension and being gently reworked by a low energy current. The majority of the bar showed cross strata of dunes, implying bed load sediment transport (Fig. 4.16b, d, and e). The only other exception to the bed load transport was found in trenches at the downstream end of the bar, where there are fine mud grain mud drape deposits ($D_{50}$=0.09mm), further evidence of sediment settling out of suspension.

These two exceptions in the sediment transport style on Bar One are due to topography driving of bedload transport around rather than over the bar. The steep adverse and lateral slopes at the upstream end of Bar One reduced the bedload transport over this surface and directed essentially all gravel into the thalweg. At the downstream end of this bar a zone of flow separation allows for fine grains to rain out of suspension and deposit in the form of mud drapes.

Bar Two has a greater grain size range than Bar One because its topography does steer the coarsest sediment away from the inner bank. A larger portion of the bed load moves directly up and over the bar. The differences in topographic steering of the bed load are portrayed in the cartoons drawn as Figures 4.20a and 4.21a. Deposition of sand from suspension dominates the upstream end of the bar where the surface slopes keep bedload transport to a minimum. At the back of the bar, flow separation caused by the curvature of the bed allows fine sediment to fall out of suspension and form mud drapes. The bend will continue to adjust over time. As the front of the bar is eroded the upstream angle of the bend will relax and through continuous sedimentation and erosion Bar Two is expected to develop a form similar to Bar Two.

**Bend Two – Persistent Bend Migration**

Bar Two exhibits all of the signs of deposition under condition of continuous bend migration. The bend and bar exhibit fairly symmetrical shapes, with apices positioned just downstream of the centroid (Fig. 4.7c). Year to year the bend pushes slightly outward and downstream (Fig. 4.8b). The bar exhibits gentle upstream and downstream slopes (Fig. 4.13). The elevation of the bar reaches its peak just after its centroid (Fig. 4.14). Based on stratigraphic evidence in the trenches dug across the bar it appears that the bar is constructed exclusively of sediment deposited from bed load.

As the water flows over the bar, grains are transported via bed load and suspended load transport. The gentle upstream slope of the bar facilitates both styles of transport over the bar top (Fig. 4.14). One unexpected finding in this study was the grain size comparison between Bar One and Bar Two. Because Bar One is upstream of Bar Two (Fig. 4.7), it would be expected for Bar One to have a larger mean grain size compared to Bar Two. Like bars, rivers typically fine in the downstream direction. However, Bar Two's mean grain size was larger than Bar One's mean grain size. The reason this occurs is not because of the sediment supply available in the individual bends, but the distribution of grain sizes able to be transported up and onto the bar surface. The steep slope of Bar One redirects the bed load transport of larger grains into the thalweg. In contrast, the gentle front slope of Bar Two allows for the transport of large grains up and over Bar Two.

## CONCLUSIONS

Freely meandering rivers migrate in two fashions. Most bends migrate by consistent erosion of the cut bank and deposition on the inner bank. Through time the bends push outward and downstream. The bars are built largely built by bedload transport and fine in the downstream direction. This style of sediment deposition and migration was well represented by Bar Two.

The other style of migration is more dramatic and associated with bend cutoffs or channel straightening. The consequence of this style of bend migration is exhibited by Bar One. Response driven migration is more rapid than typical bend migration. As a result, the lateral growth of Bar One has fallen behind the erosion of its cut bank. Notice that the bar topography does not cross the entire channel width (Fig. 4.12). There is a wide section of flat, deep river bottom produced by the widening of the channel. Over time it is predicted that sedimentation and erosion will replace this teardrop shaped bar with one that is topographically similar to Bar Two.

**FIGURES**

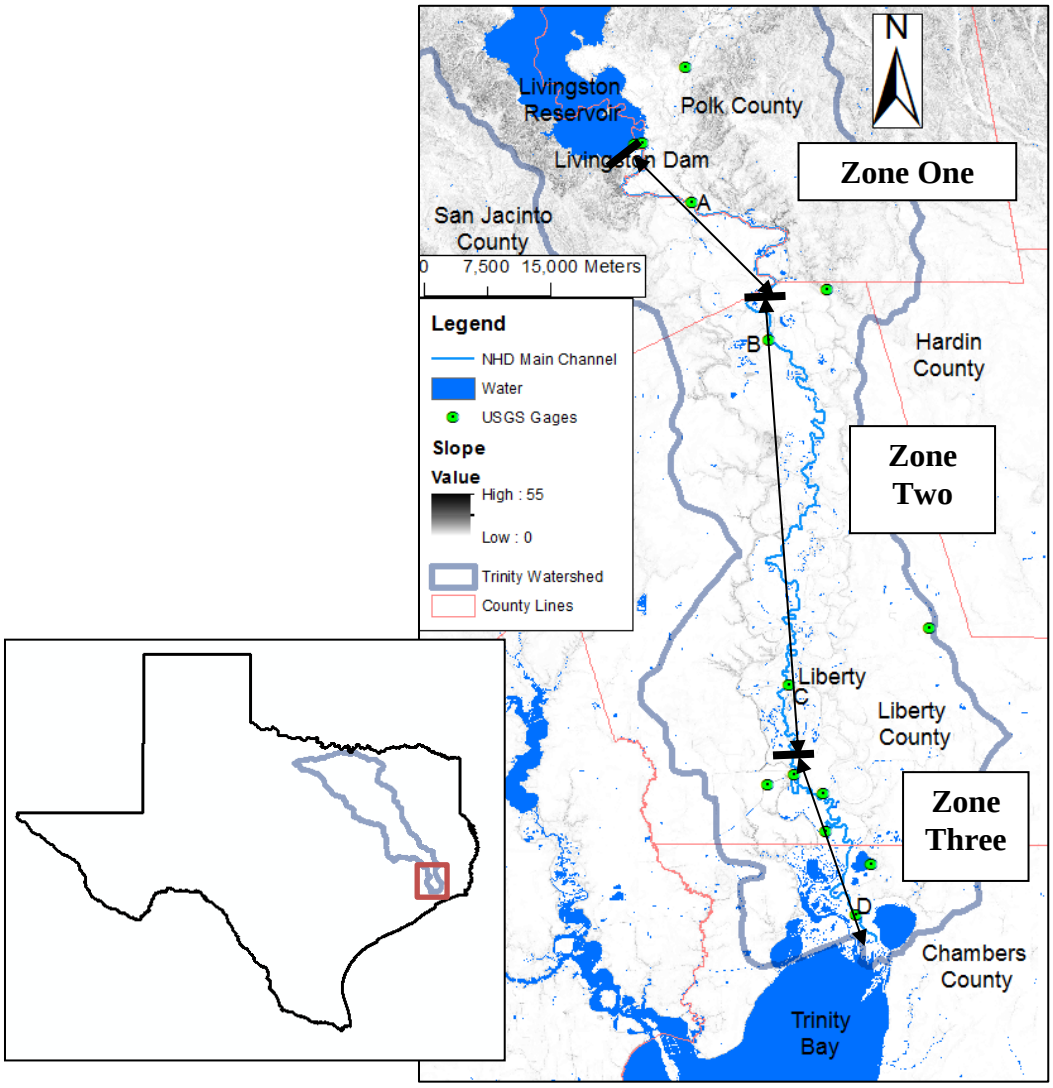


Figure 4.1: Map of the lower Trinity study. The Trinity watershed within the state of Texas is outlined in blue, running across the eastern portion of the state. The red box marks the section of the watershed that is the study area. The study area is bounded by Livingston Dam to the north and Trinity Bay to the south. On this map the counties are outlined in red. The town of Liberty, TX is labeled near gage C. The green circles mark USGS gages at Goodrich, TX (A; USGS number 08066250), Romayor, TX (B; USGS number 08066500), Liberty, TX (C; USGS number 08067000), and Wallisville, TX gage (D; USGS number 08067252). Zone One is the first 60 kilometers downstream of the Livingston Dam (labeled at the top/north of the map). Zone Two is the middle zone of the river, 100 river kilometers long. The most downstream zone of the river is Zone Three, the final 60 kilometers of the river.

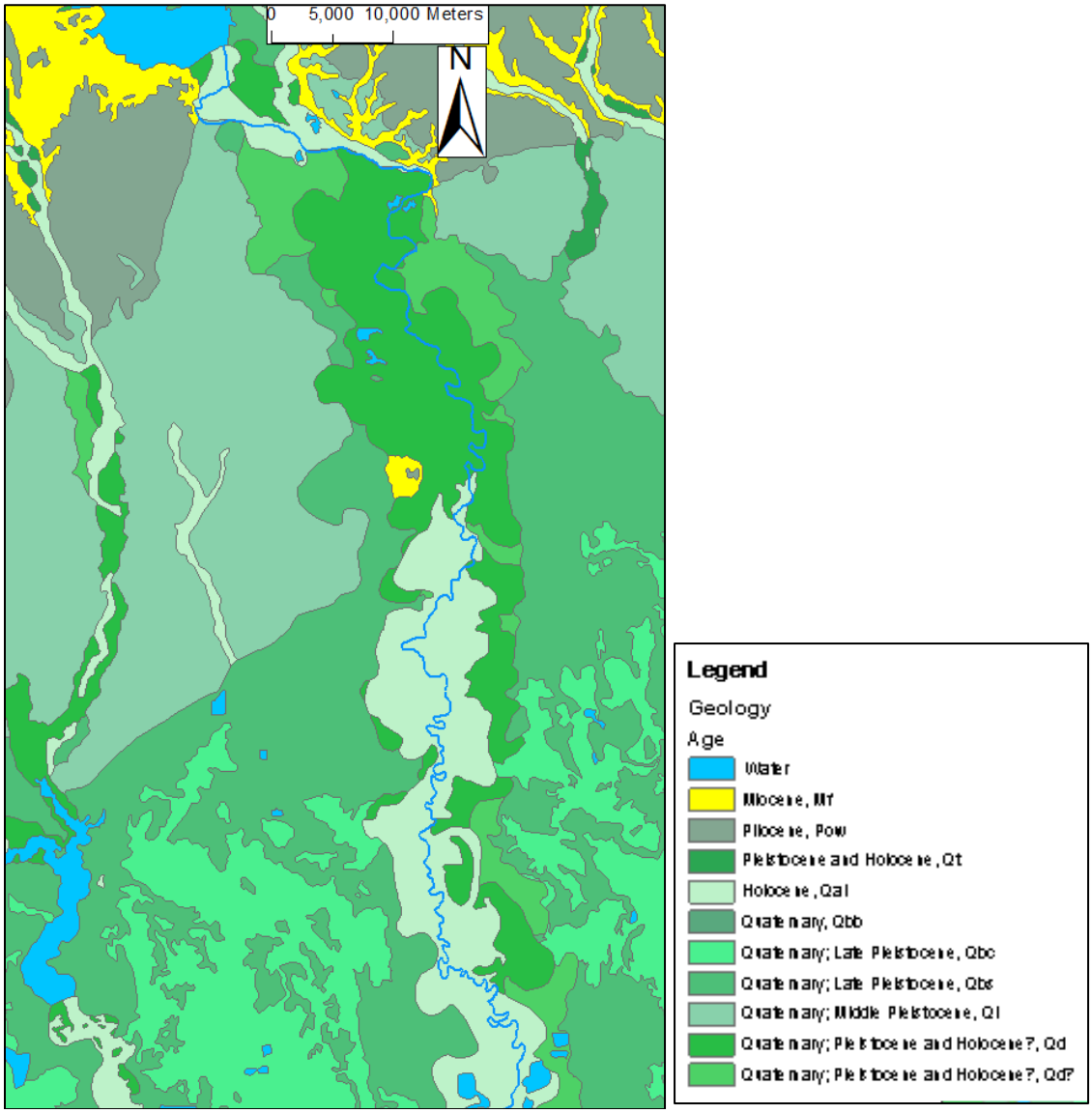


Figure 4.2: (A) Geologic map of the study area. Nearly the entire region is composed of Quaternary deposits shown in green. The blue marks major water bodies for spatial reference. The northern portion of the map has some deposits Pliocene and Miocene in age.

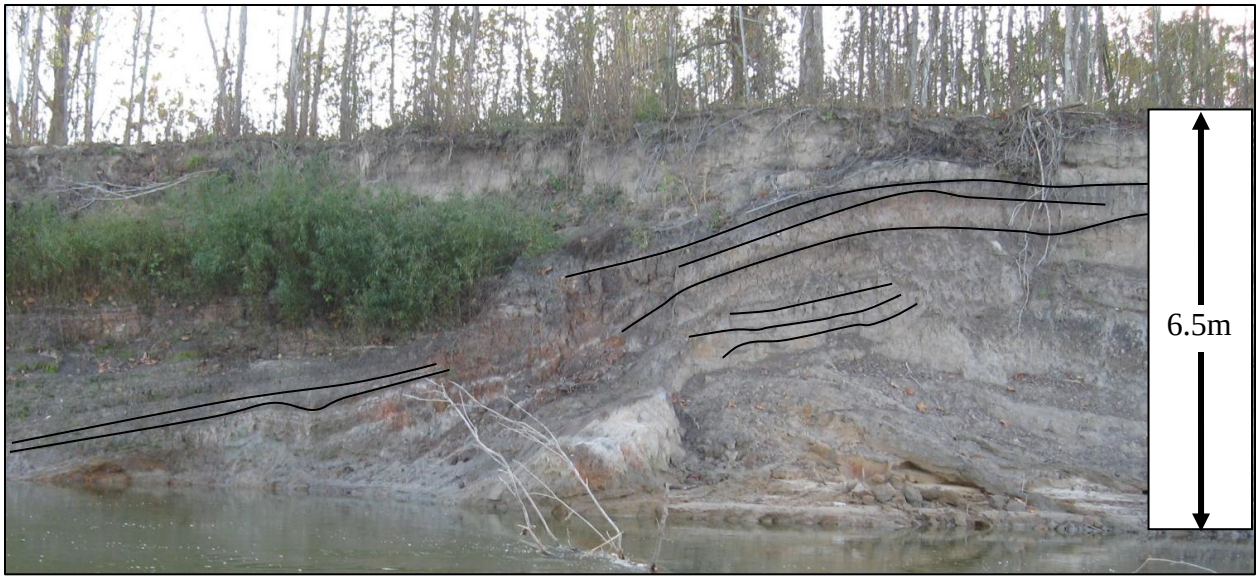


Figure 4.3: Cut bank in Zone Two, approximately 118 river kilometers from Livingston Dam. The height of the bank is approximately 6.5 meters. The black outlines show previous channel surfaces.

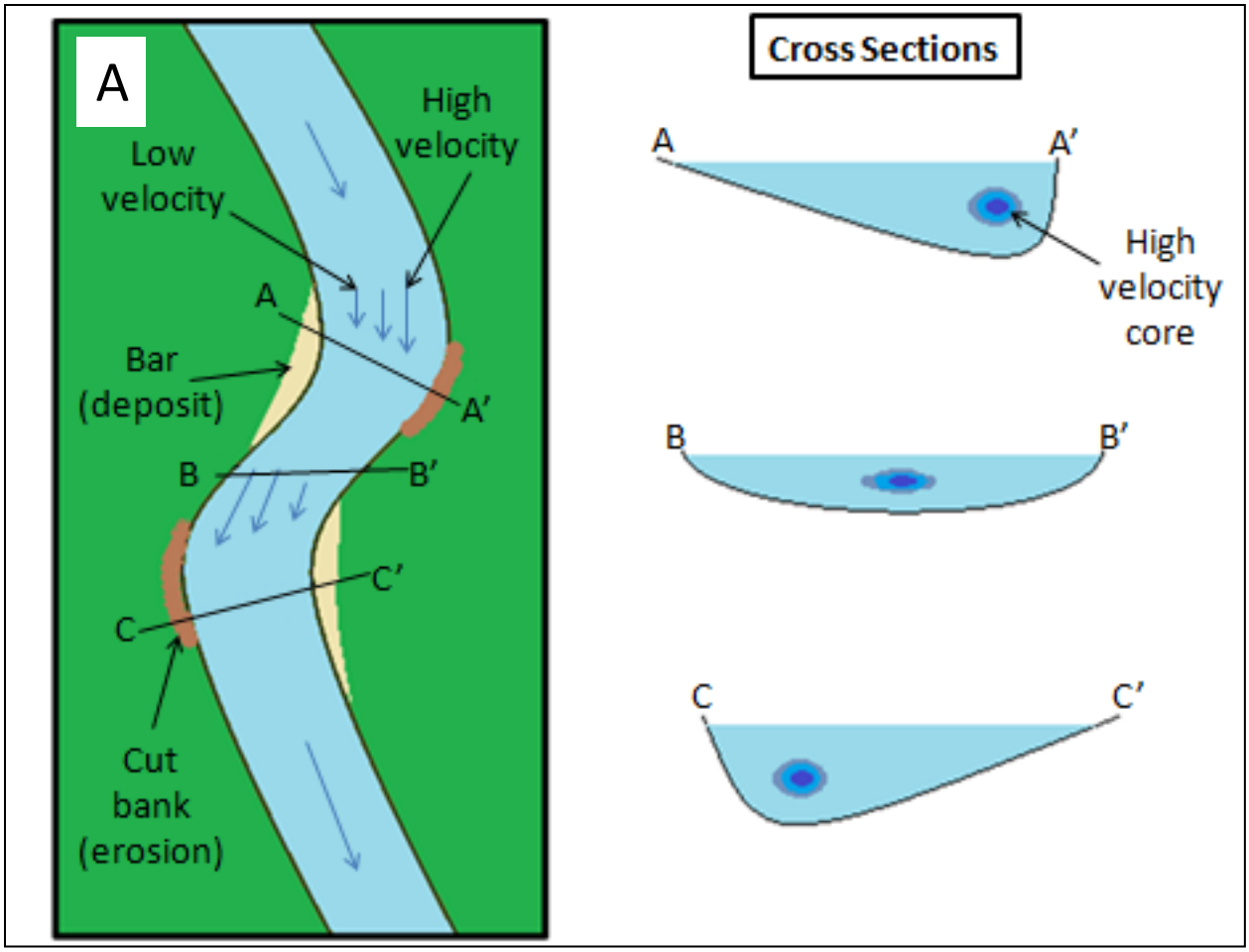


Figure 4.4: (A) River that is flowing from the top of the image to the bottom on the image through two bends. The cut bank, or outer bank is shown in brown and the bar, or depositing bank is shown in beige. The blue lines show flow. In the bends the flow is stratified across the channel, with higher flow near the cut bank and slower flow at the depositing bank. There are three lines transecting the channel labeled A-A', B-B' and C-C'. This transects correspond with the cross sections shown on the right. Transect A-A' shows the apex of the first bend. The chann-el is very asymmetrical with a high velocity core near A', or the outer bank. Transect B-B' shows a cross section of the transition between the two bends. There is no longer a substantially deep thalweg and the highest velocity water is in the center of the channel. Transect C-C' shows the apex of the second bend. It is the mirror of Transect A-A'. The high velocity shifts to the other side of the channel near the new cut bank.

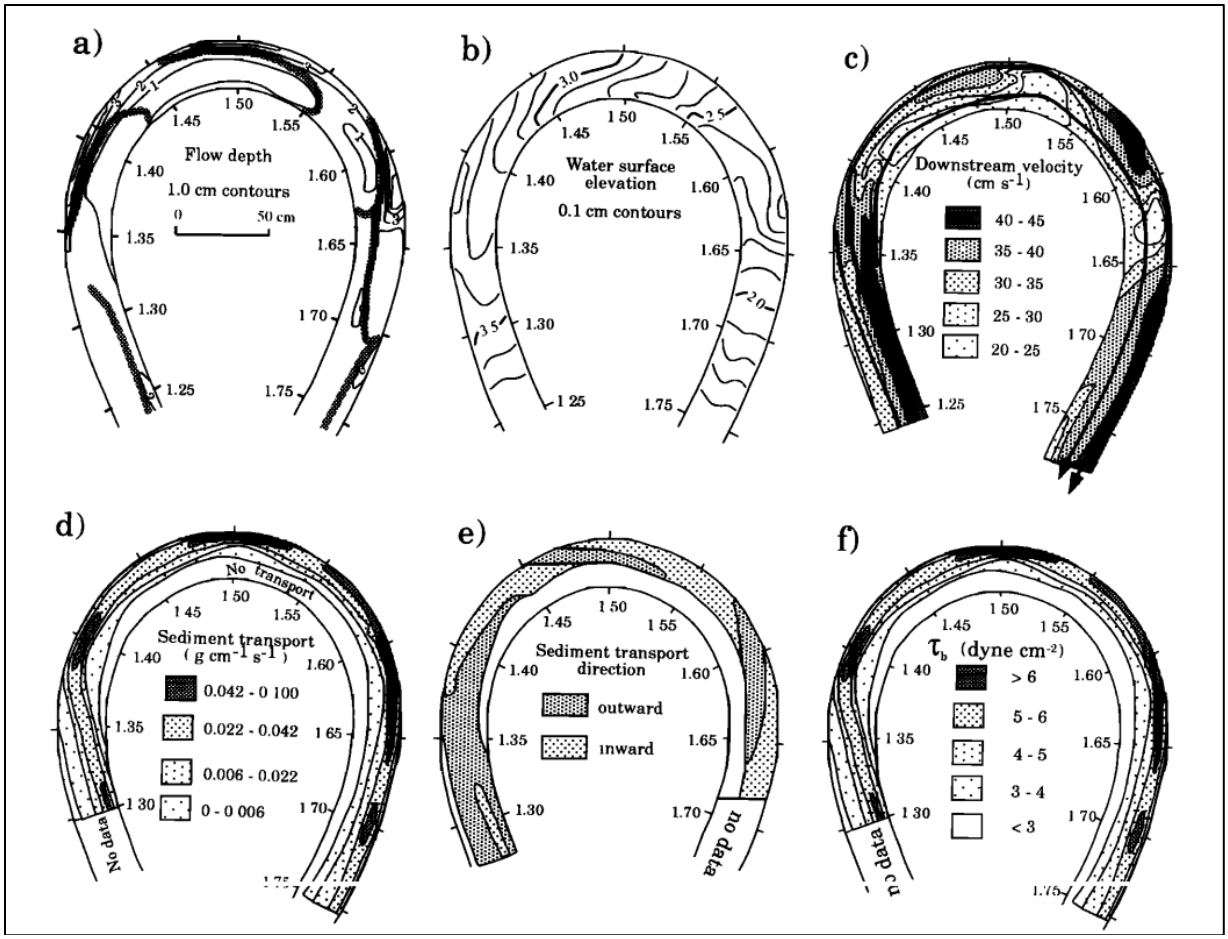


Figure 4.5: Produced from experiments on flow through a bend (*Whiting and Dietrich*, 1993). The images in this figure represent the following: a.) bathymetry, b.) water surface elevation, c.) downstream velocity, d.) sediment transport, e.) sediment transport direction, f.) local boundary shear stress. These images illustrate the mechanical changes in the flow through a bend.

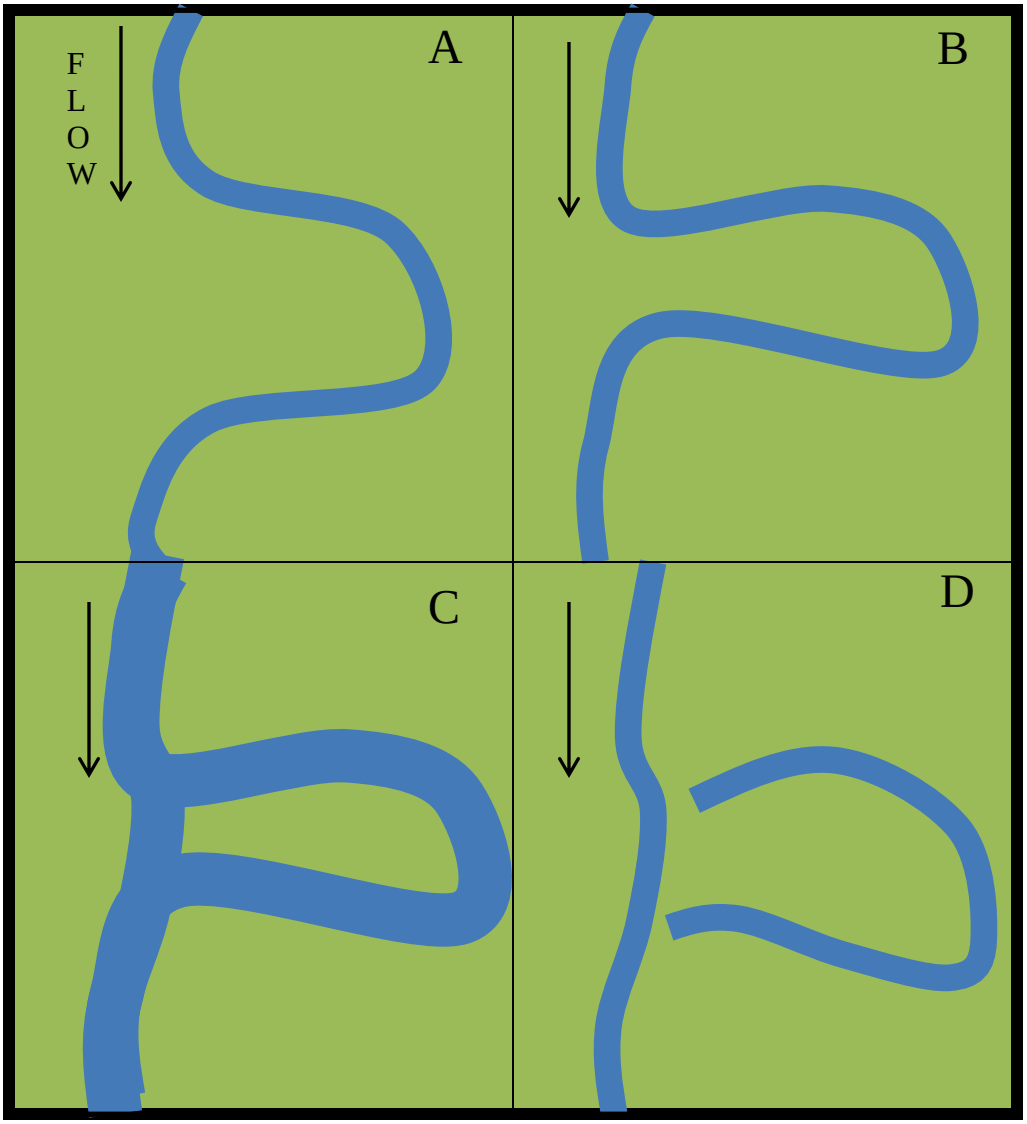


Figure 4.6: The cutoff process in a river. The blue line represents a river flowing from top to bottom of the image. The river is flowing through a bend (A), the bend tightens (B), there is a flood event (C). The flood waters top the banks of the river and rejoin the main stream at the downstream neck of the bend and when the flood waters retreated a new a channel and an oxbow lake remain as a result of the cutoff (D).

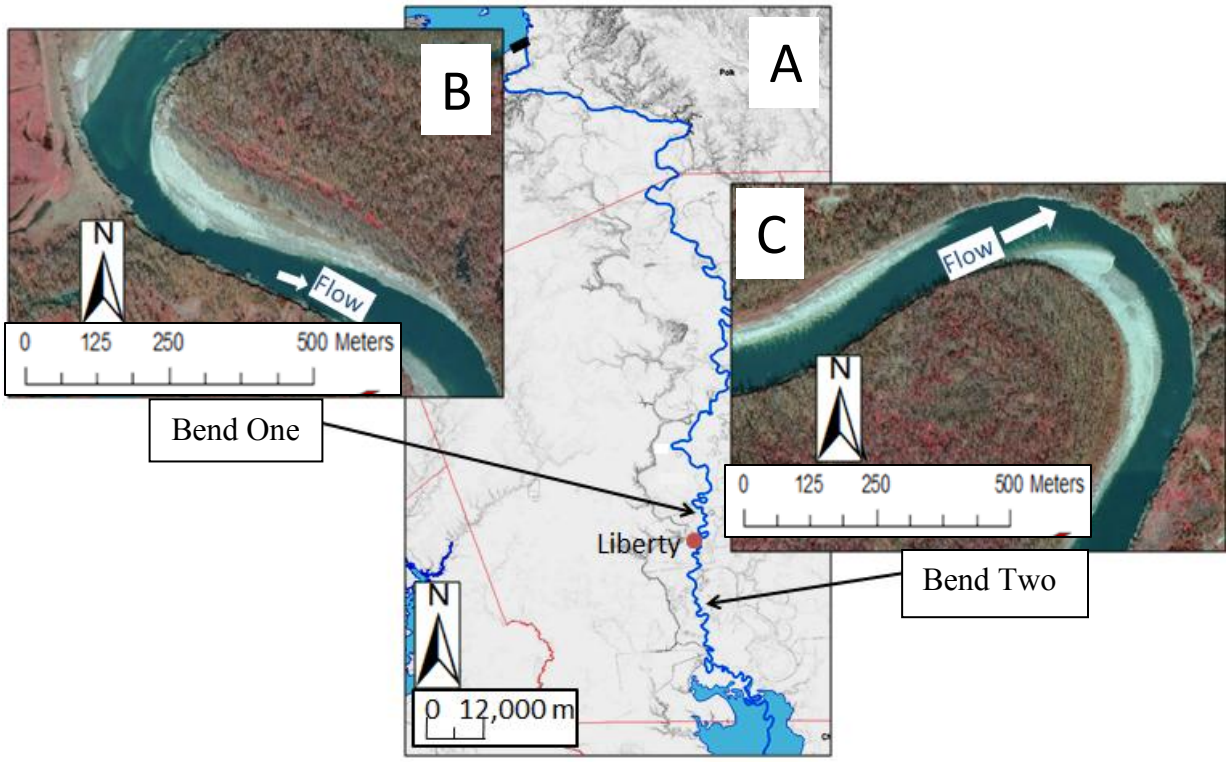


Figure 4.7: The two bends discussed in this chapter are both located in Zone Two. (A) Map of the study area, with arrows pointing out the location of Bend One (B) and Bend Two (C). Bend One is shown on the left and Bend Two is shown on the right. Both bends are located in Zone Two.

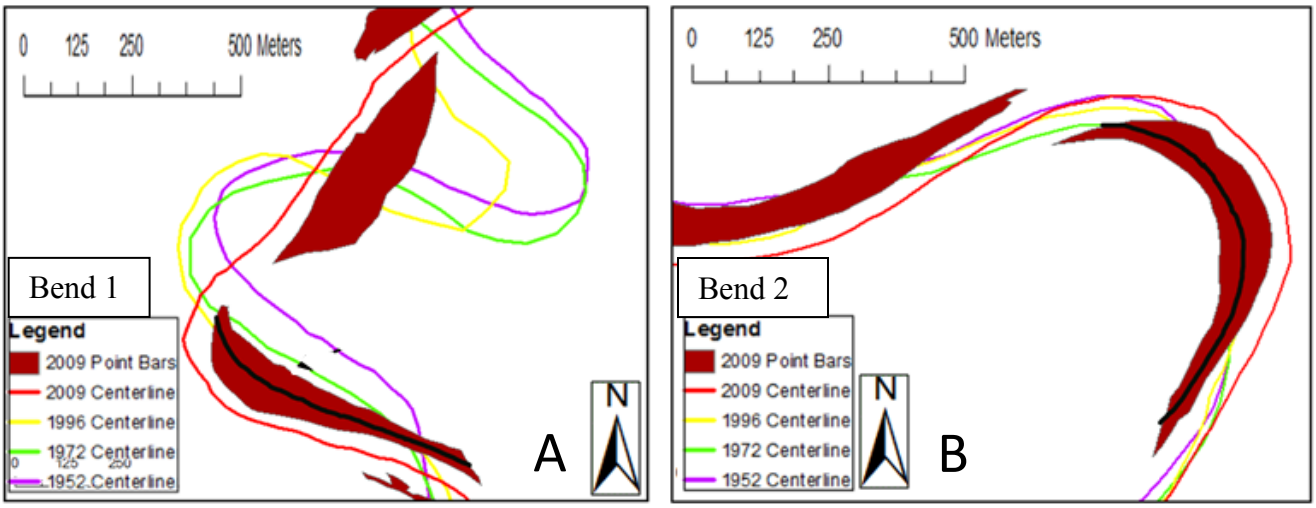


Figure 4.8: (A) The centerline history of Bend One. (B) The history of Bend Two. The centerlines of the channel from 1952, 1972, 1996 and 2009 for each bend. The centerlines were traced from aerial photographic surveys. The bar shapes were traces from the 2009 aerial photographic survey. The river straightens upstream of Bend One, resulting in an accelerated rate of migration between 1996 and 2009. Bend Two migrates at a more constant rate.

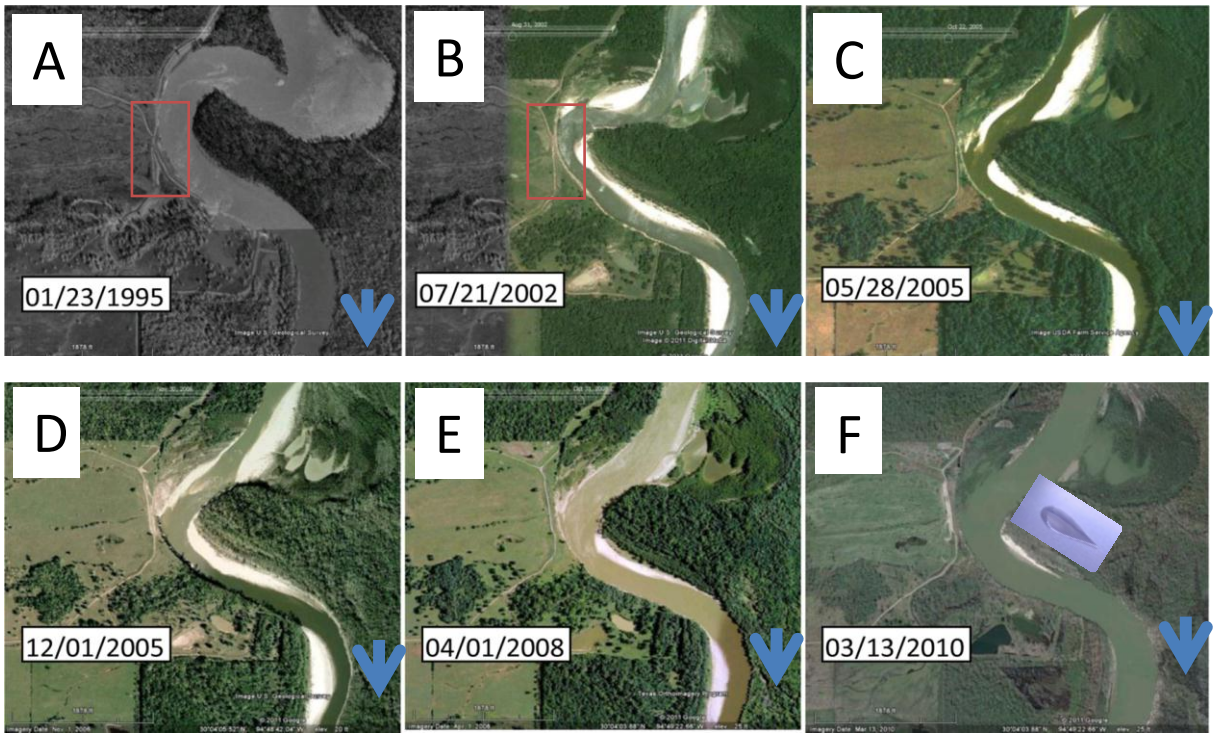


Figure 4.9: Series of aerial photographs from 1995 to 2010 depict the cutoff event that occurred upstream of Bend One. The event occurred over several years, shown on the top row from left to right (A), (B), and (C). (D), (E) and (F) the bend adjustment to the event. The accelerated migration downstream of the cutoff can be seen in the images. The red box in (A) and (B) show road that was washed away in the event. (F) was taken several months before the physical survey was done. By this stage the bar had clearly merged into the teardrop shape.

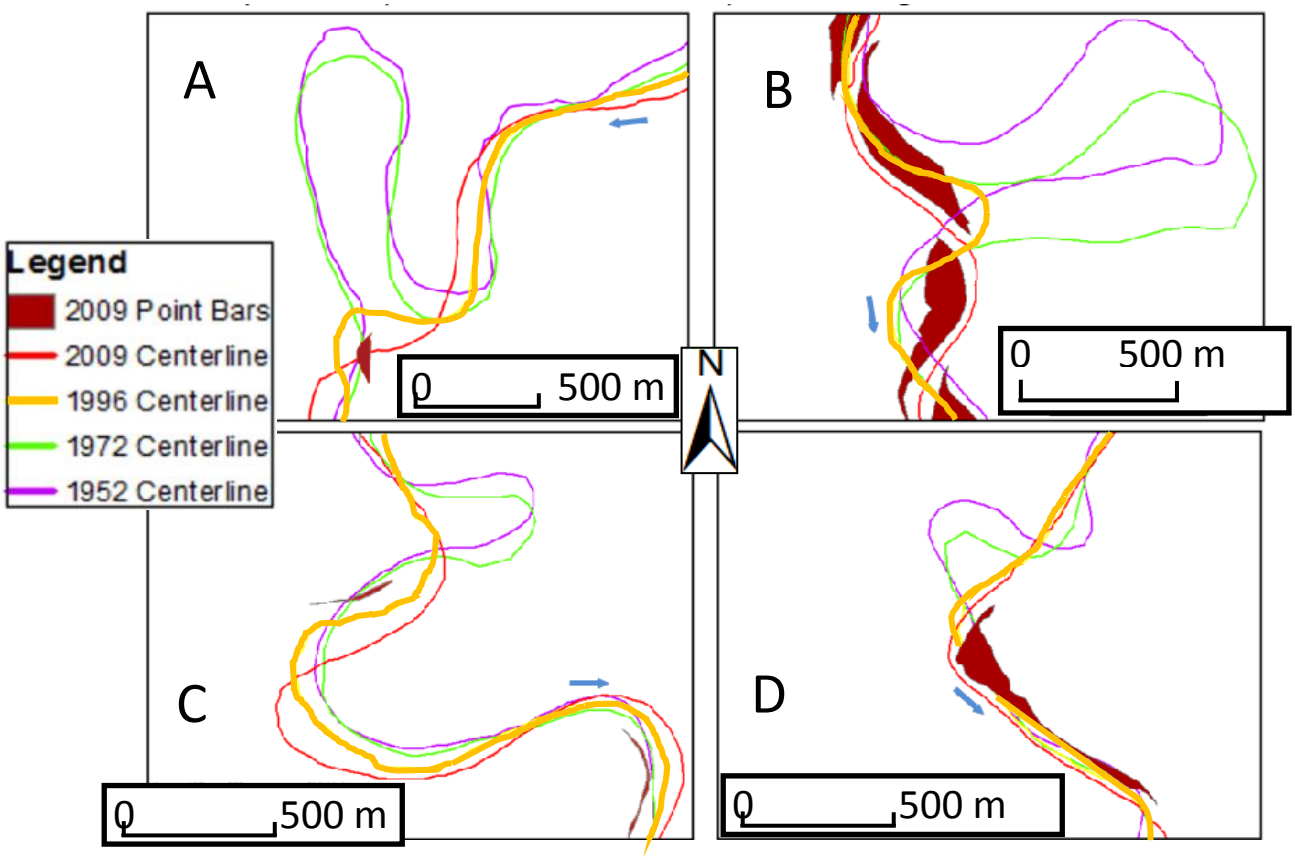


Figure 4.10: Four examples from Zone Two of recent cutoffs were taken from the Lower Trinity River, TX. (A) is 85 river kilometers from Livingston Dam. (B) is 110river kilometers from Livingston Dam. (C) is 124 river kilometers from Livingston Dam. (D) is 129 river kilometers from Livingston Dam. All of the resulting bars share the teardrop shape.

| Survey Dates | |
|---|---|
| Posted Date | Observed Dates |
| 1952 | 10/18/1952 11/12/1952 |
| 1972 | 11/4/1968 1/14/1972 |
| 1996 | 9/13/1995 1/19/1995 |
| 2009 | 1/23/2008 2/1/2008 |

Table 4.1: aerial photographs collected by the Texas Natural Resource Information System (TNRIS) for the Trinity River over approximately 60 years were used for this study. The surveys were finalized in 1952, 1972, 1996 and 2009. However, the survey date was slightly earlier in some cases.

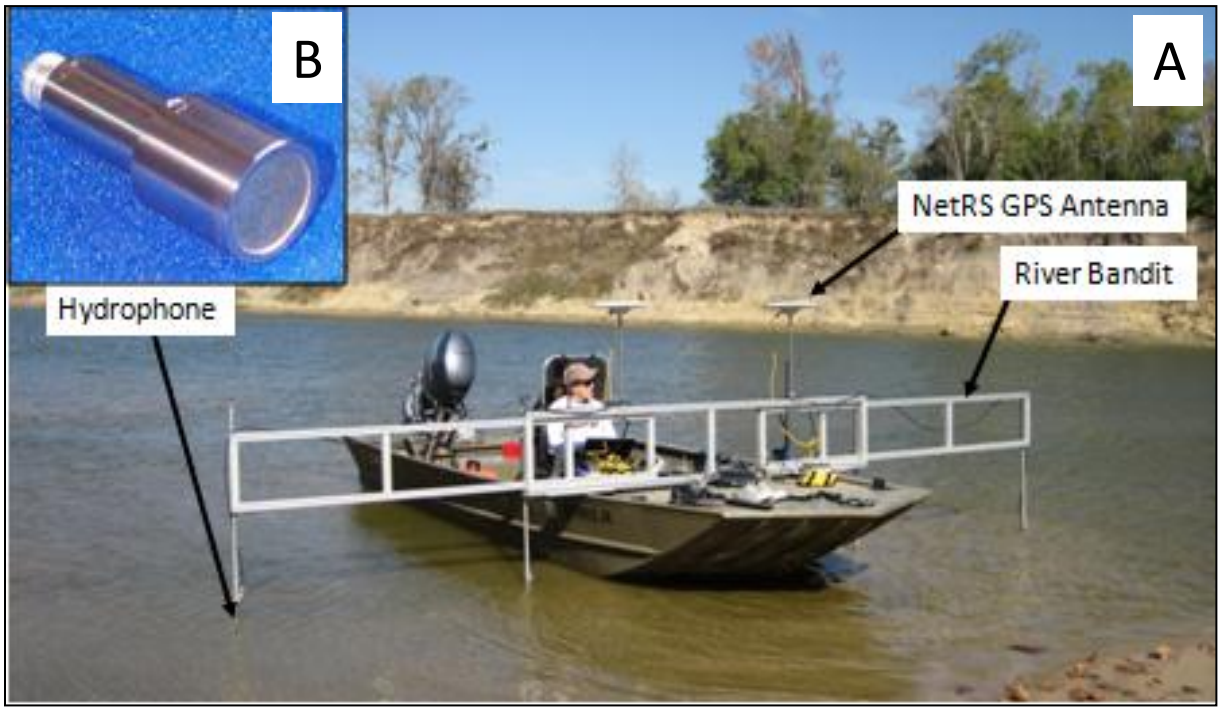


Figure 4.11: (A) The River Bandit deployed on the lower Trinity River. The metal lattice across the front of the boat supports two NetRS antenna above the lattice and four hydrophones below the water. An example of one of the single ping hydrophones (B).

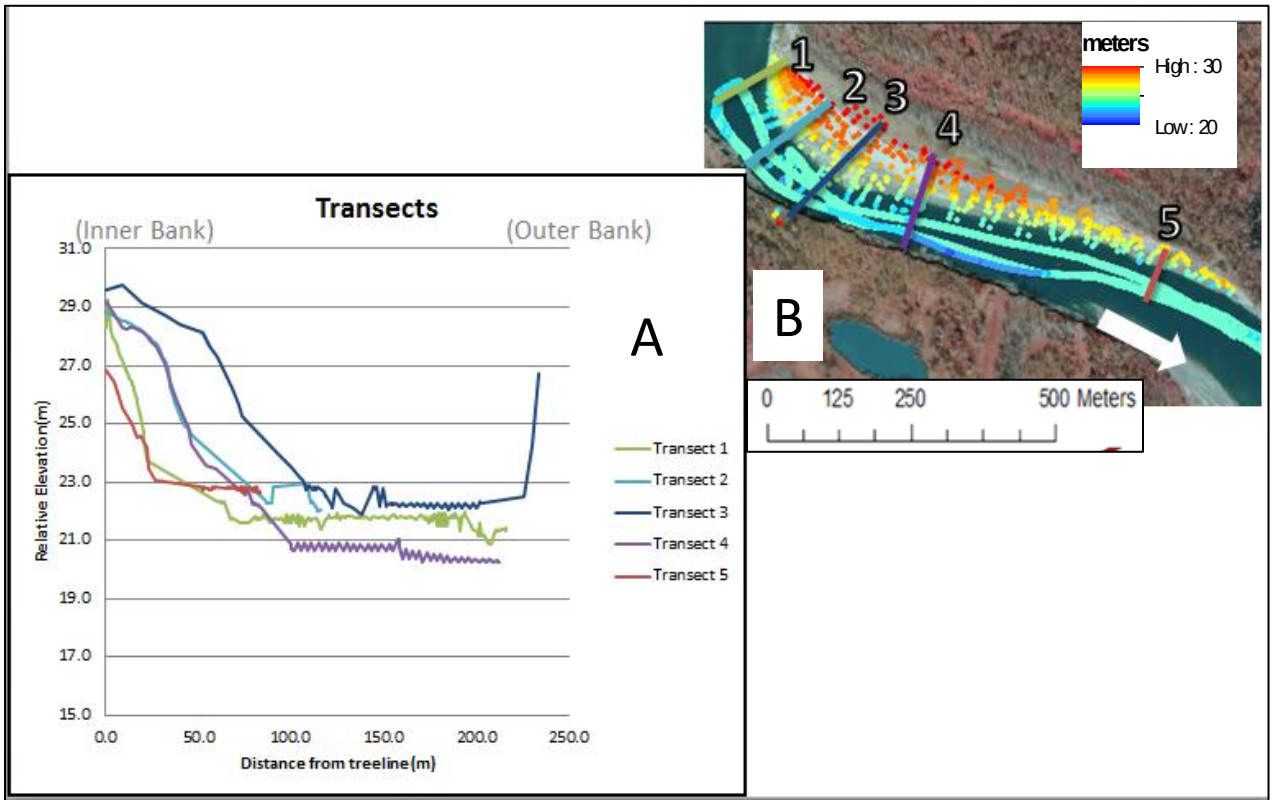


Figure 4.12: The colors of the transects in (A) correspond with the transects (B). The transects start at the vegetation line (0m) and run into the channel. Elevation of the bed is shown on the y-axis. The transects cross the bar and extend into the channel. Transect Three includes points from the cut bank. The bar in (B) shows a 2009 aerial photograph of Bar One overlain with the physical survey done.

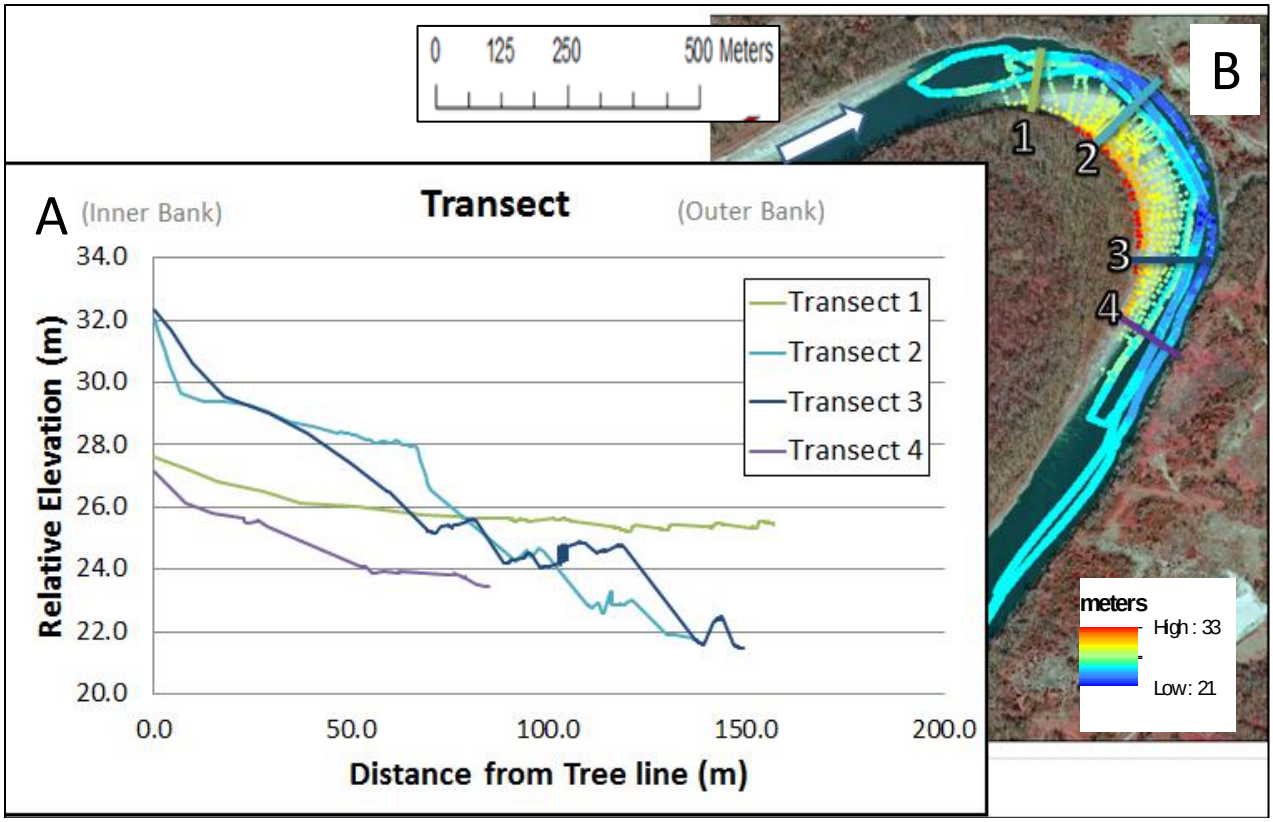


Figure 4.13: The colors of the transects in (A) correspond with the transects (B). The transects start at the vegetation line (0m) and run into the channel. Elevation of the bed is shown on the y-axis. The transects cross the bar and extend into the channel. Transect Three includes points from the cut bank. The bar in (B) shows a 2009 aerial photograph of Bar One overlain with the physical survey done.

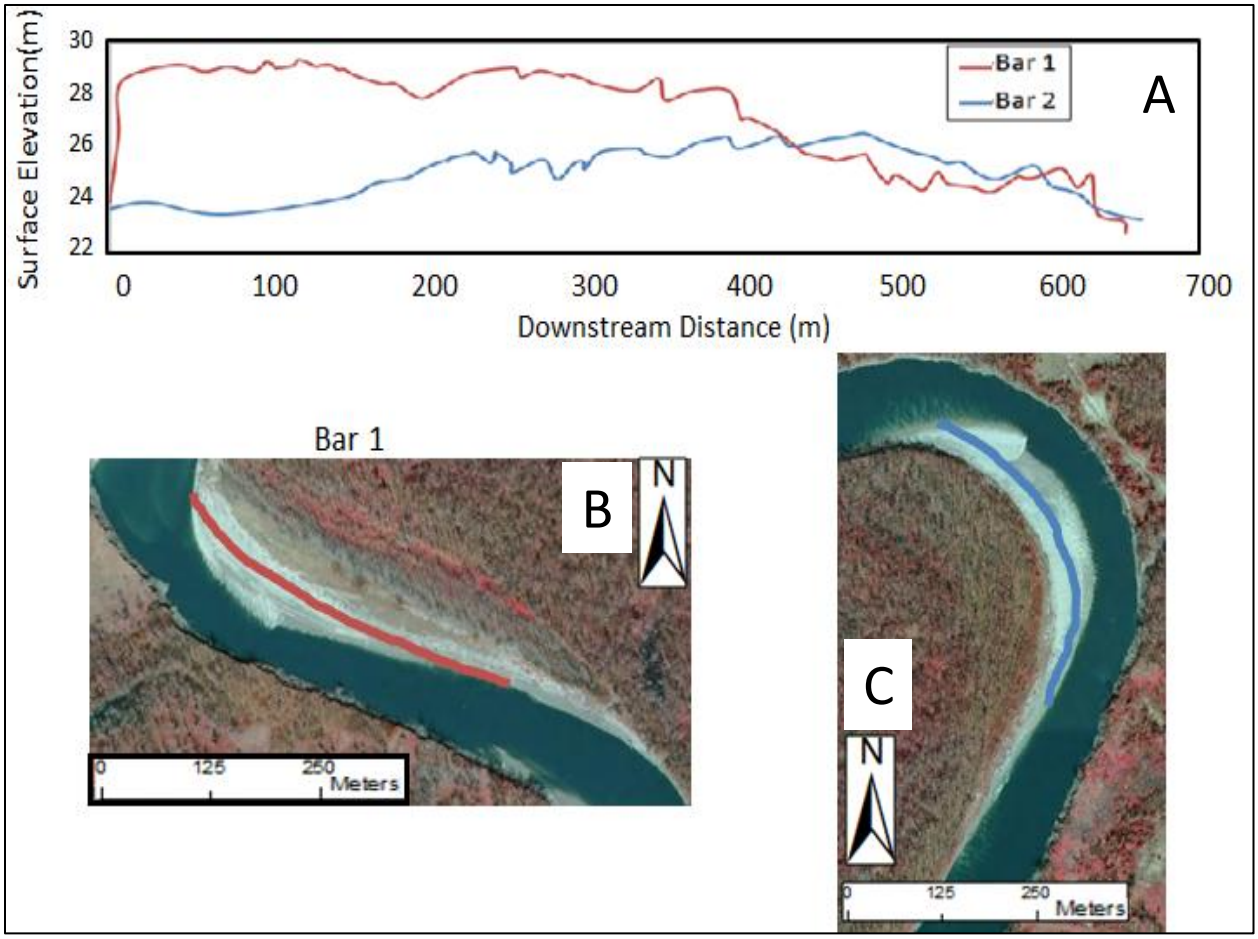


Figure 4.14: (A) Transects lengthwise, from upstream to downstream, across Bar One and Bar Two. Bar One is shown in red, and corresponds with the red line in (B). Bar Two is shown in blue, and corresponds with the blue line in (C). The background in (B) and (C) are taken from the 2009 aerial photograph survey. The transects in image A start at the upstream end (0m) and to the downstream end of the bar, on the x-axis.

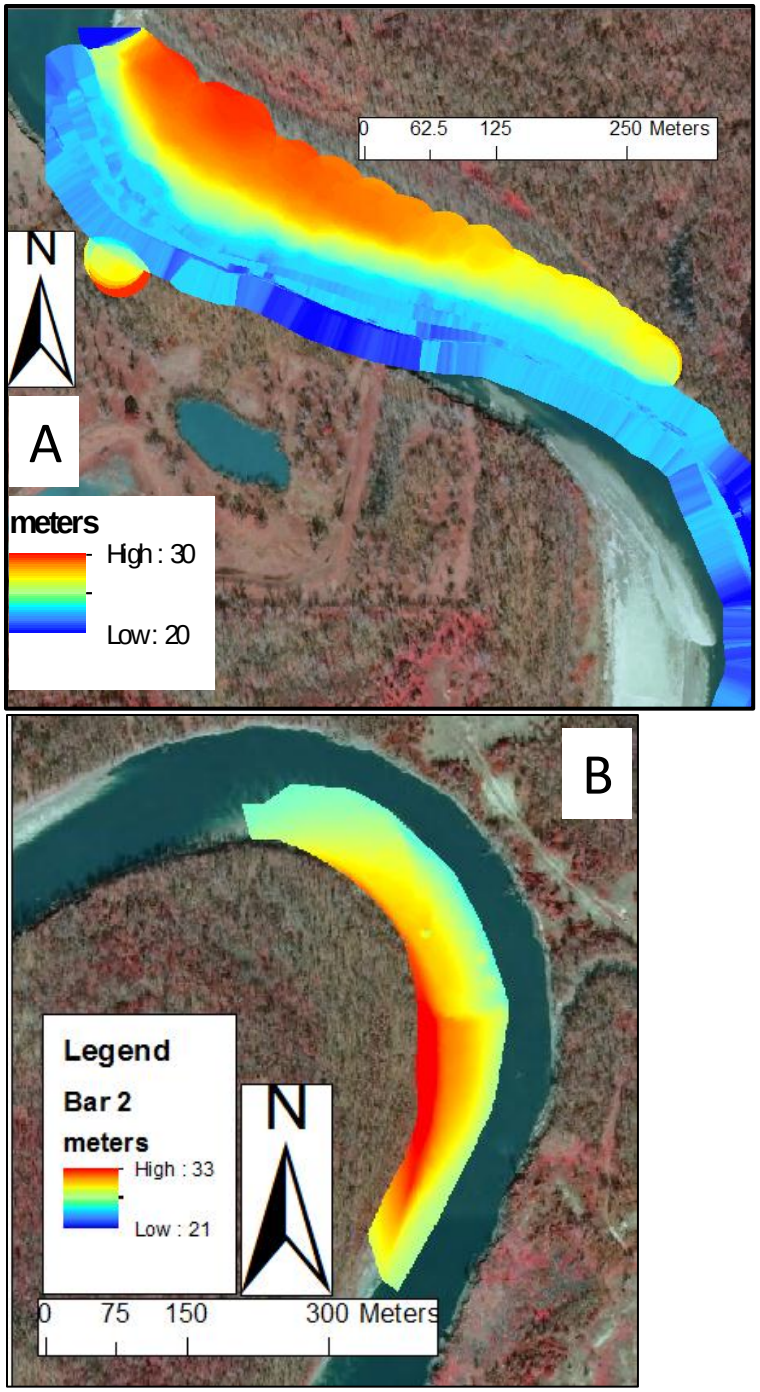

Figure 4.15: (A) 2009 aerial photograph of Bar One, overlain with a raster DEM from the physical survey. The warm colors show high elevations and the cool colors depict low elevations. (B) 2009 aerial photograph of Bar Two overlain with a raster from the physical survey.

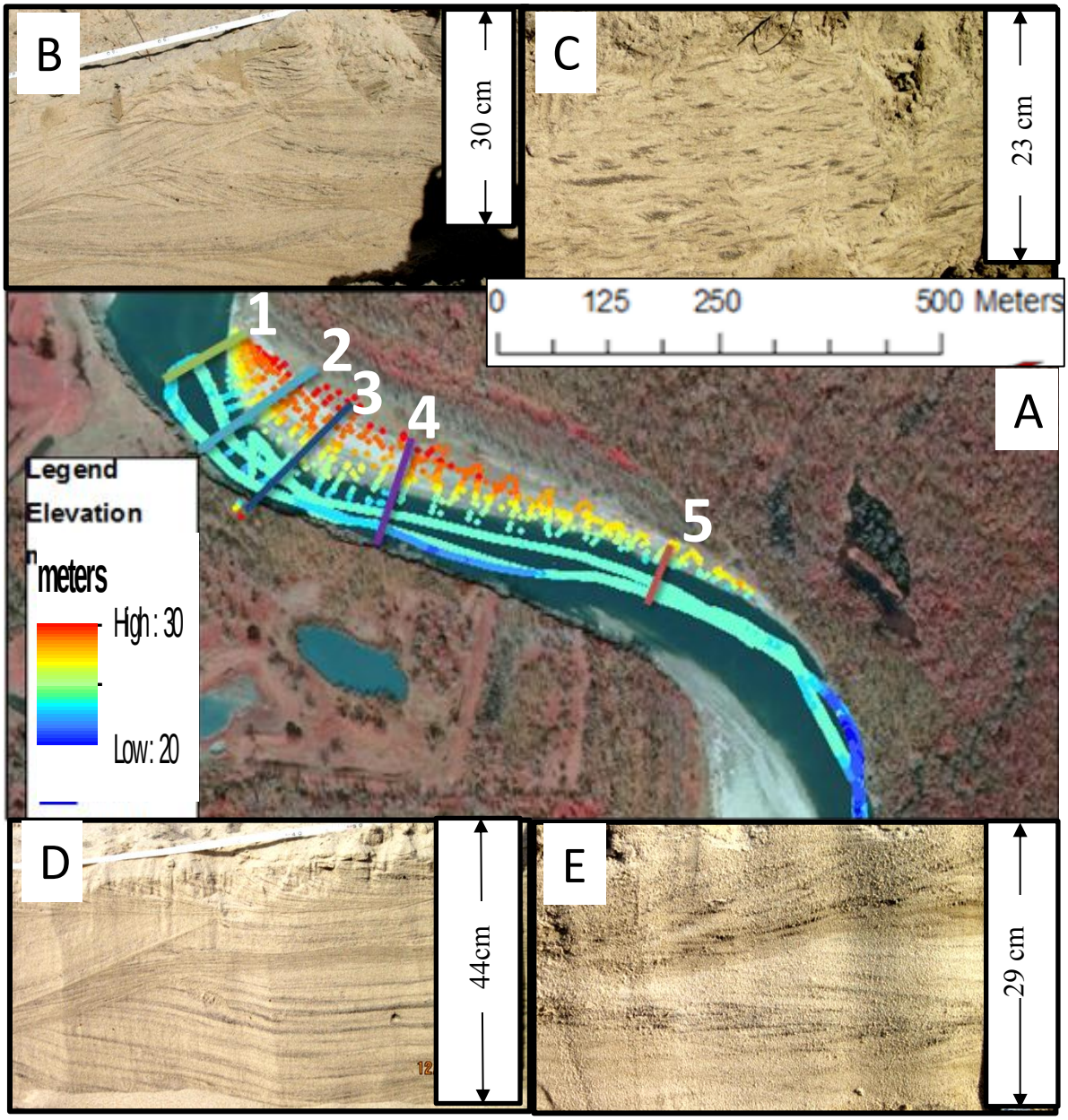


Figure 4.16: Photographs of the ditches dug transecting the Bar One. (A) 2009 aerial photograph of Bar One overlain with elevation points from the physical survey and the transects that were surveyed. (B), (C), (D) and (E) are from the sidewalls of the ditches dug across the bar: (B) the lower end of Transect One near the water's edge; (C) the upper end of Transect One, near the vegetation line; (D) near the water's edge in Transect Three; and (E) was taken from closer to the vegetation line in transect three.

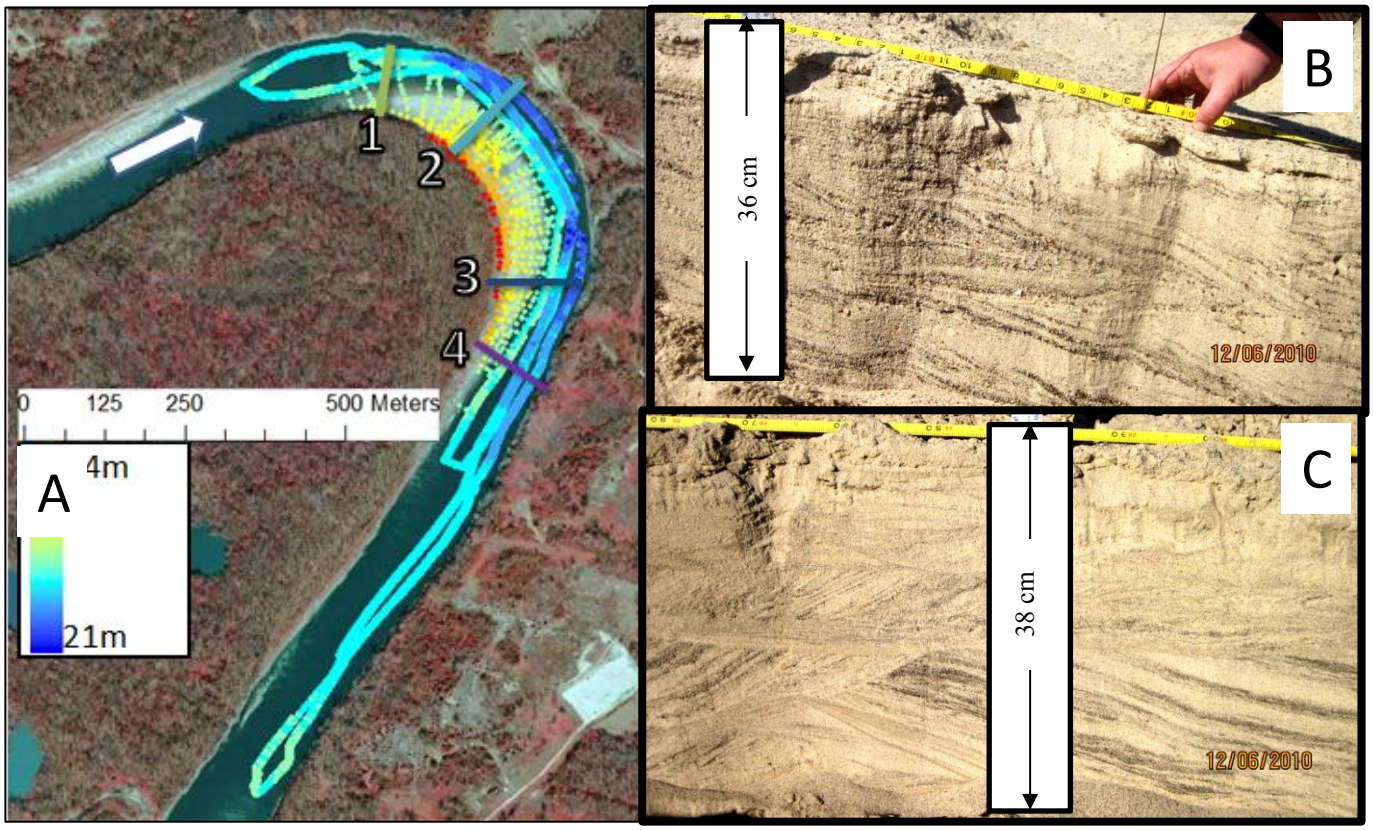


Figure 4.17: Photographs from the ditches dug transecting Bar Two. (A) 2009 aerial photograph of Bar Two. The image is overlain with elevation points from the physical survey and the transects that were surveyed. (B) and (C) are from the sidewalls of the ditches dug across the bar: (B) near the center of Transect Two; (C) near the center of Transect Three.

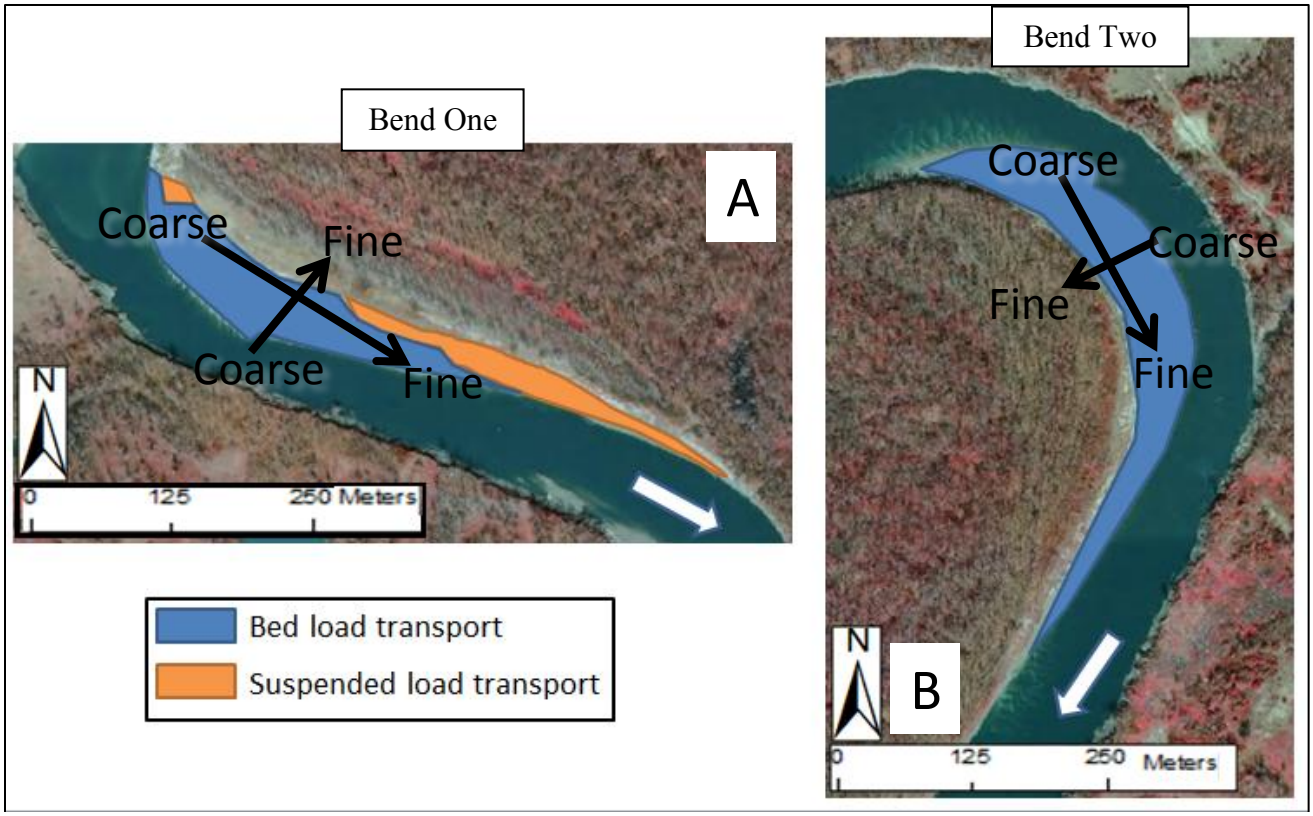


Figure 4.18: 2009 aerial photograph of Bar One (A) and Bar Two (B). The photgraphs are overlain with maps of the general grain distribution across each point bars. Both bars fine in the downstream direction and cross sectional direction toward the vegetation line.

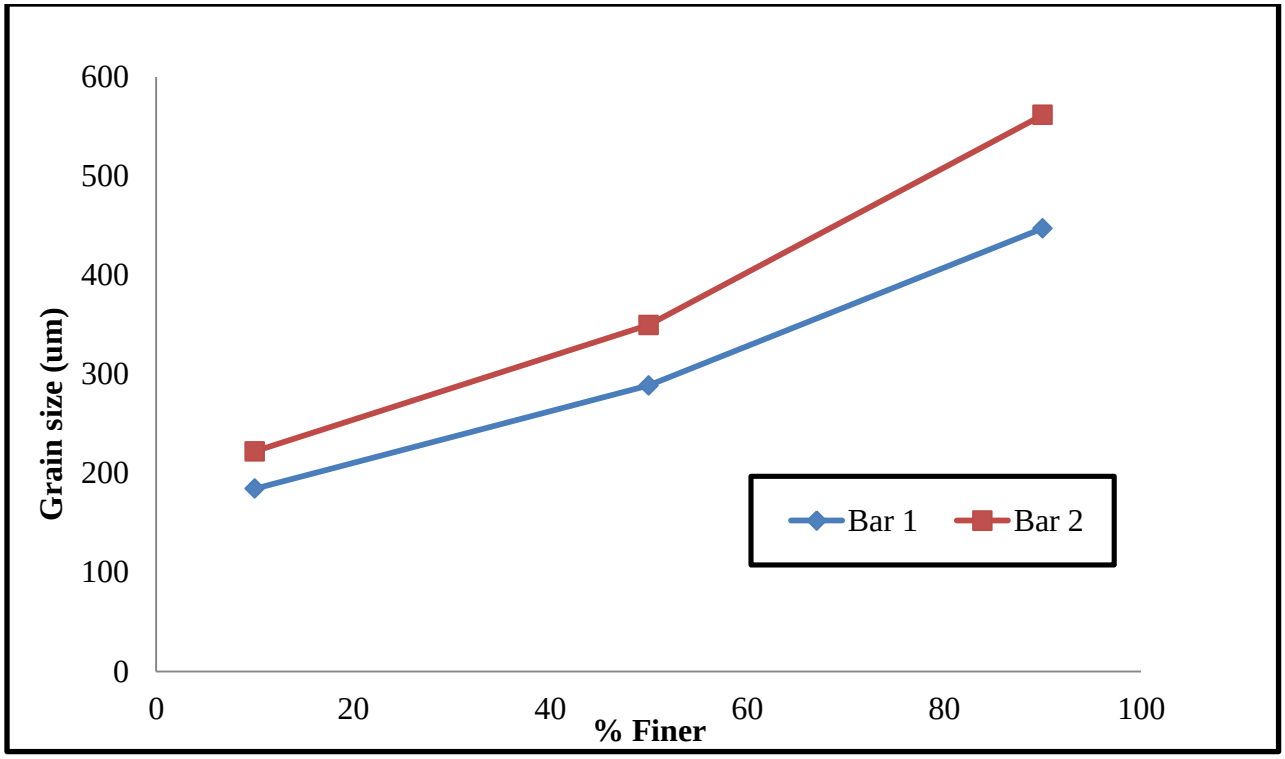


Figure 4.19: Grain size distributions for both bars. The blue line represents the grain size variation on Bar One. The red line represents the grain size variation on Bar Two. To create these lines all of the samples from the transects on each of the bars were averaged. The x-axis shows the percent of the samples that are finer that the rest of the sample. The y-axis shows the associated grain size in micrometers.

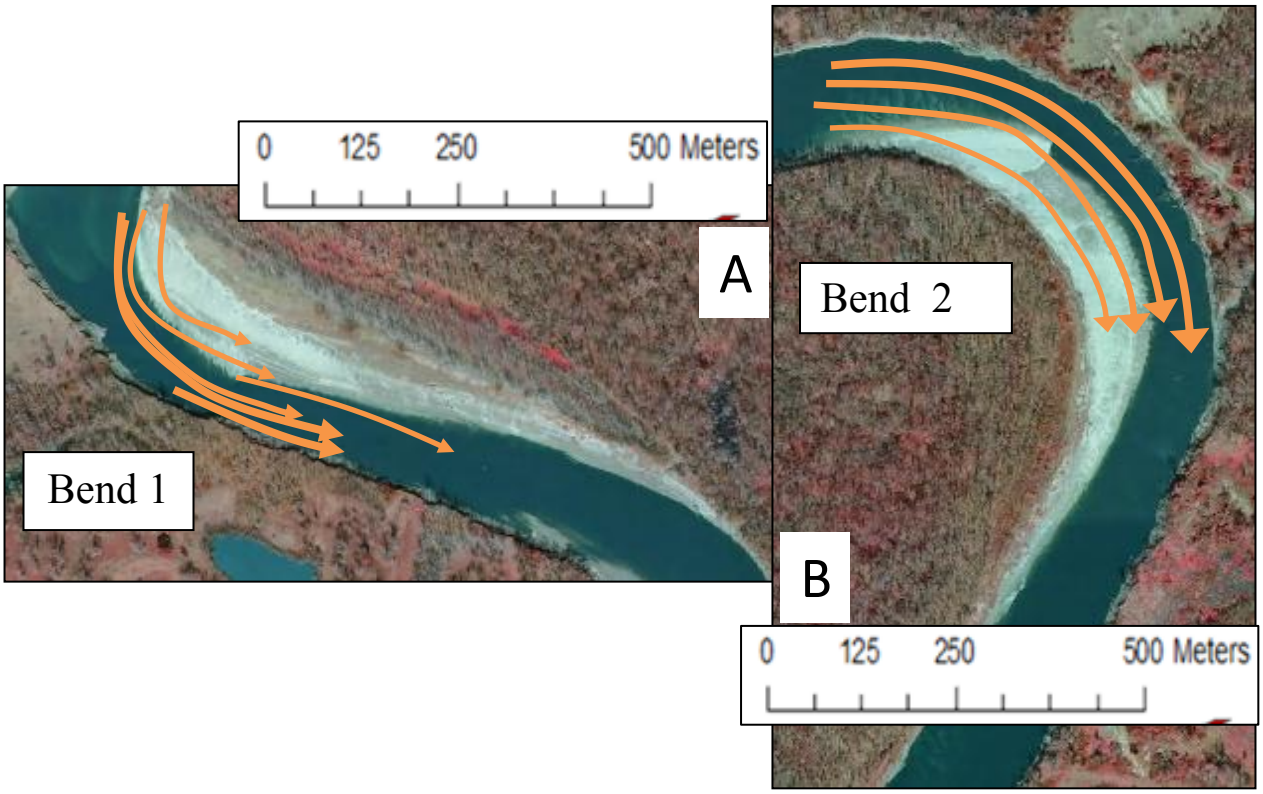


Figure 4.20: 2009 aerial photograph of Bar One (A) and shows Bar Two (B). The images are overlain with arrows (in orange) in the direction of bed load transport during high flow. On Bar One the bed load is not transported up over the front of the bar. The bed load is transported over the entire bar in Bar Two.

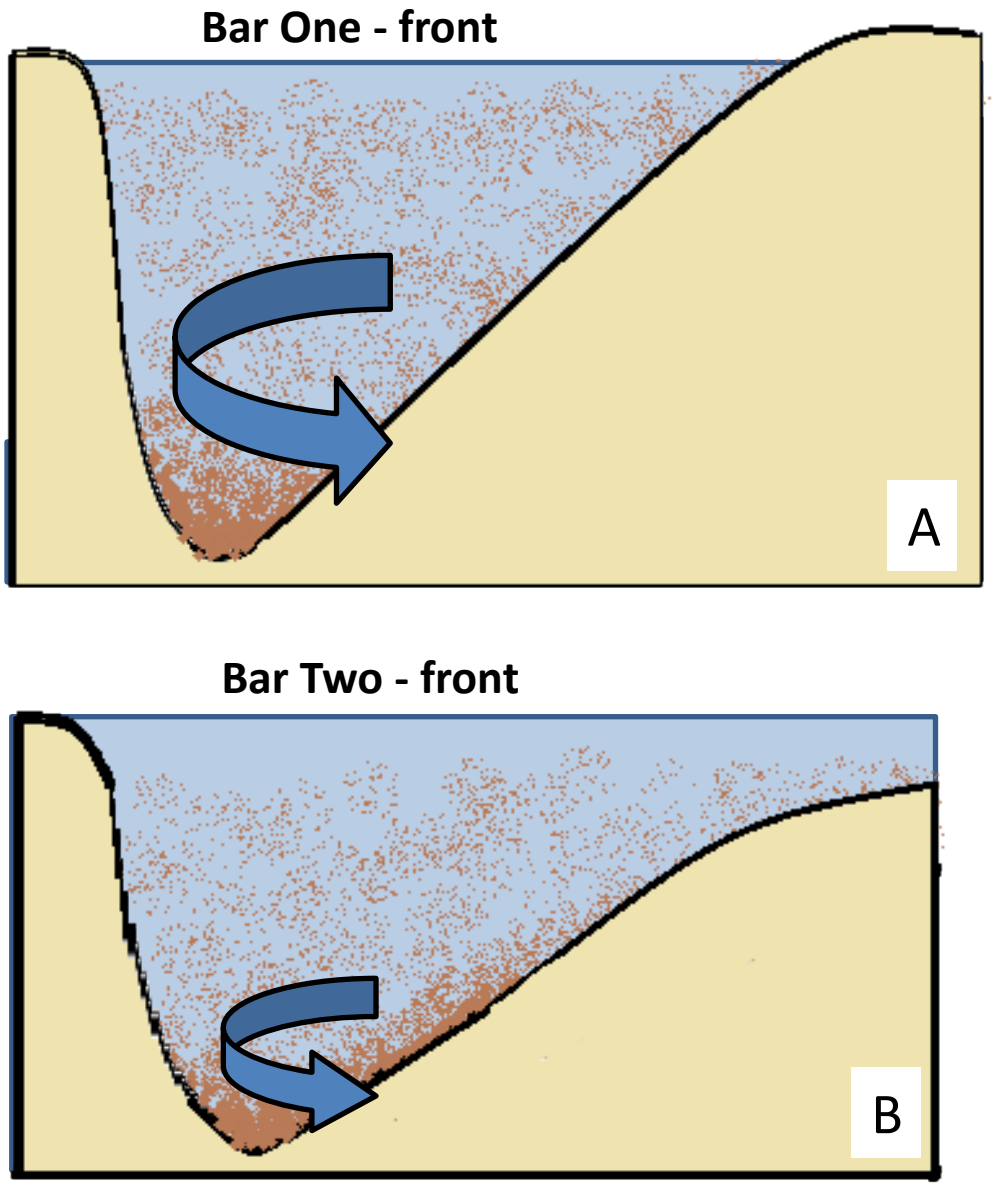


Figure 4.21: Two schematics represent sediment transport around/over Bar One and Bar Two. These images show a cross section of the channel near the front of each bar. As the flow rises the sediment transport increases. The bed load is able to roll up over Bar Two, but very little bedload is able to roll up the steep slopes of Bar One.

**REFERENCES**

Bridge, J.S., 1977. “Flow, bed topography, grain-size and sedimentary structure in bends: a three dimensional model.” *Earth Surface Processes*, vol. 2, p. 401-416.

Carson, M.A. and M.F. Lapoionte, 1983. “The inherent asymmetry of river meander planform.” *Journal of Geology,* vol. 91, no. 1, p. 41-55.

Dietrich, William E., 1987. "Chapter 8: Mechanics of Flow and Sediment Transport in River Bends." *River Channels: Environment and Process: Institute of British Geographics Special Series*. Ed. K. Richards. Vol. 18, p. 179-227.

Dietrich, William E. and John D. Gallinatti, 1991. "Chapter 5: Fluvial geomorphology." *Field Experiments and Measurement Programs in Geomorphology*. University of British Columbia Press, Vancouver, Ed. O. Slaymaker.

Dietrich, William E., J Dungan and Thomas Dune, 1979. "Flow and sediment transport in a sand bedded meander." *The Journal of Geology*, vol. 87, no. 3, p. 305-315.

Dietrich, William E. and Peter J. Whiting, 1989. “Boundary shear stress and sediment transport in river meanders of sand and gravel,” in S. Ikeda and G. Parkers (Eds.), *River Meandering, American Geophysical Union Water Resources Monograph 12*, p. 1-50.

Furbish, D.J., 1988. “River-bend curvature and migration: How are they related?” *Geology*, vol. 16, p. 752-755.

Gagliano, S.M., and P.C. Howard, 1984. "The neck cutoff Oxbow Lake cycle along the Lower Mississippi River." *River Meandering*, p.147-158.

Jackson, R.G., 1976 "Depositional model of point bars in the lower Wabash River." *Journal of Sedimentary Petrology,* vol. 46, no.3, p. 579-594.

Lauer, J. Wesley, 2006. "Channel Planform Statistics: An ArcMap Project," The National Center for Earth Surface Dynamics, Stream Restoration Toolbox.

Leeder, M.R., and P.H. Bridges, 1975. "Flow separation in meander bends." *Nature*, vol.253, p. 338-339m.

Leopold, Luna B., M. Gordon Wolman, and John P. Miller. 1964. *Fluvial Processes in Geomorphology*. San Francisco: W.H. Freeman.

Nanson, G.C., 1980. "A Regional Trend to Meander Migration," *Journal of Geology*, Vol. 88, p/ 100-108.

Nelson, J.M. and J.D. smith, 1989. "Flow in meandering channels with natural topography," in S. Ikeda and G. Parkers (Eds.), *River Meandering*, *American Geophysical Union Water Resources Monograph 12*, p. 1-50.

Mosley, M.P., 1975. "Meander cutoffs on the River Bollin, Cheshire, in July, 1973." *Revue de Geomorphologie Dynamic,* vol. 24, no. 1, p.21-31.

Parker, Gary and Edmund D. Andrews, 1986. “On the time development of meander bends.” *Journal of Fluid Mechanics,* Vol. 162, p. 139-156.

Phillips, Jonathan, Michael Slattery, and Zachary Musselman, 2005. "Channel adjustments of the lower trinity River, Texas downstream of Livingston Dam." *Earth Surface Processes and Landforms,* Vol. 30, p. 1419-1439.

Whiting, Peter J and William E. Dietrich, 1993. “Experimental constraints on bar migration through bends: Implications for meander wavelength selection.” *Water Resources Research,* Vol. 29, p.1091-1102.

Whiting, Peter J and William E. Dietrich, 1993. “Experimental studies of bed topography and flow patterns in large-amplitude meanders: 1. Observations.” *Water Resources Research,* Vol. 29, p.3605-3614.

Whiting, Peter J and William E. Dietrich, 1993. “Experimental studies of bed topography and flow patterns in large-amplitude meanders: 2. Mechanisms.” *Water Resources Research,* Vol. 29, p.3615-3622.

Zinger, Jessica A., Bruce L. Rhodes and James L. Best, 2011. “Extreme sediment pulses generated by bend cutoffs along a large meandering river,” *Nature Geoscience,* Vol. 4, P. 675-678.

# Chapter 5: Conclusions-

## Pathways to Future Work and Scientific Contributions

Rivers are a critical part of water resources. Coastal rivers maintain in particular the supply of water and sediment needed to sustain coastal environments, support population hubs and sustain industry. To best protect and manage rivers it is critical to understand their dynamic functions. This is especially important in the lower Trinity River, where growing populations have put an increased demand on the River's water resources. There are currently plans for seventeen new reservoirs in the lower Trinity Basin.

This project improves the understanding of features and mechanics characterizing three types of alluvial river environments: incisional, normal flow and backwater. Creating a comprehensive three-dimensional study of the river channel allowed for the identification of the three channel zones and how they correspond to spatial changes in sediment transport properties. Through this extensive dataset a comprehensive view of the lower Trinity River's channel geometry and channel mechanics was established. Making connections between channel geometry, migration dynamics, sediment transport dynamics and fluid mechanics in each zone provides a more complete understanding of the relationships between channel shape and the mechanics at play. This showed the methods and means of the construction of bars, the influence of dams and the changes that occur on coastal rivers over time.

Chapter Two showed the downstream influence of Livingston Dam. The sandy composition of the lower Trinity made this study unique from most of the published studies on dam influenced channels; which have predominately focused on gravel-bed rivers. By adjusting the input variables of the "One-Dimensional Morphodynamical Model" the downstream incision due to Livingston Dam's impoundment was able to accurately model. Furthermore, modeling the channel response showed that unlike gravel-bed rivers the sandy lower Trinity River is continually adjusting several decades later. The bed of the river never armors allowing a constant incision that is propagated downstream with time. The abundant supply of the sediment allows the river to re-establish sediment transport capacity downstream of the Dam.

Chapter Three investigated the physical changes of the geometry between each of the zones. Each zone has a unique sediment transport that gives way to unique channel features. The channel shape and the sediment transport cause the river to behave differently, migrating at different rates, in each of the zones. In Zone One the Dam influence on bedload transport causes the channel to straighten. The Bay influences the flow and sediment transport in Zone Three, altering the sediment transport and channel migration. In Zone Two the river has negligible outside influences, allowing the river to meander freely. In Zone Two this investigation showed that the radius of curvature over width can describe propensity of the channel to laterally migrate through a probability density function.

Chapter Four showed two fashions of channel migration, cutoff response and gentle translation. The style of migration controls the bar construction and shape. In the case of cutoff response the channel shows an accelerated migration response to a major

upstream change. The response is reflected in the unique teardrop shape and grain-size distribution of the downstream bar. The extreme slopes of the bar's frontal lope force a combination of suspended load and bed load for bar construction. The more common case of translation migration is less dramatic. Through time the bend slowly migrates, eroding in an outward and downstream direction and depositing on the inner bank. The associated bar shape for this style of migration is crescent, wrapping around the bend. This bar was built exclusively of bed load transport.

In completing this research there are a multitude of additional research questions that become evident within the three zones, their transition, and how the fluid mechanics and sediment transport kinematics of each zone influence other aspects of the river. The drastic adjustment of the profile raises questions about how profiles adjust on the decadal time scale to dam removal. In Zone Two, flow in one bend of the river drives flow downstream, but it can also influence upstream flow. It is important to understand this upstream and downstream relationship to fully describe flow through bends and its effects on sediment transport and channel kinematics. In Zone Three the backwater effects begin to appear when the channel bed reaches sea level, phenomena that has not been observed or explained in the literature. Furthermore, this will open the door to understanding the driving influences and mechanisms controlling the transition zones between the river segments. The fluid dynamics differ depending on the flow of the zones of a river. While this investigation seeks to understand and identify the mechanics behind these distinct regimes, within a coastal river there is still much to be developed in the understanding of how these regimes influence and drive each other. The fluid mechanical interactions occurring at transition zones between flow regimes pose many great scientific questions.

Additionally, understanding the mechanisms of sediment transport in an alluvial river opens many doors for interdisciplinary research. Currently, many important river management questions circulate around fluvial geomorphology. For example, this research could advance ideas in managing contaminated sediment, understanding flood prediction and flood management. Fields with a vested interest in this research include ecology, water resource planning, management agriculture and many more.

# Appendix (or Appendices)

*Moasics of the point bar trenches are too large to fit on this paper. These are available upon request.

## Bibliography

Aksoy, S., 1971. "River-bed degradation downstream of dams." *Proceedings of the 14th Congress*, IAHR, Paris, France, Vol. 3, No. C33, p. 275-282.

Bates, R.E., 1939. "Geomorphic history of the Kickappo Region," *Geological Society of America Bulletin*, Vol. 50, p. 819-879.

Begin, Z.B., 1981, "Stream curvature and bank erosion: a model based on the momentum equation," *The Journal of* Geology, vol. 89, no. 4, p. 497-504.

Biedenharn, D., N. Raphett, and C. Montague, 1989. "Long-term stability of the Ouchita River," In: C.M. Elliot (ed.), River Meandering, *Proceedings of the Conference Rivers'83,* New Orleans, LA, p.126-137.

Blondeaux , P., and G. Seminara, 1985. "A unified bar-bend theory of river meanders," *Journal of Fluid Mechanics*, vol. 157, p. 449-470.

Brandt, S.A., 2000. "Classification of geomorphological effects downstream of dams," *Catena,* Vol.**40**, p. 375–401.

Braudrick, Christian A., William E. Dietrich, Glen T. Leverich and Leonard D. Sklar, 2009. "Experimental evidence for the conditions necessary to sustain meandering in coarse-bedded rivers," Proceedings of the National Academy of Sciences of the United States of America, Vol. 106, no. 40, p. 16936-16941.

Brice, J.C., 1974. “Evolution of Meander Loops,” *Geological Society of America Bulletin,* Vol. 85, p.581-586.

Bridge, J.S., 1977. “Flow, bed topography, grain-size and sedimentary structure in bends: a three dimensional model.” *Earth Surface Processes,* vol. 2, p. 401-416.

Brune, Gunnar M., 1953. “Trap Efficiency of Reservoirs,” *Transactions,* American Geophysical Union, Vol. 34, No. 3, p.407-418.

Bullet, Bob. "Feb 20th, 2004 Trinity River Bridge Collapse W/Train on Bridge."*Webshots!* Webshots!, 09 May 2003. Web. 29 Aug. 2012. <http://rides.webshots.com/album/72572243DSKXLk>.

Carson, M.A. and M.F. Lapoionte, 1983. “The inherent asymmetry of river meander planform,’ *Journal of Geology,* vol. 91, no. 1, p. 41-55.

Cantelli, A., M. Wong, G. Parker, and C. Paola, 2007. “Numerical model linking bed and bank evolution of incisional channel created by dam removal,” *Water Resources Research,* vol. 43.

Chien, Ning, 1985. “Changes in river regime after the construction if upstream reservoirs.” *Earth Surface Processes and Landforms*, Vol. 10, p. 143-159.

Chow, Ven Te, David Maidment and Larry Mays, 1988. Applied Hydrology, McGraw, New York, p. 281.

Collins, B. and T. Dunne, 1990. "Fluvial geomorphology and river gravel mining: A guide for planners, case studies included," California Division of Mines and Geology Special Publication 98. Sacramento, California.

Crossland, Christopher J., Hartwig H. Kremer, Han J. Lindeboom, Janet I. Marshall Crossland, Martin D.A. Le Tissier, 2005. "Costal Fluxes in the Anthropocene: The land-ocean interactions in the coastal zone project of the International Geosphere-Biosphere Programme," Global Change, IGBD Series, Springer Publishing, Berlin.

Dietrich, William E., 1987. "Chapter 8: Mechanics of Flow and Sediment Transport in River Bends." *River Channels: Environment and Process: Institute of British Geographics Special Series*. Ed. K. Richards. Vol. 18, p. 179-227.

Dietrich, William E. and John D. Gallinatti, 1991. "Chapter 5: Fluvial geomorphology." *Field Experiments and Measurement Programs in Geomorphology*. University of British Columbia Press, Vancouver, Ed. O. Slaymaker.

Dietrich, William E., J Dungan and Thomas Dune, 1979. "Flow and sediment transport in a sand bedded meander." *The Journal of Geology*, vol. 87, no. 3, p. 305-315.

Dietrich, William E., and Peter Whiting, 1989. "Boundary shear stress and sediment transport in river meanders of sand and gravel." *American Geophysical Union*, p. 1-50.

Dingman, S. Lawrence, 1991. Fluvial Hydrology, W.H. Freeman and Company, New York, p. 184-193.

Engelund, F., 1974. "Flow and bed topography in channel bends," *Journal of Hydraulics*, Vol. 100, p.1631-1648.

Engelund, F., and E. Hansen, 1967. "A monograph on Sediment Transport in Alluvial Streams," Technisk, Vorlag, Copenhagen, Denmark.

Furbish, D.J., 1988. "River-bend curvature and migration: How are they related?", *Geology*, vol. 16, p. 752-755.

Furbish, D.J, 1991. "Spatial autoregressive structure in meander evolution", *Geological Society of America Bulletin*, vol. 103, p. 1576-1589.

Gagliano, S.M., and P.C. Howard, 1984. "The neck cutoff Oxbow Lake cycle along the Lower Mississippi River." *River Meandering*, p.147-158.

Graf, William L., 2005. "Geomorphology and American dams: the scientific, social, and economic context," *Geomorphology,* Vol. 71, p. 3-26.

Graf, William L., 2006. "Downstream hydrologic and geomorphic effects of large dams on American rivers," *Geomorphology*, Vol. 79, p. 336-360.

Harvey, Michael D., 1989. "Meanderbelt dynamics of the Sacramento River, CA," *USDA Forest Service Gen. Tech. Rep.*, PSW-110, p.54-59.

Hickin, E.J., 1974. "The Development of Meanders in Natural River-channels", *the American Journal of Science*, vol. 274.

Hooke, J.M., 1995. "Processes of channel planform change on meandering channels in the U.K.", In: Gurnell, A and Petts, G. (eds), Changing River Channels, John Wiley and Sons Chichester, U.K., p. 87-115.

Hooke, J.M., 2003. "River meander behavior and instability: a framework for analysis", *Transactions of the Institute of British Geographers*, vol. 28, no. 2, p. 238-253.

Hooke, J.M., 2007. "Spatial variability, mechanisms and propagation of change in an active meandering river," *Geomorphology*, vol. 84, p. 277-296.

Howard, A.D. and T.R. Knutson, 1984. "Sufficient conditions for river meandering: A simulation approach", *Water Resource Research*, vol. 20, no. 11, p. 1659-1667.

Hudson, Paul F. and Richard H. Kesel, 2000. "Channel migration and meander-bend curvature in the lower Mississippi River prior to major human modification," *Geology*, Vol. 28, No. 6, p. 531-534.

Ikeda, Syunsuke, Gary Parker and Kenji Sawai, 1981. “Bend theory of river meanders. Part 1. Linear development,” *Journal of Fluid Mechanics,* Vol. 112, p. 363-377.

Inglis, C.C., 1937. “The relationships between meander belts, distance between meanders on axis of stream, width and discharge of rivers in flood plains and incised rivers: Annual Report,” Central Board of Irrigation (India) 1938-1939, p. 49.

Ikeda, Syunsuke, Gary Parker and Kenji Sawai, 1981. “Bend theory of river meanders. Part 1. Linear development,” *Journal of Fluid Mechanics,* Vol. 112, p. 363-377.

Jackson, R.G., 1976 “Depositional model of point bars in the lower Wabash River.” *Journal of Sedimentary Petrology,* vol. 46, no.3, p. 579-594.

Jefferson, M., 1902, “Limiting width of meander belts,” *National Geographic Magazine*, vol. 13, p. 373-384.

Jain, Subhash C., and Inbo Park, 1989. “Guide for estimating riverbed degradation,” *Journal of Hydraulic Engineering,* Vol. 115, No. 3, p. 356-366.

Jerolmack, Douglas J., 2009. “Conceptual framework for assessing the response of delta channel networks to Holocene sea level rise,” *Quaternary Science Reviews,* Vol. 28, p. 1786-1800.

Lagasse, P.F. et al., 2004. “Methodology for Predicting Channel Migration,” *National Cooperative Highway Research Program Transportation Research Board of the National Academies* Document 67.

Larsen, E. and H.W. Shen, 1989. "The evolution of meander bends of the Mississippi River," In: Yalin, M.S. (Chair), Hydraulics and the Environment, *Proceedings of the XXIII Congress of the IAHR*, Vol. B, Fluvial Hydraulics, p. B33-B39.

Lauer, J. Wesley, 2006. "Channel Planform Statistics: An ArcMap Project," The National Center for Earth Surface Dynamics, Stream Restoration Toolbox.

Lauer, J Wesley and Gary Parker, 2007. "Net local removal of floodplain sediment by river meander migration," *Geomorphology* Vol. 96, p.123-144.

Lauer, J. Wesley and Gary Parker, 2008. "Modeling framework for sediment deposition storage, and evacuation in the floodplain of a meandering river: Theory," *Water Resources Research* Vol. 44.

Leeder, M.R., and P.H. Bridges, 1975. "Flow separation in meander bends." *Nature*, vol.253, p. 338-339.

Lewin, J., 1978. "Meander bend development and floodplain sedimentation: A case study from mid-Wales," *Geology Journal*, vol. 13, part 1, p. 25-36.

Leopold, Luna B,and M. Gordon Wolman, 1957. "River channel patterns: Braided, meandering and straight," U.S. Geological Survey Professional Paper 282B, p. 85.

Leopold, Luna B,and M. Gordon Wolman, 1960. “River Meanders,” *Geological Society of America,* vol. 71, p. 769-794.

Leopold, Luna B., M. Gordon Wolman, and John P. Miller. 1964. *Fluvial Processes in Geomorphology*. San Francisco: W.H. Freeman.

Leliavsky, Serge, 1955. “An introduction to fluvial hydraulics: London”, Constable and Co, p.255.

Kondolf, G. Mathis, 1997. “Hungry Water: Effects of dams and gravel mining on river channels.” *Environmental Management,* Vol. 21, No. 4, p. 533-551.

Kondolf, G.M. and M.G. Wolman, 1993. “The sizes of salmonid spawning gravels,”*Water Resources Research*, Vol. 29, No. 7, p:2275-2285.

MacDonald, T.E., G. Parkers, D.P. Leuthe, 1991. “Inventory and analysis of stream meander problems in Minnesota,” St. Anthony Falls Hydraulic Laboratory Project Report No. 321, p. 38.

Mackin, J. Hoover, 1948. “Concept of the Graded River,” Bulletin of the Geological Society of America, Vol. 59, p: 463-512.

Meyer-Petter, E., and R. Muller, 1948. "Formulas for bed load transport," Report on second meeting of international association for Hydraulics Research, Stockholm, Sweden, p. 39-64.

Mosley, M.P., 1975. "Meander cutoffs on the River Bollin, Cheshire, in July, 1973." *Revue de Geomorphologie Dynamic,* vol. 24, no. 1, p.21-31.

Musselman, Zachary A., 2006. "Tributary response to the Lake Livingston impoundment—the Lower Trinity River, Texas," Doctoral Dissertation, University of Kentucky.

Musselman, Zachary A., 2011. "The localized role of base level lowering on channel adjustment of tributary streams in the Trinity River basin downstream of Livingston Dam, Texas, USA," *Geomorphology,* Vol. 128, p.42-56.

Murray B, and C. Paola, 1994. "A cellular model of braided rivers," *Nature,* Vol. 371, p. 54-57.

Nanson, G.C., 1980. "A Regional Trend to Meander Migration," *Journal of Geology,* Vol. 88, p/ 100-108.

Nelson, J.M. and J.D. Smith, 1989. "Flow in meandering channels with natural topography," in S. Ikeda and G. Parkers (Eds.), *River Meandering, American Geophysical Union Water Resources Monograph 12*, p. 1-50.

Nelson, J.M., 1990. “The initial instability and finite-amplitude stability of alternate bars in straight channels,” *Earth-Science Reviews*, vol. 29, p. 97-115.

Nicholls, Robert J., 2003. “Coastal flooding and wetlands loss in the 21st century: changes under the SRES climate and socio-economic scenarios,” *Global Environmental Change*, Vol. 14, No. 1, p. 69-86.

Norris, Chad W., and Gordon W. Linam. 1999. "Ecologically Significant River and Stream Segments - Region H." *TPWD: Ecologically Significant River/Stream Segmentsof Region H, Regional Water Planning Area*. Texas Parks and Wildlife Department, n.d.

Nittrouer, Jeffery, 2010. “Sediment transport dynamics in the lower Mississippi River: Non-uniform water flow and affects on river-channel morphology,” Dissertation, University of Texas at Austin.

Nittrouer, Jeffery, David Mohrig, and M.A. Allison, 2012. “Punctuated transport of bed materials in the lowermost Mississippi River,” *Journal of Geophysical Research-Earth Surface.*

Nittrouer, Jeffery, John Shaw, Michael Lamb, and David Mohrig, 2012. “Spatial and temporal trends for water-flow velocity and bed-material sediment transport in the lower Mississippi River,” *GSA Bulletin*, Vol. 124, No. ¾, p. 400-414.

Paola, Chris, and David Mohrig, 1996. “Paleohydraulics revisited: Paleoslope estimation incoarse-grained braided river, *Basin Resvoirs*, vol. 9, p. 243-254.

Parker, Gary, 1976. “On the cause and characteristic scales of meandering and braiding in rivers,” *Journal of Fluid Mechanics,* Vol. 76, p. 457-480.

Parker, Gary, 1990. “Surface-based bedload transport relation for gravel rivers,” *Journal of Hydraulic Research*, Vol. 28, No. 4, p. 417-436.

Parker, Gary, 2004. “1D Sediment Transport Morphodynamics with Applications to Rivers and Turbidity Currents: E-book.” St. Anthony Falls Laboratory, University of Minnesota, Minneapolis, http://vtchl.uiuc.edu/people/parkerg/morphodynamics_e-book.htm, August 20, 2010.

Parker, Gary and Edmund D. Andrews, 1986. “On the time development of meander bends,” *Journal of Fluid Mechanics,* Vol. 162, p. 139-156.

Parker, G., T. Muto, Y. Akamatsu, W. E. Dietrich, and J. W. Lauer, 2008. “Unravelling the conundrum of river response to rising sea-level from laboratory to field. Part II. The Fly–Strickland River system, Papua New Guinea”, *Sedimentology*, Vol. 55, p. 1657–1686.

Parker, Gary, Kenji Sawai and Syunsuke Ikeda, 1982. “Bend theory of river meanders. Part 2. Nonlinear deformation of finite-amplitude bends,” *Journal of Fluid Mechanics*, Vol. 115, p. 313-314.

Parker, G., Y. Shimizu, G.V. Wilkerson, J.D. Abad, J.W. Lauer, C. Paola, W.E. Dietrich, and V.R. Voller, 2011. “A new framework for modeling the migration of meandering rivers,” *Earth Surface Processes and Landforms*, vol. 36, no. 1, p. 70-86.

Parker, Gary, Tetsuji Muto, Yoshihisa Akamatsu, William E. Dietrich, and J. W. Lauer, 2006. “Unraveling the conundrum of river response to rising sea level from laboratory to field. Part II. The Fly-Strickland River System, Papua New Guinea.” MS 2. National Center for Earth-surface Dynamics.

Petts, Geoffrey E. and Angela M. Gurnell, 2005. “Dam and geomorphology: Research progress and future directions.” *Geomorphology*, Vol. 71, p. 27-47.

Peyret, Aymeric-Pierre B., David Mohrig, Virginia Smith, and John Shaw, 2012. “A code to compute some geometrical elements of rivers in planform,” submitted to *Elsevier*.

Phillips, Jonathans and Michael Slattery, 2007. “Downstream trends in discharge, slope, and stream power in a lower coastal plain river," *Journal of Hydrology*, Vol. 334, p. 290-303.

Phillips, Jonathans, Michael Slattery, and Zachary Musselman, 2004. "Dam-to-delta sediment inputs and storage in the lower Trinity River, Texas," *Geomorphology,* Vol. 62, No.1-2, p. 17-34.

Phillips, Jonathan, Michael Slattery, and Zachary Musselman, 2005. "Channel adjustments of the Lower Trinity River, Texas downstream of Livingston Dam," *Earth Surface Processes and Landforms,* Vol. 31, p. 1419-1439.

Podolak, Charles Joseph Pena, 2012. "Channel bed response to an increasesd sediment supply," Dissertation, Johns Hopkins University.

Prus-Chacinski, T.M., 1954. "Patterns of motion in open-channel bends," *International Association of Hydrology*, pub. 38, vol, 3, p. 311-318.

Rzhanitzin, N.A., E.K. Rabkovam, P.A. Artemiev, 1971. "Deformation of alluvial channel downstream from large hydro-projects," *Proceedings of the 14$^{th}$ Congress,* IAHR, Paris, France, Vol. 3, No. C32, p. 265-274.

Schumm, S.A., 1993. "River Response to Baselevel Change: Implications for sequence stratigraphy," *The Journal of Geology,* Vol. 101, No. 2, p. 279-294.

Slattery, Michael, 2007. "Sediment budgeting in the upper and middle basins of the Brazos and Trinity Rivers, TX: An assessment of methods and directions for future work," Jun. 2007, Texas Water Development Board.

Slattery, Michael C. and Jonathan D. Phillips, 2007. "Sediment monitoring in Galveston Bay – Final Phase," *Final Report,* Texas Water Development Board.

Smith, J.D. and McLean, 1984. "A Model for meandering rivers," *Water Resources Research,* Vol. 20, p. 1311-1315.

Sun, Tao, Paul Meakin and Torstein Jossang,, 1996. "A simulation model for meandering rivers," *Water Resources Research,* Vol. 32, No. 9, p. 2937-2954.

Sun, Tao, Paul Meakin and Torstein Jossang, 2001. "A computer model for meandering rivers with multiple bed-load sediment sizes, 1. Theory," *Water Resources Research,* Vol. 37, No. 8, p. 2227-2241.

Syvitski, et al., 2005. "Impacts of humans on the flux of terrestrial sediment to the global coastal ocean," *Science* Vol. 308, p. 3376-380.

*The Handbook of Texas: the Trinity River*. Web. 19 Aug. 2010. http://www.tshaonline.org/handbook/online/articles/TT/rnt2.html

*Trinity River Audubon Center: home page*. Web. 23 Nov. 2009. <www.trinityriveraudubon.org>.

*Trinity River Basin Master Plan.* Trinity River Authority, 2010.

"Trinity River Bridge, State Highway 105." *Texas Department of Transportation.* p.1-9. Print.

*USGS Water Data for the Nation*. Web. 20 Aug. 2010. <http://waterdata.usgs.gov/nwis>.

Van Rijn, Leo C., 1984. "Sediment transport, Part III: Bed forms and alluvial roughness," *Journal of Hydraulic Engineering*, Vol.110, No.10, p. 1431-1456.

Web. 23 Sept. 2012. http://www.tpwd.state.tx.us/publications/pwdpubs/pwd_rp_t3200_1059c/index.phtml

Whiting, Peter J and William E. Dietrich, 1993. "Experimental constraints on bar migration through bends: Implications for meander wavelength selection," *Water Resources Research*, Vol. 29, p.1091-1102.

Whiting, Peter J and William E. Dietrich, 1993. "Experimental studies of bed topography and flow patterns in large-amplitude meanders: 1. Observations," *Water Resources Research*, Vol. 29, p.3605-3614.

Whiting, Peter J and William E. Dietrich, 1993. "Experimental studies of bed topography and flow patterns in large-amplitude meanders: 2. Mechanisms," *Water Resources Research*, Vol. 29, p.3615-3622.

Wiberg, P. L. and Smith, J. D., 1989. "Model for calculating bedload transport of sediment," *Jounral Hydraulic. Engineering,* Vol. 115, No. 1, p.101-123.

Williams, G.P., 1986. "River Meanders and channel size," *Journal of Hydrology*, vol. 88, p. 147-164.

Williams, G.P. and M.G. Wolman, 1984. "Downstream effects of dams on alluvial rivers," Geological Survey Professional Paper 1286, U.S. Government Printing Office, Washington, DC, vol. 83.

Wilson, K. C., 1966. "Bed load transport at high shear stresses", *Journal of Hydraulic Engineering,* Vol, 92, No. 6, p: 49-59.

Wolman, M. Gordon, 1954. "A method of sampling coarse river-bed material," *Transactiona of the American Geophyscial Union,* Vol. 35, No. 6, p. 951-956.

Wright, Scott and Gary Parker, 2004. "Flow resistance and suspended load in sand-bed rivers: Simplified stratification model," *Journal of Hydraulic Engineering,* Vol. 130, No. 8, p. 796-805.

Zinger, Jessica A., Bruce L. Rhodes and James L. Best, 2011. "Extreme sediment pulses generated by bend cutoffs along a large meandering river," *Nature Geoscience,* Vol. 4, P. 675-678.

## Vita

Virginia Smith is a PhD candidate at the University of Texas at Austin (UT), studying fluvial geomorphology and hydrology at the Jackson School of Geosciences. She began her colligate academic career at the Georgia Institute of Technology where she received a BS in civil and environmental engineering. Upon graduation Virginia joined the Peace Corps, where she spent two years serving as a volunteer in Samoa working on the National Water Project. Virginia then came to UT to begin graduate school, where she receive a master's degree in environmental and water resource engineering before being her doctoral studies. Virginia doctoral research focuses on hydrology and geomorphology of sandy coastal rivers. In addition to her studies, Virginia serves as the president of Bridging Waters and is an avid runner. She is the daughter of Patti and Roger Smith, and the finance of Bryan Enslein.

Email: Virginia.smith@utexas.edu

This dissertation was typed by Virginia Smith